

UNIVERSITA' VITA-SALUTE SAN RAFFAELE

**CORSO DI DOTTORATO DI RICERCA
INTERNAZIONALE IN MEDICINA MOLECOLARE**

**CURRICULUM IN MEDICINA CLINICA E
SPERIMENTALE**

**WOLFRAM SYNDROME:
FROM POINT MUTATION
TO CELL DYSFUNCTION**

DoS: Prof. Lorenzo Piemonti

Second Supervisor: Prof. Fabrizio Barbetti

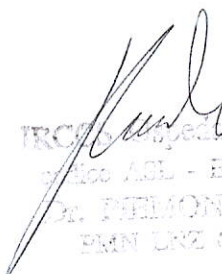
Tesi di DOTTORATO di RICERCA di SILVIA TORCHIO

Matr. 014375

Ciclo di dottorato XXXIV

SSD BIO/11

Anno Accademico 2020/2021


IRCCS Ospedale San Raffaele
Ufficio ASL - ENTE 300-035161
DR. PIEMONTE LORENZO
P.N. L. 03/16 87297

CONSULTAZIONE TESI DI DOTTORATO DI RICERCA

La sottoscritta/I Silvia Torchio

Matricola / registration number 014375

nata a/ born at Milano, Italy

il/on 28/12/1994

autore della tesi di Dottorato di ricerca dal titolo / author of the PhD Thesis titled
“Wolfram Syndrome: from point mutation to cell dysfunction”

- AUTORIZZA la Consultazione della tesi / AUTHORIZES *the public release of the thesis*
- NON AUTORIZZA la Consultazione della tesi per 6 mesi /DOES NOT AUTHORIZE *the public release of the thesis for 6 months*

a partire dalla data di conseguimento del titolo e precisamente / *from the PhD thesis date, specifically*

Dal / *from* 1/5/2022 Al / *to* 1/11/2022

Poiché /*because*:

l'intera ricerca o parti di essa sono potenzialmente soggette a brevettabilità/ *The whole project or part of it might be subject to patentability;*

ci sono parti di tesi che sono già state sottoposte a un editore o sono in attesa di pubblicazione/ *Parts of the thesis have been or are being submitted to a publisher or are in press;*

la tesi è finanziata da enti esterni che vantano dei diritti su di esse e sulla loro pubblicazione/ *the thesis project is financed by external bodies that have rights over it and on its publication.*

E' fatto divieto di riprodurre, in tutto o in parte, quanto in essa contenuto / *Copyright the contents of the thesis in whole or in part is forbidden*

Data /Date 11/04/2022

Firma /Signature



DECLARATION

This thesis has been composed by myself and has not been used in any previous application for a degree. Throughout the text I use both 'I' and 'We' interchangeably.

All the results presented here were obtained by myself, except for:

- 1) iPSC reprogramming was performed in collaboration with Dr. Greta Rossi from the Division of Neuroscience, IRCCS San Raffaele Scientific Institute;
- 2) Differentiation of iPSCs into β cells was performed by Dr. Valeria Sordi, Silvia Pellegrini, Marta Tiffany Lombardo, Alessandro Cospito, Elisa Landi, Aida Moncada and Valentina Zamarian from the Beta cell Differentiation Unit, DRI, IRCCS San Raffaele Scientific Institute;
- 3) Analyses of Ca^{++} fluxes, *WFS1* isoforms sequencing and Single Cell RNAseq dataset, gRNA design and correction of *Wfs1*-mutated iPSCs, and apoptosis tests were performed by Dr. Raniero Chimienti from the Beta cell Biology Unit, DRI, IRCCS San Raffaele Scientific Institute;
- 4) Dynamic perfusion experiments were performed by Fabio Manenti from the Beta cell Biology Unit, DRI, IRCCS San Raffaele Scientific Institute;
- 5) Human pancreatic islet preparations were isolated by Dr. Raffaella Melzi, Alessia Mercalli and Rita Nano from the Pancreatic Islet Processing Unit, DRI, IRCCS San Raffaele Scientific Institute.

All sources of information are acknowledged by means of reference.

ABSTRACT

Wolfram Syndrome 1 (WS1) is a devastating genetic disease manifesting with diabetes mellitus, diabetes insipidus, optic nerve atrophy and deafness. It is caused by dominant or recessive mutations in the *WFS1* gene, coding for Wolframin, a transmembrane protein implicated in ER stress response, autophagy, Ca^{++} handling and insulin secretion.

In the present study, we sought to investigate the case of a patient carrying novel *WFS1* heterozygous mutations, aiming to characterize the genetic, molecular and functional components that determine WS1 manifestation. To do so, we employed iPSC technology, reprogramming mononucleated blood cells into pluripotent progenitors.

Concerning genetics, we determined that one of the two mutations, falling at an acceptor splice site, causes the appearance of multiple alternative isoforms lacking variable portions of the original mRNA; some of them retain the reading frame and code for internally truncated isoforms of the protein. In light of this, we genetically corrected with CRISPR/Cas9 said allele and obtained a syngeneic counterpart.

We demonstrated that WS1-derived iPSCs differentiate in the endocrine lineage, but they show anomalies in the composition of the endocrine subpopulations and β cell subtypes.

We investigated molecular alterations both in iPSCs and iPSC-derived β cells: we found that β cells have higher basal levels of ER stress response, and stress induction further exacerbates their anomalous response. Additionally, both WS1 iPSCs and iPSC-derived β cells have abnormal activation of the autophagic flux.

Functional studies were performed on β cells, highlighting irregularities in Ca^{++} fluxes and insulin secretion in response to glucose stimulation. Lastly, all the individuated mechanisms concur to predispose WS1 cells to undergo apoptosis more than controls in response to ER stress and inflammatory stimuli.

Of interest, we show that administration of Liraglutide, a GLP-1 receptor agonist that proved effective in clinics for the patient, can ameliorate molecular and functional parameters in WS1-derived cells.

In conclusion, this study provides a novel perspective on the molecular basis of a peculiar case of WS1, connecting the genetic mutations with a unique molecular signature and with downstream functional alterations.

Table of contents

1.	Acronyms and Abbreviations.....	4
2.	List of figures and tables	7
2.1.	Figures	7
2.2.	Tables.....	8
3.	Introduction.....	10
3.1.	Wolfram syndrome	10
3.1.1.	Disease phenotype and genetics.....	10
3.1.2.	Protein structure and function	15
3.1.2.1.	ER stress	18
3.1.2.2.	Ca ⁺⁺	21
3.1.2.3.	Mitochondrial alterations	23
3.1.2.4.	Protein trafficking and maturation: Golgi and secretory granules ..	25
3.1.2.5.	Autophagy	29
3.1.3.	Treatments.....	33
3.1.3.1.	Current gold standard	33
3.1.3.2.	Experimental drugs.....	33
3.1.3.3.	Advanced therapies: gene and cell therapy	41
3.2.	iPSCs.....	43
3.2.1.	Origin and development.....	43
3.2.2.	Disease modelling	46
3.2.3.	Therapeutic potential.....	49
3.3.	Patient clinical characterization	53
4.	Aim of the work	56
5.	Results.....	58
5.1.	Generation and stabilization of WS1-derived iPSCs.....	58

5.2.	Genetic characterization of the patient's mutations	60
5.3.	Gene correction of the 316-1 A>T allele	65
5.4.	Differentiation of iPSC-derived β cells.....	68
5.5.	Wolframin expression during iPSCs differentiation	75
5.6.	ER stress in WS1-derived iPSCs.....	77
5.7.	ER stress in WS1-derived β cells	81
5.8.	Autophagy in WS1	87
5.9.	Ca ⁺⁺ imaging	92
5.10.	Insulin secretion	97
5.11.	Apoptosis.....	102
6.	Discussion.....	105
7.	Methods and Materials	115
7.1.	Sequencing	115
7.2.	Cell reprogramming	116
7.3.	Cell culture	116
7.3.1.	iPSCs and differentiation.....	116
7.3.2.	Human pancreatic islets.....	118
7.3.3.	Fibroblasts	119
7.4.	Gene correction via CRISPR/Cas9	119
7.5.	Dynamic perfusion	120
7.6.	Protein extraction and Western blot.....	121
7.7.	RNA extraction, retrotranscription and PCR/RT-qPCR	122
7.8.	FACS.....	123
7.9.	Immunofluorescence	123
7.10.	Ca ⁺⁺ imaging	124
7.11.	Single cell RNAseq	124

7.12. Statistical analysis.....	127
7.13. Antibody table.....	127
7.14. Primer table.....	129
8. References.....	131

1. Acronyms and Abbreviations

#

4-PBA: 4-Phenylbutyric acid

A

AAV: Adeno-associated virus

ALS: Amyotrophic Lateral Sclerosis

AUC: Area under the curve

B

B2M: Beta-2 Microglobulin

BDNF: Brain derived neurotrophic factor

Bp: Base pair

BSA: Bovine serum albumin

C

CACNA1D: calcium voltage-gated channel subunit $\alpha 1 D$; coding for Cav1.3

CaM: Calmodulin

cDNA: Complementary DNA

CREB: cAMP responsive element binding

D

DFNA6: Deafness, autosomal dominant 6

DI: Diabetes insipidus

DIDMOAD: Diabetes insipidus, diabetes mellitus, optic atrophy and deafness; alternative name for WS

DM: Diabetes mellitus

DMEM: Dulbecco's modified Eagle's medium

DPP-4: Dipeptidyl peptidase-4

E

E3: HECT-type ubiquitin ligase

ER: Endoplasmic reticulum

ERAD: Endoplasmic-reticulum-associated protein degradation

ERIS: Endoplasmic reticulum intermembrane small

ERSE: ER stress response elements

ESC: Embryonic stem cell

F

FACS: Fluorescent activated cell sorting

FBS: Fetal bovine serum

G

GAPDH: Glyceraldehyde 3-Phosphate Dehydrogenase

GLP-1: Glucagon-like peptide-1

GLP-1R: Glucagon-like peptide-1 receptor

GMP: Good manufacturing practice

gRNA: Guide RNA

H

HLA: Human leukocyte antigen

HRD1: ERAD-associated E3 ubiquitin-protein ligase

HRP: Horseradish peroxidase

I

IL: Interleukin

iPSC: Induced pluripotent stem cell

K

KGF: Keratinocyte growth factor

L

LHON: Leber hereditary optic neuropathy

M

MAM: Mitochondria-associated membrane

MANF: Mesencephalic astrocyte-derived neurotrophic factor

MEF: Mouse embryonic fibroblast

MHC: Major histocompatibility complex

MODY: Mature-onset diabetes of the young

MRI: Magnetic Resonance Imaging

N

NCS1: Neuronal calcium sensor 1

NGS: Next generation sequencing

NK: Natural killer

NMD: Nonsense-mediated decay

O

OA: Optic atrophy

P

PAM: Protospacer adjacent motif

PBMCs: Peripheral blood mononuclear cells

PBS: Phosphate buffered saline

PCR: Polymerase chain reaction

P.I.: Propidium Iodide

PVDF: Polyvinylidene difluoride

R

RA: Retinoic acid

RGC: Retinal ganglion cells

rh: recombinant human

ROS: Reactive oxygen species

RT-qPCR: Real time quantitative PCR

S

S1R: Sigma-1 receptor

SEM: Standard error of the mean

SERCA: Calcium-dependent ATPase of sarco-endoplasmic reticulum

SLR: Sel1-like repeat

SMURF1: Smad ubiquitination regulatory factor 1

SSC: Side scatter

ssODN: Single-strand oligodeoxynucleotide

T

T1D: Type 1 diabetes mellitus

T2D: Type 2 diabetes mellitus

T3: L-3,30,5-Triiodothyronine

T_a: Annealing temperature

TBST: TBS Tween 20 Buffer

TEM: Transmission electron microscopy

TG: Thapsigargin

TM: Tunicamycin

TUDCA: Tauroursodeoxycholic acid

U

UPR: Unfolded protein response

W

WS: Wolfram syndrome

2. List of figures and tables

2.1. Figures

Figure 1. Probability of WS1 symptom development based on age.	12
Figure 2. Frequency distribution for the five subclasses of WFS1 mutations.	15
Figure 3. WFS1 gene and Wolframin protein structure.	16
Figure 4. ER stress response and UPR.	19
Figure 5. Ca ⁺⁺ -related roles of Wolframin.	23
Figure 6. MAMs' connection to Wolframin.	25
Figure 7. Wolframin role in insulin secretion.	28
Figure 8. Main stages of autophagy.	30
Figure 9. Wolframin connection to autophagy.	32
Figure 10. Therapeutic approaches for WS1.	34
Figure 11. Mechanism of action for Ibudilast and Calpain inhibitor in WS1 β cells.	38
Figure 12. Signalling downstream the activation of GLP-1R axis in β cells.	39
Figure 13. Results from the clinical trial of Liraglutide in pediatric WS1 patients (Frontino et al., 2021).	41
Figure 14. Steps of pancreatic differentiation in vitro.	45
Figure 15. Main current approaches in regenerative medicine for diabetes.	51
Figure 16. Mechanism of T and NK cell recognition of mismatched HLA and escape of B2M ^{-/-} , HLA-E expressing cells from immune rejection.	52
Figure 17. Graphical aims of the project.	57
Figure 18. Characterization of iPSCs newly generated from reprogramming of a WS1 patient.	59
Figure 19. Localization of the patient's mutations.	60
Figure 20. WFS1 mutations generate multiple splicing isoforms in affected cells.	62
Figure 21. Results from deep sequencing of PCR products from WFS1 transcripts.	64

Figure 22. Characterization of corrected Wfs1 iPSCs.	67
Figure 23. Morphology and differentiation efficiency in iPSC-derived β cells.	71
Figure 24. Single Cell Transcriptomics of iPSC-derived endocrine subpopulations.	75
Figure 25. Study of Wolframin in terminally differentiated cells.	77
Figure 26. Gene and protein expression of ER stress markers in iPSCs.	79
Figure 27. Timecourse of gene expression in iPSCs stimulated with TG.	81
Figure 28. Gene and protein expression of ER stress markers in iPSC-derived β cells.	84
Figure 29. ER stress response to TG and inflammatory cytokines in β cells.	86
Figure 30. Study of autophagy markers in iPSCs, in basal conditions and upon stress induction.	88
Figure 31. Study of autophagy markers in β cells, in basal conditions and upon stress induction.	91
Figure 32. Experimental plan and examples of Ca^{++} fluxes on differentiated iPSCs.	93
Figure 33. Spike profiles of Ca^{++} measurements in Wfs1 and Wfs1 corrected β cells.	96
Figure 34. Gene expression of Ca^{++} -related genes.	97
Figure 35. Insulin secretion quantification after dynamic perfusion.	100
Figure 36. Quantification of secretion-related factors.	102
Figure 37. Apoptosis rate after stress induction in iPSCs.	103
Figure 38. Apoptosis rate after stress induction in β cells.	104
Figure 39. Model of WS1 pathogenesis.	112

2.2. Tables

Table 1. Panoramic view of WS1 symptoms.	11
Table 2. Comparison of the two main papers reporting iPSC-derived WS1 β cells, Shang et al, 2014 and Maxwell et al, 2020.	48
Table 3. Drugs employed in vitro for cell treatments.	118

Table 4. Repartition of cells from control samples of the Single Cell Transcriptomics experiment.

126

3. Introduction

3.1. Wolfram syndrome

3.1.1. *Disease phenotype and genetics*

Wolfram syndrome 1 (WS1) is a genetic condition (OMIM: 222300) first described in 1938 by Wolfram and Wagener (Wolfram & Wagener, 1938), indicating a complex clinical presentation also known as DIDMOAD in light of its main symptoms: diabetes insipidus, diabetes mellitus, optic atrophy, and deafness. These four signs are progressive, with non-autoimmune diabetes mellitus (DM) developing in the first decade of life, while optic atrophy (OA), diabetes insipidus (DI) and deafness in the second decade. In the absence of a genetic test, clinical diagnosis can be performed based upon discovery of optic nerve atrophy and concomitant DM before sixteen/eighteen years old, especially if family history is positive for similar clinical presentations (Urano, 2016).

Differential diagnoses include: type 1 DM (T1D), Leber hereditary optic neuropathy (LHON), Alström syndrome, Bardet-Biedl syndrome, Myotonic dystrophy type 1, Friedreich ataxia, some mitochondrial DNA deletion syndromes, Thiamine-responsive megaloblastic anemia syndrome, Optic atrophy type 1, Charcot-Marie-Tooth neuropathy X type 5, Deafness-dystonia-optic neuronopathy syndrome (Tranebjærg *et al*, 2020; Ma & Sadun, 2021).

Life expectancy is greatly reduced, since most patients die around the third decade because of brainstem atrophy-induced central respiratory failure or progressive renal disease (Kinsley *et al*, 1995; Bueno *et al*, 2018; Pallotta *et al*, 2019).

Other symptoms, which may present in a minority of patients, include: urinary dysfunctions, hypogonadism, ataxia, loss of smell and taste, incomplete development of the brain, psychiatric illness of various nature. To generalize, the most common clinical symptoms are either of pancreatic origin, for DM, or neurological (Rigoli *et al*, 2011; Rigoli & Di Bella, 2012; Rigoli *et al*, 2018). A very thorough description of the morphological features of macular microvasculature in WS1 by optical coherence tomography-angiography has been published recently (Battista *et al*, 2022). Compared to T1D, which also presents with diabetes mellitus during childhood, insulin requirements are lower and microvascular complications are less frequent: however, it is quite clear that the prognosis is way worse both by means of quality of life and life expectancy.

A complete presentation of all described symptoms for WS1 is encompassed in **Table 1**, while **Figure 1** reports the probability of symptom onset according to age.

Major clinical signs	Other common clinical signs
<u>Diabetes mellitus</u>	Fatigue, hypersomnolence
<u>Optic nerve atrophy</u>	Neurological manifestations/autonomic dysfunctions: central apnea, dysphagia, areflexia, epilepsy, decreased ability to taste and detect odors, headache, orthostatic hypotension, hypothermia, hyperpyrexia, gastroparesis, constipation
<u>Central diabetes insipidus</u>	Psychiatric symptoms: depression, psychosis, panic attacks, sleep abnormalities, mood swings
<u>Sensorineural hearing loss</u>	Endocrine disorders: hypogonadism, deficient growth hormone secretion, deficient corticotrophin secretion, delayed menarche in females
	Ataxia
	Urinary tract problems: neurogenic bladder, bladder incontinence, urinary tract infections

Table 1. Panoramic view of WS1 symptoms.
Summarized from (Urano, 2016).

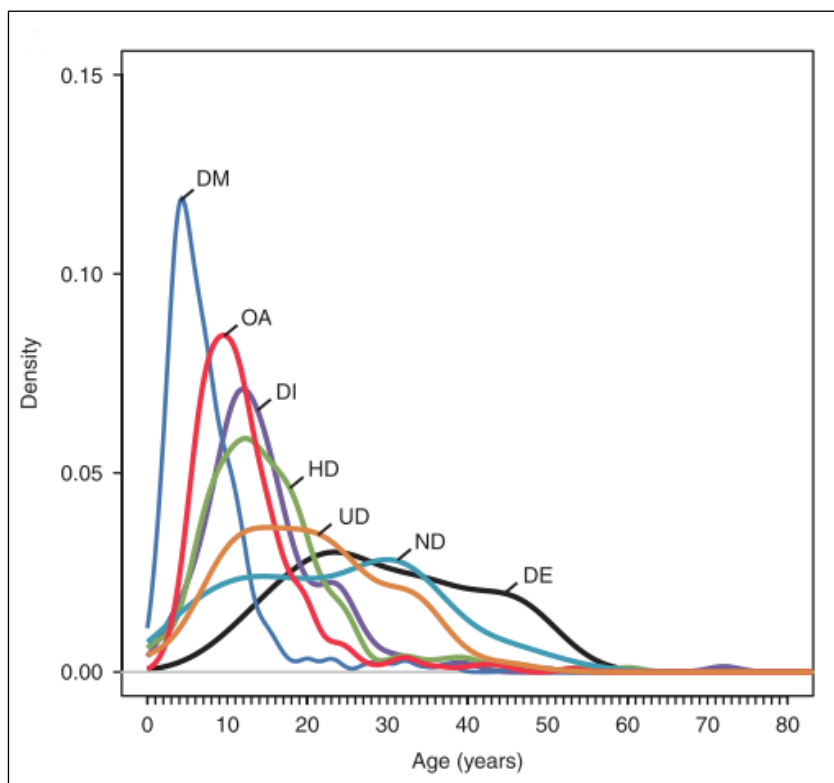


Figure 1. Probability of WS1 symptom development based on age.

Taken from (De Heredia *et al*, 2013). DE, deceased; DI, diabetes insipidus; DM, diabetes mellitus; HD, hearing defects; ND, neurological, psychiatric, and developmental defects; OA, optic atrophy; UD, urological or renal defects.

Incidence of WS1 is probably determined by region-specific factors, since it is estimated around 1 in 770000 in the UK and 1 in 710000 in Japan, but rises up to 1 in 100000 in North America and even 1 in 68000 in Lebanon and 1 in 54478 in a district of North-Eastern Sicily (Barrett *et al*, 1995; Pallotta *et al*, 2019; Delvecchio *et al*, 2021).

Autosomal recessive inheritance in WS1 has been described in most affected families, presenting with apparently healthy parents and affected children. However, in recent years many groups reported in literature cases of autosomal dominant inheritance, although this phenomenon is probably limited to a small number of WS-affected families (Aloi *et al*, 2012; Berry *et al*, 2013; De Franco *et al*, 2017; Batjargal *et al*, 2020; Nkonge *et al*, 2020). Furthermore, dominant mutations in the *WFS1* locus are correlated to other diseases, such as Wolfram-like syndrome and autosomal dominant deafness 6 (DFNA6). Wolfram-like syndrome presents as a severe form of WS1, with congenital progressive hearing impairment, optic atrophy and adult-onset DM (Valéro *et al*, 2008; Tranebjærg

et al, 2020); DFNA6 is a form of low frequency (<2000Hz) sensorineural hearing loss, without DM or visual impairment (Fukuoka *et al*, 2007; Hildebrand *et al*, 2008).

Global data for WS1 highlight no mutational hotspots and a wide range of mutation classes: nonsense (25%), frameshift (21%), splice site mutations (2%), in frame deletions/insertions (13%) or missense mutations (35%) (Hardy *et al*, 1999; Khanim *et al*, 2001).

The mode of inheritance and presentation suggested for years a mitochondrial origin for the disease, similar to other known neurodegenerative conditions like LHON (Rigoli *et al*, 2011). Early reports of altered mitochondrial DNA suggested that maternally-inherited deletions or point mutations could underlie the condition, although this was in open contrast with the apparent recessive inheritance (Ballinger *et al*, 1992; Vora *et al*, 1993).

Repeated genetic testing of this hypothesis was inconclusive and in 1998, WS1 was finally correlated with mutations in a locus on chromosome 4p16, harboring the *WFS1* gene coding for a novel protein, therefore called Wolframin (Strom *et al*, 1998; Inoue *et al*, 1998).

Patients carrying mutations in heterozygosity do not express a clinical phenotype, although multiple studies tried to find a correlation between a single altered *WFS1* locus and diabetes, deafness or psychiatric disorders, often reaching inconclusive or contradictory findings (Torres *et al*, 2001; Young *et al*, 2001; Martorell *et al*, 2003; Kato *et al*, 2003; Wasson & Permutt, 2008; Sandhu *et al*, 2009; Fawcett *et al*, 2010; Munshani *et al*, 2021).

Meanwhile, in 2000, clinical evidence started to support the existence of two classes of WS and the WS2 subtype (OMIM: 604928) was first postulated (El-Shanti *et al*, 2000): *CISD2* gene, located at chromosome 4q22-q24, was correlated to WS2 in 2007, encoding for the endoplasmic reticulum (ER) intermembrane small (ERIS) protein (Amr *et al*, 2007). WS2 has a similar presentation to WS1, including DM, OA and deafness but not DI, accompanied by peptic ulcers and impaired platelet aggregation. Only a few families have been reported so far to be affected by WS2, therefore making it problematic to define specific traits of the disease and clinically distinguish it from the more frequent WS1

variant (Mozzillo *et al*, 2014; Rondinelli *et al*, 2015; Danielpur *et al*, 2016; Cattaneo *et al*, 2017; Tranebjærg *et al*, 2020). To make the issue even more complicated, in 2017 a patient was tested for differential diagnosis, since the presentation exactly matched that of WS1: however, a novel pathogenic mutation in *CISD2* was found, suggesting the possibility that WS1 and WS2 are actually a continuous pathological spectrum and, equally, Wolframin and ERIS are related to the same molecular pathway (Rouzier *et al*, 2017).

The conventional classification of WS1 patients was proposed by De Heredia and colleagues, giving systematic organization to previous studies with smaller patient cohorts (Cano *et al*, 2007; Rohayem *et al*, 2011; Chaussonot *et al*, 2011). An increasing number of patients that do not precisely fit the scheme are being described worldwide: for example, Mirrahimi and colleagues report three siblings carrying homozygous missense mutations (c.1885C>T) on exon 8 of *WFS1* gene, but presenting with a non-uniform severity, suggesting incomplete penetrance at least for some manifestations of the disease (Mirrahimi *et al*, 2021). Similar discrepancies in patients with the same genotype, even within the family, were spotted also in other reports (Smith *et al*, 2004; Tarcin *et al*, 2021).

Still, De Heredia's work constitutes a general guide for understanding genotype-phenotype correlation and remains applicable in most cases (De Heredia *et al*, 2013).

Three groups of mutations are described, according to the effect on protein production:

- i. Type I, when Wolframin production is not allowed due to extreme instability of the mRNA, for example because of very premature stop codons, which are detected and degraded by nonsense-mediated decay (NMD) mechanism
- ii. Type II, in which Wolframin is rapidly degraded after production due to the presence of missense mutations that impair the folding or stability
- iii. Type III, that includes all cases in which an incomplete but mostly stable protein form is produced

Similarly, five genotypic classes can be individuated that allow a sufficiently precise prediction of disease progression:

- A. No Wolframin produced, severe phenotype

- A1. No Wolframin due to mRNA degradation only
- A2. No Wolframin due to both mRNA and protein degradation
- A3. No Wolframin due to protein degradation only
- B. Reduced expression of a defective protein, mostly severe phenotype
- C. Normal production of an abnormal protein, milder phenotype

Frequency distribution for each genotypic class is presented in **Figure 2**.

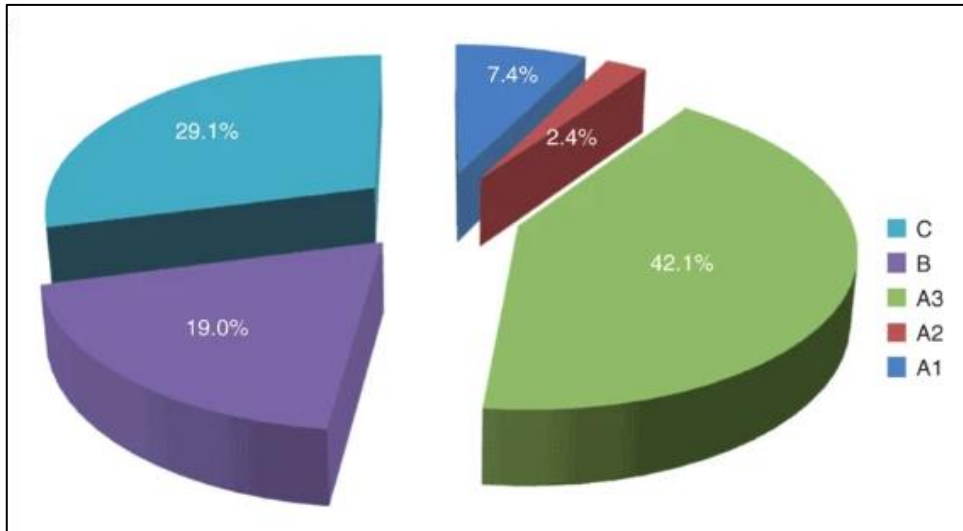


Figure 2. Frequency distribution for the five subclasses of WFS1 mutations. Taken from (De Heredia *et al*, 2013).

3.1.2. Protein structure and function

Phylogenetically speaking, Wolframin is a protein with common orthologues in all metazoans: no structurally related proteins are known in any species, making Wolframin the only protein of its own family. It is ubiquitously expressed during development and basically in all adult tissues, particularly in pancreatic β cells and in the brain (Takeda *et al*, 2001; Philbrook *et al*, 2005); a complete expression pattern in human tissues, both fetal and adult, is reported by De Falco and colleagues (De Falco *et al*, 2012).

A diagram showing gene and protein structure for Wolframin is seen in **Figure 3**.

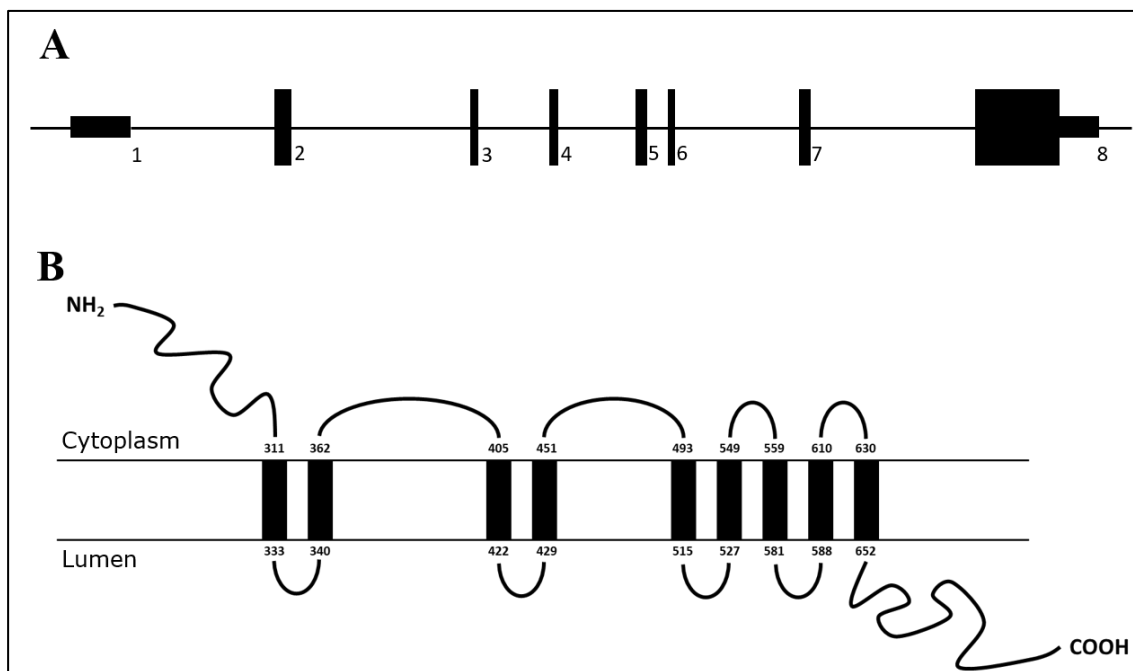


Figure 3. WFS1 gene and Wolframin protein structure.

A) Scheme of the WFS1 gene showing exons and intronic regions. B) Predicted protein structure for Wolframin, highlighting the functional N-term and C-term domains and the putative nine transmembrane helices.

The gene comprises eight exons, of which the first one is not coding. The resulting protein has no known alternative splicing isoforms and is 890aa long. No crystallographic structure has been described, but it is believed to possess nine transmembrane helices, with experimental data pointing towards a localization in the ER, in the Golgi and in secretory granules. Mitochondrial localization has been excluded, sustaining the fact that WS1 is not a mitochondrial disease, but recent reports highlighted that a fraction of Wolframin binds Neuronal Calcium Sensor 1 (NCS1) and localizes at the mitochondria-associated membranes (MAMs), connective structures that act as a bridge between ER and mitochondria (Delprat *et al*, 2018; Angebault *et al*, 2018). A paper reporting Wolframin localization at the plasma membrane has been retracted due to the use of aspecific antibodies that invalidated most of the findings, but it is still inappropriately cited in some contemporary works (Fonseca *et al*, 2012).

Multiple bioinformatics and biochemical approaches tried to shed light on the two main functional portions of the protein, without ever getting a full picture: the presence of transmembrane domains impairs the application of classical crystallographic approaches. So far, we know that the N-terminal is cytosolic and contains four Sell1-like

repeats (SLRs) for protein-protein interaction, namely with Calmodulin (CaM), H⁺ V-ATPase, SEC24, and possibly others; CaM binding in particular is mediated by the region comprised between Glu90 and Trp186. EF-hand domains are also present, which represent a putative dimerization/multimerization domain, in line with the observation by Western blot that a fraction of Wolframin runs at an apparent molecular weight of exactly four times its predicted one (Yurimoto *et al*, 2009; Gharanei *et al*, 2013; Schäffer *et al*, 2020; Wilf-Yarkoni *et al*, 2021; Wang *et al*, 2021a).

The C-terminal is oriented towards the lumen of the organelle; it has OB fold-containing domains which possibly mediate protein-protein interactions, such as with ATP1B1, a subunit of Na⁺/K⁺-ATPase. The C-terminal also mediates interactions with cargoes for ER export. Six conserved cysteine residues are present, with no clear function but a hypothesized role in intramolecular cross-linking, as seen in other proteins that are implicated in Ca⁺⁺ storage. Residues Asn661 and Asn746, also located in the C-terminal, are subjected to N-glycosylation in the ER, which protects from degradation. Residues 667–700 form the putative degron: they allow interaction with the HECT-type ubiquitin ligase (E3) Smad ubiquitination regulatory factor 1 (SMURF1), destining Wolframin to ubiquitination and proteasomal degradation.

Interestingly, loss of just the last seven residues of the protein is sufficient to induce a severe WS1 phenotype, suggesting that a lot still has to be unpacked to fully understand Wolframin structure (Hofmann *et al*, 2003; Yamaguchi *et al*, 2004; Yurimoto *et al*, 2009; Fonseca *et al*, 2010; Alimadadi *et al*, 2011; Guo *et al*, 2011; Cao & Zhang, 2013; Schäffer *et al*, 2020).

Wolframin production is certainly controlled by ER stress: its expression is decreased in IRE1 α ^{-/-} and PERK^{-/-} cells, and it is induced by ER stressors such as Thapsigargin, a non-competitive inhibitor of calcium-dependent ATPase of sarco-endoplasmic reticulum (SERCA) (Fonseca *et al*, 2005); other stress inducers such as Ionomycin, cyclopiazonic acid, 4-chloro-m-cresol, and Tunicamycin all induce the expression of *WFS1* gene (Ueda *et al*, 2005).

WFS1 promoter is regulated by SP1 and SP3 transcription factors (Ricketts *et al*, 2006), while the 3'-UTR region is regulated by miR-185 in a negative way (Elek *et al*, 2015): in pancreatic β cells, miR-185 promotes insulin biosynthesis and secretion (Lang

et al, 2018). Apart from this information, transcriptional regulation of *WFS1* remains elusive, since none of the postulated transcription factors have an actual binding capability to the promoter: this is the case for XBP1, which positively regulates *WFS1* transcription in an indirect way (Kakiuchi *et al*, 2006).

3.1.2.1. ER stress

Interestingly, a growing body of evidence has linked diabetes insurgence with a deregulated ER stress response, both in the more common T1D and T2D and in rarer forms, such as maturity-onset diabetes of the young (MODY) (Fonseca *et al*, 2009; Lemaire & Schuit, 2012; Morita *et al*, 2017; Nkonge *et al*, 2020; Stone *et al*, 2020).

The best example is given by Wolcott-Rallison Syndrome, a hereditary genetic condition in which the *EIF2AK3* gene, encoding for PERK, is mutated: patients display permanent neonatal DM, skeletal dysplasia, hepatic failure and other variable systemic manifestations (Vattem *et al*, 2004; Delépine *et al*, 2000).

Physiological and pathological stimuli that put pressure on the ER, like misfolded protein accumulation, trigger an innate cellular response aimed at reducing engulfment, slowing down translation, and activating transcription of chaperones. The system that tightly regulates such activity, so that it lasts as little as possible with maximal efficacy, is called unfolded protein response (UPR).

The UPR has three main branches, dependent on PERK, IRE1 α and ATF6 signalling (Urrea *et al*, 2013; Schröder, 2006).

A summary of ER stress-related pathways and UPR is presented in **Figure 4**.

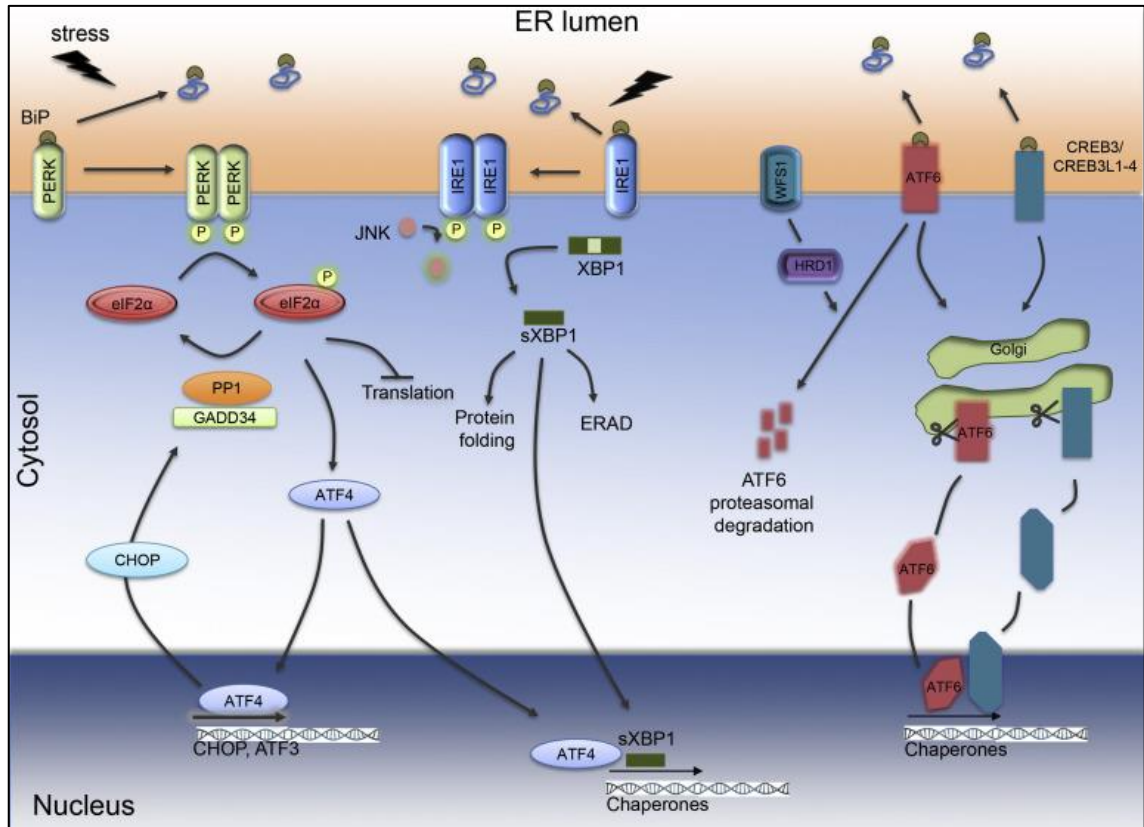


Figure 4. ER stress response and UPR.

Representation of the three main branches of the UPR (*PERK*, *IRE1 α* and *ATF6*), taken from (Cnop *et al*, 2017).

Briefly, the UPR is able to sense the presence of stress-inducing stimuli such as misfolded proteins accumulation, translation overload, reactive oxygen species (ROS) presence through BiP, which inhibits stress signalling in normal conditions; if ER homeostasis is lost, BiP triggers activation of *PERK*, *IRE1 α* and *ATF6*, orchestrating a molecular response to correct the underlying issue (Shen *et al*, 2005; Sitia *et al*, 2019).

PERK activation and dimerization induces *eIF2 α* phosphorylation, which in turn stabilizes *ATF4*. *ATF4* is part of a small selection of mRNAs which are preferentially translated in the cell upon general translation inhibition, keeping the number of new proteins low in order to manage the already existing ones before fully engulfing the ER. *ATF4* is a key transcription factor which triggers the production of novel chaperones and of *GADD34*, that has a negative feedback role on the axis (Harding *et al*, 2000; Yamaguchi *et al*, 2008); downstream and in parallel to *ATF4*, *ATF3* intervenes in glucose metabolism, mediating inflammation and apoptosis (Ku & Cheng, 2020). There is general

consensus around the notion that Wolframin loss alters this pathway, as represented by eIF2 α , ATF4 and GADD34 dysregulation (Shang *et al*, 2014; Maxwell *et al*, 2020).

IRE1 α has to dimerize and trans-phosphorylate in order to be activated: the active form is an endoribonuclease and performs mRNA processing on *XBPI*, producing the *XBPI-s* isoform, which is translated into a transcription factor: this also induces the expression of chaperones and protein degradation components. Moreover, IRE1 α can activate other targets such as JNK, whose phosphorylation mediates cell death (Schröder, 2006). Recently, it was described that IRE1 α deletion in β cells can protect from T1D insurgence, possibly by partial dedifferentiation and subsequent masking from the autoreactive CD8⁺ T cells (Lee *et al*, 2020). It has been reported that in *WFS1*-deficient cells, spliced *XBPI* is increased (Shang *et al*, 2014); however, another paper in a similar model does not confirm this data (Maxwell *et al*, 2020).

ATF6 is also an ER membrane-resident protein, which upon stress detection detaches from the ER and moves to the Golgi via COPII transport; here, it undergoes S1P and S2P cleavage to produce an N-term fraction, which translocates to the nucleus as an active transcription factor. ATF6 binds genomic locations defined ER stress response elements (ERSE), activating the transcription of chaperones on top of multiple Endoplasmic-reticulum-associated protein degradation (ERAD) components, ER resident proteins, Ca⁺⁺ binding factors and more (Adachi *et al*, 2008; Ariyasu *et al*, 2017). Examples include, but are not limited to: *CAT*, *EDEMI*, *HERPUDI*, *HYOUI*, *PDIA4* and *SELIL* (Belmont *et al*, 2008). In the ER, Wolframin stabilizes ERAD-associated E3 ubiquitin-protein ligase (HRD1) interaction with ATF6, directing it for degradation and keeping low the UPR: loss of Wolframin frees ATF6 from HRD1, allowing its translocation from the ER to the Golgi (Fonseca *et al*, 2010; Guo *et al*, 2011).

Among the other proteins connected to UPR, ERO1 α is an oxidase implicated in the correct restoration of the oxidized/reduced balancing of protein isoforms, especially in β cells: it controls ER steady-state disulphide content by oxidation of PDI and production of H₂O₂ as a byproduct, balancing glutathione buffering (Appenzeller-Herzog *et al*, 2010; Wright *et al*, 2013). It has been reported that *Wfs1*-KO INS-1 cells display elevated levels of ERO1 α (Fonseca *et al*, 2005).

PDI is an ER-resident disulphide isomerase whose oxidation state also acts as a switch between activation/repression of PERK and IRE1 α (Kranz *et al*, 2017; Yu *et al*, 2020): similarly to ERO1 α , *Wfs1*-KO retinas of mice had significantly increased levels of PDI protein, consistent with chronic UPR activation in WS1 models (Bonnet Wersinger *et al*, 2014).

Another ER-resident protein acting in quality control and protein folding, with a special regard to glycosylated proteins, is Calnexin. No specific reports on Calnexin expression have been published yet in the context of WS1, but it is known to colocalize with ERIS and could therefore be implicated in the pathogenesis of WS2 (Amr *et al*, 2007; Hetz *et al*, 2011).

Macroscopically, chronic ER stress results in the enlargement of ER cisternae to accommodate the growing load of proteins to be modified and folded: this is clearly visualized via transmission electron microscopy (TEM) (Pavelka & Roth, 2015). Such cellular phenotype has been reported in WS1-affected cells, both in patient-derived material and in mice genetically lacking *Wfs1* (Riggs *et al*, 2005; Akiyama *et al*, 2009; Shang *et al*, 2014; Maxwell *et al*, 2020).

If stress is too strong or prolonged, cells can undergo apoptotic cell death in order to prevent aberrant transformations. This is usually achieved through CHOP, which as a transcription factor upregulates pro-apoptotic factors such as GADD34, ERO1 α and BH3-only proteins (Zinszner *et al*, 1998; Schröder, 2006; Urra *et al*, 2013): in particular, ERO1 α induces ROS and ER Ca⁺⁺ release through IP3R activation (Li *et al*, 2009). Loss of Wolframin is associated with higher *DDIT3* (the gene coding for CHOP protein) expression in a chronic fashion; increased *TXNIP* and *JNK* expression and Caspase 3 activation are also described. This, as we said, results in apoptotic cell death (Fonseca *et al*, 2005; Yamada *et al*, 2006; Shang *et al*, 2014; Abreu *et al*, 2020; Maxwell *et al*, 2020).

To summarize, Wolframin exerts a negative regulation on the UPR and protects cells from ER stress and apoptosis.

3.1.2.2. Ca⁺⁺

Ca⁺⁺ homeostasis is crucial for β cell health and secretory ability. Insulin secretion itself requires a regulated ion flux in order to promptly respond to hormone request and

generate a coordinated secretion within the islet (Sabatini *et al*, 2019; Idevall-Hagren & Tengholm, 2020). Multiple mechanisms probably connect Wolframin function with Ca^{++} homeostasis.

Wolframin is able to induce an increase in Ca^{++} concentration inside the ER, mainly by inducing a faster uptake (Takei *et al*, 2006) and by binding to SERCA, which is kept at stable levels by Wolframin-mediated degradation. Wolframin-deficient cells display altered Ca^{++} fluxes in response to glucose challenge and leaking from the ER, which upregulates SERCA as a compensatory mechanism (Zatyka *et al*, 2015; Abreu *et al*, 2020).

Fibroblasts from WS1 patients display reduced ER Ca^{++} release and cytosolic Ca^{++} after Bradykinin stimulation in the absence of mitochondrial or ATP perturbations, indicating that this is a primary feature of the disease and not a consequence of other molecular mechanisms (La Morgia *et al*, 2020).

Wolframin binds CaM through its N-terminal domain in a Ca^{++} -dependent manner, and mutations in this region abolish the interaction: therefore, Wolframin is implicated in Ca^{++} signal transduction mechanisms (Yurimoto *et al*, 2009). Moreover, ER stress due to Wolframin mutants impairs the ability of IP3R to control and maintain Ca^{++} homeostasis, at least in neurons (Cagalinec *et al*, 2016).

Wolframin loss and subsequent Ca^{++} dysregulation is an activating trigger for Calpain 2, a mediator of ER stress-induced apoptosis in β cells, using the same mechanism seen in T2D (Huang *et al*, 2010; Lu *et al*, 2014).

A single paper postulates the possibility that, according to protein structure prediction and biochemical data, Wolframin is sufficient to induce a Ca^{++} current across a lipid bilayer and, therefore, is a cationic channel by itself (Osman *et al*, 2003).

Some of the Ca^{++} -related functions of Wolframin are reported in **Figure 5**.

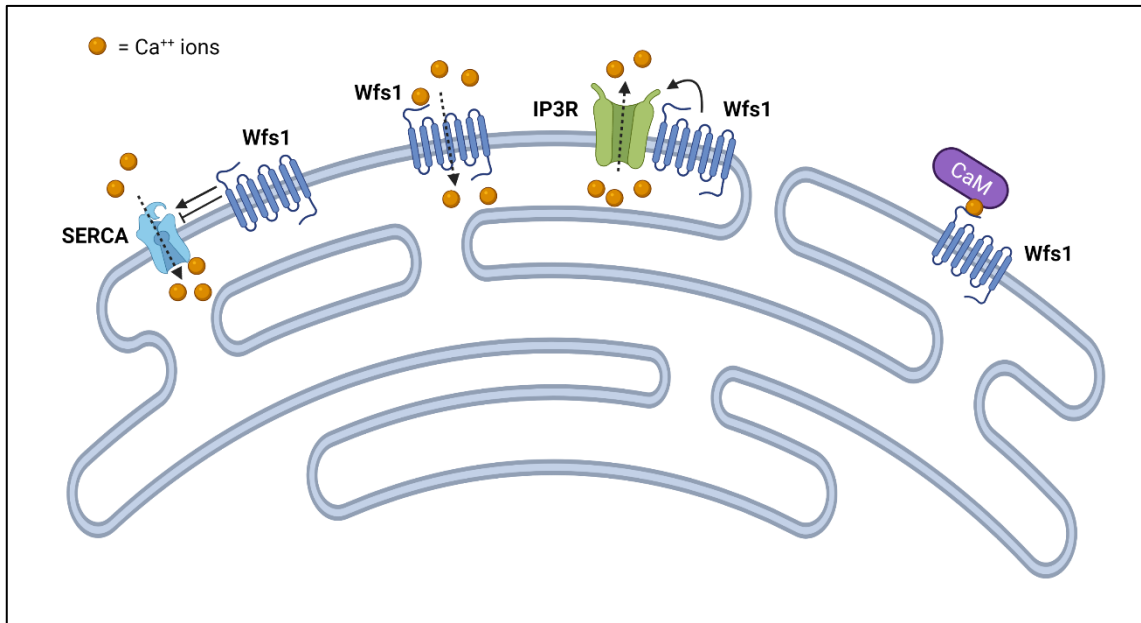


Figure 5. Ca⁺⁺-related roles of Wolfram.

Wolfram is implicated in SERCA regulation, Ca⁺⁺ transportation across the ER membrane, IP3R stabilization and CaM binding.

In summary, Wolfram is able to directly and indirectly promote the correct cycling of Ca⁺⁺ from the cytoplasm to organelles and back, maintaining homeostasis.

3.1.2.3. Mitochondrial alterations

As we discussed before, the striking similarity of WS1 to mitochondrial diseases suggests that these organelles could play a role in pathogenesis. Since the first histological and molecular investigations, gross functional abnormalities in respiratory chain function were excluded (Jackson *et al*, 1994), although other authors report conflicting data (Bunday *et al*, 1992), possibly due to the limited availability of patients and techniques of the time.

Recent reports still face similar challenges in replicability, with some authors finding normal mitochondrial bioenergetics and morphology (Angebault *et al*, 2018; La Morgia *et al*, 2020), and some others reporting the exact opposite (Cagalinec *et al*, 2016). In this instance, the inconsistency is heavily influenced by the considered tissue model: fibroblasts in the first case, which are not affected by WS1, and neurons in the second.

From a mechanistic point of view, coupling of ER and mitochondria is essential for the proper functioning of both neurons and β cells: such tight connection is mediated by MAMs, complex proteic platforms in which linker proteins physically connect the

cytosolic domains of mitochondrial and ER-bound proteins, or directly insert through the phospholipidic bilayer. Such conformation, which has a limited flexibility due to mechanical constraints, allows to keep a precise distance and reciprocal orientation of the organelles. Lipid exchange, Ca^{++} transfer, autophagy, ROS transfer are all dependent on the maintenance of this distance, but organelle shaping also occurs preferentially at ER-mitochondria contact sites.

Specifically, selective Ca^{++} release from the ER to mitochondria is dependent on the IP3R–GRP75–VDAC1 complex formation, so that the total distance for ion transport must be under 100nm, ideally between 10nm and 30nm: therefore, all components have to be concentrated at the ER-mitochondria contact sites for optimal transfer (Rieusset, 2018; Csordás *et al*, 2018).

It is also important to remember that the UPR and MAMs are connected: PERK, but not its kinase activity, is necessary for ER-mitochondria appropriate interaction, while IRE1 α regulates IP3R localization at MAMs and its channel activity, allowing rewiring of energy metabolism in response to ER stress (Delprat *et al*, 2018; Carreras-Sureda *et al*, 2019).

Similarly to ER stress, mitochondrial stress is sensed through organelle-specific factors that regulate mitochondrial chaperones and proteases transcription, for example ATF5. ATF5 is a close homologue of ATF4: it promotes cell proliferation and maintenance of mitochondrial functionality upon stress, mainly acting on basal and maximal respiration rates and overall respiratory capacity (Fiorese *et al*, 2016). ATF5 is crucial in the context of β cell biology because, as a target of PDX1, it cooperates with ATF4 in order to attenuate global translation in response to stress, thus enhancing the survival of β cells to stress-induced apoptosis (Juliana *et al*, 2017).

Going back to the context of WS1, Wolframin impairment in neurons causes a reduced turnover, motility and energy production in mitochondria, mainly mediated by the underlying ER stress and IP3R-dependent Ca^{++} dysregulation: this causes neurodevelopmental delays *in vitro* and reduced survival, similar to what is observed in patients (Cagalinec *et al*, 2016).

Interestingly, loss of Wolframin impairs the proper formation of MAMs without altering mitochondrial structure, limiting mitochondrial Ca^{++} uptake and functionality in patient-derived fibroblasts. Wolframin activity on MAMs is performed through binding of NCS1, an IP3R interactor: in fact, Wolframin controls NCS1 half-life (Angebault *et al*, 2018). This has relevant implications in β cells, considering that NCS1 is found both in the ER and in secretory granules (Gromada *et al*, 2005). The putative role of Wolframin in MAMs is presented in **Figure 6**.

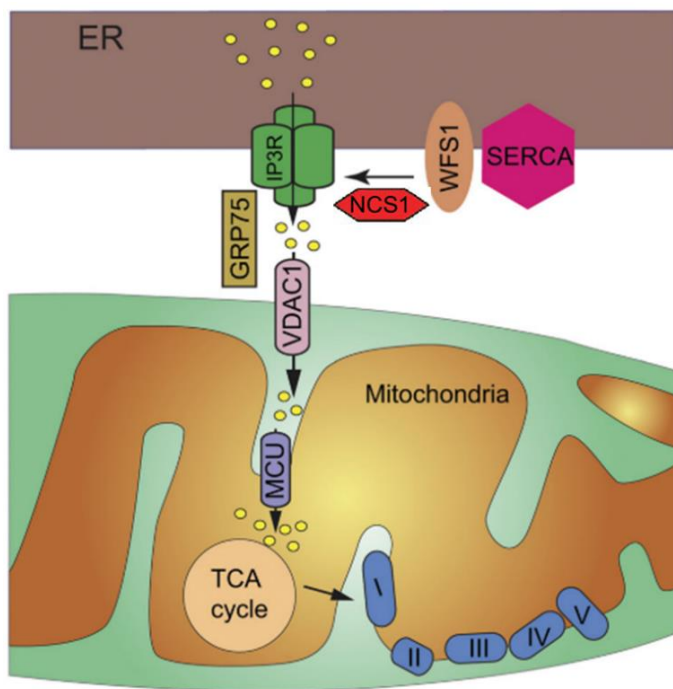


Figure 6. MAMs' connection to Wolframin.
Adapted from (Delprat *et al*, 2018).

Collectively, current knowledge on WS1 molecular mechanisms supports the existence of mitochondrial alterations predominantly in neurons, while the fact that this mechanism is a primary alteration of the condition and not a later consequence of multiple impairments is still debated.

3.1.2.4. Protein trafficking and maturation: Golgi and secretory granules

Insulin granule processing, packaging and secretion is the main task a successful β cell has to perform. Insulin secretion deficiency was described early on in WS1, and it soon became clear that loss of circulating hormone was mainly due to β cell death (Karasik *et al*, 1989); however, the remaining β cells also showed impaired insulin secretion ability,

poorly responding to secretagogues and showing increased susceptibility to apoptosis (Ishihara *et al*, 2004).

As we discussed before, part of Wolframin impact on β cell secretory capacity is due to its interaction with NCS1. NCS1 is important for the sustenance of the readily releasable pool of insulin, which is made of granules directly docked to the plasma membrane. Since Wolframin and NCS1 were shown to bind, it is possible that part of the impaired stimulus-secretion coupling observed in WS1 β cells is due to loss of such interaction (Gromada *et al*, 2005; Angebault *et al*, 2018).

Moreover, a fraction of Wolframin localizes at the secretory granules, at least in β cells and in a neuroblastoma cell line. Interestingly, WS1 β cells show impaired pH adjustment of insulin granules, which suggests a defect in the acidification process necessary for insulin processing. The phenomenon was subsequently linked to the direct interaction of Wolframin with V1A subunit of the H^+ V-ATPase, a proton pump implicated in granule acidification; this is ER stress-independent, as BiP overexpression corrects ER stress but does not recover V1A expression (Hatanaka *et al*, 2011; Gharanei *et al*, 2013).

Proinsulin processing performed by prohormone convertase enzymes, PC1/3 and PC2, is also pH-dependent: as a consequence, it is not surprising that WS1 β cells have normal proinsulin levels, but show a decreased conversion to insulin in the granules and therefore a scarce ability to secrete it. Curiously, PC1/3 levels are also significantly reduced, although the mechanism is not understood: it is possible that Wolframin exerts a role in the correct maturation of the enzyme in the ER (Gharanei *et al*, 2013).

To summarize, Wolframin loss causes impaired insulin secretion by lack of granule maturation in the cell: a simple scheme of insulin secretion impairment in WS1 is presented in **Figure 7**.

In line with the observation that Wolframin protein is found in the ER, but also in secretory granules, it is only logical to speculate that the cellular connection between the two organelles would be the Golgi. However, previous investigations excluded the possibility of a Golgi localization for Wolframin, as seen from fractionation of human primary fibroblasts (Takeda *et al*, 2001). Nevertheless, a more recent report clearly demonstrates that Wolframin, indeed, is implicated in the trafficking of peptides from the

ER to the Golgi cisternae, and several Wolframin missense mutations impair this specific function (Wang *et al*, 2021a).

This builds up on the previous observation that loss of Wolframin results in impaired proinsulin/insulin ratio, due to lack of granule maturation; in INS-1 cells, this is due to lack of proinsulin trafficking to the Golgi, which, as discussed above, is crucial for its proper processing. Therefore, proinsulin levels are conserved, but its localization is altered and it remains stuck in the ER.

Specifically, Wolframin uses its N-terminal domain to interact with the COPII complex, in particular with its subunit SEC24, which is responsible for anterograde vesicle transportation from the ER to the cis-Golgi network (**Figure 7**). The C-terminal side, instead, mediates the recognition of several cargo proteins, such as INS1, NPY, CPE and SCG5. For both domains, known missense mutations were tested and found to impair Wolframin functionality as a cargo receptor, by lack of engagement with COPII complex or with cargoes, respectively.

The authors conclude that since COPII-mediated cargo trafficking block can in turn induce protein accumulation and ER stress, this could be one of the underlying mechanisms for apoptosis in pancreatic β cells of WS1 patients.

Curiously, the same mechanism of anterograde transport disruption is found in another condition due to mutations in the *YIPF5* gene. YIPF5 is a cis-Golgi protein, responsible for the trafficking of vesicles from the ER to the Golgi in mammalian cells (Kranjc *et al*, 2017): its mutations, in humans, underlie a rare form of monogenic neonatal DM with neurological features.

In vitro modelling through *YIPF5*-KO human embryonic stem cell (ESC)-derived β cells and patient-derived induced pluripotent stem cells (iPSCs) differentiated into β cells shows a marked proinsulin accumulation in the ER, causing increased ER stress signaling and reduced insulin content: YIPF5, in fact, interacts with SEC23 and SEC24 to promote COPII-dependent trafficking (De Franco *et al*, 2020).

The similarities between the clinical presentations in the two syndromes suggest that the ER-Golgi trafficking impairment may be a common and crucial feature in pathogenesis, but the differences in timing and severity of affected organs also indicate

that YIPF5 and Wolframin each have unique functions that do not overlap completely and justify a peculiar disease progression.

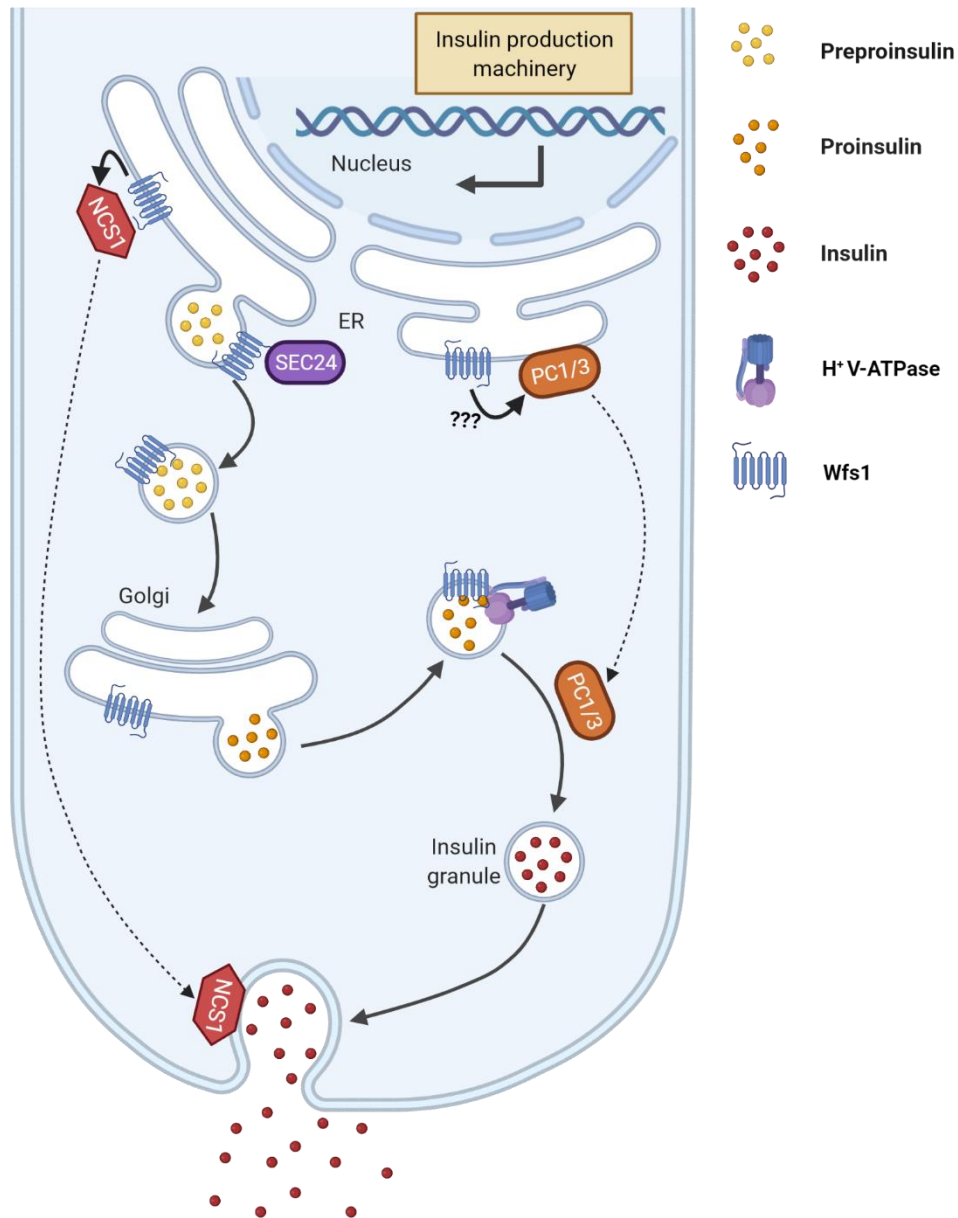


Figure 7. Wolframin role in insulin secretion.

Wolframin controls insulin secretion by exerting its regulatory activity on component of the maturation and secretory machinery: PC1/3, NCS1 and H⁺ V-ATPase.

To conclude this matter, it is interesting to note also that a close relationship exists between ER stress and COPII-dependent anterograde protein transport: on one hand, ER stress inhibits vesicle formation, impairing export from the ER in presence of misfolded

proteins (Amodio *et al*, 2013), while on the other hand activation of COPII machinery promotes the reallocation of said misfolded proteins into discrete compartments of the ER, favoring ubiquitination and subsequent proteasomal degradation (Kakoi *et al*, 2013).

3.1.2.5. Autophagy

Autophagy is a cellular process that mediates the recycling of old and damaged organelles and proteins, allowing the cell to retrieve their basal components and synthesize new ones. Autophagy is fundamental in β cell biology since it is necessary to preserve the structure, mass and function of pancreatic β cells: patients affected by T2D show signs of impaired autophagic flux and this is thought to contribute to the pathogenesis (Yin *et al*, 2012; Pearson *et al*, 2021). Multiple proteins and pathways cooperate in order to perform autophagy, but five main stages can be individuated: induction, nucleation, elongation, fusion to the lysosome and degradation.

Induction of autophagy is regulated by multiple signalling pathways in the cell, that converge in AMPK activation, mTORC1 inhibition, and triggering of ULK1/2 complex. Such complex, when active, induces the large macromolecular Beclin1 complex and the formation of the phagophore, through a process called nucleation. According to most reports, autophagic vesicles stem from the double membrane of the ER to recruit cargos (Rubinsztein *et al*, 2012).

Elongation and closure of the phagophore are mediated by subsequent reactions similar to ubiquitin ligation, performed through the ATG12-ATG5-ATG16L1 complex, mediating LC3-I conversion into the membrane-bound, lipidated form, LC3-II. Fully formed and loaded autophagic vesicles then use cytoskeletal transport to reach the lysosomes and fuse with them through the small GTPase RAB7A and LAMP1/2: at this point, degradation of the cargo is performed in the acidic environment of the lysosomal lumen (Rashid *et al*, 2015; Kocaturk & Gozuacik, 2018).

After complete degradation of the autophagosomes, LC3-II is converted back to LC3-I and recycled, cycling back and forth in the process and allowing to appreciate its dynamism (Mizushima *et al*, 2010). The outline of autophagy steps and players is reported in **Figure 8**.

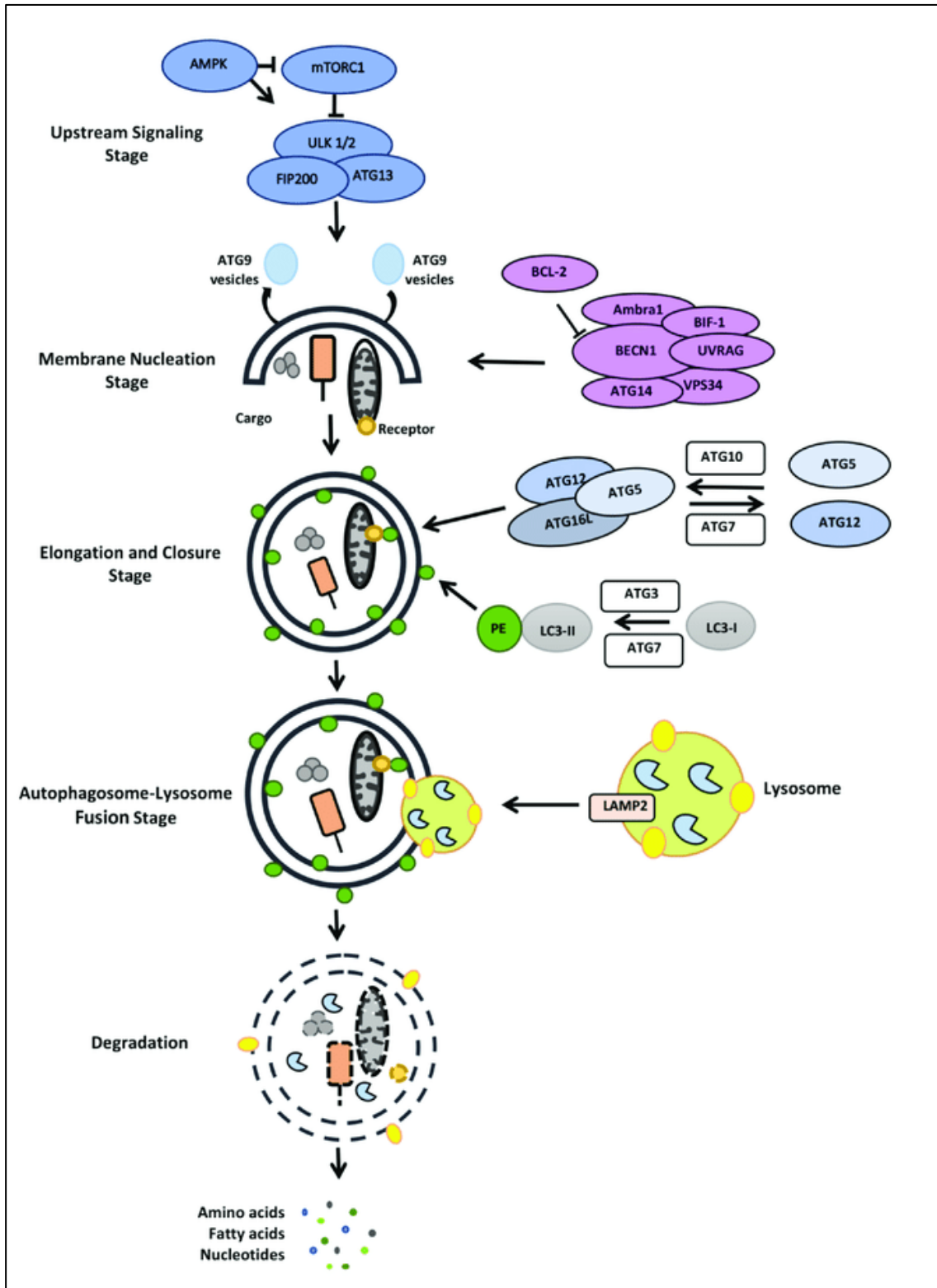


Figure 8. Main stages of autophagy.
Adapted from (Kocaturk & Gozuacik, 2018).

Autophagy is triggered by cellular sensing of material to be removed. In general, the process is not cargo-specific, but recently different kinds of specialized autophagic removal of targets have been reported and their mediators characterized. In yeast and in mammals, studies are ongoing about the understanding of aggrephagy, ER-phagy, mitophagy, glycophyagy, lipophagy, lisophagy, zymophagy, and many more: collectively they are referred to as mechanisms of selective autophagy (Gubas & Dikic, 2021). Recently, PGRMC1 was reported to be the cargo receptor driving ER-phagy of prohormones carrying mutations, for example *Akita* proinsulin (Chen *et al*, 2021).

Autophagy can be triggered in response to ER stress due to accumulated misfolded proteins, since it can exert a cleaning role on intracellular aggregates due to misfolding and on ruined organelles, two hallmarks of stressed cells. Notably, a dynamic interconnection between UPR and autophagy has been reported in literature, making it clear that the two processes can regulate each other. On one hand, all three branches of the UPR can induce transcriptional activation of autophagy-related genes such as *ATG10*, *BECN1*, *ATG12*, *ATG8* and *SQSTM1*, coding for p62 protein; also, BiP is required for stress-induced autophagy (Li *et al*, 2008).

On the other hand, under some conditions, ER stress and its mediators can block autophagic flux at the initiation stage or before fusion with the lysosome. On top of that, dysregulated Ca^{++} concentrations in the cytoplasm are responsible for the missed activation of many cellular processes, including autophagy kinases (Bernales *et al*, 2006; Rashid *et al*, 2015; Song *et al*, 2018).

Moreover, autophagy is tightly interconnected with COPII-dependent protein transport: phosphorylation of SEC24, a COPII complex subunit and Wolframin interactor, regulates autophagosome number during starvation, acting as a switch to promote autophagic flux at the expense of ER-Golgi transport (Davis *et al*, 2016).

Autophagic dysfunction has been linked to WS2, because ERIS interacts with BCL-2 to mediate its inhibitory role on Beclin1 and therefore autophagy, but not on apoptosis induction: in light of the role of ERIS in Ca^{++} homeostasis, it is further clear that ERIS loss impairs the fine tuning of autophagic flux necessary for the cells' wellbeing (Wang *et al*, 2014; Shen *et al*, 2021).

In the context of WS1, one group recently started investigating and publishing about autophagy as a pathogenic mechanism. In 2016, Cagalinec and colleagues showed that inhibition of Wolframin activates autophagy and, conversely, overexpression of Wolframin impairs it, as measured by LC3-II/LC3-I ratio (**Figure 9A-B**). However, this first paper mostly focused on mitochondrial dynamics and Pink1-Parkin-dependent mitophagy, without going into detail in the autophagic flux study (Cagalinec *et al*, 2016).

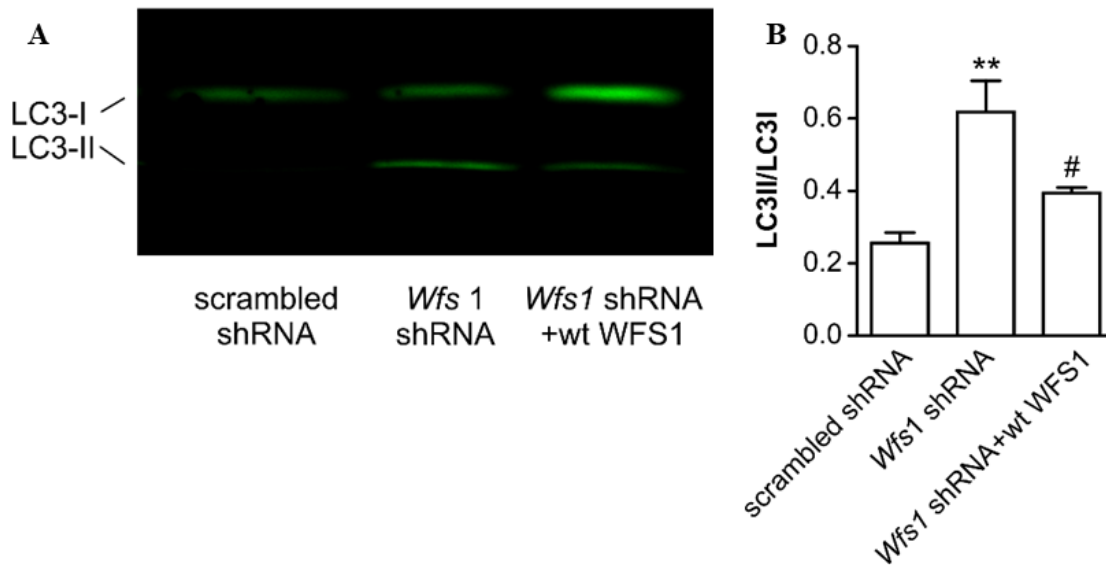


Figure 9. Wolframin connection to autophagy.

PC6 cells transfected with scrambled shRNA or *Wfs1* shRNA or wt *WFS1*, taken from (Cagalinec *et al*, 2016). A) Western blot showing LC3 in the transfected groups. B) Quantification of the experiment in A).

In 2022 the same group followed up with an ulterior study about the involvement of autophagy. They detected increased autophagic flux in *WFS1*-KO fibroblasts, demonstrating that the sigma-1 receptor (S1R) agonist PRE-084 reverts this effect: reduced ER-mitochondrial Ca^{++} transfer in the model causes an impaired energy production and ATP scarcity, which is a trigger for autophagy (Crouzier *et al*, 2022).

Generally speaking, autophagy is not a well-understood pathway in WS1, but its relevance in diabetes pathogenesis and its connections to ER stress make it a very promising topic to be investigated.

3.1.3. *Treatments*

3.1.3.1. *Current gold standard*

WS1 and WS2 are orphan diseases. As such, the current standard of care is focused on alleviating symptoms and trying to guarantee the highest quality of life; however, to this day, WS1 provokes severe manifestations since adolescence and it is lethal at a median age of 30 years (Rigoli & Di Bella, 2012).

A multidisciplinary team is required in order to tackle all the manifestations that may arise in patients, from the most common ones (DM, ocular involvement, deafness, balance, respiratory function) to the rarer ones (urological dysfunctions, psychiatric disorders, developmental delays, speech and others).

DM is managed by insulin injections similar to T1D, although often with a better glycemic control and lower dosage (also because WS patients can keep detectable levels of secreted C-peptide for decades after diagnosis); hearing loss can be corrected by appropriate aids, while no approach to prevent or ameliorate vision loss has proven effective so far. Physical therapy can assist in retaining gross and fine motor skills for a longer time. Brain stem dysfunction is the most risky aspect, as central sleep apnea is the most frequent cause of death in WS1: patients may benefit from assisted ventilation at least during the night.

Given that the autosomal recessive mode of inheritance is the most common, parents of affected kids are obligated carriers; genetic counselling is recommended for siblings, in order to check genetic status and start therapy as soon as possible, if appropriate (Wolfram Syndrome Guideline Development Group, 2014; Tranebjærg *et al*, 2020).

3.1.3.2. *Experimental drugs*

Excellent reviews on prospective drug therapies for WS1 have been collected by other groups (Pallotta *et al*, 2019; Abreu & Urano, 2019; Mishra *et al*, 2021): I will try to expand and update their very complete work.

A summary of all the therapeutic approaches currently being explored for WS1, both drug-based and centered on more cutting-edge technology, is available in **Figure 10**.

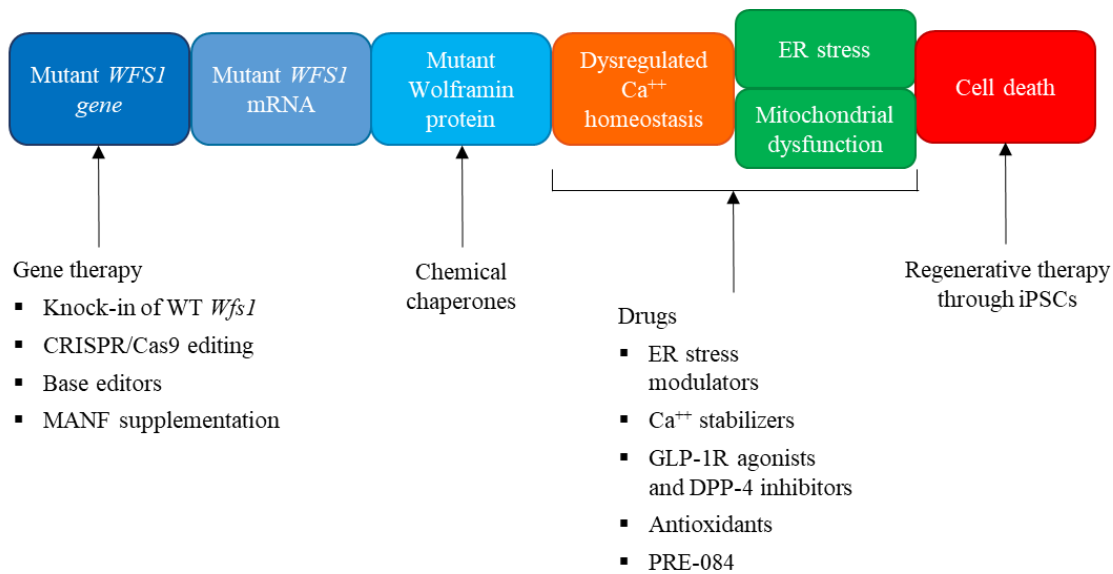


Figure 10. Therapeutic approaches for WS1.

A promising class of drugs currently under investigation is the one of chemical chaperones. Since excessive ER stress is the best characterized cause of WS1 pathogenesis, administration of drugs that can relieve the load of misfolded proteins and thus decrease UPR activation should be beneficial. The best known compounds are 4-Phenylbutyric acid (4-PBA) and Tauroursodeoxycholic acid (TUDCA): both of them protect cells from apoptosis in neurodegenerative, retinal and metabolic disorders. In the context of WS1, 4-PBA showed efficacy also on dominant forms and in iPSC-based models *in vitro* (Shang *et al*, 2014; Batjargal *et al*, 2020). A proprietary formulation of taurursodiol 50 μ M and sodium phenylbutyrate 500 μ M, AMX0035, is commercialized by Amylyx Pharmaceuticals Inc. for the treatment of Amyotrophic Lateral Sclerosis (ALS) (Paganoni *et al*, 2020). In November 2020 the FDA has granted orphan drug designation to AMX0035 for the treatment of WS1, but no clinical experimentation has started yet: the company assumes to get approval for experimentation in WS1 patients in the first half of 2022. An interesting aspect is that AMX0035 also shows beneficial effects on mitochondrial function. Chaperone compounds offer the unique possibility to stabilize Wolfram mutants that retain some protein expression, like in the case of missense mutations, and therefore mitigate the pathology by sustaining at least a partial functionality of residual Wolfram.

Targeting ER stress response is a reasonable approach in order to limit WS1 progression. A well-known compound is mesencephalic astrocyte-derived neurotrophic

factor (MANF), a protein first discovered in the brain and capable of protection from apoptosis both in β cells and in neurons (Hellman *et al*, 2011; Hakonen *et al*, 2018), possibly by acting through BiP-client interaction modulation (Yan *et al*, 2019). MANF also induces proliferation in primary human pancreatic islets: similar results were observed in *Wfs1*^{-/-} mice islets, along with reduction of known proapoptotic ER stress markers such as Chop (Mahadevan *et al*, 2020).

Another neurotrophic factor similar to MANF is brain derived neurotrophic factor (BDNF). The BDNF mimetic 7,8-dihydroxyflavone was tested in the rat model of WS1, where it prevented optic nerve damaging, protected from vision loss, recovered some behavioral parameters and downregulated UPR activation in the brain (Seppa *et al*, 2021).

Another ER stress modulator is Valproate. Valproate is currently employed as a mood stabilizer in bipolar disorder, but it can also induce *WFS1* gene expression by promoter activation. Curiously, the original paper reporting such mechanism ascribes it to the binding with GRP94, a UPR component, but this interaction is only partially demonstrated and should therefore be treated with caution (Kakiuchi *et al*, 2009). Nonetheless, cells transfected with dominant negative Wolframin mutants benefit from Valproate treatment *in vitro* (Batjargal *et al*, 2020), and data collected in ALS models indicate a positive effect on autophagy which could contribute to the effectiveness (Wang *et al*, 2015). A very recent paper reports beneficial effects *in vitro* in WS-derived iPSCs differentiated into neurons: the authors observe that patient-derived cells display altered elongation and branching of axons, and they associate defective axonal pathfinding during development to the generalized brain atrophy seen in magnetic resonance imaging (MRI) of patients (Hershey *et al*, 2012; Lugar *et al*, 2019; Samara *et al*, 2019, 2020). Multiple clinical trials for Valproate are ongoing, for example the AUDIOWOLF study directed by professor Barrett from University of Birmingham, expected to end in 2022 and repurposed for a new round of patients until 2025 (NCT03717909 and NCT04940572, respectively).

Another molecule known to modulate ER stress and proven effective in the *ob/ob* mouse model is Azoramide (Fu *et al*, 2015): testing it in the context of WS1 would be interesting, especially since it recently demonstrated neuroprotective ability in an iPSC-based model of dopaminergic neurons affected by Parkinson disease (Ke *et al*, 2020).

In the context of increased ROS production and impaired mitochondrial function, which has been reported at least in some models of WS1, the use of antioxidants could improve cellular metabolism and protect from apoptosis. Idebenone is a coenzyme Q derivative that was tested in a single patient affected by WS1, providing some visual recovery (Bababegy *et al*, 2012).

Ca⁺⁺ dysregulation is a hallmark of WS1 molecular pathogenesis, and as such many experimental approaches try to target this mechanism. Currently, the most advanced compound is Dantrolene, a drug already prescribed for malignant hyperthermia and muscle spasticity, since it suppresses ion leakage from the ER to the cytoplasm by blocking ryanodine receptor RyR2, preventing Calpain activation. It was reported effective in an *in vitro* screening and shown to protect from apoptosis both β cell and neuronal models of WS1 (Lu *et al*, 2014): the promising preclinical data prompted a clinical trial in 2016 (NCT02829268), whose results were recently published. Out of the nineteen patients who completed the study, only a portion seemed to benefit from the drug and no statistically significant differences in β cell function, visual acuity or disease severity could be measured, although at the 6-month follow-up the drug was well tolerated (Abreu *et al*, 2021).

The same *in vitro* study cited above identified more compounds which protected a β cell model from Thapsigargin-induced cell death by acting on Ca⁺⁺, and these were: PARP inhibitor, NS398, Pioglitazone, Calpain inhibitor III, Docosahexaenoic acid, Rapamycin, and Glucagon-like peptide-1 (GLP-1). However, no further experiments to validate the screening were performed in this context, apart from the ones on Dantrolene (Lu *et al*, 2014).

A different study from the same group investigates the role of Pioglitazone and Rapamycin on a β cell model of ER stress: they act by enhancing SERCA expression levels and suppressing IP3R signalling, respectively. Both drugs can reduce the number of Ca⁺⁺-depleted and apoptotic cells in response to Thapsigargin, but they still do not mediate a complete recovery of the phenotype (Hara *et al*, 2014).

JTV-519 is also, like Dantrolene, a stabilizer of ryanodine receptor RyR2, which is postulated to be dysfunctional in WS1 and cause Ca⁺⁺ leak from the ER. The compound

is currently being tested *in vitro*, *in vivo* and a future phase 1b clinical trial is under preparation (Loncke *et al*, 2021).

A way to amplify glucose-stimulated insulin secretion through IP3R activation and Ca⁺⁺ flux induction is to act on the other receptors present on β cell surface: the M3 muscarinic receptor has a relevant role in β cell function and its agonist Carbachol increased insulin secretion in a WS1 mouse model (Toots *et al*, 2019). Alternatively, the S1R has been proposed as an effective target both *in vitro* and *in vivo*: its agonist, PRE-084, acts on IP3R favoring the transit of Ca⁺⁺ from the ER to the mitochondria, improving cellular energetics and alleviating in turn behavioral symptoms of WS1 in animal models (Crouzier *et al*, 2022).

Ca⁺⁺ antagonists Verapamil and Diltiazem were found effective in an unbiased *in vitro* screening performed in a shWFS1 cell line, reducing Caspase 3/7 activation (Henderson *et al*, 2021); this paper also reports convincing results using Bromocriptine in the same cell model, although the authors exclude that the beneficial effects could be mediated by its canonical dopamine receptor 2: the mechanism is Ca⁺⁺-related, but remains elusive.

Another recent paper investigated the inhibition of Calpain as a tool to protect WS1 cells from apoptosis, and they correlate the use of Calpain inhibitor XI and Ibudilast with improved Ca⁺⁺ handling, insulin secretion and survival in WFS1-KO cells (Nguyen *et al*, 2020). The mechanism of action is reported in **Figure 11**.

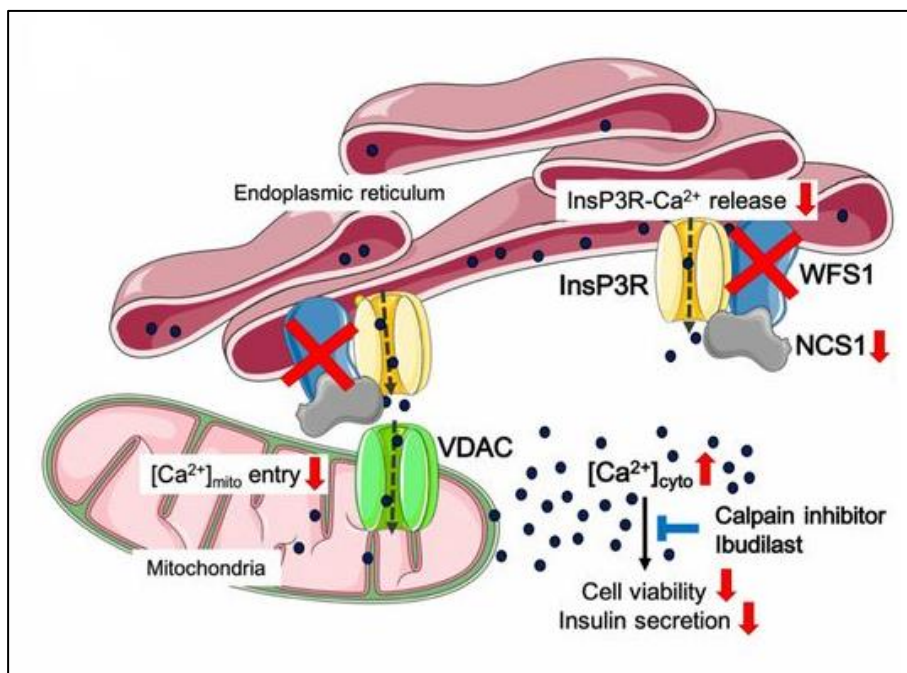


Figure 11. Mechanism of action for Ibutilast and Calpain inhibitor in WS1 β cells.

Taken from (Nguyen *et al.*, 2020).

GLP-1 receptor (GLP-1R) agonists are a class of drugs very commonly used for T2D: notably, they can both ameliorate diabetic control and lower the risk of long term complications such as cardiovascular events, as assessed in very large cohorts of patients (González-González *et al.*, 2021). In 2019 Liraglutide, possibly the most used GLP-1R agonist, was approved for use in the pediatric age for the co-treatment of T2D (Tamborlane *et al.*, 2019); multiple subtypes of MODY also benefit from co-treatments with Liraglutide (Deiss *et al.*, 2011; Docena *et al.*, 2014; Urakami *et al.*, 2015; Terakawa *et al.*, 2020).

The GLP-1R pathway is physiologically activated by GLP-1, secreted by enteroendocrine L-cells in the gut to potentiate glucose-dependent insulin release; in the long term, it triggers the cAMP responsive element binding (CREB) signalling, which promotes survival, stimulates proliferation, protects against Ca^{++} depletion and ER stress, and regulates autophagy (Rowlands *et al.*, 2018). A complete depiction of the pathways controlled by GLP-1R activation is presented in **Figure 12**.

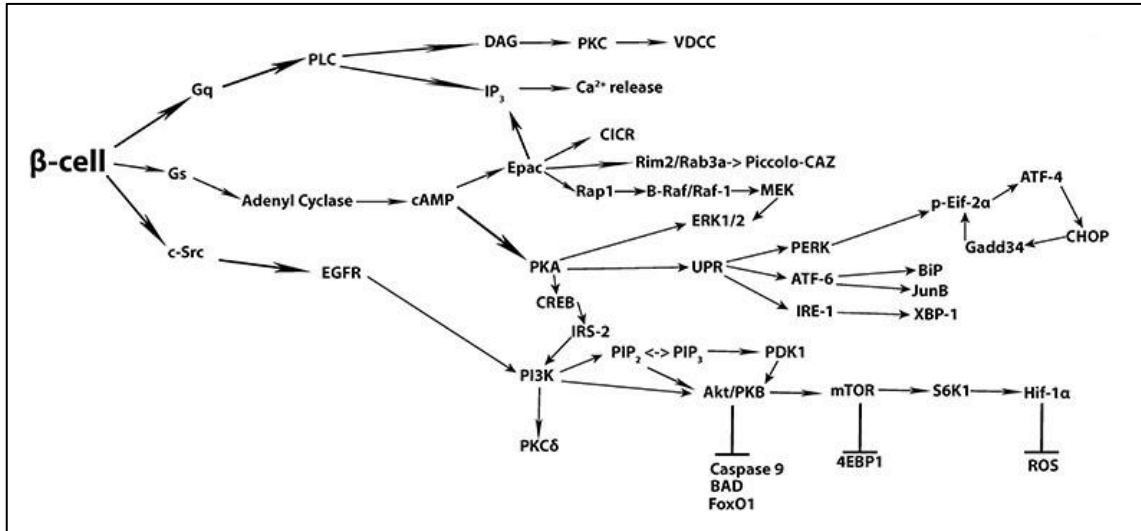


Figure 12. Signalling downstream the activation of GLP-1R axis in β cells.
Adapted from (Rowlands *et al*, 2018).

While synthetic GLP-1R agonists like Liraglutide and Exenatide are designed to last in the bloodstream and exert an almost chronic effect, endogenous GLP-1 has a short half-life in the circulation, since it is rapidly degraded by the dipeptidyl peptidase-4 (DPP-4) enzyme. Chemical inhibitors of DPP-4, like Sitagliptin, Vildagliptin and Linagliptin, raise the circulating levels of endogenous incretins: Vildagliptin showed promising results in the *Wfs1*^{-/-} mouse model, both with a single administration and after long term use (Tanji *et al*, 2015). Linagliptin was administered to two sisters affected by WS1 and carrying the same mutations, with variable benefit: this was probably due to the differences in clinical presentation and age at therapy beginning (Tarcin *et al*, 2021).

Given the very broad spectrum of mechanisms on which the GLP-1 axis acts that also overlap with known dysfunctions in WS1, it is not surprising that a considerable amount of papers came out, testing various agonists on WS1 models.

Exenatide was the first GLP-1R agonist to show promising effect in glycaemia lowering in the WS1 mouse model (Sedman *et al*, 2016), followed by studies performed with Liraglutide in both rats and mice with WS1. Interestingly, the ability of Liraglutide to cross the brain-blood barrier conferred a protective effect not only on β cells, but also in neurons: β cell function is improved, neuronal degeneration is slowed down, but most importantly both cell types are more protected by early intervention, treating as early as before the onset of symptoms (Toots *et al*, 2018; Kondo *et al*, 2018; Seppa *et al*, 2019,

2021). The most recent publication from Plaas group reports important beneficial effects of a lifelong administration of the drug in their WS1 rat model: early Liraglutide treatment delayed the onset of diabetes and protected against vision loss and optic nerve atrophy, but it was not effective on sensorineural hearing loss (Jagomäe *et al*, 2021).

Notably, Liraglutide also exerted a neuroprotective effect in a mouse model of Parkinson disease, whose pathogenic mechanism of neurodegeneration has been postulated to share similarities with the ones seen in WS1 (Zhang *et al*, 2020; Lin *et al*, 2021): the results were so convincing that this prompted the initiation of a clinical trial, justifying the high expectations about the possible neurological benefit (NCT02953665).

Likewise, the preclinical data from WS1 models prompted the initiation of pilot trials of GLP-1R agonists on patients: a single WS2 patient treated with Exenatide for 9 weeks in 2016 (Danielpur *et al*, 2016), a 25-year-old Japanese woman who received Liraglutide for 24 weeks (Kondo *et al*, 2018), and a report on a patient with autosomal dominant WS1 who received weekly subcutaneous administration of Dulaglutide for six weeks (Scully & Wolfsdorf, 2021). All of these studies, however, followed only a single patients for a limited amount of time and did not manage to reach any definitive conclusion due to intrinsic limitations, more than lack of efficacy of the drugs.

In this context, our group recently published, to our knowledge, the clinical trial with the most patients and the longest follow up in the field of GLP-1R agonists in WS1 (Frontino *et al*, 2021): notably, both examination of DM-related parameters and neurological evaluation were performed. Four pediatric patients affected by WS1 were treated daily with Liraglutide for up to 27 months, with variable results. One patient showed improved glycometabolic parameters, while the other three remained stable in the observed timeframe; visual impairment did not show the rapid decline that is frequently encountered in WS1 patients, although no improvements could be seen. Concerning neuroradiologic findings, all patients remained stable up until the latest follow-up. A graph showing clinical characteristics of the four patients and the progression of C-peptide area under the curve (AUC) during treatment is presented in **Figure 13**.

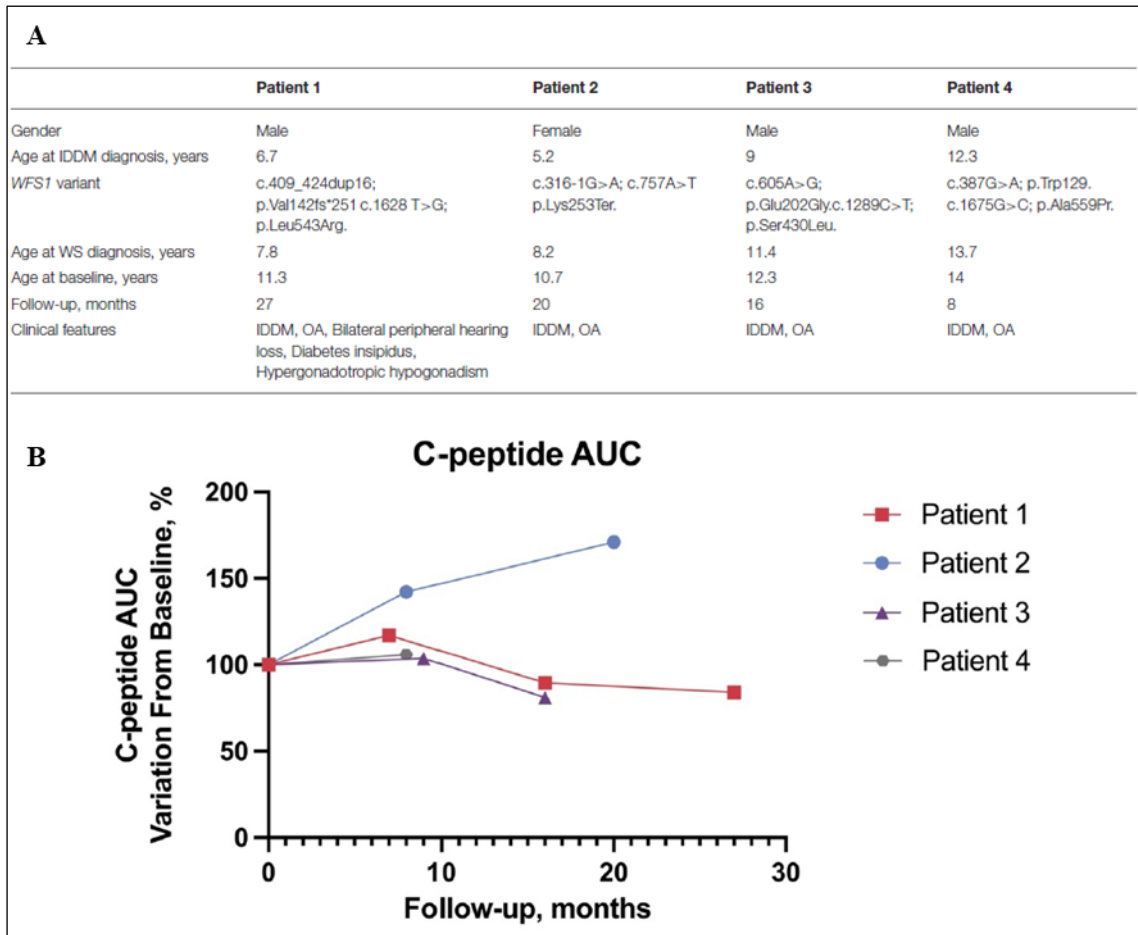


Figure 13. Results from the clinical trial of Liraglutide in pediatric WS1 patients (Frontino et al., 2021).

A) Clinical attributes of patients at trial recruitment. IDDM=insulin-dependent diabetes mellitus. B) Variation from baseline of C-peptide AUC in the four patients.

3.1.3.3. Advanced therapies: gene and cell therapy

In spite of the great effort in developing pharmacological therapies, it is likely that no drug will be able to completely stop disease progression, let alone recover the cell loss that is virtually always present at diagnosis. To actually tackle the necessities of patients and develop a cure for WS1, gene and cell therapy are being investigated.

Gene therapy is particularly attractive to approach neurons, since physically replacing them is almost impossible due to loss of synaptic connections and accessibility. In particular, gene therapy with adeno-associated viruses (AAVs) targeting retinal ganglion cells (RGCs) has made considerable progress in recent years in other forms of OA, like Leber congenital amaurosis and LHON (Bainbridge et al, 2015; Newman et al, 2021): this is mainly due to the fact that the eye is an immune privileged compartment, eliciting

no vector-related toxic immune responses, and the retina in particular can be targeted via direct intravitreal injection (Boye *et al*, 2013).

RGCs are the most affected cell type in the WS1 eye, making them the ideal model for gene therapy; the AAV2-CMV-WFS1 vector has been shown to efficiently target RGCs in a WS1 mouse model, restoring the expression of *WFS1* gene and improving visual function (Hamel *et al*, 2017); other studies are ongoing in Vania Broccoli's lab at Ospedale San Raffaele (personal communication).

Moreover, the increasing availability of CRISPR/Cas9 technology could assist in precise correction of existing mutations directly in patients, although *in vivo* applications are still far from clinically available (Abreu & Urano, 2019); nevertheless, CRISPR/Cas9-mediated correction of patient derived cells has been implemented as a disease modelling tool (Maxwell *et al*, 2020). An ulterior development of gene editing is constituted by base editors, a technique which allows precise single base correction without the introduction of double strand breaks and decreasing off targets; a proof of concept for the use of base editors *in vitro* in WS1 has recently been published (Nami *et al*, 2021).

Another application for gene therapy is the possibility to deliver pro-survival molecules through viral vectors: the promising results seen in MANF-treated *in vitro* and *in vivo* models prompted to develop AAV vectors encoding for MANF to be employed in WS1 patients, but no clinical experimentation has been launched so far (Mahadevan *et al*, 2020).

Once target tissues are too far gone to be modulated by drugs or corrected by gene therapy, the remaining option is to replace them with new ones. Regenerative medicine has made steady progress in the last years, improving transplantation rates by means of surgical techniques, immunosuppressive regimens, and expanding potential sources for cells and organs.

Cadaveric pancreatic islet transplantation is nowadays applied to T1D patients exhibiting difficult-to-control blood glucose levels, in order to obtain normoglycemia and prevent the development of long term complications (Ontario Health Quality, 2015). WS1 patients could benefit from the same procedure, but the lack of organ donors and the fact that islet transplantation is not a lifelong achievement severely limit this application; in

fact, slow graft revascularization and immune rejection impair the ability of transplanted cells to engraft indefinitely, meaning that islet transplantation does not provide permanent insulin independence (Bourgeois *et al*, 2021). Moreover, nervous tissues, which are severely affected in the condition, are mostly not suitable for transplantation.

Nevertheless, at least regarding WS1-induced DM, a regenerative approach could be beneficial to patients. To this aim, looking for new cell sources from which to obtain transplantable material is a considerable task: in recent years, iPSCs have paved the way in this sense.

In order to better understand implications, advantages and drawbacks of iPSC technology, a brief excursus presenting them is needed.

3.2. iPSCs

3.2.1. *Origin and development*

The proof of concept that adult, specialized cells still retained the potential to go back in time and become undifferentiated, pluripotent ones dates back to the 1950s (Gurdon *et al*, 1958). However, while information concerning how cells became differentiated grew with time, little was still known about the mechanisms that could trigger the inverse process.

In 1981, two groups independently published the establishment of a culture protocol for inner cell mass-derived cells of the mouse, which were deemed ESCs (Evans & Kaufman, 1981; Martin, 1981); later on, in 1998, the same result was obtained with human cells (Thomson *et al*, 1998). The discovery allowed to perform unprecedented progress in understanding the early phases of development and the actual concept of self-renewal and pluripotency, which had been poorly studied and understood up until then; however, ESCs quickly encountered difficulties in their diffusion due to ethical and safety concerns. In fact, ESCs have to be derived from early embryos, which poses moral issues in many countries including Italy, where their derivation is prohibited by the 40/2004 law; on the other hand, the extreme differentiation potential of such cells caused doubts concerning the risk of developing teratomas if not properly handled.

Between 2006 and 2007, Yamanaka's group published for the first time a protocol for the reprogramming of murine and human fibroblasts into undifferentiated, primitive cells,

which were called iPSCs, using just four factors: OCT3/4, SOX2, c-MYC, and KLF4 (Takahashi & Yamanaka, 2006; Takahashi *et al*, 2007). The same technique worked in reprogramming virtually any differentiated cell type, with increasing efficiency and progressively less genomic manipulation: the first protocols included retrovirus-mediated transfection, while non integrating Sendai virus-based approaches are currently the most common (Ban *et al*, 2011).

Very soon, since pancreatic development had been extensively studied and the master genes regulating organogenesis were known, many groups started publishing protocols of differentiation to produce β cells and the other endocrine subtypes starting from ESCs and iPSCs (D'Amour *et al*, 2006; Zhang *et al*, 2009).

In spite of the very low yield and purity achieved by the first protocols, progressive adjustments managed to improve both parameters: nowadays, gold standard protocols of differentiation reach up to 70% C-peptide⁺ cells, most of which are non-polyhormonal, mature β cells, exhibiting the proper first and second phase of secretion in response to glucose (Nair *et al*, 2019; Velazco-Cruz *et al*, 2019; Hoglebe *et al*, 2020, 2021; Balboa *et al*, 2022).

Briefly, iPSCs reach the stage of definitive endoderm, followed by specification into primitive gut tube. From there, cells acquire a pancreatic phenotype, differentiating into pancreatic progenitors; a subsequent commitment to the endocrine lineage defines the subset of cells that will originate the islets of Langerhans, from which insulin producing cells are then derived, at first as polyhormonal cells, and after appropriate maturation stages as *bona fide* β cells. The entire process takes around three weeks to be completed, plus several optional weeks for ulterior acquisition of the mature phenotype.

Regardless of the specific approach, pancreatic differentiation aims to recapitulate ontogenesis in a dish: a prospect of the passages is presented in **Figure 14**.

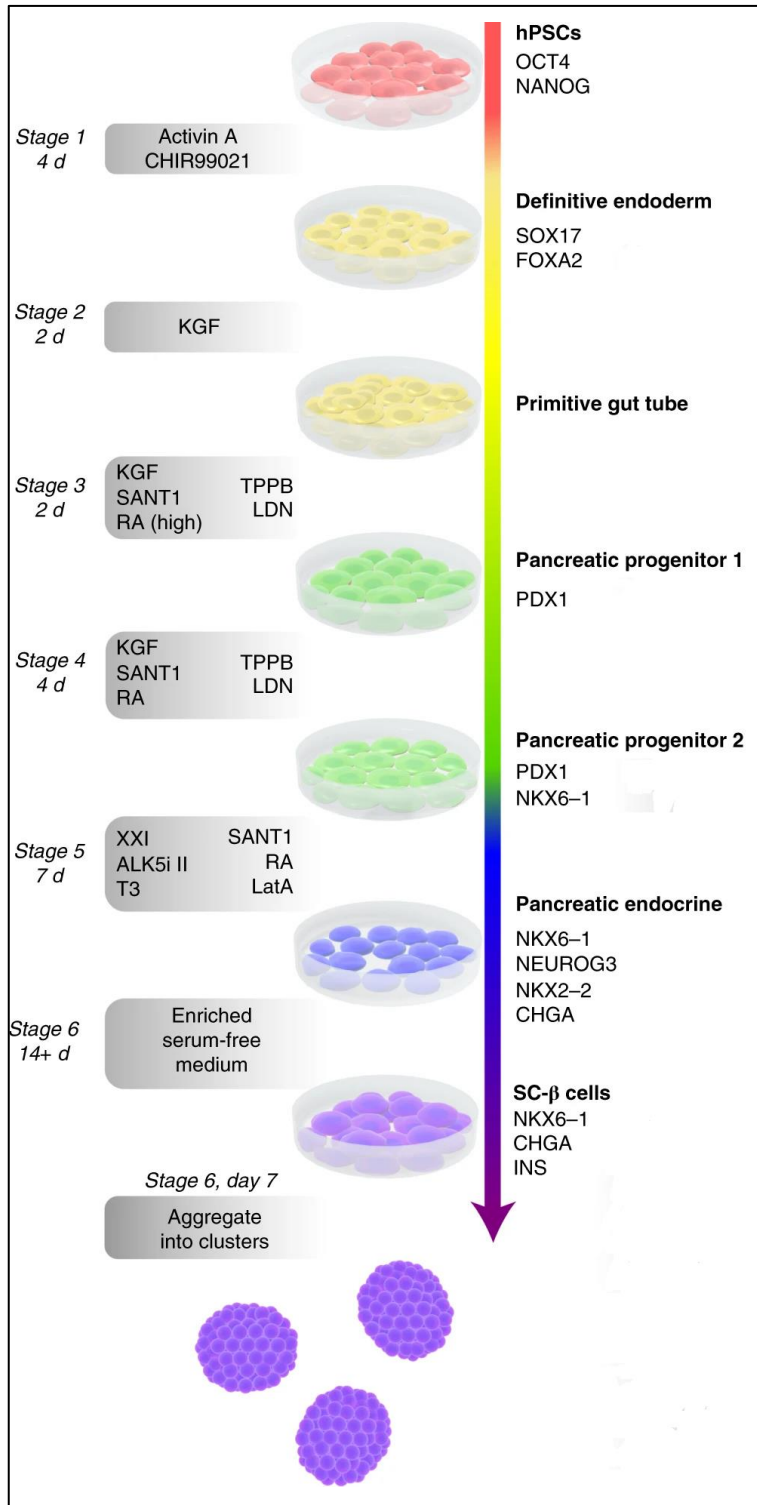


Figure 14. Steps of pancreatic differentiation in vitro.
 Adapted with permission from Springer (Hogrebe et al, 2021).

As we discussed before, iPSCs can be derived from any cell type. Moreover, they can also be derived by a theoretically infinite number of individuals: differently from ESCs,

which are amplified from a selected number of donors and are mostly commercial cell lines, iPSCs with the desired genotype can be produced. For example, stem cells from all Human leukocyte antigen (HLA) haplotypes can be derived, or from people with complex polygenic traits (such as in T2D), or from patients who carry a specific genetic disease and, among those, patients carrying a specific mutation. The possibilities, as it is clear at this point, are endless. For this reason, iPSCs technology has risen as a disease modelling tool.

3.2.2. *Disease modelling*

Disease modelling aims to develop easy systems in which pathological mechanisms can be recapitulated, dissected, understood, and hopefully corrected. Patient-derived iPSCs can aid in this task by allowing to produce platforms characterized by a precise disease-associated genetic background and unlimited growth potential.

Engineered cell lines mutated for relevant genes implicated in differentiation have been studied to elucidate the molecular pathways guiding pancreatic development: this allowed to understand the exact temporal and sequential activation of lineage determinants such as PDX1, ARX, NEUROG3 and many more (Zhu *et al*, 2016).

iPSC lines have been derived from multiple diseases manifesting with diabetes: at least ten from WS1 (Lu *et al*, 2014; Maxwell *et al*, 2020; Grzela *et al*, 2020; Pourtoy-Brasselet *et al*, 2021; Hoglebe *et al*, 2021), one from WS2 (La Spada *et al*, 2018), different lines from most MODY subtypes (Pellegrini *et al*, 2021; Cardenas-Diaz & Cardenas, 2018; more reviewed in Skoczek *et al*, 2021 and Heller *et al*, 2021), genetically diverse cases of permanent neonatal diabetes, T1D and T2D (Balboa *et al*, 2019; Maxwell & Millman, 2021); the list is quickly expanding.

Especially for monogenic forms of diabetes, such as WS and MODY, the opportunity to model pathogenesis *in vitro* is a useful tool in order to understand general mechanisms that can be applied to the more common forms, T1D and T2D, which are less efficiently modelled due to the complex immune and environmental involvement, respectively.

Concerning WS1, Shang and colleagues and Maxwell and colleagues (Shang *et al*, 2014; Maxwell *et al*, 2020) report the most complete analysis of iPSC-derived β cell modelling, and I will briefly describe their most significant findings, as seen in **Table 2**.

	Shang <i>et al</i>, 2014	Maxwell <i>et al</i>, 2020																												
<u>Mutations</u>	1 patient missense/frameshift, 1 patient frameshift/frameshift, 2 patients missense/nonsense	2 patients missense/nonsense, 1 patient frameshift/nonsense																												
<u>Wolframin protein?</u>	Not determined	Yes, half than control iPSCs, does not increase at beta cell stage																												
<u>Controls</u>	2 healthy, 1 carrier, HUES42 cells	Corrected isogenic line																												
<u>Differentiation protocol</u>	<p>Adhesion protocol</p> <table border="1"> <thead> <tr> <th>Stage</th> <th>Day</th> <th>Basic Medium</th> <th>Supplement</th> </tr> </thead> <tbody> <tr> <td>Stage 1: Definitive Endoderm</td> <td>1</td> <td>RPMI</td> <td>Activin A (100 ng/ml) Wnt3A (25 ng/ml) 75 uM EGTA</td> </tr> <tr> <td>Stage 2: Primitive Gut Tube</td> <td>2-3</td> <td>RPMI</td> <td>Activin A (100 ng/ml), 0.2% FBS</td> </tr> <tr> <td>Stage 2: Primitive Gut Tube</td> <td>4-5</td> <td>RPMI</td> <td>FGF10 (50 ng/ml), KAAD-cyclopamine (0.25 uM) 2% FBS</td> </tr> <tr> <td>Stage 3: Posterior Foregut</td> <td>6-8</td> <td>DMEM</td> <td>FGF10 (50 ng/ml), KAAD-cyclopamine (0.25 uM) Retinoic acid (2 uM) LDN-193189 (250 nM) B27</td> </tr> <tr> <td>Stage 4: Pancreatic Endoderm</td> <td>9-12</td> <td>CMRL</td> <td>Exendin-4 (50 ng/ml) SB431542 (2uM) B27</td> </tr> <tr> <td>Stage 5: Endocrine</td> <td>13+</td> <td>CMRL</td> <td>B27</td> </tr> </tbody> </table>	Stage	Day	Basic Medium	Supplement	Stage 1: Definitive Endoderm	1	RPMI	Activin A (100 ng/ml) Wnt3A (25 ng/ml) 75 uM EGTA	Stage 2: Primitive Gut Tube	2-3	RPMI	Activin A (100 ng/ml), 0.2% FBS	Stage 2: Primitive Gut Tube	4-5	RPMI	FGF10 (50 ng/ml), KAAD-cyclopamine (0.25 uM) 2% FBS	Stage 3: Posterior Foregut	6-8	DMEM	FGF10 (50 ng/ml), KAAD-cyclopamine (0.25 uM) Retinoic acid (2 uM) LDN-193189 (250 nM) B27	Stage 4: Pancreatic Endoderm	9-12	CMRL	Exendin-4 (50 ng/ml) SB431542 (2uM) B27	Stage 5: Endocrine	13+	CMRL	B27	<p>Cytoskeletal modulation in adhesion (suspension protocol doesn't work)</p>
Stage	Day	Basic Medium	Supplement																											
Stage 1: Definitive Endoderm	1	RPMI	Activin A (100 ng/ml) Wnt3A (25 ng/ml) 75 uM EGTA																											
Stage 2: Primitive Gut Tube	2-3	RPMI	Activin A (100 ng/ml), 0.2% FBS																											
Stage 2: Primitive Gut Tube	4-5	RPMI	FGF10 (50 ng/ml), KAAD-cyclopamine (0.25 uM) 2% FBS																											
Stage 3: Posterior Foregut	6-8	DMEM	FGF10 (50 ng/ml), KAAD-cyclopamine (0.25 uM) Retinoic acid (2 uM) LDN-193189 (250 nM) B27																											
Stage 4: Pancreatic Endoderm	9-12	CMRL	Exendin-4 (50 ng/ml) SB431542 (2uM) B27																											
Stage 5: Endocrine	13+	CMRL	B27																											
<u>Differentiation efficiency</u>	20% C-peptide ⁺ , same as controls	22% C-peptide ⁺ versus 50% in corrected ones																												
<u>Gene expression in differentiation</u>	Not determined	Single Cell Transcriptomics: low % of fully endocrine cells, lots of off target beginning at Stage2 (neural progenitors, acinar, unknown...)																												
<u>ER stress</u>	Increased in fibroblasts, iPSCs and differentiated cells; enlarged ER only after TG	Increased, by single cell transcriptomics; swollen ER																												
<u>Mitochondria</u>	Not determined	Altered OCR, fragmented mitochondria																												
<u>Insulin secretion</u>	Less insulin content and # of granules, normal proinsulin/insulin ratio	Basically no response to high glucose, high proinsulin/insulin ratio, low insulin content																												
<u>Stressors</u>	Differential sensitivity of mutant cells to TG and TM in basically all parameters considered	TG makes WT cells lose glucose response and increases ER stress, while WS1 cells are apparently unaffected in secretion and less affected in ER stress induction																												
<u>Other</u>	No increased cell death																													
<u>In vivo</u>	Lower fold of secretion after glucose challenge in mice, loss of 50% C-peptide production a month after transplantation	Very low insulin production; no reversal of diabetes in mice, while corrected cells revert diabetes																												

Table 2. Comparison of the two main papers reporting iPSC-derived WS1 β cells, Shang et al, 2014 and Maxwell et al, 2020.

Both works highlight an altered UPR in the model, as we already discussed. Regardless of the specific gene analyzed, it is clear that at the basal level, Wolframin loss or alterations are sufficient to drive ER stress even in the absence of external stimuli: the situation is only worsened by application of stressors such as Thapsigargin (TG) and Tunicamycin (TM), which heighten differences with controls. Therefore, iPSC-based systems are apt for ER stress studies.

Functionality *in vitro* and *in vivo* is also impaired: mutant differentiated cells have an altered insulin content and display poor secretory ability, also after transplantation in mice. Hence, functional studies can be performed in the WS1 iPSC model.

Interestingly, while some findings are in common, some others differ profoundly between the two works.

First of all, while Shang and colleagues report no impairment in differentiation capacity, Maxwell and colleagues report a halved percentage of C-peptide⁺ cells compared to the genetically corrected counterpart. The difference could be due to genetic heterogeneity, but considering that both papers study more than one patient with several kinds of mutations it is unlikely that this is the only underlying reason.

If we consider differentiation methodology, instead, Maxwell and colleagues use a more advanced combination of small molecules in adhesion, which allows the authors to obtain a high percentage of mature β cells at the end of differentiation. Such an aggressive approach could very well operate a stronger selection on fully committed cells, while Shang and colleagues might be producing less mature cells and therefore less dependent on Wolframin upregulation, which, as shown in the paper itself, is increased and possibly critical at the very end stage of differentiation. This is in line with the observation that WS1 is not a developmental disease and it is rarely manifest in the neonatal period and early infancy, suggesting that most mutations require time and/or additional stresses to become clinically manifest.

Another indication for this hypothesis is the fact that Maxwell and colleagues state they were not able to apply their newest differentiation protocol in suspension to WS1-derived cells, while it is well characterized and efficient in wild type cells (Velazco-Cruz

et al, 2019). In this context, differentiation technique could be the discriminant between manifestation and latency of the disease at the cell level, in the absence of further stimuli. Therefore, we can conclude that caution is needed when comparing iPSC lines with different genetics or differentiation protocols.

Overall, iPSCs are a valuable tool to recapitulate some crucial aspects of WS1 pathogenesis, and as such they raise the possibility to use them not only for passive modelling, but also for developing new therapeutic strategies.

3.2.3. *Therapeutic potential*

Human islet transplantation gave the proof of concept that diabetes can be effectively cured, given the right conditions. As soon as ESC and iPSC technology proved to be able to produce *bona fide* β cells, it could have been speculated that the search for a definitive cell source was concluded.

In fact, both cell types have been extensively studied and characterized for their ability to produce glucose-responsive, insulin-secreting cells, and the newest protocols improved the quality to a point where engraftment *in vivo* in mouse models was reached (Agulnick *et al*, 2015; Haller *et al*, 2019). In particular, the best stage to be transplanted was demonstrated to be the pancreatic progenitor stage, since *in vitro* maturation protocols are still not as effective as having cells undergo *in vivo* glycemic fluctuations to “train” them (Brusko *et al*, 2021).

However, most studies were conducted in nude mice, where the immune system is abolished, limiting xenograft rejection but also alloimmunity and autoimmunity.

Both T1D and T2D patients face the common backlash of transplants that is imperfect histocompatibility: especially with ESCs, the idea would be to develop a single or, at best, a few well-characterized cell lines to be used on all patients, but of course this does not take into account HLA variability in the population. iPSCs can theoretically be derived from each individual for personalized medicine, but rationally it would take an insurmountable amount of time and money to develop that many cell lines according to Good Manufacturing Practice (GMP).

Moreover, patients with T1D display autoimmune attack against the β cells, which is the cause of DM insurgence: the mere substitution of dead cells with new ones is to no

avail if autoreactive T cells are still present in the body, as it has been demonstrated, in some cases, for up to decades after diagnosis (Keenan *et al*, 2010; Coppieters *et al*, 2012; Pugliese, 2017).

Stem cell transplantation faces the serious challenge of having to perform immune escape. This can be achieved through three main roads: immunosuppression, encapsulation, or gene engineering.

Immunosuppressive regimens taken from the experience in human islet transplantation could be employed, although they are one of the most relevant pitfalls in the procedure (Shapiro *et al*, 2016; Vantyghem *et al*, 2019). Lifelong immunosuppression can severely impair the quality of life for patients, especially if we think that for WS1 patients this is not the only clinical manifestation to treat, and DM insurgence is even earlier than in T1D.

Encapsulation describes the procedure of hiding the cells to be transplanted in a scaffold with the aim to ease engraftment, give mechanic support, make them retrievable for any quality control or possible side effect, but most importantly to shield them from the immune system. Encapsulation devices made up of different materials have been produced in multiple works *in vivo* in animal models, obtaining encouraging results (Agulnick *et al*, 2015; Haller *et al*, 2019; Wang *et al*, 2021c).

The promising preclinical data prompted the launch of clinical trials starting in 2014 by the ViaCyte company (NCT02239354 and NCT04678557), subcutaneously implanting pouches containing ESCs differentiated into pancreatic progenitors. The first device, VC-01, was designed to protect the cells inside from immune attacks, allowing at the same time hormones, oxygen and nutrients to freely flow in and out of it by diffusion: encouraging preliminary results have been published recently, paving the way for further experimentation (Ramzy *et al*, 2021; Shapiro *et al*, 2021).

Notwithstanding the positive outcomes obtained in the first transplanted patients, a second trial following a different procedure was begun in 2017 (NCT03162926). This time, ViaCyte employed its VC-02 device, an open one in which the host would directly vascularize the implant to improve nutrient availability and graft survival; of course, this

protocol requires systemic immunosuppression in combination with the transplantation procedure.

The co-existence of both approaches (full encapsulation and encapsulation plus immunosuppressants) operated by the same company highlights how complicated it is to define the perfect strategy in order to tackle immune escape: on one hand, closed devices perfectly handle the job, but suffer from progressive fibrotic deposition that limits the graft survival in time; on the other hand, open devices still get caught up in the old need for systemic immunosuppression. Currently, the indication for VC-02 is to enroll patients with a severe presentation of T1D, including hypoglycemia unawareness or significant glycemic lability; meanwhile, VC-01 has a broader indication for all T1D patients who are eligible for the transplantation procedure.

The most employed cell sources for transplantation in ongoing clinical trials or in clinical routine are presented in **Figure 15**.

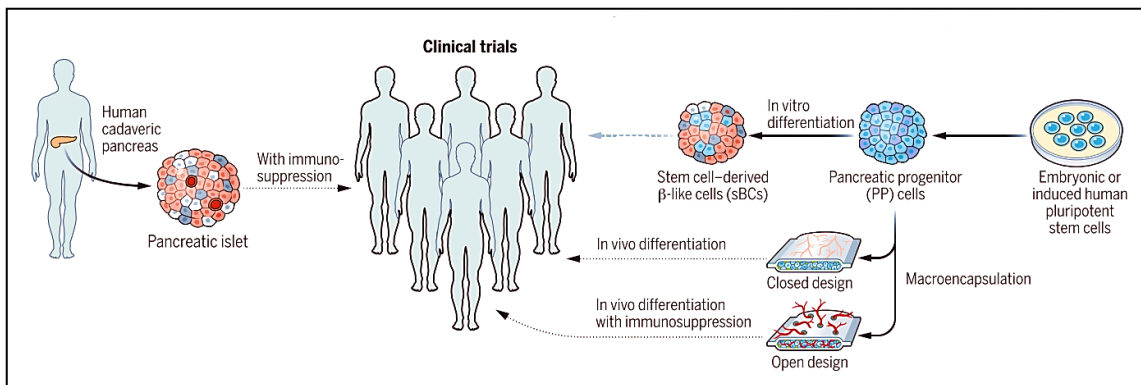


Figure 15. Main current approaches in regenerative medicine for diabetes. Adapted from (Brusko *et al*, 2021). Reprinted with permission from AAAS.

In parallel with systemically suppressing immune cells and isolating the graft so that it does not come in close contact with them, the third option is to engineer the transplanted cells as to make them invisible. A similar technique could be beneficial to all kinds of stem cell-based transplantation procedures, not only for β cells: therefore, multiple groups aimed at generating a universally transplantable ESC or iPSC line, which could be then differentiated into any cell type.

In HLA-mismatched transplantation, major histocompatibility complex (MHC) class I is recognized as non-self by T cells and therefore triggers graft rejection by the host.

Due to the highly polymorphic nature of HLA haplotypes, total transplant compatibility is extremely difficult to achieve and this limits the large scale applicability of stem cell-based methods. Abolishment of MHC class I expression by knock-out of its supporting Beta-2 Microglobulin (B2M) molecule renders cells invisible to T cells, but triggers a natural killer (NK) response from missing-self recognition (Riolobos *et al*, 2013).

A pioneering work by Russell's group in 2017 demonstrated that concomitant abolishment of endogenous MHC class I and knock-in of the tolerogenic HLA-E single-chain trimer (fused to B2M and a peptide antigen) is effective in both avoiding T cell recognition and inhibiting NK cell response, *in vitro* and *in vivo* (Gornalusse *et al*, 2017): the mechanism is presented in **Figure 16**.

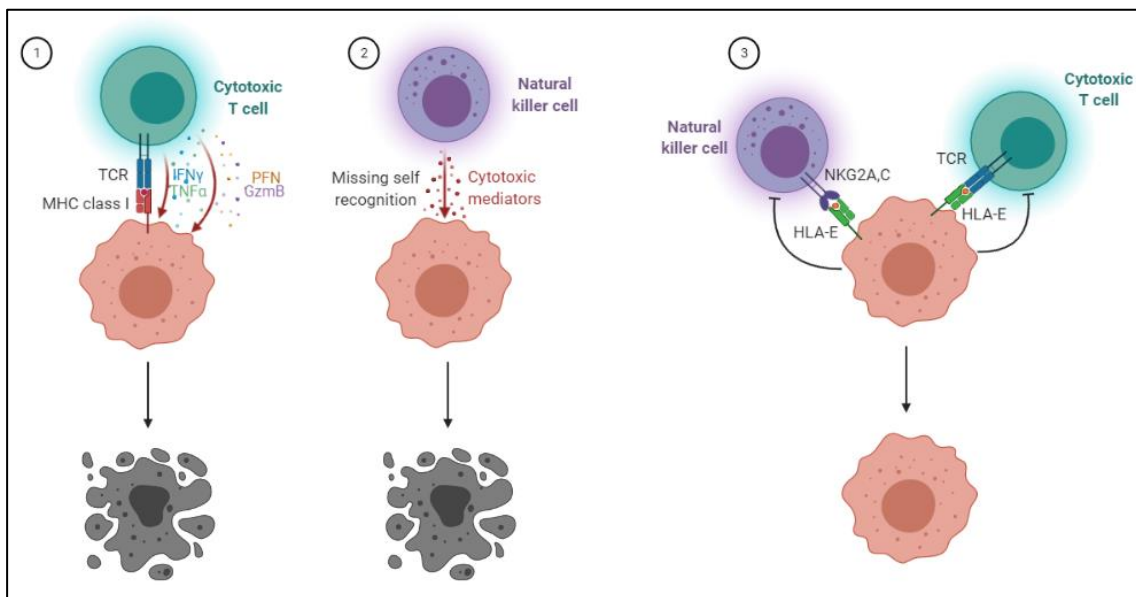


Figure 16. Mechanism of T and NK cell recognition of mismatched HLA and escape of $B2M^{-/-}$, HLA-E expressing cells from immune rejection.

Following this proof of concept, other non-polymorphic MHC class I molecules such as HLA-G were evaluated as a prospective tool for tolerance induction. Other approaches include the knock-in of other tolerogenic molecules like PD-L1 and CD47, which are known to suppress NK-mediated lysis (Flahou *et al*, 2021).

Our lab recently established an iPSC line genetically modified to lack the expression of two NK ligands with activating roles, B7H3 and CD155. The triple knock-out line, $B2M^{-/-}B7H3^{-/-}CD155^{-/-}$, can escape immune attack from both $CD8^{+}$ T cells and NK cells,

both *in vitro* and *in vivo*, at the iPSC stage and after differentiation into pancreatic progenitors and insulin-secreting β cells (Chimienti *et al*, under revision).

Also ViaCyte has been exploring the possibility to employ an immune-evasive version of their signature PEC-01 cell line, which they have employed in all of their devices so far; in 2018 they established a partnership with CRISPR Therapeutics in order to develop the new cell line, VCTX210. A phase 1/2 clinical trial in patients has been approved in 2021 in Canada and is expected to start treating patients soon. Such combination of open device and hypoinmunogenic cells is of great interest, as it could both bypass the need for immunosuppression and improve graft vascularization and durability.

3.3. Patient clinical characterization

To conclude this introduction, I will present the clinical characterization of the patient around whom my thesis will revolve. Curiously, our patient has been reported in literature three separate times by three different groups, including ours: I will try to sum up all the findings and report the clinical case as completely as possible.

The patient had an unremarkable medical history up until 5 years of age, when she was diagnosed with T1D at Ospedale San Raffaele. Further testing highlighted the absence of known autoantibodies, which, combined with the early age at onset and very initial signs of OA, prompted for referral to a geneticist and screening for a panel of monogenic diabetes-related genes: at age 8, two compound heterozygous mutations in the *WFS1* gene were confirmed by next generation sequencing (NGS), c.316-1G>A and c.757A>T. None of them had ever been reported in literature. Family investigations confirmed that indeed the patient inherited the c.316-1G>A mutation from the father, and c.757A>T from the mother; her younger brother has inherited healthy alleles from both parents. Family history includes T2D in her grandfather and T1D in a second cousin, but all relatives were otherwise healthy. No family history of visual loss or other *WFS1*-related symptoms were reported, nor consanguinity.

In 2018, off-label treatment protocol with Liraglutide was approved by The Regional Network Coordination Center for Rare Diseases and Pharmacological Research IRCCS Mario Negri, and at age 10 she started taking the drug up to 1.8mg/die; her current follow up is of three years of treatment, with no recorded significant adverse events, and a report is seen in the paper from Frontino and colleagues (Frontino *et al*, 2021).

Generally speaking, she exhibits a mostly mild presentation for the disease: at age 13, following Liraglutide treatment, her residual C-peptide secretion has increased to 170% compared to the baseline, while retinal nerve fiber layer thickness and optic nerve thickness have remained stable. Very initial signs of intracranial and intraorbital optic nerve atrophy are seen, although this does not impair vision: best corrected visual acuity remained stable at zero (expressed as LogMAR), which indicates standard vision. She is not colorblind. Mild brainstem/pontine atrophy is present.

Following WS1 diagnosis, the patient was referred to a specialist for copper and other metals status evaluation. No information about metal metabolism has ever been reported in WS1, but it is known that in T1D high copper concentrations can be found in patients. Unexpectedly, our patient displayed low levels of circulating copper and ceruloplasmin, suggesting an unrelated, genetic reason for this alteration. Further investigations showed that this is not a common finding in other WS1 cases, but our patient was found to carry a novel heterozygous mutation in the *ATP7B* gene (c.1870-3A>G), a copper-transporting ATPase. The mother of the proband is a compound heterozygote for two variants: c.98T>C and c.1870-3A>G.

ATP7B gene mutations cause Wilson disease, a disorder of copper metabolism which usually presents with hepatic failure, neurological features, psychiatric symptoms and the characteristic Kayser Fleischer corneal rings (Rodriguez-Castro *et al*, 2015). Curiously, neither the proband nor her mother presented any of those symptoms apart from altered copper and ceruloplasmin serum levels, and therefore are asymptomatic Wilson patients. The patient underwent three months of omega-3 fatty acids and eicosapentaenoic acid supplementation, which led to normalization of all parameters.

Our patient also manifested low Ca⁺⁺ serum levels, according to literature and molecular knowledge for WS1 patients, and very high levels of Vanadium of uncertain significance, like her mother. All of the reported findings on metal metabolism in our patient have been published (Squitti *et al*, 2019).

The third paper covering our patient is very recent (Panfili *et al*, 2021). The authors investigate the novel mutations directly in peripheral blood mononuclear cells (PBMCs) of the proband, finding no expression of the c.316-1G>A mutation-carrying allele, but only from the one with c.757A>T. No protein production is seen. PBMCs from the patient

do not display basal ER stress, but they are more responsive to ER stress induction than controls, although this specific cell type is not known to be affected by WS1.

Interestingly, patient-derived PBMCs secrete high levels of TNF α , IL1 β and IL6: such inflammatory profile is not due to DM *per se*, since the specific upregulated cytokines are different than in T1D.

The authors conclude that the presence of WS1 mutations induces perturbations in adaptive immunity, causing what they define “proinflammatory hypercytokinemia”. Of note, inflammatory statuses in chronic diseases are frequently associated with unbalanced T cell subtype repartition. Actually, the patient’s PBMCs have lower levels of *FOXP3* and higher levels of *ROR γ t* transcripts, which are markers of regulatory Treg cells and proinflammatory Th17 ones, respectively; the data indicate that a Th17/Treg ratio imbalance is present due to increased apoptosis of Tregs.

The strongest point in this paper is that the authors are the first ones to report an involvement of the immune compartment in WS1; however, this is also the greatest limitation, as performing their analysis in a single patient characterized by a unique clinical and genetic presentation hinders to draw conclusions about WS1 in general.

Collectively, the novelty of the mutations, the mild clinical phenotype observed, and the availability of tools to perform a deeper study on the molecular mechanisms underlying WS1 in the patient of interest drove us to follow through with the present study.

4. Aim of the work

In this project, we aimed at generating iPSCs from a WS1 patient carrying novel mutations in the *WFS1* gene, in order to elucidate the mechanisms underlying the onset of DM from a molecular point of view. iPSCs represent a powerful mean for the modelling of genetic diseases, in light of their relative ease of derivation and differentiation capacity.

Starting from this tool, we followed three main questions that guided all the project:

- 1) What are the phenotypic and functional effects of the patient's mutations on differentiated β cells?
- 2) Which molecular mechanisms drive or are part of WS1 pathogenesis, specifically concerning our patient?
- 3) What are the transcriptional and translational effects of the aforementioned mutations, and can they be corrected genetically?

Concerning the work on β cells, we took advantage of a well-established differentiation protocol available in our lab, which allowed us to obtain good proportions of iPSC-derived β cells. In this model, we managed to study β cell-specific functions, such as Ca^{++} signalling and insulin secretion. Moreover, we investigated the potential beneficial effects of a drug, Liraglutide, on β cell phenotype.

Among the molecular mechanisms underlying WS1 pathogenesis, we dug into literature and opted to focus onto two main aspects: ER stress response and autophagy. While the first one is a well-known process in the condition, autophagy role had not been clarified yet and therefore constituted a novel piece of the puzzle for WS1. We decided to employ both targeted techniques, looking at single genes and proteins, and to perform a more in-depth screening through Single Cell Transcriptomics.

Last, but not least, we performed an in-depth characterization of the transcripts resulting from the patient's mutations, especially from the 316-1 A>T allele, since no accurate predictions could be made bioinformatically. Subsequently, we studied the ulterior effect on protein production. We also supposed that gaining knowledge on the biological meaning of the mutations would give us a helpful insight into how to correct them and recover a normal phenotype.

Collectively, all three branches of the project were expected to cooperate in gaining original insights into WS1 pathogenesis, and possibly offering novel therapeutic strategies.

The graphical representation of the aims for this project can be seen in **Figure 17**.

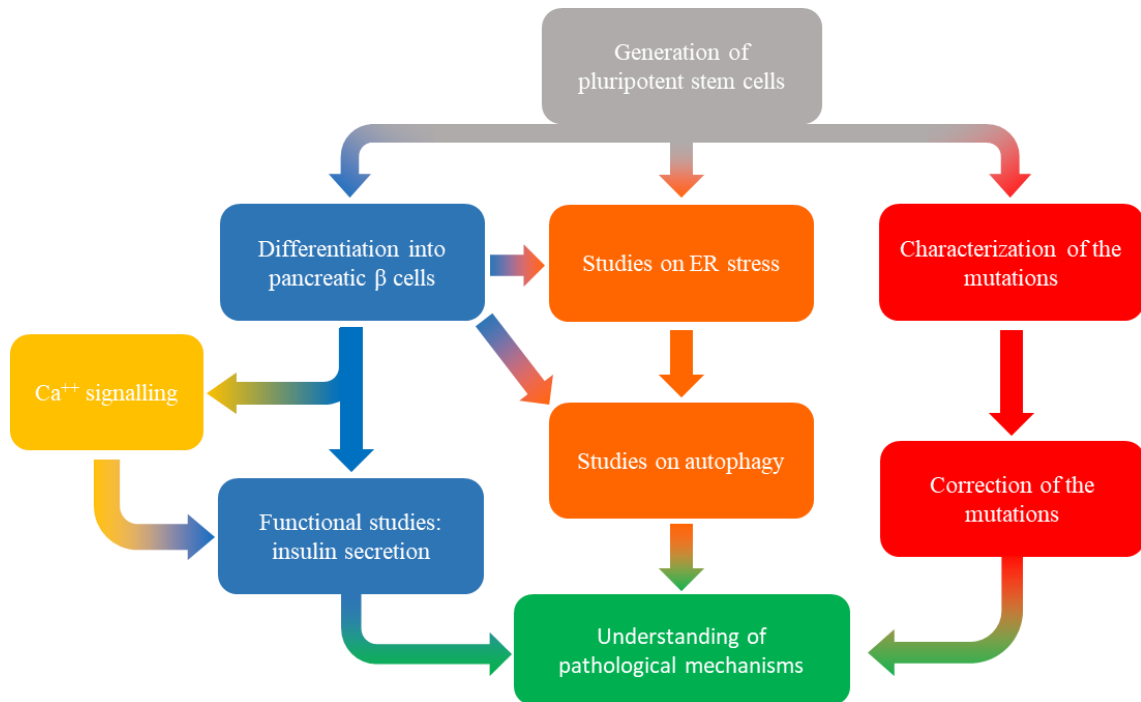


Figure 17. Graphical aims of the project.

5. Results

5.1. Generation and stabilization of WS1-derived iPSCs

The first step of the project consisted in the derivation of iPSCs from the WS1 patient, starting from PBMCs isolated during a routine blood draw, as described in the corresponding **Methods and Materials** section.

We managed to obtain eight stable clones of iPSCs from the patient, with typical stem cell morphology since early passages (**Figure 18A**) and confirmed normal karyotype (**Figure 18B**).

To test for pluripotency, we employed three different techniques: immunofluorescence, fluorescence-activated cell sorter (FACS), and real time-quantitative polymerase chain reaction (RT-qPCR). The three methods confirmed that all the considered clones were correctly pluripotent by means of their gene and protein expression (**Figure 18C-E**).

In conclusion, we efficiently derived multiple clones of iPSCs from the WS1 patient of interest, all of which had normal morphology, karyotype and pluripotency, allowing their use for further experiments. From now on, this cell line will be referred to as “Wfs1 iPSCs” and its derivatives will be named accordingly.

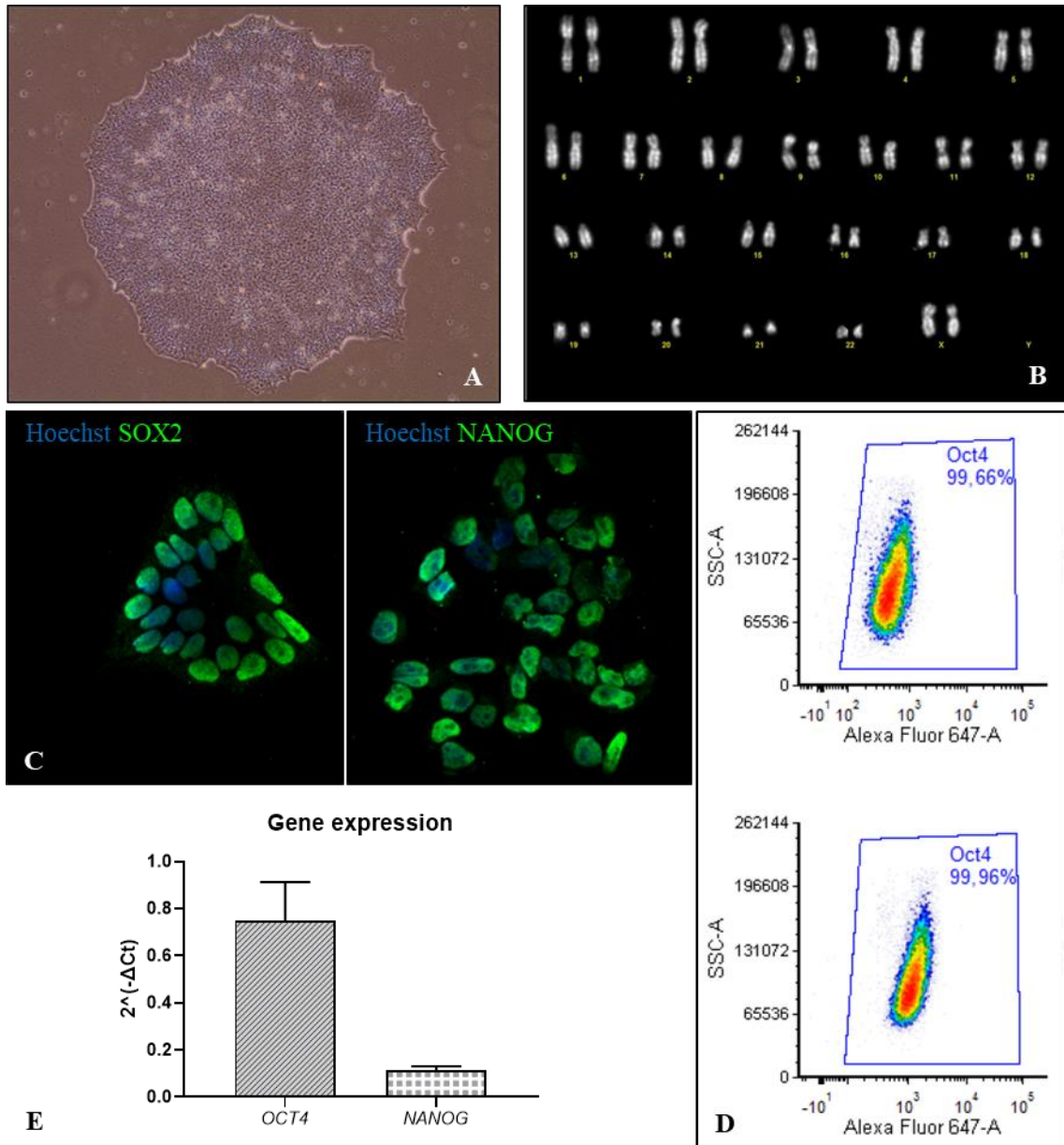


Figure 18. Characterization of iPSCs newly generated from reprogramming of a WSI patient.

A) Bright-field image of an iPSC colony after stabilization; 10x zoom. B) Example of a normal karyotype from a clone of iPSCs after reprogramming. C) Immunofluorescence for the pluripotency markers SOX2 and NANOG, showing complete positivity of the cell population; nuclei were counterstained with Hoechst. 20x zoom. D) Example of two FACS plots from Wfs1 iPSCs, showing almost complete positivity for the pluripotency marker OCT4; SSC=side scatter. E) RT-qPCR analysis showing expression of the pluripotency genes OCT4 and NANOG in Wfs1 iPSCs; Mean±SEM, N=7.

5.2. Genetic characterization of the patient's mutations

From the geneticist's report, we knew that two mutations were present in the *WFS1* gene: c.316-1G>A and c.757A>T, respectively inherited from the father and from the mother. However, we could not draw conclusions about the downstream effects of such mutations on mRNA or protein conservation. In **Figure 19**, a visual representation of the mutations with respect to the whole gene and protein is reported: as seen in the second panel, both mutated sites fall in the N-terminal domain at a very early position.

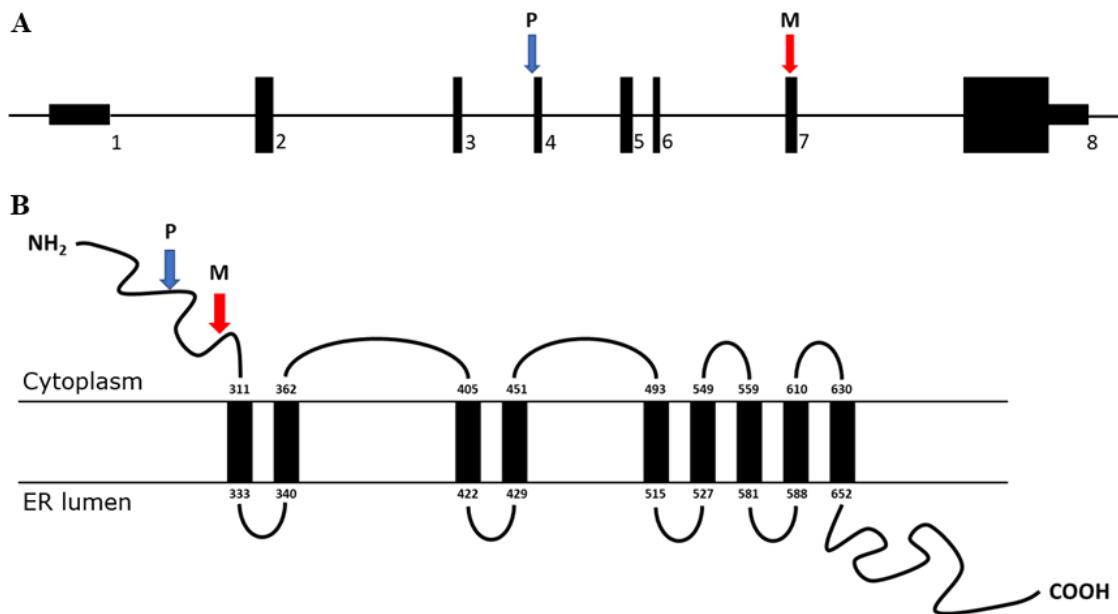


Figure 19. Localization of the patient's mutations.

A) Localization of the mutations in the *WFS1* gene; the numbers indicate the eight exons. B) Localization of the mutations on a simplified depiction of Wolframin putative structure; the numbers indicate the aminoacid that delimits functional domains. P = paternally inherited, M = maternally inherited.

Concerning the c.757A>T, bioinformatics prediction estimated the introduction of a premature stop codon in the middle of exon 7, generating the putative p.Lys253X protein: this would correspond to a 27.65kDa truncated protein without any transmembrane and C-terminal domain, likely losing localization and function.

On the contrary, the c.316-1G>A falls at the acceptor splice site upstream exon 4, abolishing it. We could not identify an intuitive molecular effect for this kind of mutation, which was not known in literature: usually, loss of splicing sites are reported in literature to generate multiple splicing isoforms which should be studied singularly (Cattaneo *et al*, 2017). Indeed, Human Splicing Finder resource (GENOMNIS SAS) clearly showed that

exon 4 itself contained at least four high-probability acceptor splice sites in relative proximity to the natural one (data not shown).

To better investigate the matter, we designed three PCR primers to amplify the whole transcriptional locus in proximity of the c.316-1G>A mutation: the position of our primers is reported in **Figure 20A**.

In **Figure 20B**, we show the results of PCR amplification of the locus on Wfs1 iPSCs and unrelated WT controls: amplification between exon 3 and exon 4 and between exon 4 and exon 5 only showed bands compatible with the expected amplicons. However, in the amplification between exon 3 and exon 5, in Wfs1 iPSCs we could detect a strong band of approximately 180 base pairs (bp) other than the expected one, but apparently not in controls.

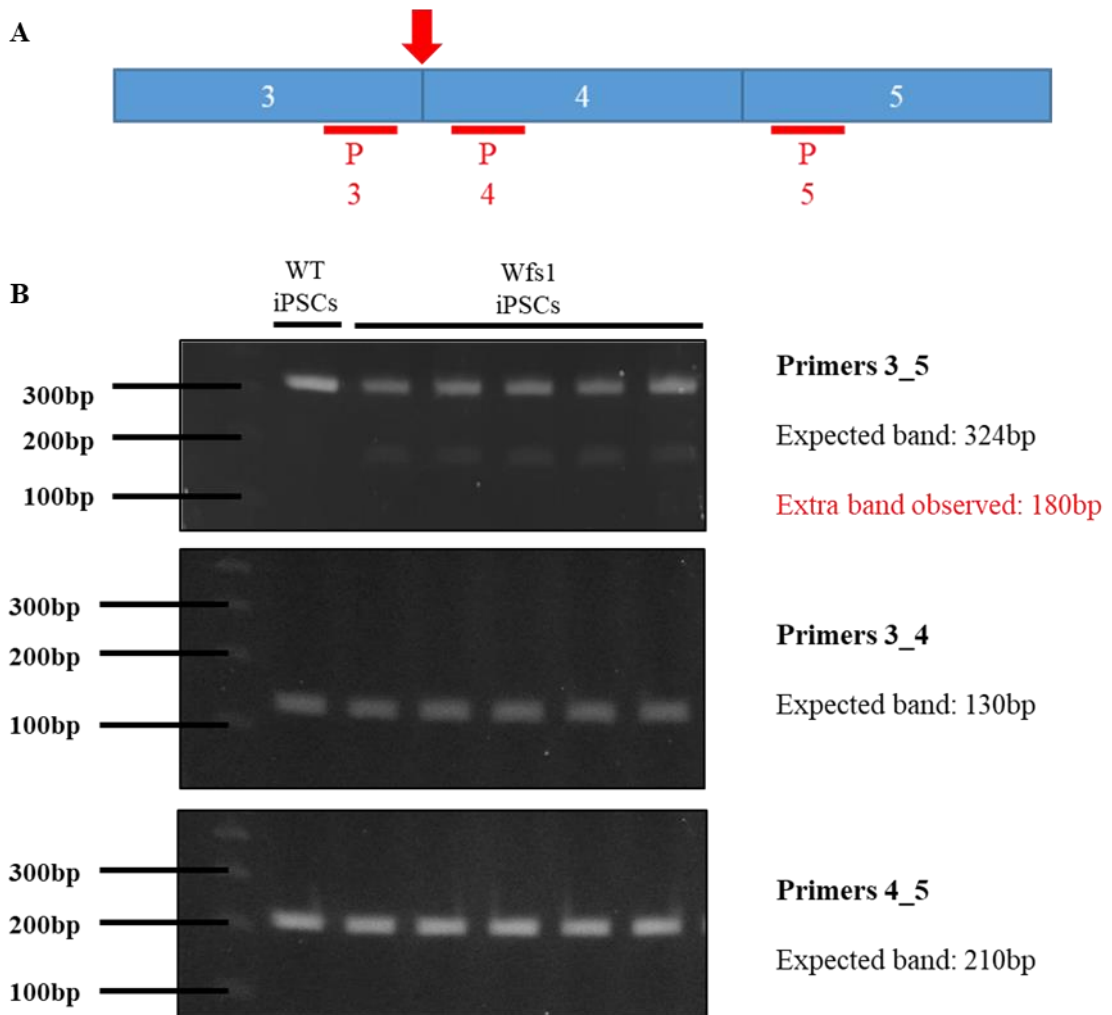


Figure 20. WFS1 mutations generate multiple splicing isoforms in affected cells.

A) Scheme of the PCR strategy to identify alternative splicing isoforms; the mutation spot is indicated by the red arrow and the three primers by the red horizontal lines. B) PCR results from the amplification of the indicated gene span, showing expected and detected amplicon size.

This result suggested the presence of alternative splicing isoforms derived from the allele carrying the c.316-1G>A mutation, with unknown significance. In light of this, we further investigated to understand the nature of such amplicon and determine its source.

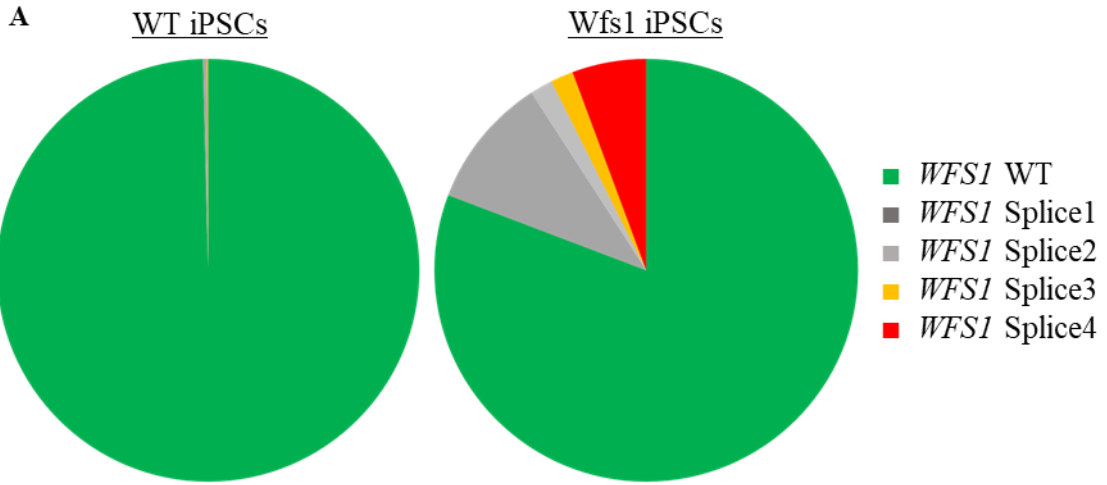
Deep sequencing of the purified PCR product from the region spanning exon 3 to 5 unexpectedly revealed the presence of four splicing isoforms different from the WT one, which in turn we deemed derived from the allele carrying the c.757A>T mutation (which, in this region, presents a normal sequence).

Interestingly, all the isoforms were present both in WT and in Wfs1 cells, although at different levels: while in WT cells the alternative isoforms account for less than 1% of all sequences, in Wfs1 cells they make up more than 15% of the total (**Figure 21A-B**).

Two isoforms, Splice3 and Splice4, determine the loss of a number of nucleotides that is a multiple of three (141bp and 240bp, respectively): this allows the retention of the frame and, potentially, the production of an internally truncated protein. Splice3 would lose the portion of the N-terminal comprised between Val106 and Gln152, while Splice4 between Leu91 and Asp171 (**Figure 21C-D**).

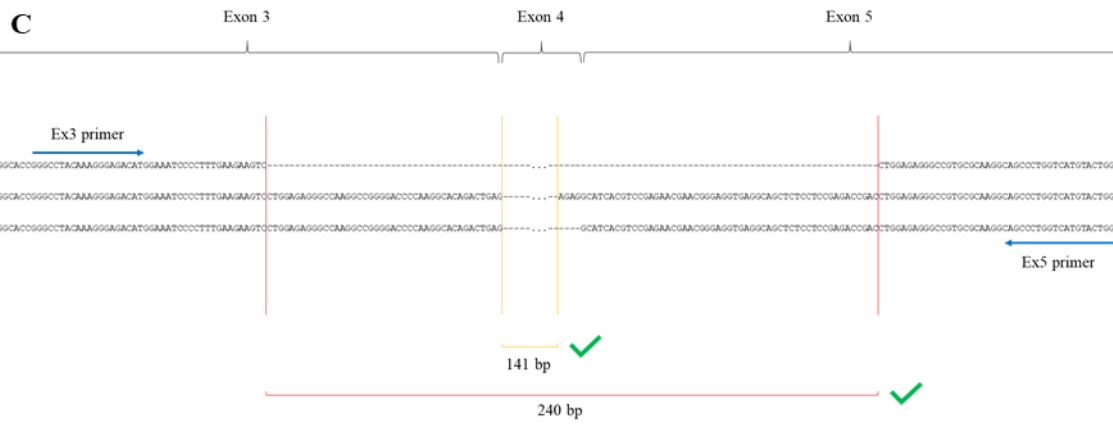
In light of these findings, we sought to investigate whether a similar mix of splicing isoforms could result in the production of a residual protein, even though lacking part of the functional N-terminal domain.

Western blot analysis revealed contrasting results: on one hand, an antibody raised against the N-terminal (Wolframin CST) only recognized the protein in WT cells; on the other hand, an antibody raised against the conserved C-terminal of the protein (Wolframin B) could detect a band at the same molecular weight also in WS1-derived iPSCs. The difference observed is likely due to the recognized epitope, which we postulate to be lost in Wfs1 cells in the case of the Wolframin CST antibody. Interestingly, Wolframin CST antibody seems more efficient in also recognizing the tetrameric form of Wolframin, weighting around 400kDa, on top of the monomer found at 100kDa (**Figure 21E-F**).



B

Isoform	WT %	Wfs1 %
WT	99,6%	84,5%
Splice1	0,2%	8%
Splice2	0,1%	2%
Splice3	0,08%	1,5%
Splice4	0,02%	4%



D

Splice3

MDSNTAFLGFSQPPPPAFQPARSRNLNATASLEQERSERFRAPGQAGFGPVRDAAAP
 AEPQAQHTRSRERADGTGPTKGDMEIPFEVLERAKAGDPKAQTEVGKHYLQLAGSDTDEE
 LNSCTAVDWLVLAARQGRREAVKLLRCLADRRGITSENEREVRLSSEDLERAVRKA
 LVMYKLNPKKKKQVAVAELENVGVNEHGGAGPVPKSLQQRMLERLVSSEKIN
 YIALDDFVEITKKYAKGVI PSSLFLQDDEDDDELAKSPEDLPLRLKVVYPLHAIMK
 EYLIDMASRAGMHWLSTIIPHTHINALIFFIVSNLIDFFAFFIPLVIFYLSFISMVIC
 TLKVFQDSKAWENFRITDILLRFEPLNLDVEQAEVNFQGNHLEPYAHFLLSVFVIFSP
 IASKDCIPCESELAVITGFFVTYSYLSLTHAEPYTRRALATEVTAGLLSLLPSMPLNWPY
 LKVLGQTFITVPGHVLVNLVSVPCLLYVYLLYLFRRMAQLRNFKGYCYLVPLVLCFMW
 CELSVILLESGLGLLRASIGYFLFALPILVAGLALVGLQFARWFTSLELTKIAVT
 VAVCSVPLLRWTKASFVVMVKSLSRSMVKLLVWLTAIVLPCWFVYVYRSEGMKVY
 NSTLTWQQYGALCGPRAWKETNMARTQILCSHLEGRVTVWTRFKYVVRVTDIDNSAESAI
 NMLPFFIGDWMRCLYGEAYPACSPGNTSTAEELCRLLKLAHPCHIKKFDYKFEITVG
 MPFSSGADGSRSEEDDVTKDIVLRASSEFKSVLLSLRQGSLEIFSTILEGRLGSKWPFV
 ELKAISCLNCAQLSPTRRHVKIEHDWRSTVHGAVKFAFDFFFPFLSAA

Splice4

MDSNTAFLGFSQPPPPAFQPARSRNLNATASLEQERSERFRAPGQAGFGPVRDAAAP
 AEPQAQHTRSRERADGTGPTKGDMEIPFEVLERAKAGDPKAQTEVGKHYLQLAGSDTDEE
 LNSCTAVDWLVLAARQGRREAVKLLRCLADRRGITSENEREVRLSSEDLERAVRKA
 LVMYKLNPKKKKQVAVAELENVGVNEHGGAGPVPKSLQQRMLERLVSSEKIN
 YIALDDFVEITKKYAKGVI PSSLFLQDDEDDDELAKSPEDLPLRLKVVYPLHAIMK
 EYLIDMASRAGMHWLSTIIPHTHINALIFFIVSNLIDFFAFFIPLVIFYLSFISMVIC
 TLKVFQDSKAWENFRITDILLRFEPLNLDVEQAEVNFQGNHLEPYAHFLLSVFVIFSP
 IASKDCIPCESELAVITGFFVTYSYLSLTHAEPYTRRALATEVTAGLLSLLPSMPLNWPY
 LKVLGQTFITVPGHVLVNLVSVPCLLYVYLLYLFRRMAQLRNFKGYCYLVPLVLCFMW
 CELSVILLESGLGLLRASIGYFLFALPILVAGLALVGLQFARWFTSLELTKIAVT
 VAVCSVPLLRWTKASFVVMVKSLSRSMVKLLVWLTAIVLPCWFVYVYRSEGMKVY
 NSTLTWQQYGALCGPRAWKETNMARTQILCSHLEGRVTVWTRFKYVVRVTDIDNSAESAI
 NMLPFFIGDWMRCLYGEAYPACSPGNTSTAEELCRLLKLAHPCHIKKFDYKFEITVG
 MPFSSGADGSRSEEDDVTKDIVLRASSEFKSVLLSLRQGSLEIFSTILEGRLGSKWPFV
 ELKAISCLNCAQLSPTRRHVKIEHDWRSTVHGAVKFAFDFFFPFLSAA

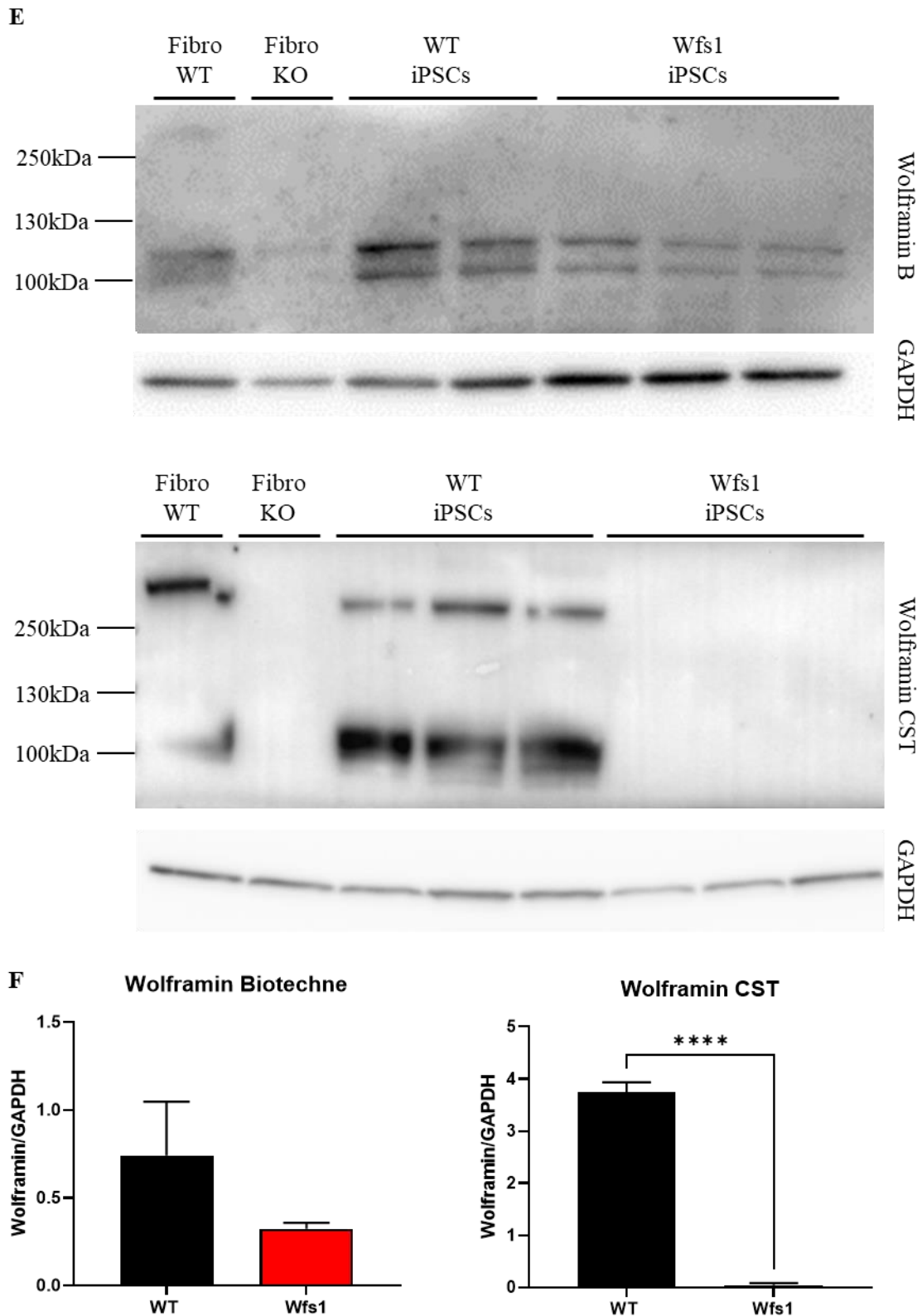


Figure 21. Results from deep sequencing of PCR products from WFS1 transcripts.

A) Example of the distribution of WFS1 isoforms in a WT and a Wfs1 clone of iPSCs. B) Mean relative percentages of the fragments that have been mapped to

each splicing isoform in WT and *Wfs1* iPSCs; N=1 for WT, N=2 for *Wfs1*. C) Graphic depiction of *Splice3* (in yellow) and *Splice4* (in red) at the mRNA level; colored brackets indicate the limits of the lost portion for each isoform. D) Complete protein sequence of Wolframin, showing the lost aminoacids for *Splice3* (in yellow) and *Splice4* (in red). E) Representative Western blots showing full-length Wolframin protein at an approximate molecular weight of 100kDa (predicted molecular weight: 96kDa); the antibody used for blotting is reported on the right. Blot for Glyceraldehyde 3-Phosphate Dehydrogenase (GAPDH) as housekeeping is also presented. B=Biotechne, CST=Cell Signalling Technology; WT and KO fibroblasts were used as controls of antibody specificity. F) Quantification relative to the Western blots presented in E). Mean±SEM, N=as shown in E); **** $p < 0.0001$.

5.3. Gene correction of the 316-1 A>T allele

In order to obtain a more stringent control, we designed a correction strategy to produce heterozygous iPSCs, correcting a single allele in *Wfs1* cells. We opted to correct the mutation located at the acceptor splice site upstream exon 4 (c.316-1G>A), because our data pointed to a residual transcriptional and translational activity of the locus: in order to avoid confounding effects of residual protein production, dampening the phenotype or on the contrary acting as a dominant negative, we deemed it easier to just retain the more predictable c.757A>T mutation and correct the other allele.

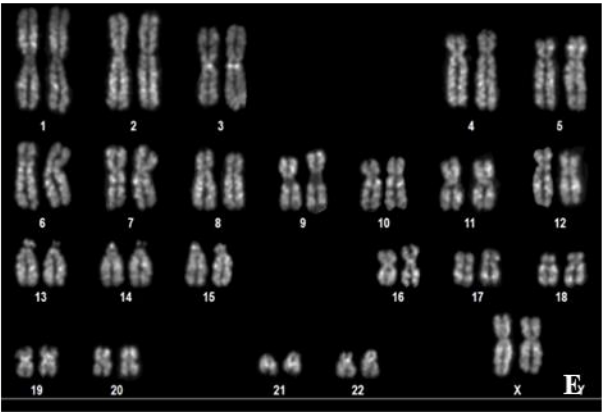
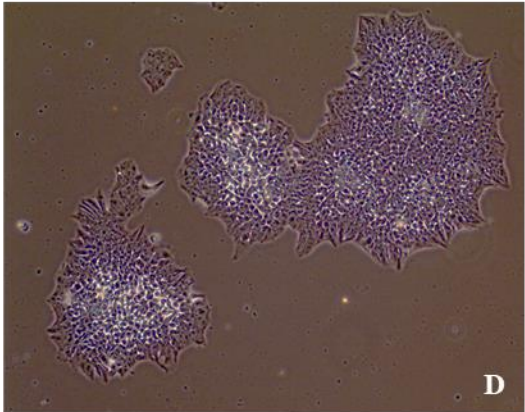
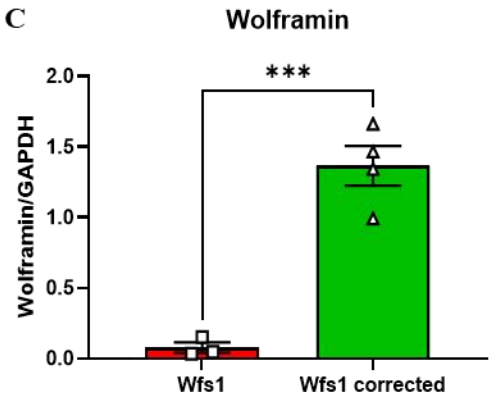
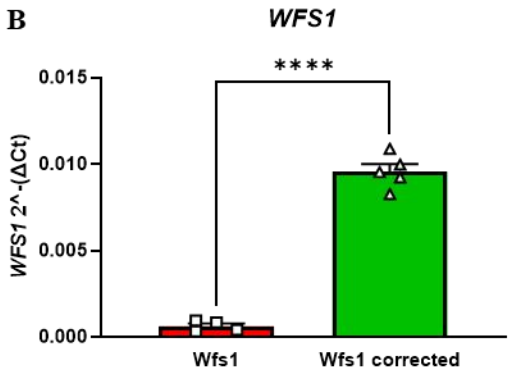
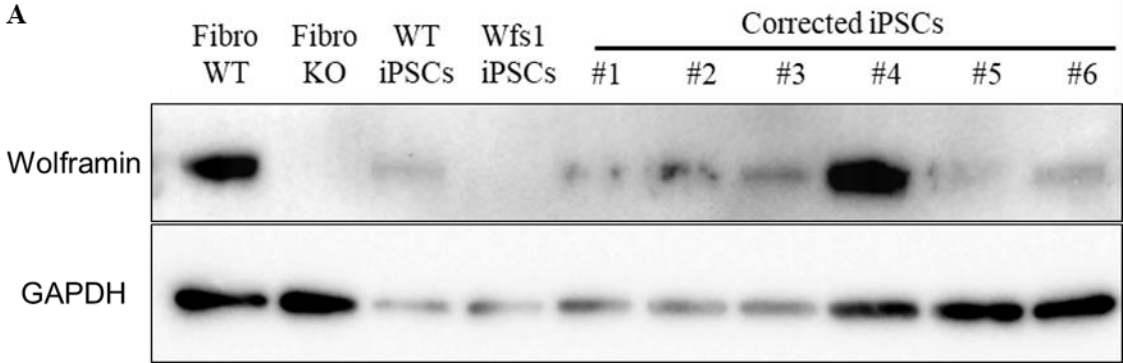
The strategy for gene correction is illustrated in the relative section of **Methods and Materials**.

We generated six clones, which were tested for their expression of both *WFS1* transcript and reexpression of full-length Wolframin protein, using an antibody that recognizes the epitope which we predict to be lost in the case of internal truncation of the N-terminal discussed before: such antibody does not recognize mutant Wolframin, but binds to the WT sequence. Western blot and RT-qPCR highlighted a strong increase in expression of both mRNA and protein levels of the target, confirming the genetic correction (**Figure 22A-C**).

Subsequently, one clone was excluded due to karyotype abnormalities: the other five had normal morphology, karyotype and pluripotency marker expression, as seen in **Figure 22D-F**.

We then investigated the presence of the splicing isoforms that we previously identified in *Wfs1* iPSCs. As shown in **Figure 22G**, genetic correction of the *WFS1* locus is able to abolish abnormal splicing isoforms and restore the same single PCR band seen

in WT iPSCs. Thus, we confirm that the aforementioned band is strictly derived from the allele carrying the c.316-1G>A mutation and is not an aspecific finding due to the genetic background.



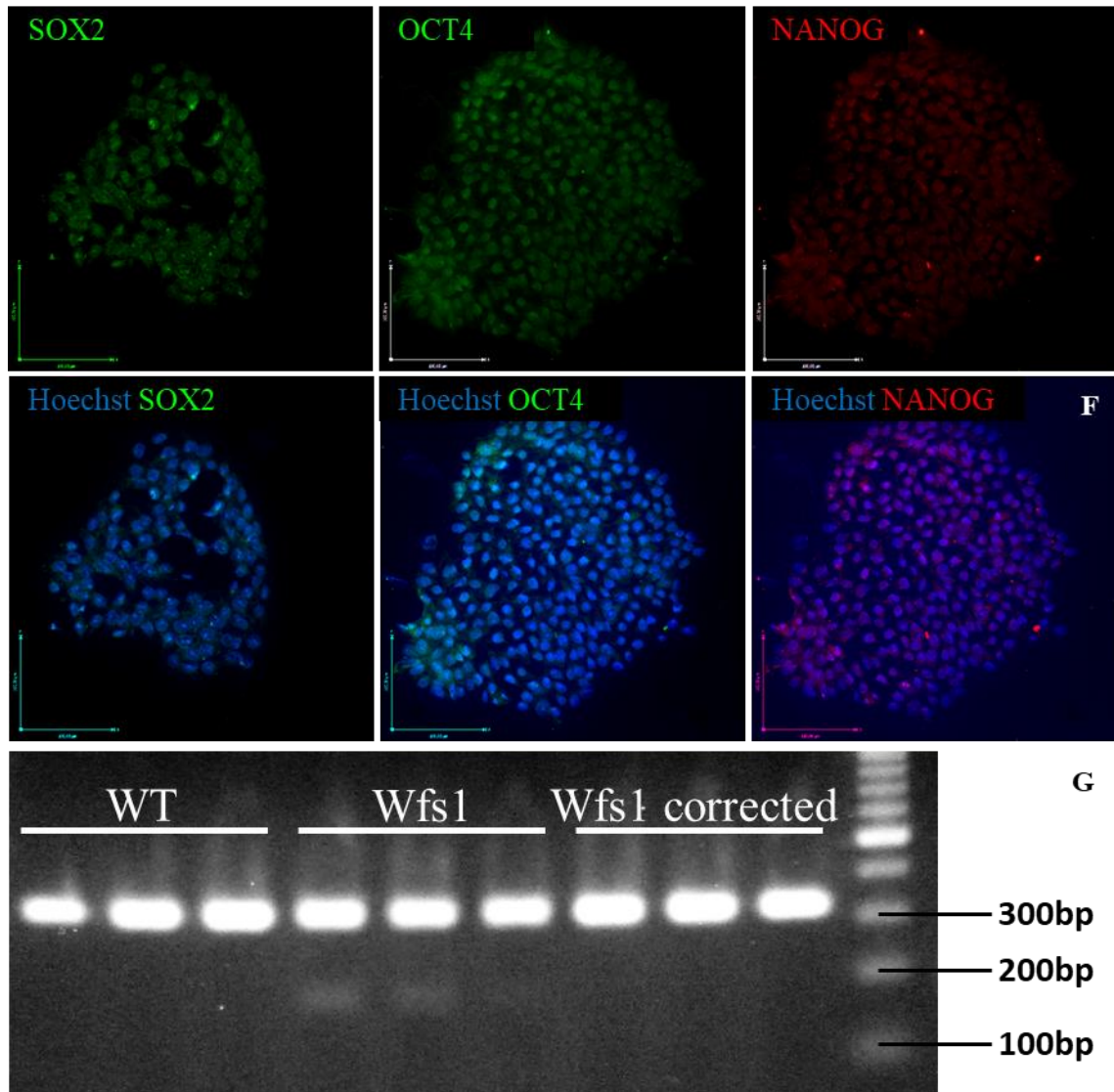


Figure 22. Characterization of corrected *Wfs1* iPSCs.

A) Western blot with Wolframin CST antibody (GAPDH as housekeeping) to assess reexpression of full-length protein; WT and KO fibroblasts were used as controls of antibody specificity. B) RT-qPCR of *WFS1* transcripts showing significant overexpression in *Wfs1* corrected over *Wfs1* iPSCs. Mean \pm SEM, N=4 for *Wfs1*, N=5 for *Wfs1*-corrected; **** $p < 0.0001$. C) Western blot quantification for the reexpression of full length Wolframin using Wolframin CST antibody. Mean \pm SEM, N=3 for *Wfs1*, N=4 for *Wfs1*-corrected; *** $p < 0.001$. D) Bright-field image of an iPSC colony after correction; 10x zoom. E) Example of a normal karyotype from a clone of iPSCs after gene correction. F) Immunofluorescence for the pluripotency markers SOX2, OCT4 and NANOG, showing complete positivity of the cell population; nuclei were counterstained with Hoechst. 20x zoom, scalebar is 100 μ m. G) PCR amplification of the exon3-exon5 span, showing expression of abnormal splicing isoforms in *Wfs1* iPSCs, but not in WT or *Wfs1* corrected ones.

5.4. Differentiation of iPSC-derived β cells

We differentiated WT, Wfs1 and Wfs1 corrected iPSCs into pancreatic β cells using a consolidated *in vitro* 2D-protocol recapitulating pancreatic development. For simplicity, I will only present the data derived from Wfs1 and Wfs1 corrected cells, keeping in mind that Wfs1 corrected cells showed to behave in line with a WT genotype.

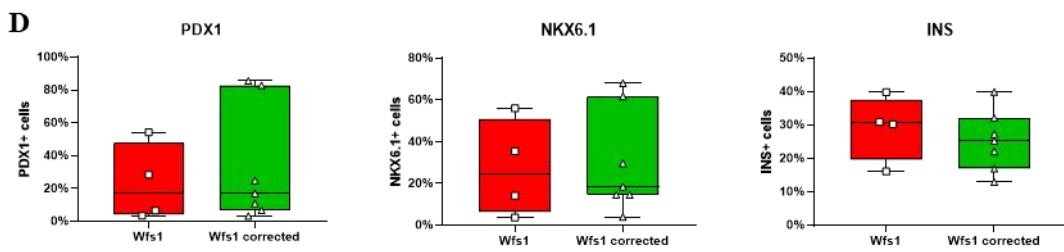
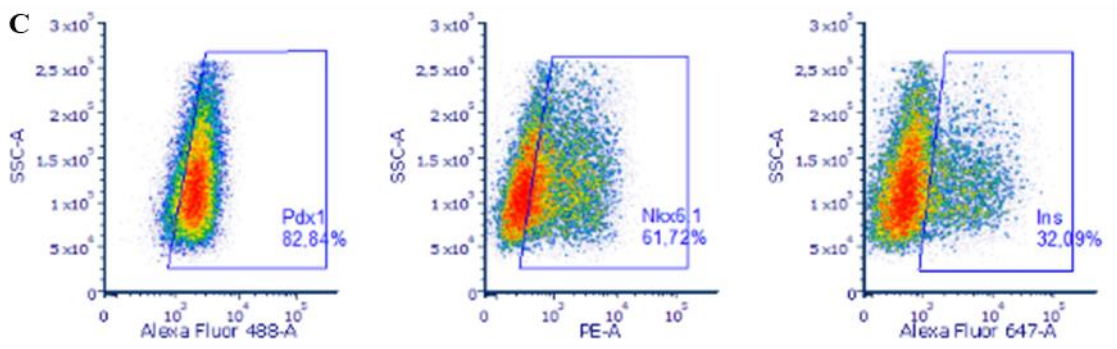
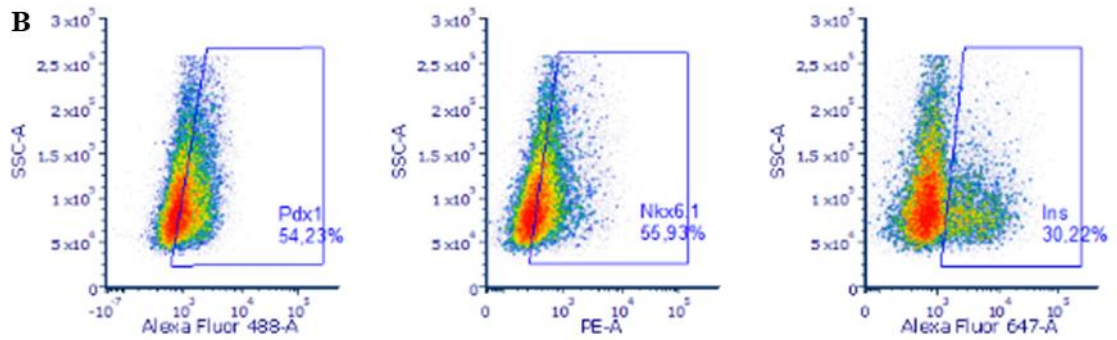
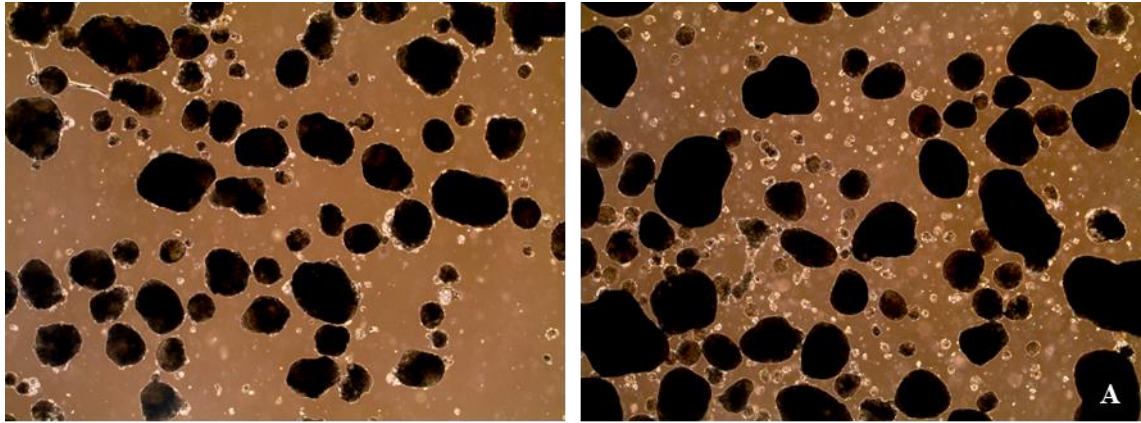
Both Wfs1 and Wfs1 corrected cells managed to get through the whole differentiation process without apparent delays or impairments, in contrast with a previous report (Maxwell *et al*, 2020): at the end of the 24 days-long protocol, they appear as cell clusters with a roundish shape, not dissimilar from the ones obtained from human islets of Langerhans kept in culture in comparable conditions (**Figure 23A**).

FACS evaluation of relevant differentiation markers (PDX1, NKX6.1 and INS) revealed that all the cell lines tested can efficiently differentiate into Insulin-positive cells, reaching comparable efficiencies (23,17% \pm 11,76% vs 33,08% \pm 13,48% for PDX1, 27,31% \pm 11,60% vs 30,14% \pm 9,44% for NKX6.1, 29,25% \pm 4,90% vs 25,21% \pm 3,44% for INS; mean \pm SEM, Wfs1 vs Wfs1 corrected), as presented in **Figure 23B-D**.

As a further proof of correct differentiation, we performed immunofluorescence on β cell clusters from Wfs1 and Wfs1 corrected cells: we found a considerable number of cells expressing Chromogranin A, Insulin, Glucagon and NKX6.1, consistent with the data from FACS analysis (**Figure 23E**).

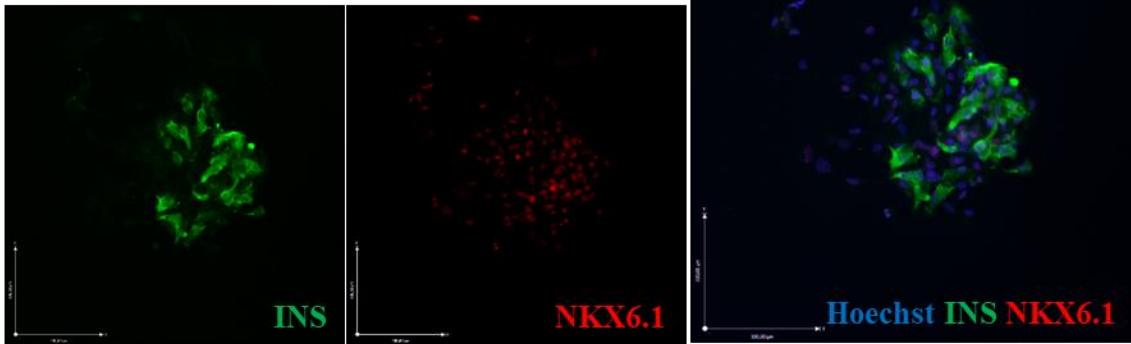
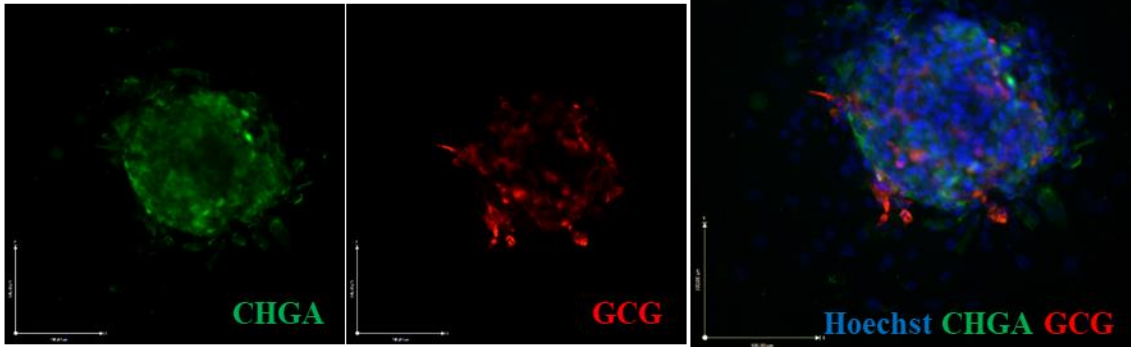
Furthermore, as seen in **Figure 23F**, differentiating Wfs1 iPSCs correctly recapitulate pancreatic ontogenesis, as assessed by their gene expression of relevant markers of the process.

Collectively, these data suggest that Wfs1 iPSCs can efficiently differentiate and express the molecular signature appropriate for a mature β cell.

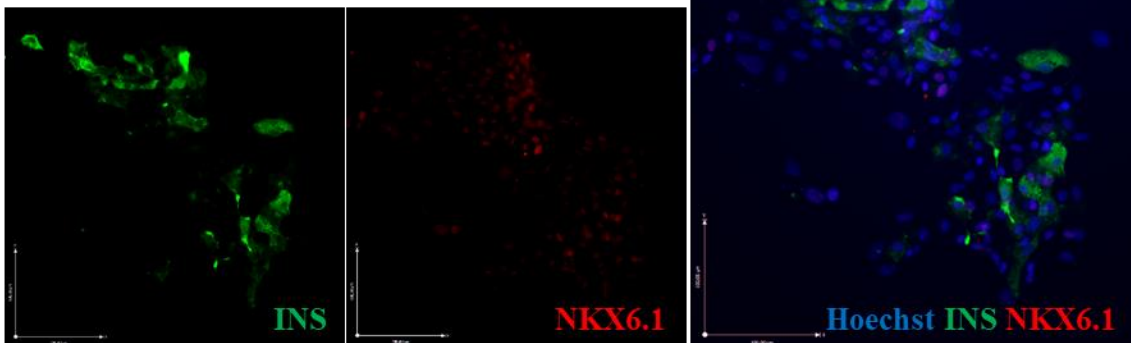
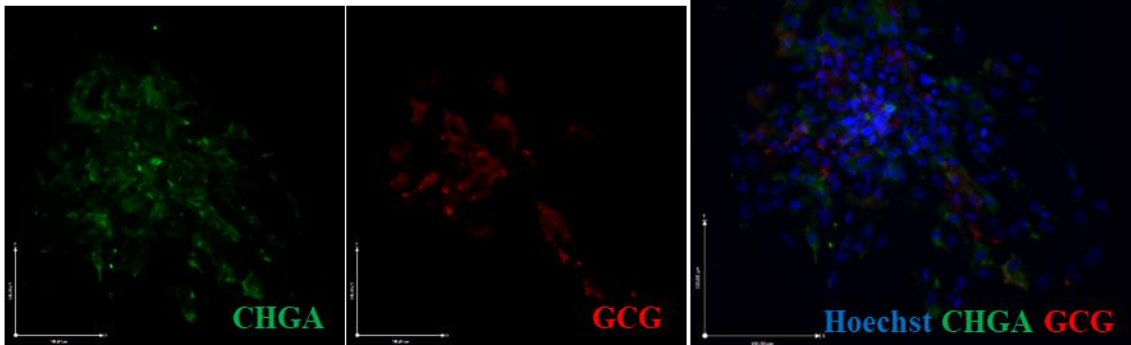


E

Wfs1



Wfs1 corrected



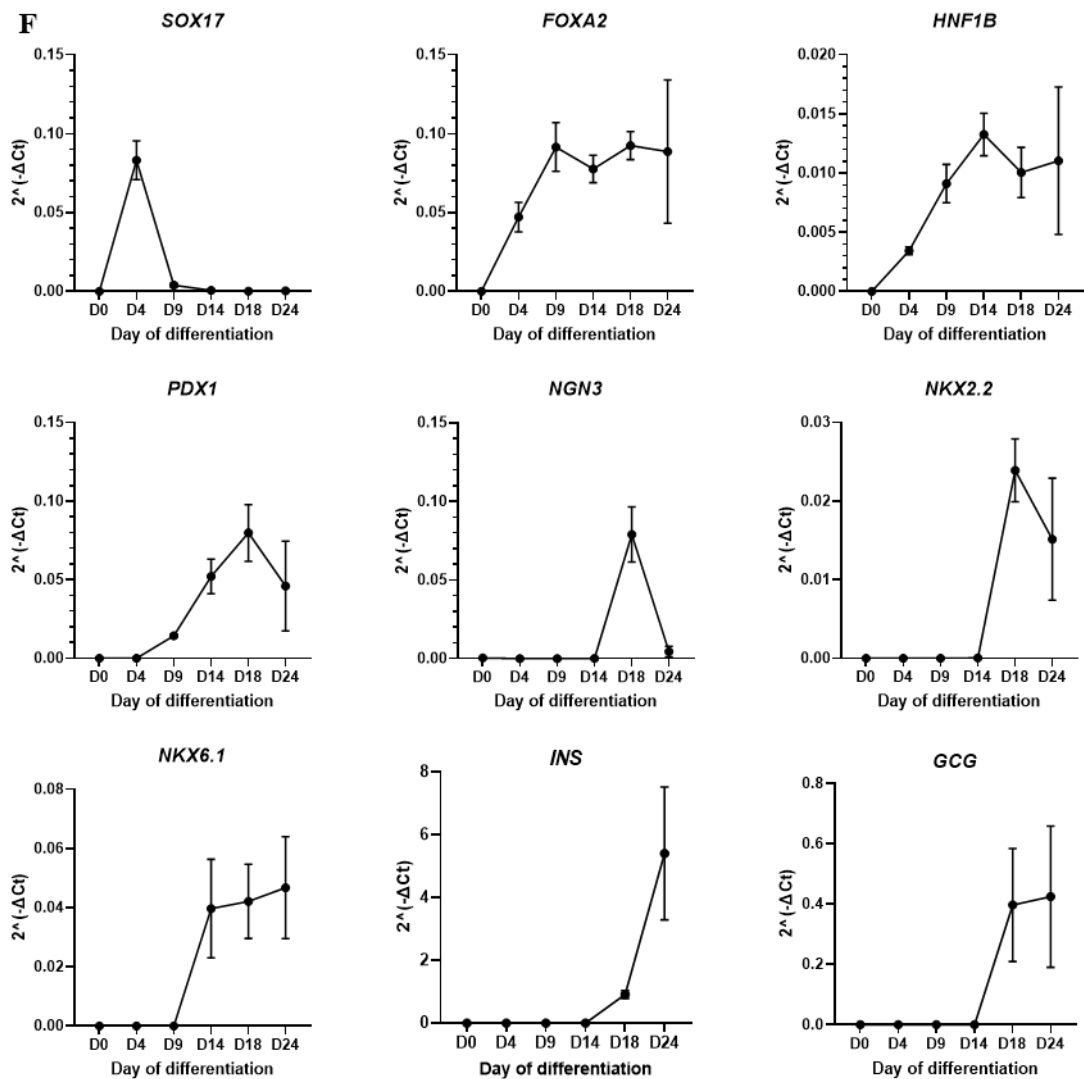


Figure 23. Morphology and differentiation efficiency in iPSC-derived β cells.

A) Brightfield image of clusters of iPSC-derived *Wfs1* (left) and *Wfs1* corrected (right) β cells cultured in suspension; 4x zoom. B) Example of FACS plots from *Wfs1* differentiated iPSCs, showing the percentage of cells positive for PDX1, NKX6.1 and INS. C) Example of FACS plots from *Wfs1* corrected and differentiated iPSCs, showing the percentage of cells positive for PDX1, NKX6.1 and INS. D) Quantification of the FACS plots presented in B) and C). Mean \pm SEM, N=4 for *Wfs1*, N=7 for *Wfs1* corrected; $p > 0.05$ for all three markers. E) Immunofluorescence panel of relevant markers in differentiated β cells, both *Wfs1* and *Wfs1* corrected. CHGA=Chromogranin A, GCG=Glucagon, INS=Insulin; scalebar is 100 μ m. F) Gene expression analysis of differentiation markers, showing correct timing of progression. Mean \pm SEM, N=4.

FACS analysis, gene expression and immunofluorescence all indicate a good efficiency of differentiation into the β cell lineage. However, we wanted to better characterize the endocrine compartment composition and the general off-targets of the process, as the literature strongly indicated that WS1-derived cells might have troubles in

their full specification (Maxwell *et al*, 2020). The authors of the paper reach this conclusion based on an experiment of Single Cell Transcriptomics, which allowed them to uncover all differentiation clusters present, as we mentioned in the introduction in **Table 2**.

Therefore, we designed a Single Cell Transcriptomics experiment to assess gene expression of our Wfs1 and Wfs1 corrected β cells.

The first parameter we considered was appropriate cell clustering. Our data indicate that cell clustering of the whole control samples is comparable between the genotypes, as seen in **Figure 24A**: both endocrine progenitors and endocrine cells, mature and immature, are present with similar proportions in the two populations, making up the majority of the cells.

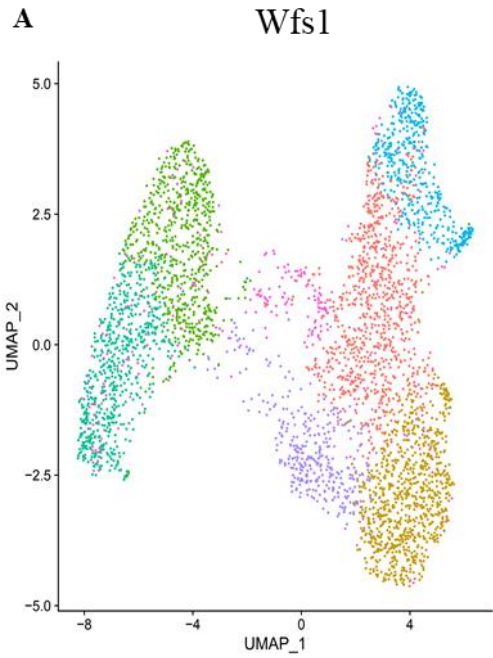
We then investigated whether the endocrine compartment contained all the appropriate cell types in the right proportions: surprisingly, we found that Wfs1 cells lack a proper formation of the α , δ and γ clusters: fully differentiated α and δ cells are greatly reduced in number, while γ cells seem to be completely absent (**Figure 24B**). Loss of glucagon-, somatostatin- and pancreatic polypeptide-secreting cells, respectively, might impact on whole islet functionality, in light of the complex paracrine communication between the various subpopulations. Conversely, the proportion of β cells was similar in both samples and represented the majority of the endocrine population, suggesting that Wfs1 cells do not have an impaired production of β cells concerning the mere number.

According to this result, we decided to dig deeper into β cell subpopulations. Heterogeneity of β cells has been postulated starting from the empirical observation that single isolated β cells do not have the same sensitivity or responsivity to glucose stimulation. From this concept, four main subpopulations were identified, named $\beta 1$, $\beta 2$, $\beta 3$ and $\beta 4$, based on the combinatorial expression of two surface markers: $CD9^- ST8SIA1^-$, $CD9^+ ST8SIA1^-$, $CD9^- ST8SIA1^+$ and $CD9^+ ST8SIA1^+$, respectively; the $\beta 1$ subtype is the most responsive to glucose challenge, while the $\beta 4$ secretes the least insulin when challenged. Moreover, it was reported that the frequencies of β cell subtypes are altered in T2D (Dorrell *et al*, 2016).

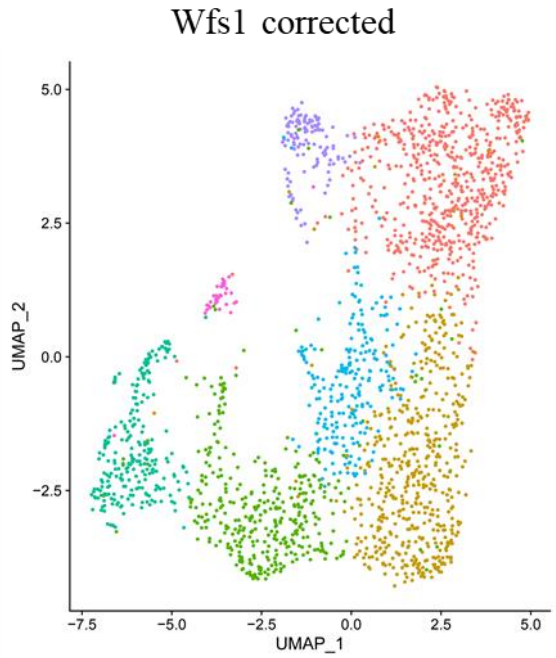
Other groups reported similar findings focusing on Ca^{++} handling across β cell subpopulations, finding that the least secreting cells (which manifested an almost immature gene signature) were responsible for cell-to-cell contacts, Ca^{++} redistribution and insulin secretion coordination (Johnston *et al*, 2016; Salem *et al*, 2019). These cells are called hub cells or leader cells, and we can postulate that they overlap with the β 3 and β 4 subtypes.

In both genotypes, we detected a vast majority of β 1 cells, which constitute the most common subtype and represent “standard” β cells, as it is usually intended. On the contrary, we did not find any β 4 cells. The main difference among the two lines was the proportion of β 2 and β 3 cells, which was inverted (high β 2 and low β 3 in *Wfs1*, low β 2 and high β 3 in *Wfs1* corrected) (**Figure 24C**). This result is of unclear interpretation, as both β 2 and β 3 cells are underrepresented in our samples compared to what is observed in normal adult islets (Dorrell *et al*, 2016): it could be due to a generalized partial maturation of the endocrine compartment.

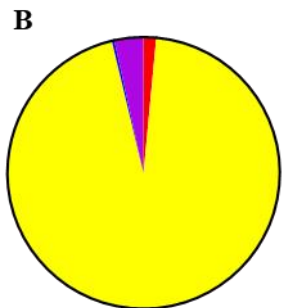
All in all, clustering of endocrine populations and β cell subtypes suggested an impaired differentiation ability of *Wfs1* cells compared to the corrected counterpart, not because of loss of true β cells, but on the contrary due to a lower differentiation capacity of the other ancillary cell types of the islet. These results pave the way for the correlation of molecular and functional alterations in *Wfs1* cells, stemming from putative defects in their correct differentiation.



- Endocrine cells (less mature: EC and polyhormonal)
- Endocrine cells (more mature: α , β , γ , δ)
- Mesenchyme
- Ductal cells
- Endocrine progenitors
- Acinar cells
- Unknown

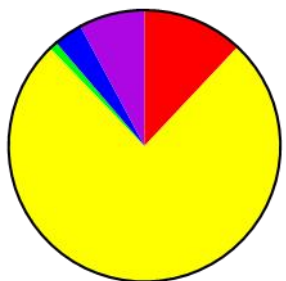


- Endocrine cells (less mature: EC and polyhormonal)
- Endocrine cells (more mature: α , β , γ , δ)
- Mesenchyme
- Ductal cells
- Endocrine progenitors
- Endothelial cells
- Unknown



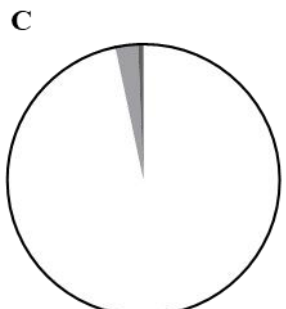
- α cells
- β cells
- δ cells
- Polyhormonal

Wfs1



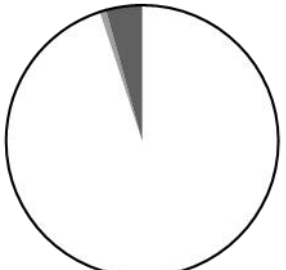
- α cells
- β cells
- γ cells
- δ cells
- Polyhormonal

Wfs1 corrected



- β 1
- β 2
- β 3

Wfs1



- β 1
- β 2
- β 3

Wfs1 corrected

Figure 24. Single Cell Transcriptomics of iPSC-derived endocrine subpopulations.

A) Clustering of the control groups from the Single Cell Transcriptomics experiment. Each dot represents a single cell, each different color is a cluster as indicated in the legend. B) Pie chart of the endocrine subpopulations, showing the prevalence of α , β , γ , δ and polyhormonal cells in the two genotypes. C) Pie chart of the β cell subpopulations, showing the prevalence of $\beta1$, $\beta2$, $\beta3$ and $\beta4$ cell types in the two genotypes. No $\beta4$ cells were found in either sample.

5.5. Wolfram expression during iPSCs differentiation

On top of true β cell identity and the definition of endocrine cluster composition, we were interested in assessing the temporal upregulation of Wolfram protein production.

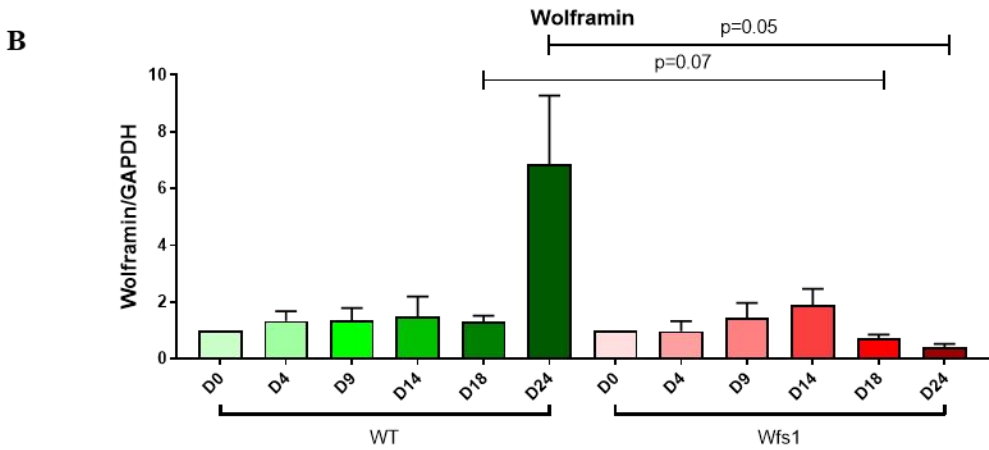
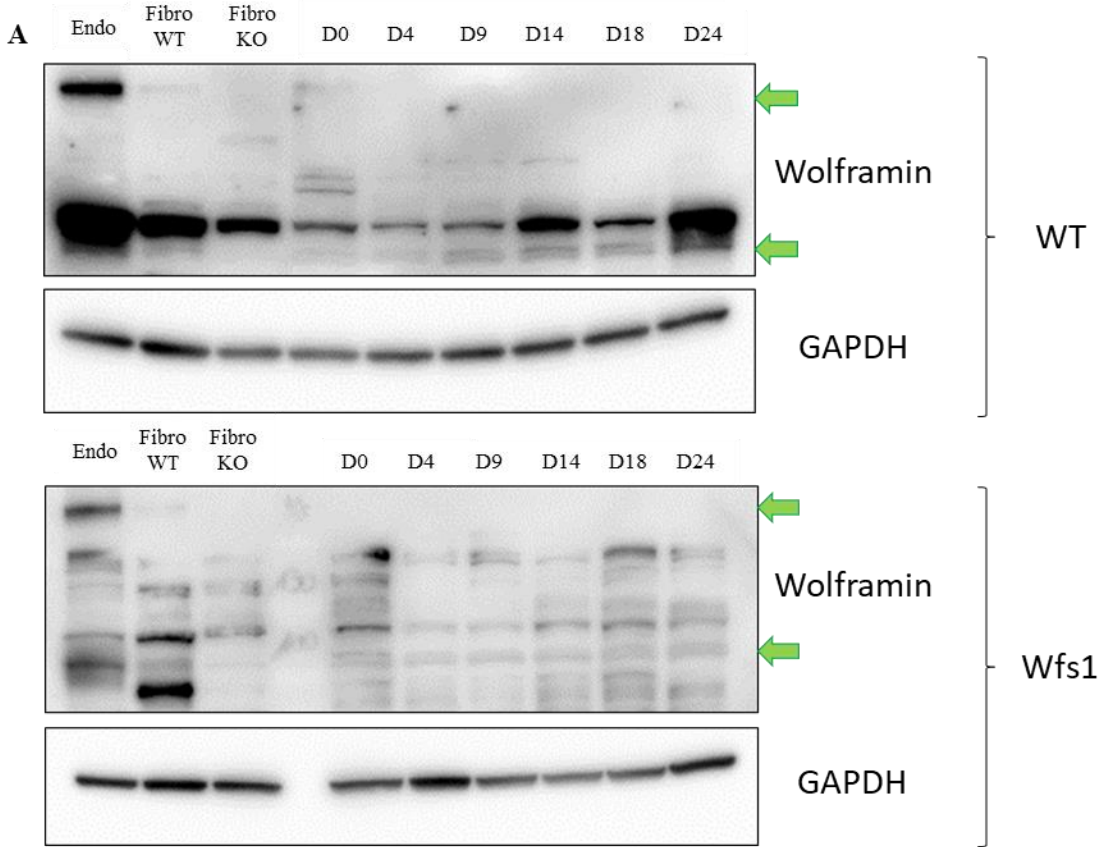
It had already been reported in literature that iPSCs express less Wolfram than the terminally differentiated counterpart (Maxwell *et al*, 2020), but the dynamics of upregulation had never been defined. In **Figure 25A-B**, we show that Wolfram levels stay low and constant up until the very last stage of β cell differentiation at Day24, where WT cells boost their protein levels to around 7-fold compared to Day0, while Wfs1 cells fail to do so and never increase their Wolfram levels.

We also investigated if the genetic characterization of *WFS1* splicing isoforms could be applied to differentiated cells. Panfili and colleagues, who reported in literature our same patient, performed a genetic investigation similar to ours, designing almost identical probes, but using PBMCs as a sample: their paper reports no detectable transcript from the allele with the c.316-1G>A variant, which the authors justify as a result of NMD (Panfili *et al*, 2021) (**Figure 25C**).

We designed a panel of samples which we tested with the same primers reported in previous figures, including: WT and Wfs1 PBMCs, WT, Wfs1 and Wfs1 corrected iPSCs, WT, Wfs1 and Wfs1 corrected iPSC-derived β cells, WT and Wfs1 iPSC-derived retinal organoids (**Figure 25D**). iPSC-derived retinal organoid samples, both controls and from the patient, were kindly given to us by Vania Broccoli's group at Ospedale San Raffaele.

Our results confirm the presence of the alternative splicing band at around 180bp in Wfs1 iPSCs and β cells, and they also reveal that this is conserved in Wfs1 PBMCs: surprisingly, they not only express the 324bp and the 180bp, but also a distinct intermediate band, of approximately 240bp, which is not detectable on agarose gel in any

other sample but is compatible with Splice4, one of the splicing isoforms identified by deep sequencing in Wfs1 iPSCs. Interestingly, retinal organoids appear to express very low levels of splice isoforms different from the WT one derived from the c.757A>T allele.



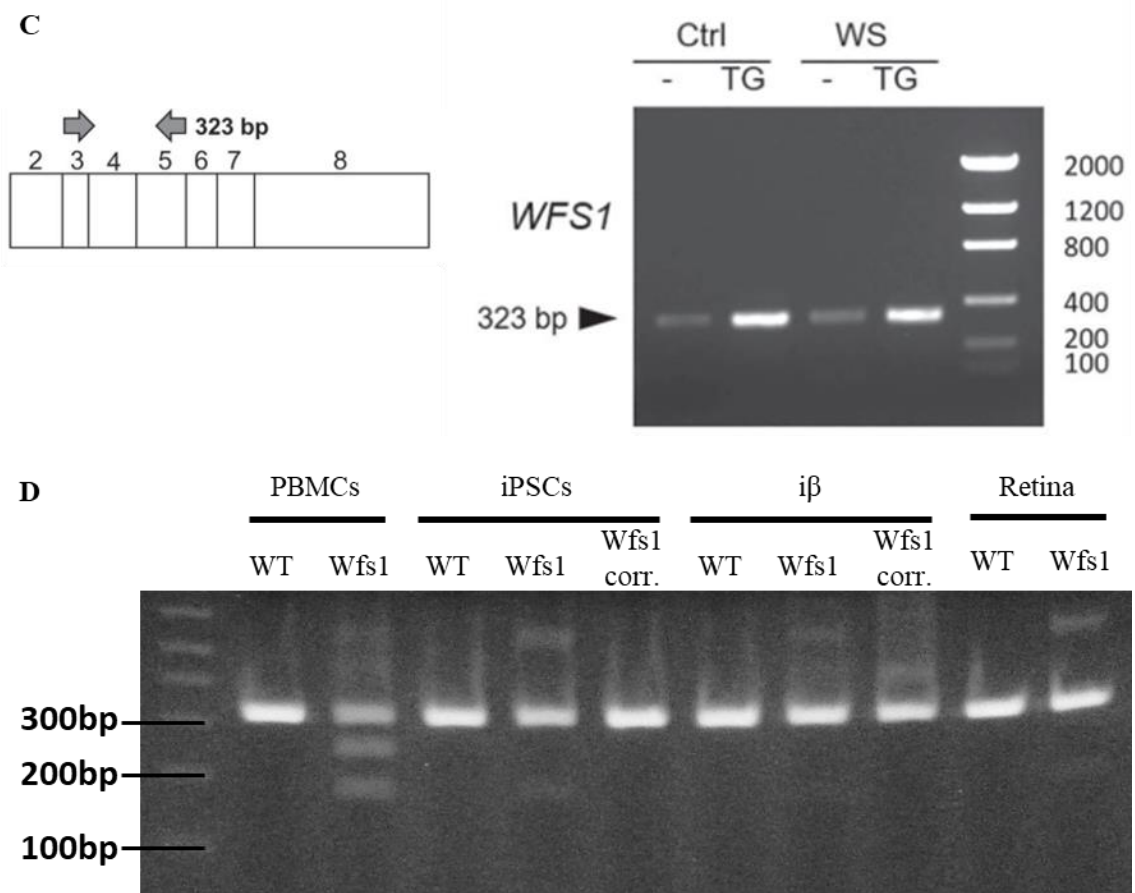


Figure 25. Study of Wolfram in terminally differentiated cells.

A) Representative Western blots showing Wolfram protein expression throughout the differentiation process from iPSCs to β cells; the antibody used is the Biotechne one, which recognizes also N-terminal mutants. Upper panel, WT cells; lower panel, *Wfs1* cells. WT and KO fibroblasts were used as controls of antibody specificity; Endo=EndoC- β H1, an immortalized human β cell line, was used as a quantitative comparison with mature β cells expression. D=Day of differentiation. B) Quantification of the Western blots exemplified in A); mean \pm SEM, N=3. C) Snapshot of Figure 1C-D from Panfili et al., 2021, showing their findings from PCR amplification of the indicated region. D) PCR amplification of the exon3-exon5 span, showing expression of abnormal splicing isoforms in *Wfs1* iPSCs, *Wfs1* PBMCs, *Wfs1* β cells and *Wfs1* retinal specimens, but not in WT or *Wfs1* corrected ones of any kind.

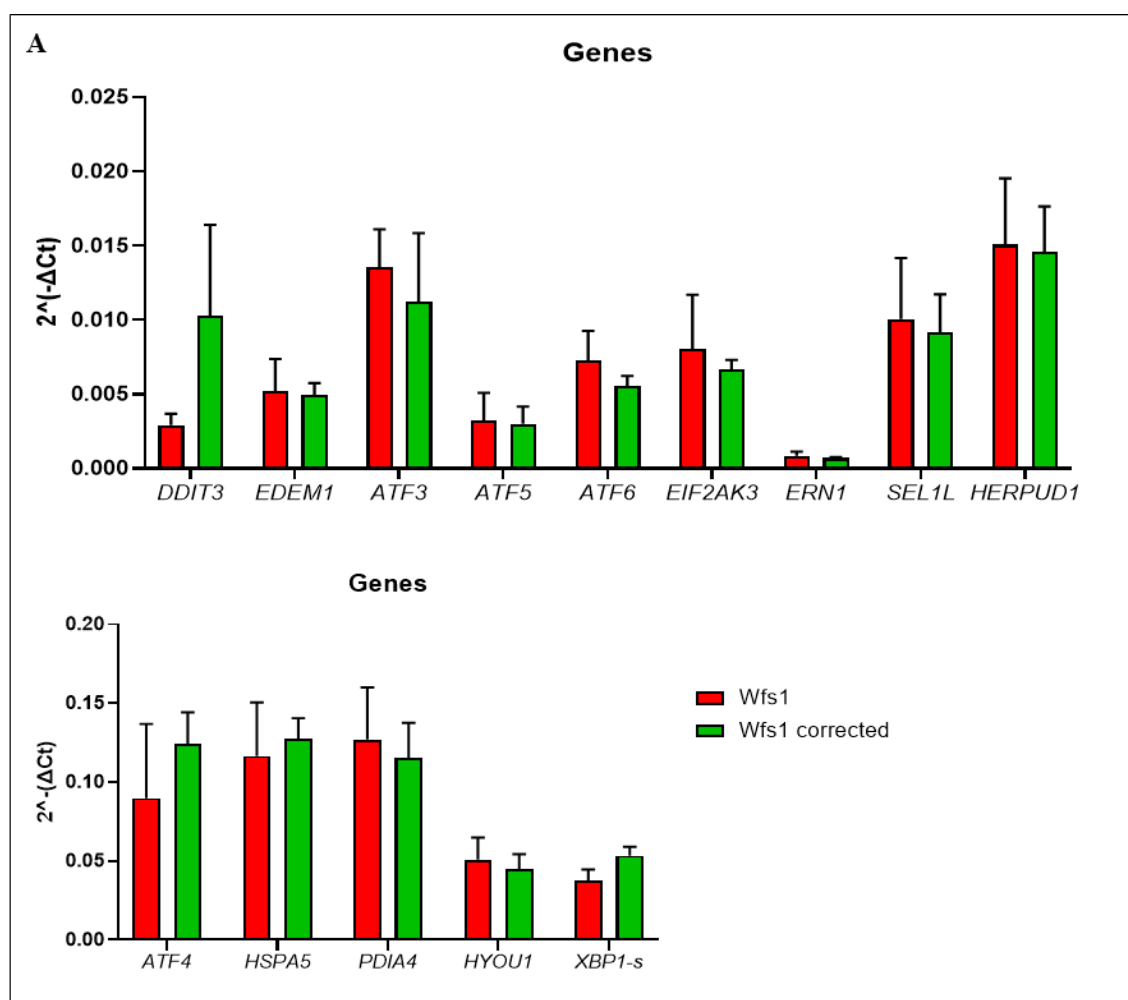
5.6. ER stress in WS1-derived iPSCs

In line with the knowledge present in literature about WS1 pathogenic mechanisms, we sought to investigate the levels of ER stress in our iPSC model of the disease.

We designed a panel of relevant genes and proteins to be measured through RT-qPCR and Western blot, respectively, in order to characterize all three branches of the UPR (PERK, IRE1 α and ATF6, including their direct and indirect targets), but also other

mechanisms which could be relevant for cell stress response, such as the mitochondrial UPR, chaperones, redox state regulators and translational suppressors. Our aim was to cover as thoroughly as possible the factors implicated in UPR orchestration, which, as discussed in the introduction, have pleiotropic functions and must be tightly coordinated in order to promptly respond to stress: any alteration in one or more of the transduction passages could have severe effects on the downstream effectiveness.

Our results clearly show that, in spite of the broad variety of markers considered, we could not detect any major differences at the basal level in any of the pathways analyzed: the only significant result came from ERO1 α protein quantification, which was higher in Wfs1 cells (**Figure 26A-B**). Our data suggest that, in the absence of external stimuli, Wfs1 iPSCs do not display an abnormal ER stress response, apart from a mild imbalance of redox regulation which would require further investigation.



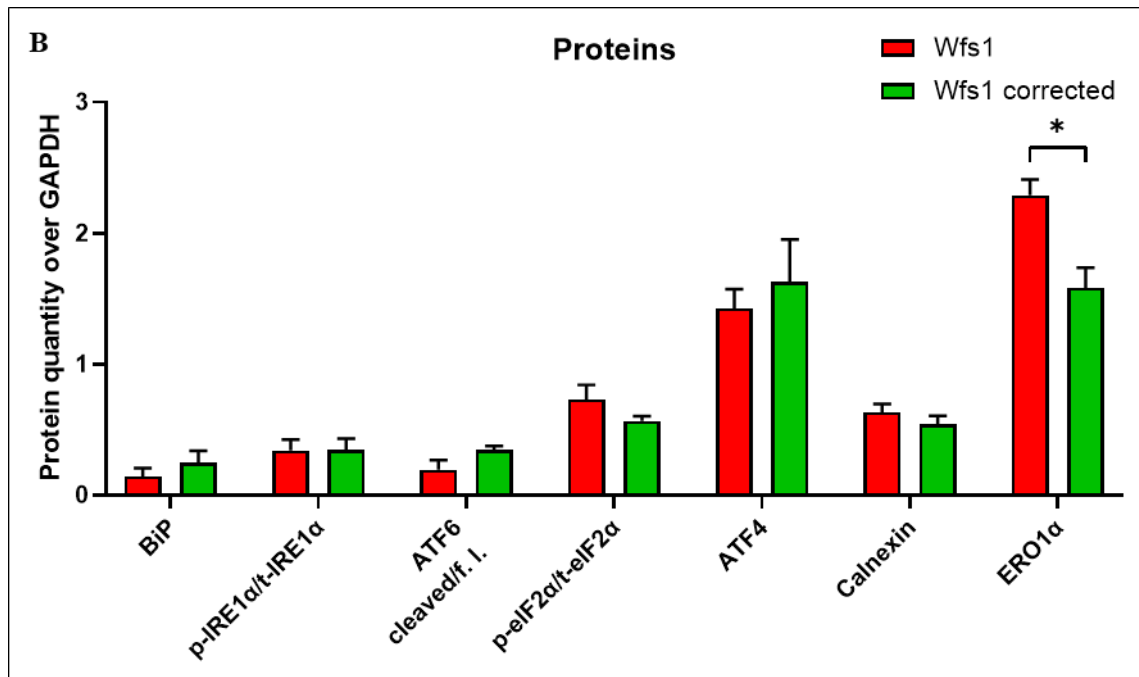


Figure 26. Gene and protein expression of ER stress markers in iPSCs.

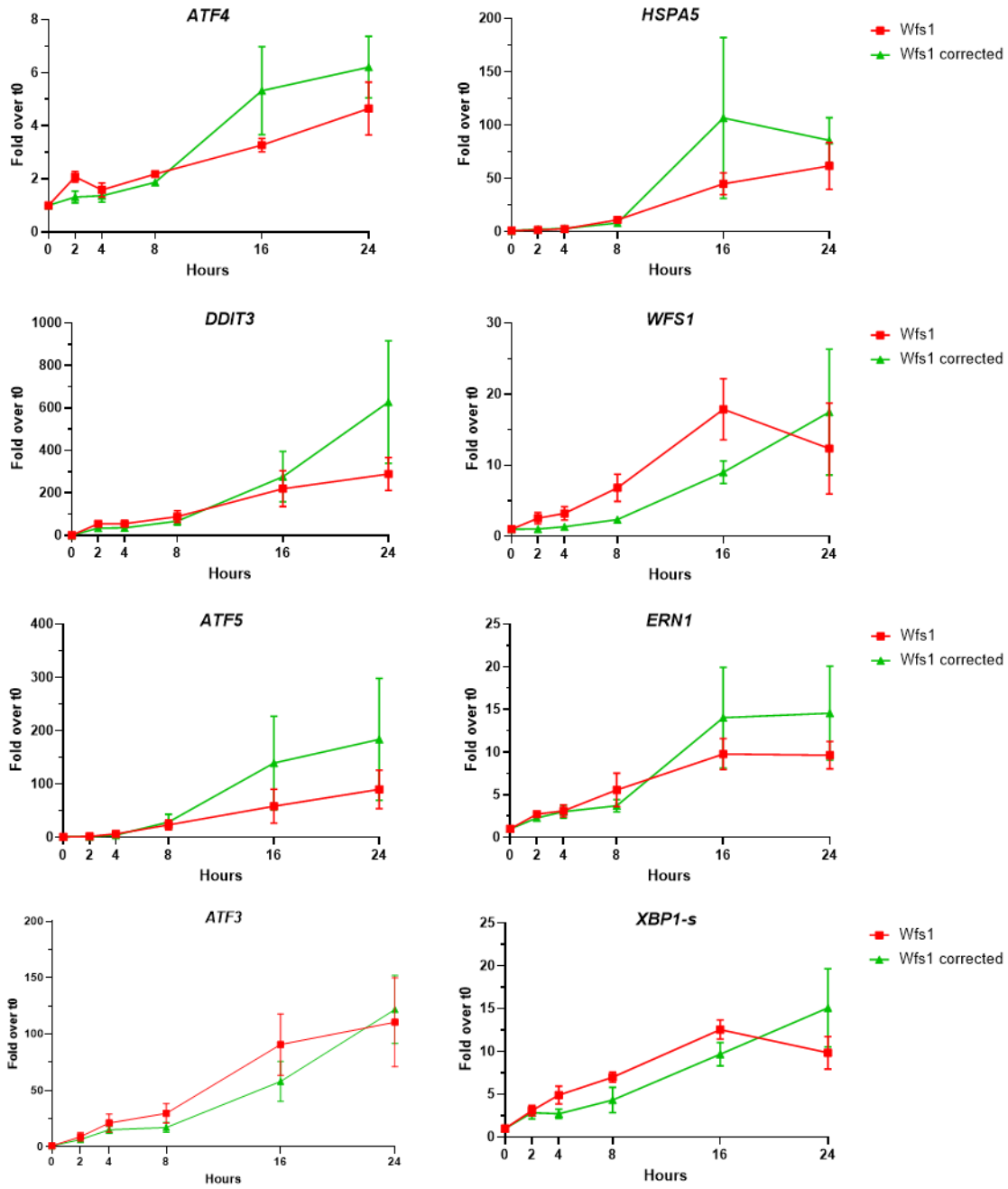
A) Quantification of RT-qPCR experiments evaluating the indicated markers of ER stress in *Wfs1* and *Wfs1* corrected iPSCs. Mean±SEM, N=4 for *Wfs1* iPSCs, N=5 for *Wfs1* corrected iPSCs. B) Quantification of Western blot experiments evaluating the indicated markers of ER stress in *Wfs1* and *Wfs1* corrected iPSCs. Mean±SEM, N=3 for *Wfs1* iPSCs, N=4 for *Wfs1* corrected iPSCs. * $p < 0.05$.

Therefore, we challenged our cells with a well-known ER stress inducer, Thapsigargin (TG). We reasoned that, probably, in the absence of further stimuli our iPSCs would not display alterations in ER stress signalling, since Wolframin is less expressed in iPSCs than in β cells. We set up a timecourse experiment, in order to assess not only if *Wfs1* cells are able to upregulate their UPR and related genes, but also if their timing reflects the right one, as seen in *Wfs1* corrected cells.

Our results indicate that, notwithstanding slight differences in the timing of upregulation of some UPR genes and proteins (such as *HSPA5* and *WFS1* itself), we couldn't detect major defects in *Wfs1* cells compared to the corrected counterpart (**Figure 27A-B**).

Collectively, this suggests that, in the short term, *WS1*-affected iPSCs still retain the ability to trigger an appropriate response to ER stress. Whether this is due to the fact that iPSCs do not rely upon Wolframin as much as differentiated cells or because they would require a longer conditioning is still up for debate.

A



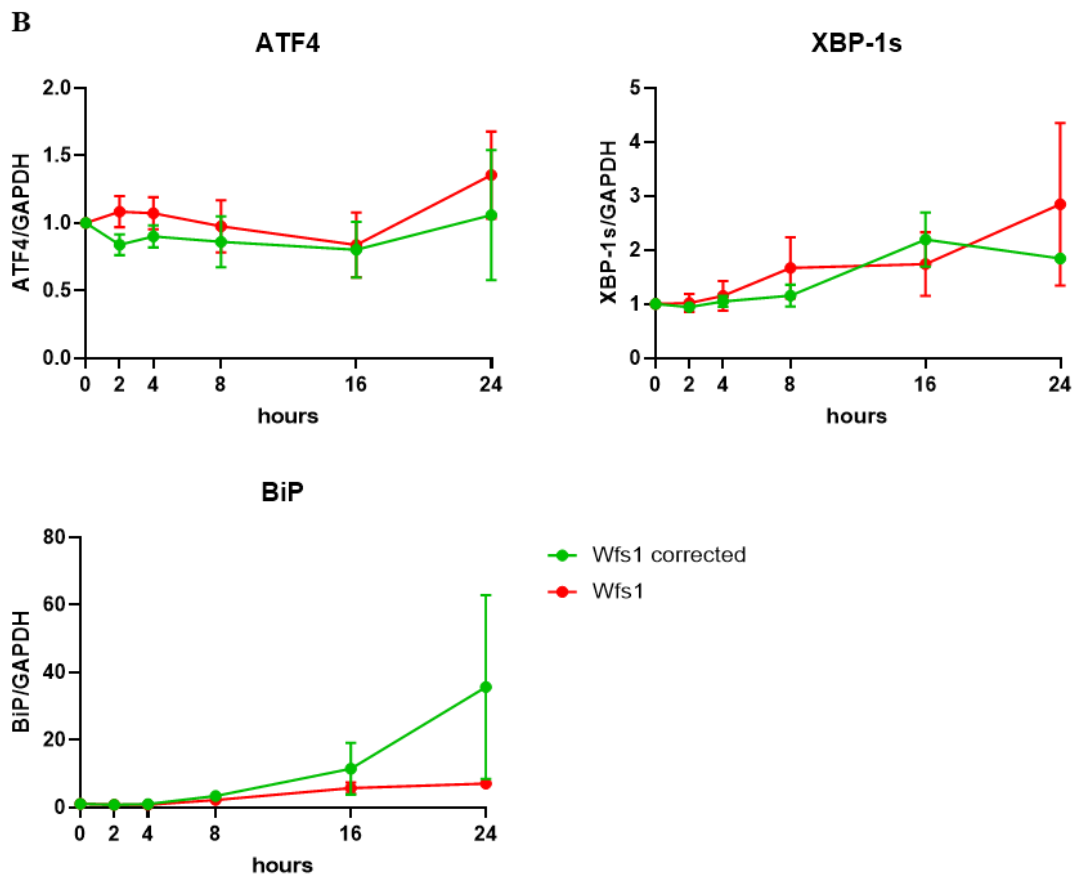


Figure 27. Timecourse of ER stress factors in iPSCs stimulated with TG.

A) Quantification of RT-qPCR experiments evaluating the indicated markers of ER stress in Wfs1 and Wfs1 corrected iPSCs after 500nM TG treatment for 0, 2, 4, 8, 16 and 24 hours. All data are expressed as a fold on 0h. Mean±SEM, N=4. B) Quantification of Western blot experiments evaluating the indicated markers of ER stress in Wfs1 and Wfs1 corrected iPSCs after 500nM TG treatment for 0, 2, 4, 8, 16 and 24 hours. All data are expressed as a fold on 0h. Mean±SEM, N=4.

5.7. ER stress in WS1-derived β cells

The poorly informative results obtained in iPSCs prompted us to move our studies in the β cell model. In this context, we were able to see more differences in the expression of UPR-related genes and proteins (**Figure 28A-B**).

Strikingly, we observed a differential regulation of the three branches of the UPR in our Wfs1 and Wfs1 corrected β cells: on one hand Wfs1 cells showed inconclusive results concerning ATF6 target genes (*HERPUD1* was higher in Wfs1 cells, but *SEL1L* was lower; both genes did not reach statistical significance), and on the other hand they expressed significantly less ATF4 and XBP1-s, both at the protein and transcript level

(*ATF4* expression almost reached statistical significance, $p=0.09$), suggesting a downregulation of the PERK and IRE1 α branches, respectively.

We also saw that ERO1 α protein is downregulated in Wfs1 β cells compared to their corrected counterpart: this is the opposite of what we previously observed in iPSCs, and suggests that an unresolved imbalance in the redox homeostasis is present in WS1-derived cells. A similar defect has already been reported in WS2 models (Wiley *et al*, 2013).

Results from Single Cell Transcriptomics confirmed a generalized alteration of the UPR in Wfs1 β cells, as illustrated in **Figure 28C**: the *ATF* family of genes was upregulated in Wfs1 corrected cells (*ATF3*, *ATF4*, *ATF5*), as well as *DDIT3* gene, coding for CHOP protein; on the contrary, *HSPA5* was significantly upregulated in Wfs1 β cells.

Furthermore, in line with our RT-qPCR data, we detected contrasting results concerning ATF6-dependent gene expression: *HERPUD1* and *HYOU1* were unchanged, *PDIA4* was significantly higher in Wfs1 cells, while *SEL1L* showed a promising trend towards an upregulation in Wfs1 corrected cells ($p=0.0631$). Collectively, these gene expression values do not support a basal alteration of the ATF6 branch of the UPR in Wfs1 β cells.

Overall, these results support the hypothesis that WS1-derived β cells already manifest molecular changes that pave the way for functional impairment. In particular, they show alterations mainly in two branches of the UPR (PERK and IRE1 α , but not ATF6) and in the redox balancing.

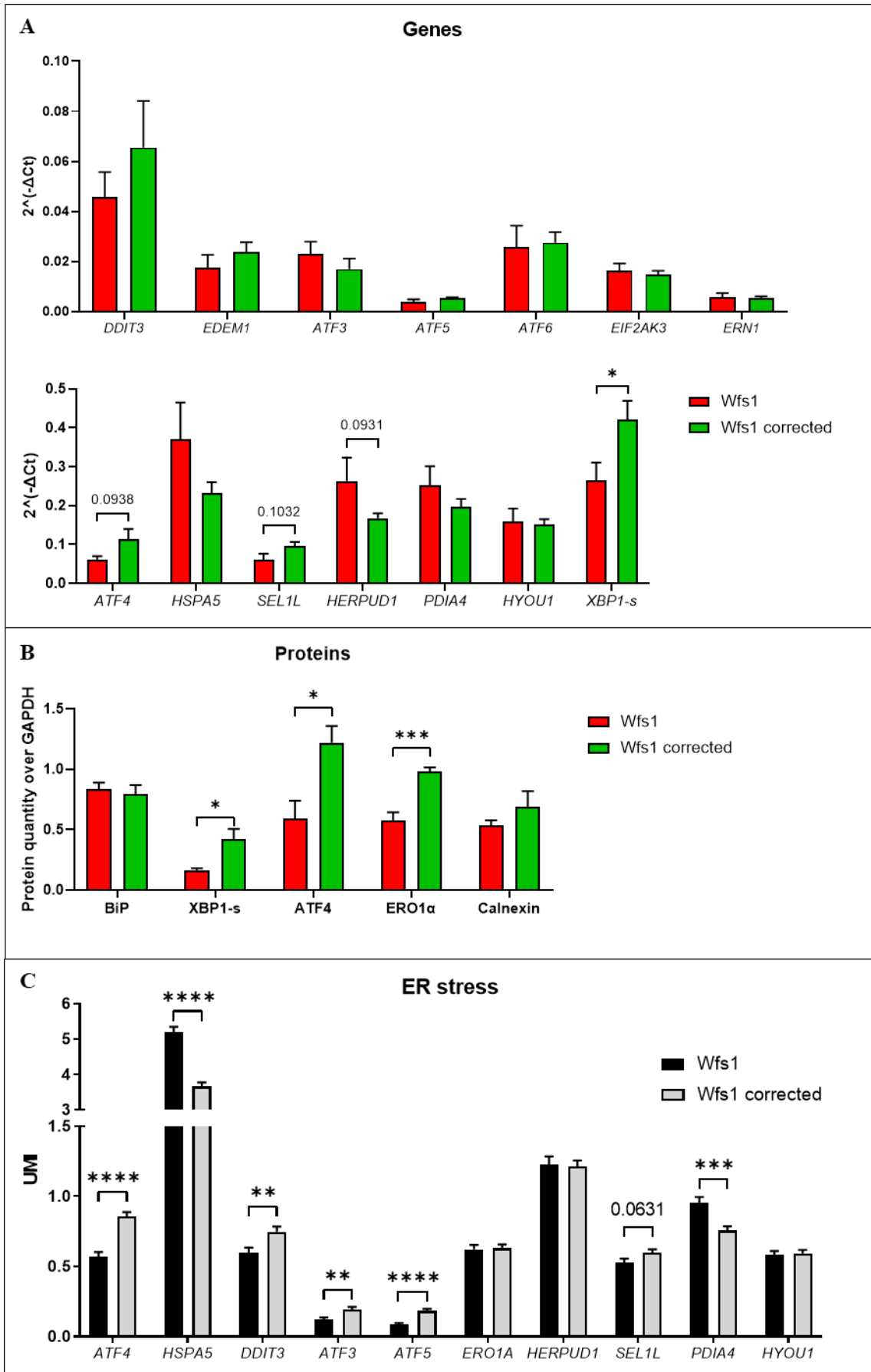


Figure 28. Gene and protein expression of ER stress markers in iPSC-derived β cells.

A) Quantification of RT-qPCR experiments evaluating the indicated markers of ER stress in *Wfs1* and *Wfs1* corrected iPSC-derived β cells. Mean \pm SEM, N=5. B) Quantification of Western blot experiments evaluating the indicated markers of ER stress in *Wfs1* and *Wfs1* corrected iPSCs. Mean \pm SEM, N=4 for *Wfs1* cells, N=5 for *Wfs1* corrected ones. * p <0.05, *** p <0.001. C) Quantification from Single Cell Transcriptomics experiment evaluating the indicated markers of ER stress in *Wfs1* and *Wfs1* corrected iPSC-derived β cells. Mean \pm SEM, N=831 for *Wfs1*, N=1140 for *Wfs1* corrected; ** p <0.01, *** p <0.001, **** p <0.0001.

These data encouraged us to test if stress induction could further exacerbate the differences in response between the two genotypes. To this aim, we used as stressors TG and inflammatory cytokines (IL1 β 50U/ml +IFN γ 1000U/ml + TNF α 10ng/ml, shortened as IL): while TG would recapitulate a classical ER stress stimulus, as well-known in literature, we chose cytokines in light of a recent paper reporting an increase in inflammatory signature in the serum of our patient (Panfili *et al*, 2021). In this line, the concept of inflammatory status in WS1 is starting to be explored and recognized more (Morikawa *et al*, 2022).

As presented in the introduction, there is reasonable evidence supporting the use of Liraglutide in WS1: this stems both from many preclinical studies and from the clinical trial of our own group, in which the patient presented in this thesis was included with good results (Frontino *et al*, 2021).

In light of the positive clinical outcome, we postulated that similar findings could also be uncovered in our iPSC-based β cell model. Our main aim in using Liraglutide would be to confirm that its administration is beneficial in the tissue of interest for the condition, and possibly to elucidate which molecular mechanisms mediate the phenotypic amelioration in the patient.

Therefore, we investigated if Liraglutide co-treatment with our stressors of choice could prevent or at least modify UPR upregulation in target cells; especially, we wondered if it could reestablish a similarity in response in *Wfs1* and *Wfs1* corrected cells (**Figure 29**).

First, we recognized that *in vitro* treatment with 50nM of TG was able to trigger ER stress in multiple conditions, but the 8h treatment was the most differential in the two

genotypes considered: in fact, we observed a significant overexpression of *HSPA5* and *DDIT3* transcripts and of BiP protein in Wfs1 β cells compared to the corrected ones ($p < 0.05$). After 16h of treatment, instead, we observed a trend towards an higher activation of the considered pathways in Wfs1 corrected cells, although not statistically significant, suggesting that UPR activation is stringently activated in time and a different kinetic is present in Wfs1 versus Wfs1 corrected cells.

Liraglutide treatment together with the stressor nullified any difference in UPR upregulation between the two lines, by promoting the transcription of *HSPA5* and the inhibition of *DDIT3*. This suggests that Liraglutide increases chaperones (namely BiP) and lowers a proapoptotic factor (CHOP), which should be beneficial for cell homeostasis and survival.

We also observed that inflammatory cytokines (IL) treatment did not trigger ER stress response in β cells, and accordingly, co-treatment with Liraglutide did not alter the ER stress response profile, neither at the transcriptional nor at the protein level. We know from literature that IL treatment can trigger ER stress response, but only the PERK branch: however, this is not necessary for IL-induced cell death, and attenuation of ER stress is not sufficient to protect β cells from undergoing apoptosis (Åkerfeldt *et al*, 2008). As a consequence, we could not assert that a lack of UPR upregulation meant our cells were not affected by the treatment, also because attentive observation of the treated and untreated samples revealed an apparent distress in the first group (data not shown).

Overall, our data show that Wfs1 β cells have an impaired UPR expression already at the basal level, which is reflected in an aberrant response to ER stress induction by TG; Liraglutide use can modulate and shrink the differences between Wfs1 and Wfs1 corrected cells, acting on crucial mechanisms implicated in the switch between cell death and survival.

These results prompted us to investigate other mechanisms which underlie WS1 pathogenesis and could benefit from Liraglutide administration, such as autophagy.

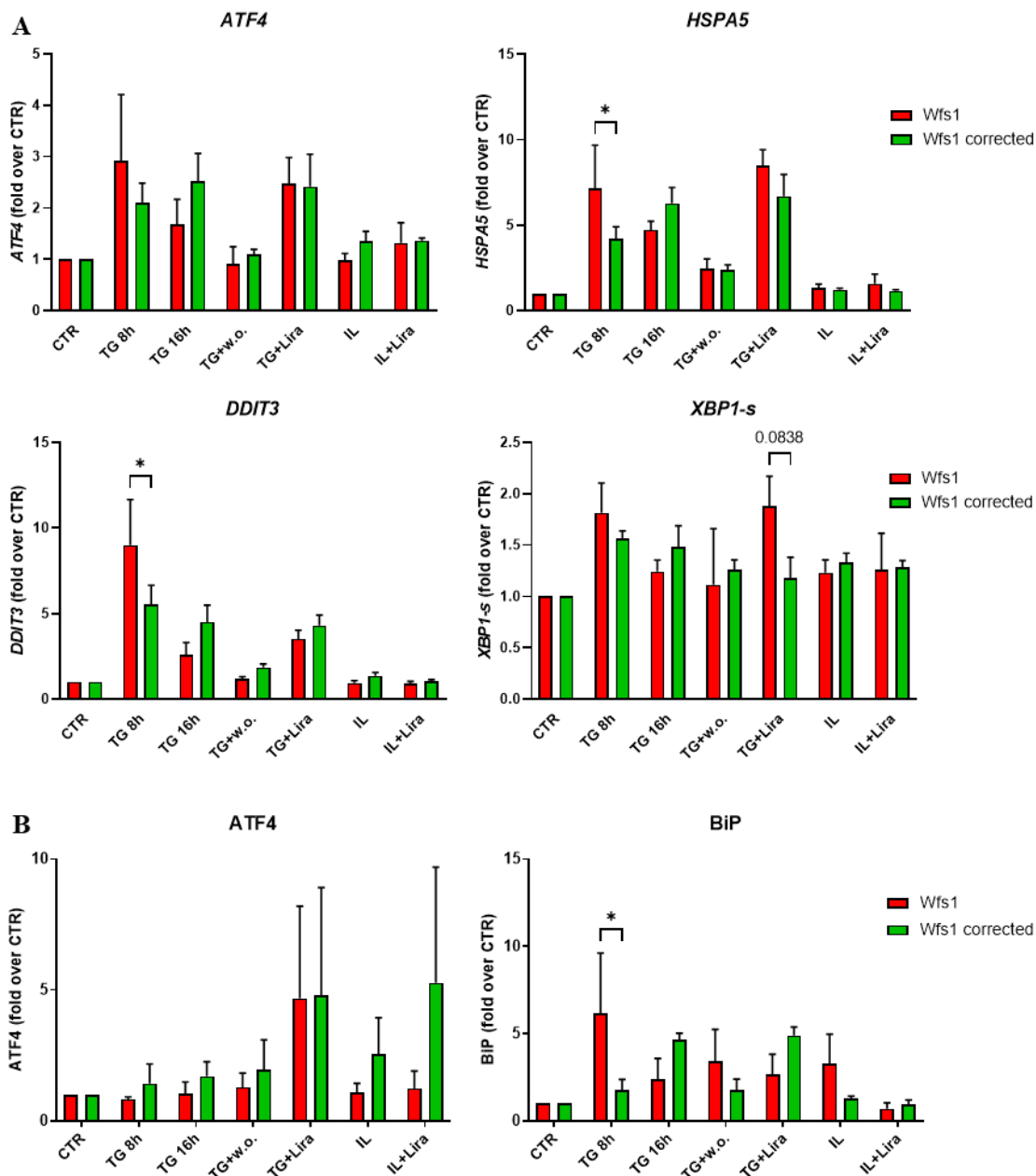


Figure 29. ER stress response to TG and inflammatory cytokines in β cells.

ER stress was induced as follows: 50nM TG treatment for the indicated time, with or without Liraglutide 1 μ M, or inflammatory interleukins (IL1 β 50U/ml + IFN γ 1000U/ml + TNF α 10ng/ml for 48h), with or without Liraglutide 1 μ M. All data are expressed as a fold on CTR.

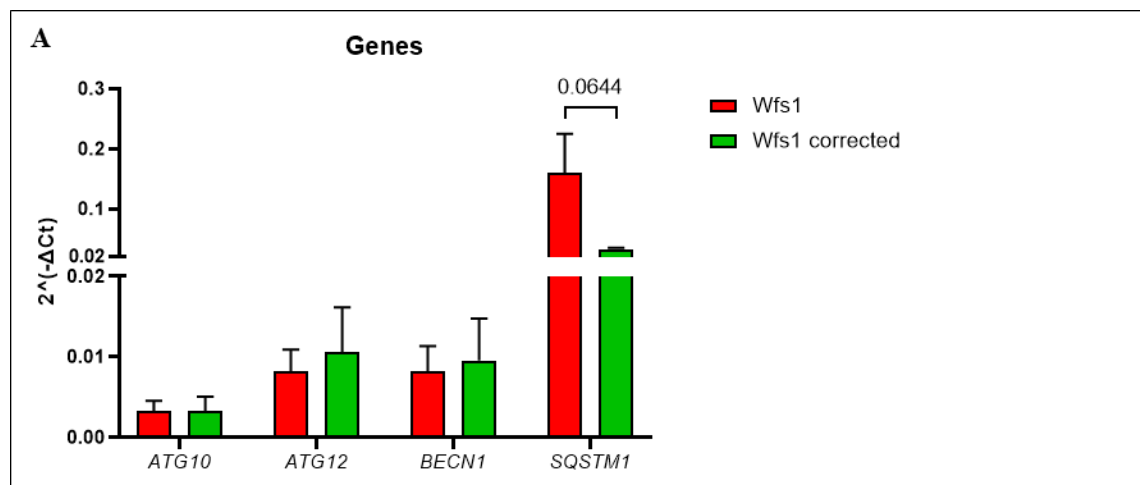
A) Quantification of RT-qPCR experiments evaluating the indicated markers of ER stress in Wfs1 and Wfs1 corrected β cells. Mean \pm SEM, N>3; *p<0.05. B) Quantification of Western blot experiments evaluating the indicated markers of ER stress in Wfs1 and Wfs1 corrected β cells. Mean \pm SEM, N>3; *p<0.05.

5.8. Autophagy in WS1

As discussed in the introduction, at the beginning of the project we had the running hypothesis that autophagy could constitute a novel piece of the puzzle for WS1 pathogenesis. It had already been demonstrated for WS2 and proof of the interconnection between ER stress and autophagy in T2D is growing at a fast pace (Gonzalez *et al*, 2011; Song *et al*, 2018); such elements prompted us to examine whether autophagy was altered in our model of WS1.

We started our investigation on iPSCs. We did not find alterations of ER stress signature in this model, therefore we did not expect to detect significant differences: considering unstimulated conditions, we only measured statistically not significant trends indicating a higher expression of *SQSTM1* gene and a downregulation of LC3 active form in Wfs1 cells compared to the corrected counterpart (**Figure 30A-B**).

We then wondered if ER stress induction could have an impact on autophagy, as reported in literature in other models (Rashid *et al*, 2015); our timecourse experiment indicates that, in iPSCs, UPR activation also triggers an induction of autophagy, but there are no major statistical differences in the process between the genotypes. However, we noted that TG induces transcription of *SQSTM1* gene already at 16h and phosphorylation of Beclin after 24h of treatment in Wfs1 corrected cells. Meanwhile, Wfs1 iPSCs never change Beclin phosphorylation status or *SQSTM1* gene transcription to the same extent, in spite of the drug: this could underlie a differential sensitivity to stress, or an impaired ability to trigger autophagic flux in response to stimuli (**Figure 30C-D**).



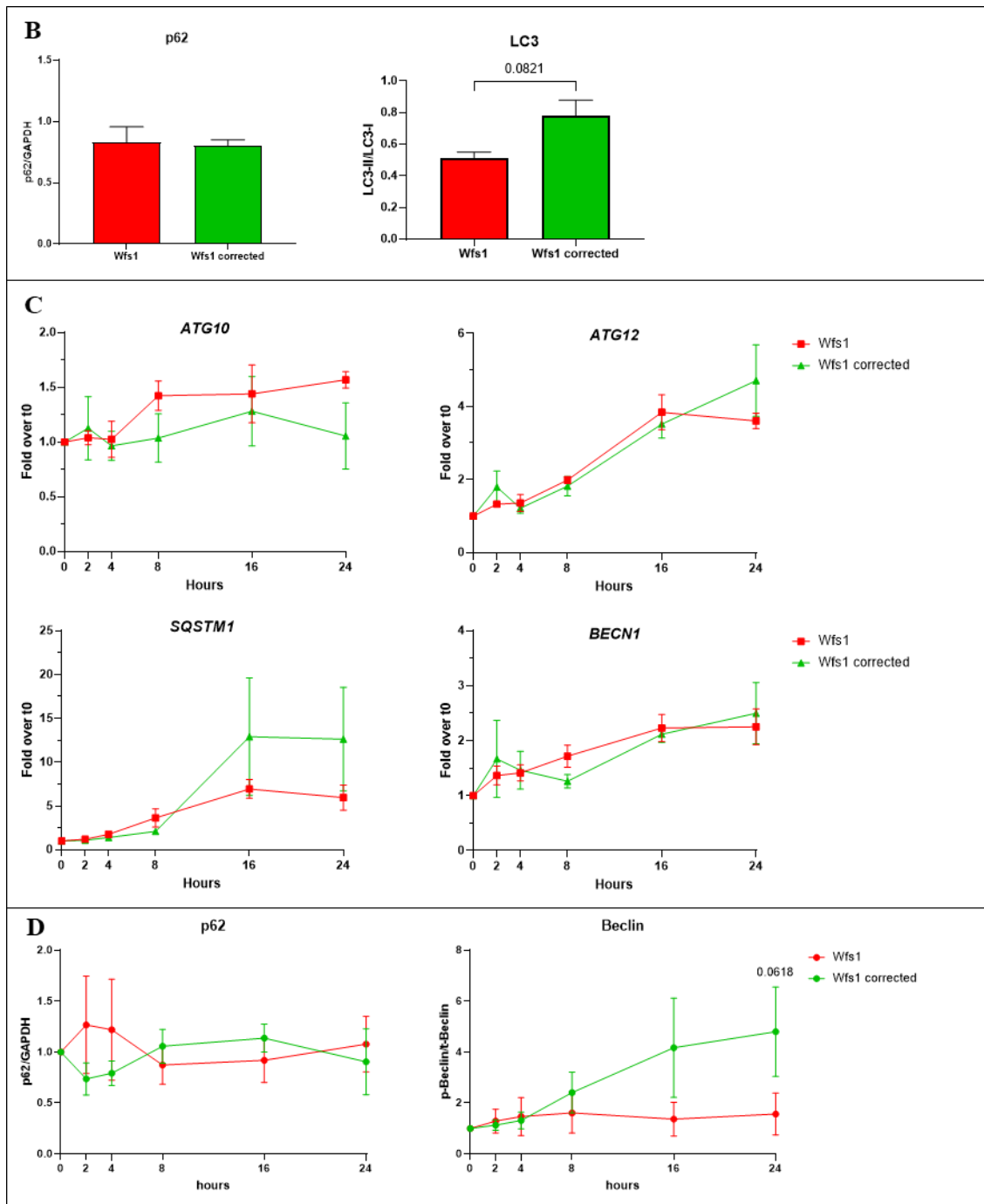


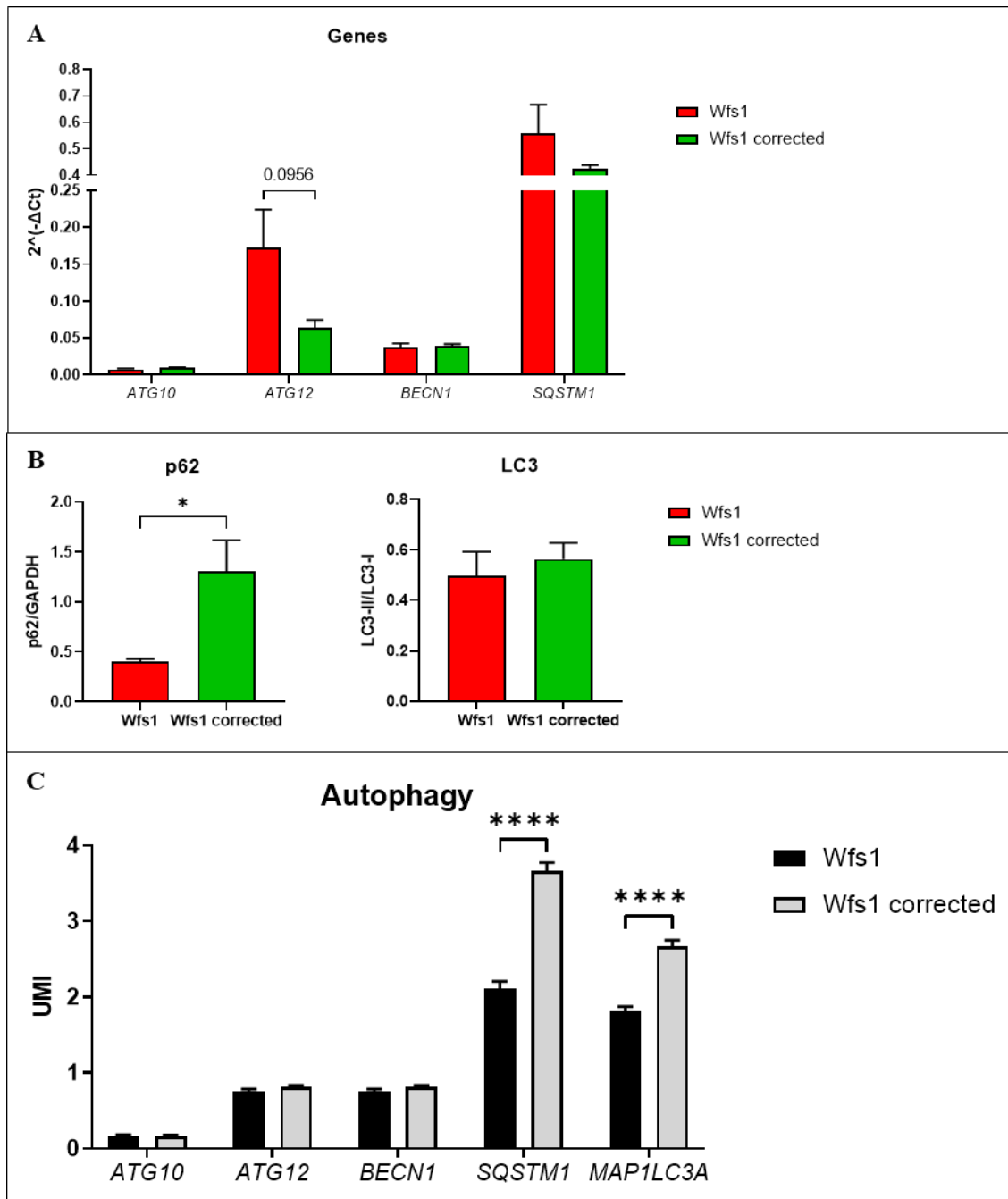
Figure 30. Study of autophagy markers in iPSCs, in basal conditions and upon stress induction.

A) Quantification of RT-qPCR experiments evaluating the indicated markers of autophagy in *Wfs1* and *Wfs1* corrected iPSCs. Mean \pm SEM, N=4. B) Quantification of Western blot experiments evaluating the indicated markers of autophagy in *Wfs1* and *Wfs1* corrected iPSCs. Mean \pm SEM, N=3. C) Quantification of RT-qPCR experiments evaluating the indicated markers of autophagy upon exposure to 500nM TG for 0, 2, 4, 8, 16 and 24h; values are expressed as a fold over 0h. Mean \pm SEM, N=4. D) Quantification of Western blot experiments evaluating the indicated markers of autophagy upon exposure to 500nM TG for 0, 2, 4, 8, 16 and 24h; values are expressed as a fold over 0h. Mean \pm SEM, N=4.

After iPSCs, we moved our attention to iPSC-derived β cells. We first measured basal levels of relevant markers, and subsequently we considered the same experimental setting as in ER stress studies, in order to see if UPR activation could trigger or inhibit autophagy.

Concerning basal levels, we saw approximately three times more p62 protein in Wfs1 corrected cells compared to Wfs1, but no striking differences in the other considered markers (**Figure 31A-B**). Accelerated turnover of p62 could indicate a sustained autophagic flux in Wfs1 β cells, similar to what was demonstrated elsewhere (Crouzier *et al*, 2022), but low p62 production could on the contrary underlie a scarce activation of the pathway. Single Cell Transcriptomics highlighted a strong upregulation of *SQSTM1* and *MAP1LC3A*, coding for LC3 protein, in Wfs1 corrected cells: a similar result supports the second hypothesis and suggests an impaired molecular induction of the autophagic flux. The results are presented in **Figure 31C**.

After stress induction, we measured again relevant proteins and genes: we saw a statistically significant difference in response to 8h of treatment with TG, when Wfs1 β cells upregulated by two fold *SQSTM1*, while Wfs1 corrected ones showed no increase at all. In general, Liraglutide co-treatment seemed to upregulate all autophagy-related genes in Wfs1 cells more than in the corrected counterpart. This could suggest that, in Wfs1 β cells, autophagy is triggered to try and escape resolvable ER stress, while corrected ones rely upon different mechanisms, or at least do not need to actively transcribe new factors in light of their higher basal levels (**Figure 31D-E**).



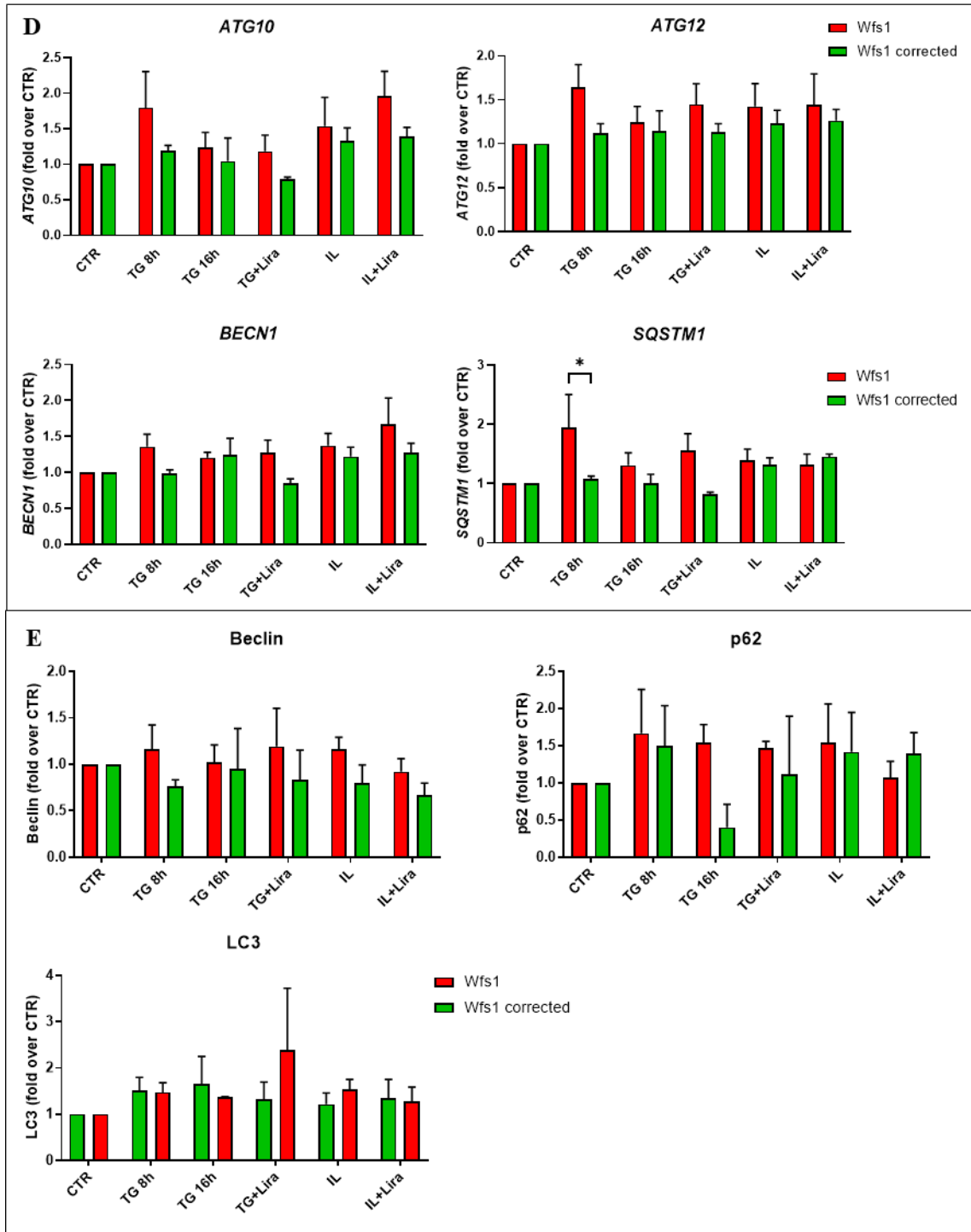


Figure 31. Study of autophagy markers in β cells, in basal conditions and upon stress induction.

A) Quantification of RT-qPCR experiments evaluating the indicated markers of autophagy in *Wfs1* and *Wfs1* corrected β cells. Mean \pm SEM, N=5. B) Quantification of Western blot experiments evaluating the indicated markers of autophagy in *Wfs1* and *Wfs1* corrected β cells. Mean \pm SEM, N=4. C) Quantification from Single Cell Transcriptomics experiment evaluating the indicated markers of autophagy in *Wfs1* and *Wfs1* corrected iPSC-derived β cells. Mean \pm SEM, N=831 for *Wfs1*, N=1140 for *Wfs1* corrected; **** p <0.0001.

In D) and E), ER stress was induced as follows: 50nM TG treatment for the indicated time, with or without Liraglutide 1 μ M, or inflammatory interleukins (IL1 β 50U/ml +IFN γ 1000U/ml + TNF α 10ng/ml for 48h), with or without Liraglutide 1 μ M. All data are expressed as a fold on CTR.

*D) Quantification of RT-qPCR experiments evaluating the indicated markers of autophagy in Wfs1 and Wfs1 corrected β cells. Mean \pm SEM, N>3; *p<0.05. E) Quantification of Western blot experiments evaluating the indicated markers of autophagy in Wfs1 and Wfs1 corrected β cells. Mean \pm SEM, N>2.*

5.9. Ca⁺⁺ imaging

Our data up until this point suggest that it would be better to investigate WS1-related pathogenesis directly in β cells, as undifferentiated iPSCs showed limited effectiveness in mimicking some processes relevant for the disease. Therefore, to further investigate the molecular mechanisms that could lead to cell dysfunction in WS1, we sought to study if Ca⁺⁺ dynamics were altered in Wfs1 β cells compared to the corrected ones.

To do so, we set up a protocol including a pretreatment phase, during which we administered no stressor or TG to the cells; then, after 16 hours, cells were washed, loaded with Fluo-4, stimulated with secretagogues, and their Ca⁺⁺ currents were recorded (**Figure 32A**).

We obtained detailed videos of cell response as exemplified in **Figure 32B-C**, which could be quantified to obtain measurements of intensity of the spikes.

As a control, we stimulated both Wfs1 and Wfs1 corrected cells with buffer only. We adapted our stimulation protocol until buffer stimulation did not trigger any fluorescence change due to mechanical stress, apart from some minor background (data not shown), and this same setting was used for all the other stimuli.

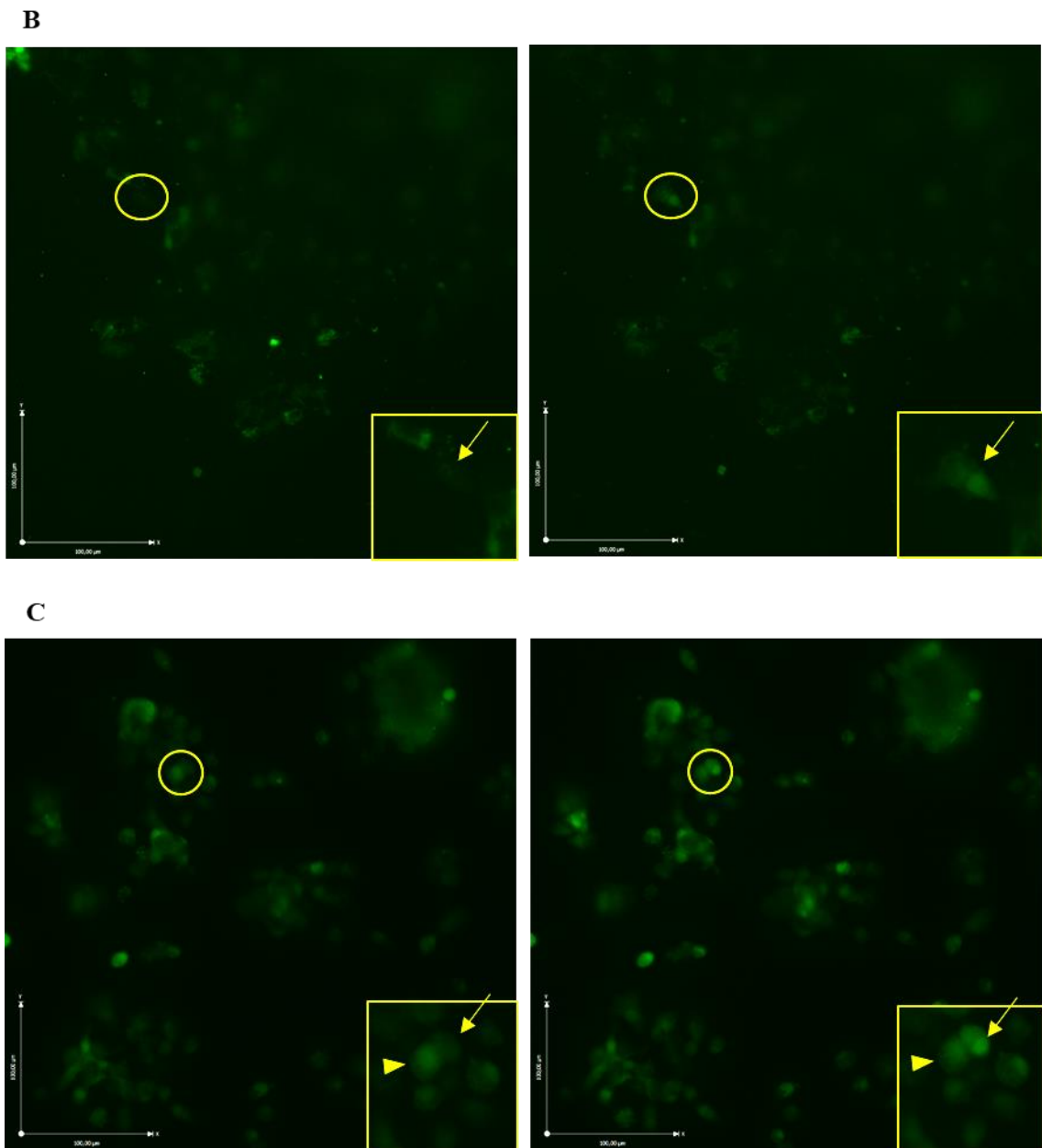
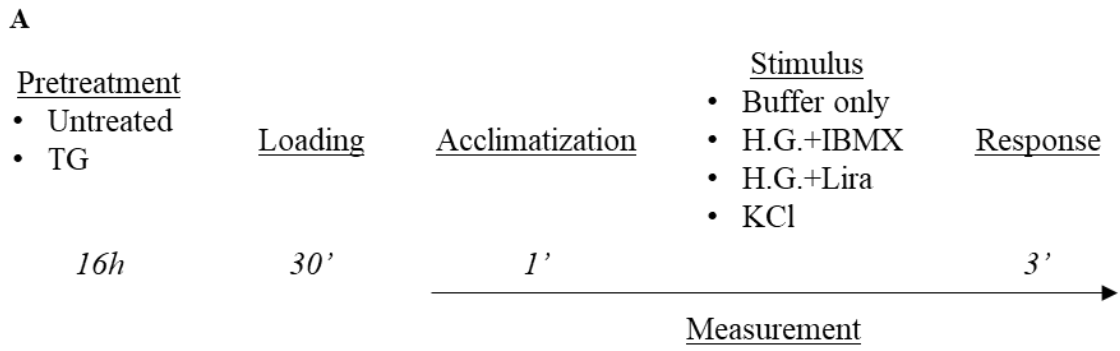


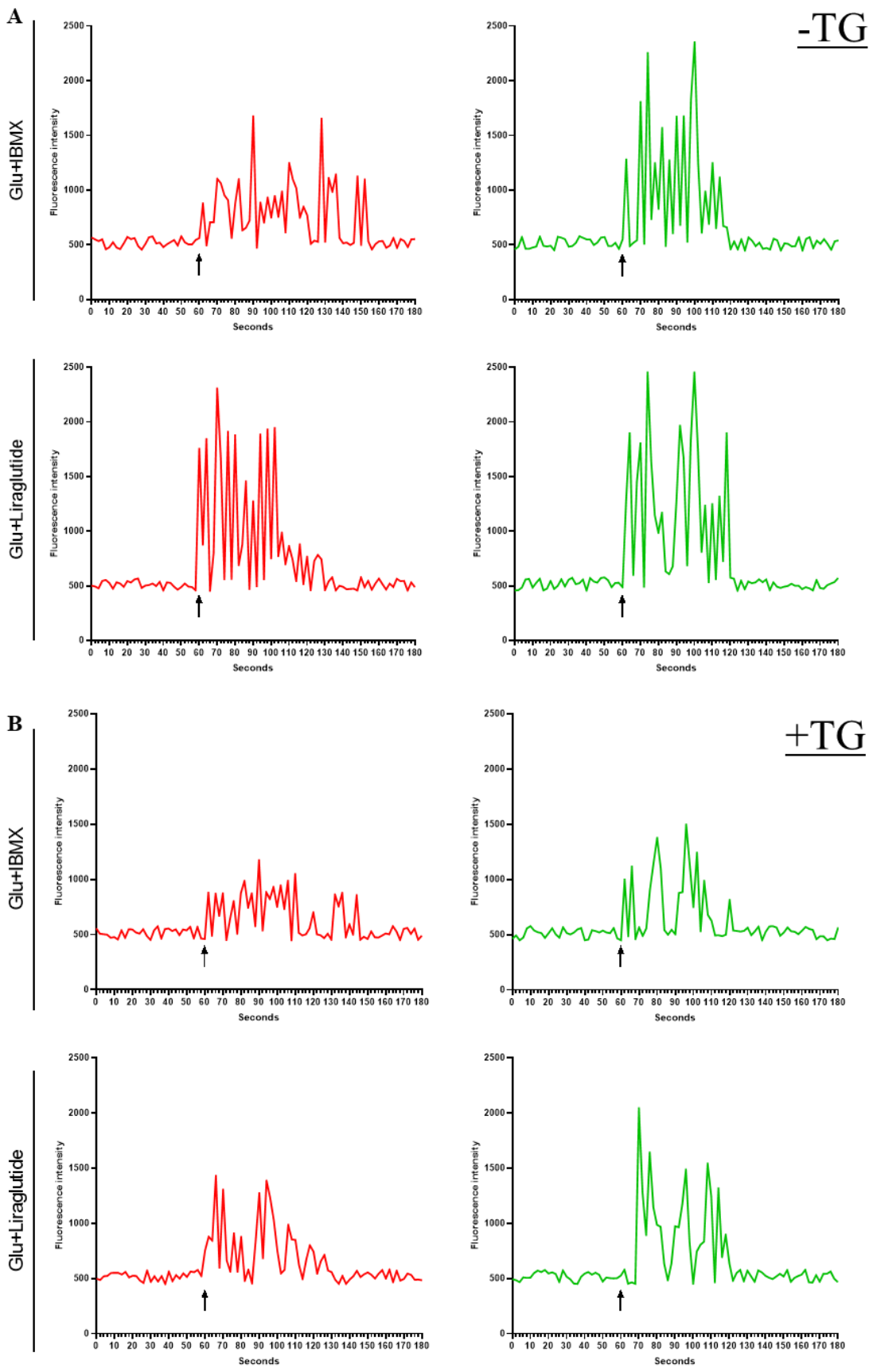
Figure 32. Experimental plan and examples of Ca⁺⁺ fluxes on differentiated iPSCs.

A) Experimental plan for Ca⁺⁺ measurements, illustrating all the possible pretreatments and stimuli. B-C) Frames from two of the videos taken on stimulated cells, showing t0 (left) and t70 (right), after administration of glucose+IBMX at t60; scalebar is 100µm. In the yellow square, enlargement of the images in the yellow circle, showing more clearly non-responder cells (triangle) and responders (arrow). B) is Wfs1 cells, C) is Wfs1 corrected ones.

Our results indicate that, in unstressed conditions, Wfs1 cells stimulated with a control solution (high glucose+IBMX) already show impairments in the shape of response spikes. The mean intensity is lower than corrected cells, and they also display a reduced control in time: while corrected cells have a sort of synchronicity in their fluxes and collectively stop responding after the first minute, Wfs1 ones never manage to synchronize enough to give rise to sharp, defined peaks, and furthermore they seem to keep fluxing for a longer time. Liraglutide administration in an acute setting, together with glucose, realigns the two genotypes and corrects the flaws seen in Wfs1 cells, although a tendency to persist fluxing longer than the corrected counterpart is still noticeable (**Figure 33A**).

TG pretreatment of cells induced a general reduction in peak intensity, which could be only partially reversed in Wfs1 corrected cells, and even less in Wfs1 ones. Collectively, TG pretreatment was not as informative as we hoped, since it affected both Wfs1 and Wfs1 corrected cells beyond what could be recovered by acute Liraglutide stimulation (**Figure 33B**).

KCl addition as a control demonstrated that all cells respond by fluxing Ca⁺⁺ in a comparable way: this result suggests that Wfs1 cells contain a normal quantity of Ca⁺⁺ and retain the ability to shuttle it between organelles. Therefore, any differences that may arise upon stimulation are related to its correct dynamicity only (**Figure 33C**).



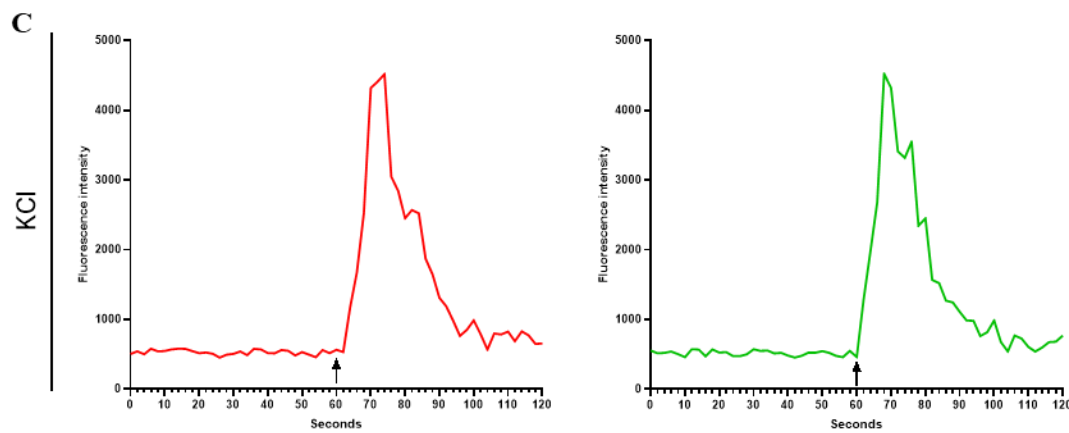


Figure 33. Spike profiles of Ca^{++} measurements in *Wfs1* and *Wfs1* corrected β cells.

A) Ca^{++} response of *Wfs1* and *Wfs1* corrected iPSC-derived β cells stimulated with glucose+IBMX or glucose+1 μ M Liraglutide. Mean, N=20 cells from 2 experiments. B) Ca^{++} response of *Wfs1* and *Wfs1* corrected iPSC-derived β cells, after pretreatment for 16h with 50nM TG, stimulated with glucose+IBMX or glucose+1 μ M Liraglutide. Mean, N=20 cells from 2 experiments. C) Ca^{++} response of *Wfs1* and *Wfs1* corrected iPSC-derived β cells stimulated with 30mM KCl. Mean, N=20 cells from 2 experiments.

In all the figure, arrows at 60 seconds indicate application of the stimulus; *Wfs1* corrected cells are always in green, *Wfs1* ones in red.

To investigate whether the deficiencies in Ca^{++} response in *Wfs1* cells were due to an abnormal expression of Ca^{++} -related channels, we quantified the gene expression of *CACNA1D* (calcium voltage-gated channel subunit α 1 D). Cav1.3, coded by the *CACNA1D* gene, is a subunit of a Ca^{++} channel mediating granule exocytosis; interestingly, *CACNA1D* transcript is reduced in T2D patients and correlates with impaired glucose-stimulated insulin release (Reinbothe *et al*, 2013). A recent study in mice showed its requirement in glucose-induced β cell voltage-dependent activation and maintenance of β cell mass and insulin release (Theiner *et al*, 2022). Intriguingly, we measured a significant reduction of about 50% in the expression levels of *CACNA1D* (**Figure 34A**).

Investigation via Single Cell Transcriptomics of other related genes confirmed a strong downregulation of both *CACNA1D* gene and its paralogue *CACNA1C* in *Wfs1* β cells, and an upregulation of *RGS4*, as seen in **Figure 34B**. *RGS4* codes for the RGS4 protein, an inhibitor of insulin secretion and Ca^{++} signalling in β cells, acting on muscarinic receptors for acetylcholine (De Azua *et al*, 2010).

Collectively, our data indicate that Wfs1 β cells display an altered Ca^{++} metabolism: this may underlie defects in a strictly interconnected mechanism, insulin secretion.

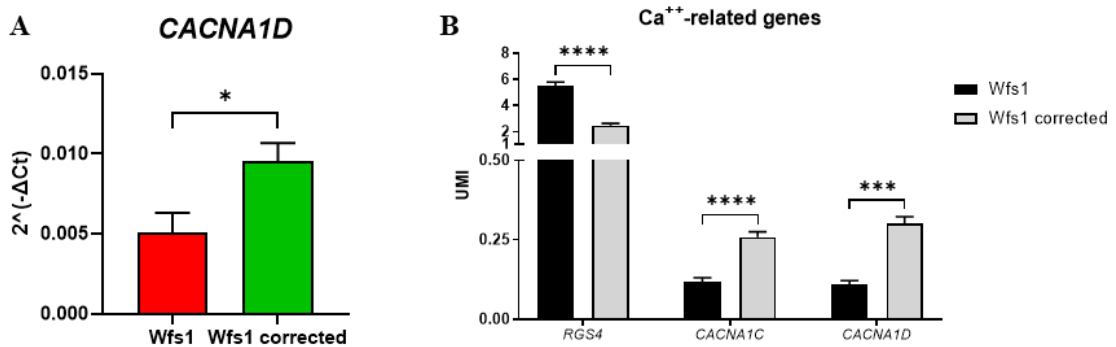


Figure 34. Gene expression of Ca^{++} -related genes.

A) RT-qPCR quantification of gene expression for *CACNA1D* in iPSC-derived β cells. Mean \pm SEM, N=6 for Wfs1, N=5 for Wfs1 corrected; * p <0.05. B) Quantification from Single Cell Transcriptomics experiment evaluating the indicated Ca^{++} -related genes in Wfs1 and Wfs1 corrected iPSC-derived β cells. Mean \pm SEM, N=831 for Wfs1, N=1140 for Wfs1 corrected; **** p <0.0001.

5.10. Insulin secretion

The most important function for a β cell is its ability to secrete insulin when challenged with an appropriate stimulus: therefore, we decided to test the insulin secretory ability of our differentiated β cells by a dynamic perfusion system. Furthermore, we wondered if acute stimulation with Liraglutide could potentiate insulin secretion in Wfs1 and Wfs1 corrected cells: we knew from literature and from our own preliminary data that Liraglutide addition to the high glucose stimulus boosted insulin secretion to more than 150% in primary human islets (**Figure 35A-B**).

Both primary human islets and iPSC-derived cells were kept in low glucose (0.5mM for differentiated cells, 2mM for human islets) and then challenged with two stimuli, high glucose concentration (11mM for differentiated cells, 20mM for human islets) and subsequently a potent depolarizing agent (KCl 30mM): the first stimulus tests the ability of the sample to respond in a physiological setting, while the second causes a massive membrane depolarization and releases all intracellular granules.

We could not compare glucose-only stimulated iPSC-derived β cells, as they poorly respond to high glucose alone irrespectively of the genotype (data not shown): therefore, we considered as our positive control of secretion the insulin release mediated by high

glucose plus IBMX, a phosphodiesterase inhibitor commonly used to boost insulin secretion. As seen in **Figure 35C-D**, both Wfs1 and Wfs1 corrected cells are able to sense secretagogues stimulation and respond accordingly.

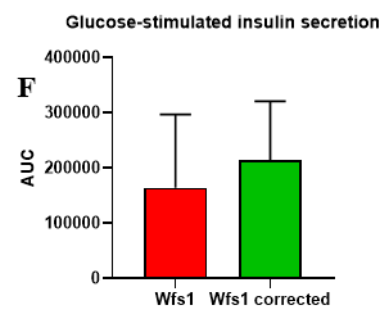
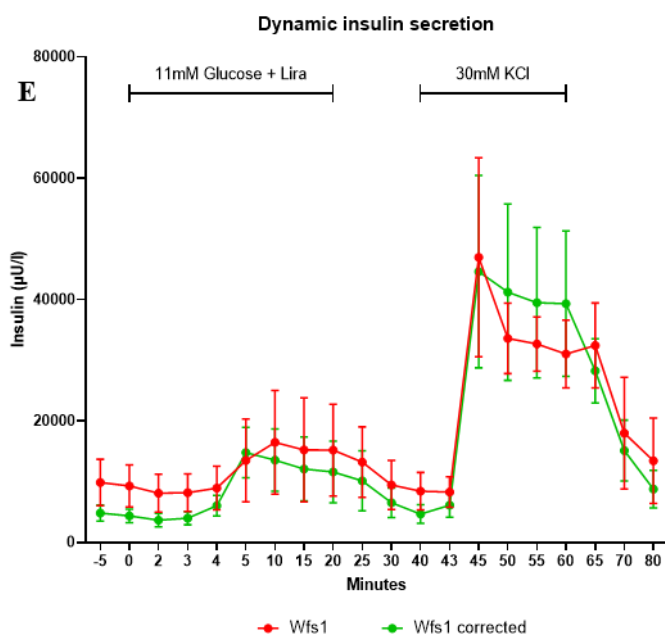
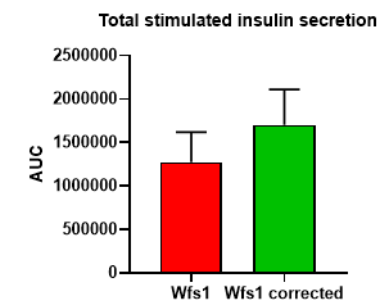
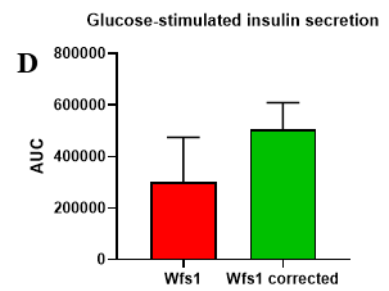
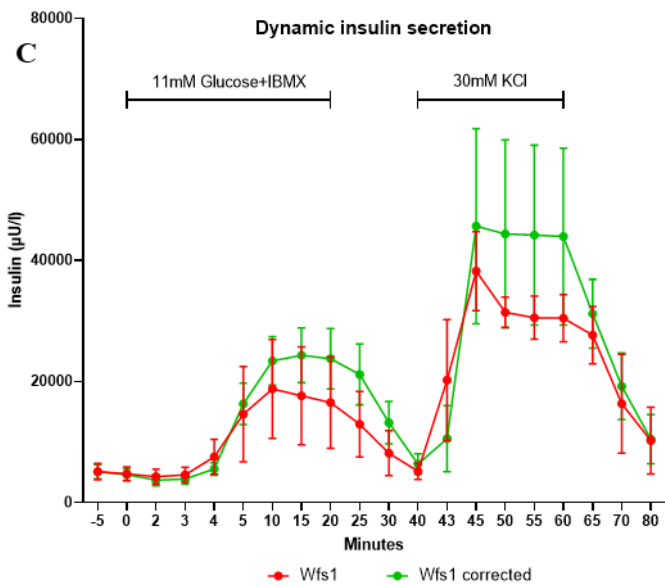
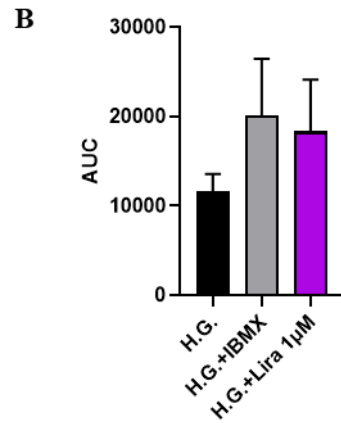
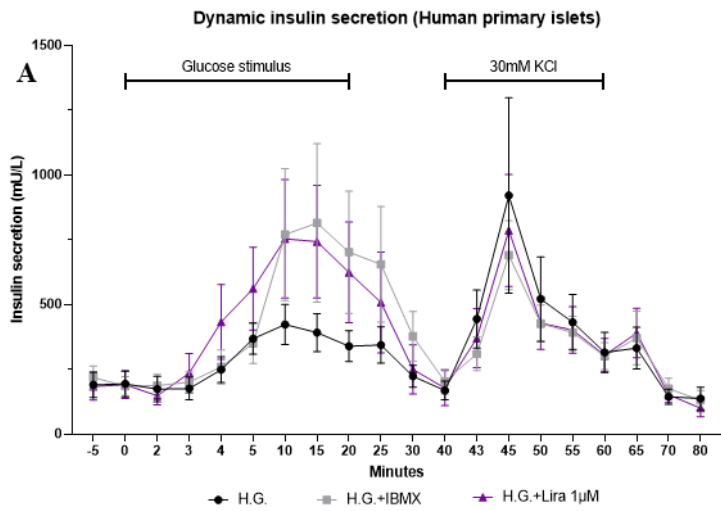
Wfs1 cells seem to secrete less insulin in comparison to the corrected counterpart: this is true when taking into account glucose-stimulated secretion (-40%), but also total secretion independent of the stimulus (-25%), both point-to-point and as a whole. The difference is not statistically significant due to high variability of the technique, but it still suggests an inferior functionality of Wfs1 cells or maybe a lower insulin content, as previously reported in literature (Shang *et al*, 2014; Maxwell *et al*, 2020).

We repeated the previous experiment of dynamic perfusion adding 1 μ M of Liraglutide in the high glucose stimulus instead of IBMX. Glucose-stimulated insulin secretion in the Liraglutide group was lower than in the IBMX group, which is in line with the molecular effect of the two compounds and with the data from primary human islets: our hypothesis, however, is that Liraglutide treatment can not only act on the secretory ability, but also on general homeostasis of the cells, particularly in the Wfs1 ones (**Figure 35E-F**).

As seen in **Figure 35G**, our results suggest that Liraglutide reduces the gap in insulin secretion between the two β cell lines by inducing a more beneficial effect on Wfs1 cells than in Wfs1 corrected ones; the mechanism for this selective advantage is unknown.

We know from literature that stressor application affects the secretory ability of β cells, both iPSC-derived and from primary islets. However, we wondered if Wfs1 ones would be more sensitive to chronic stress induction.

Our preliminary data highlight a severe effect of TG on both differentiated cell lines in total secreted insulin, more than in glucose-stimulated one (**Figure 35H**): this is compatible with a general effect on cell physiology that leads to decreased insulin production, as seen by the low rate of secretion even after KCl stimulation. Chronic addition of Liraglutide together with TG was not able to rescue the parameter, while the co-treatment plus acute administration of Liraglutide proved more effective, even if a greater impairment could still be seen in Wfs1 cells compared to the corrected ones (**Figure 35I**). However, more replicates are needed to determine if such effect is true.



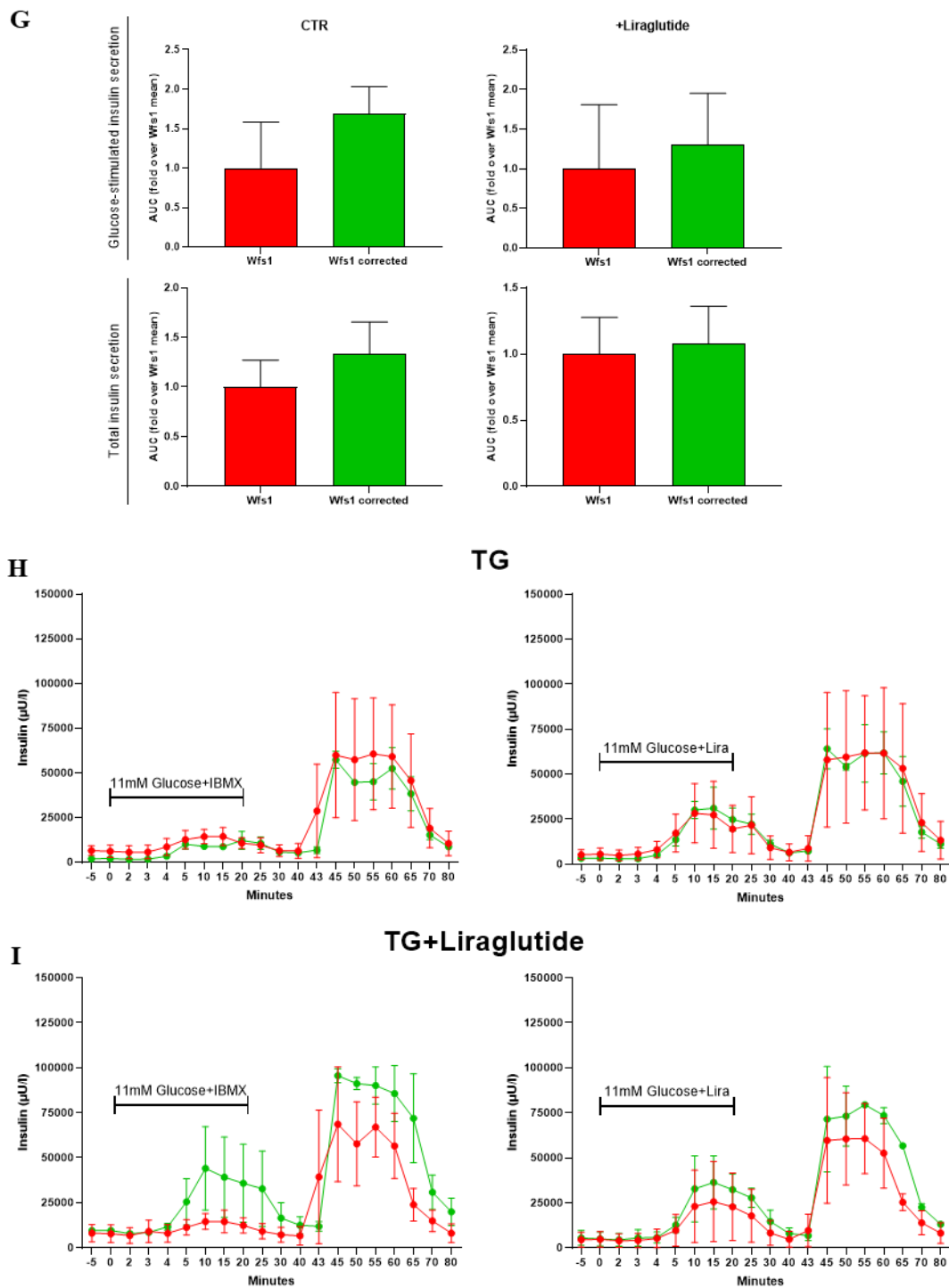


Figure 35. Insulin secretion quantification after dynamic perfusion.

In figures A-G: mean \pm SEM, N=3 for Wfs1, N=5 for Wfs1 corrected, N=6 for primary human islets.

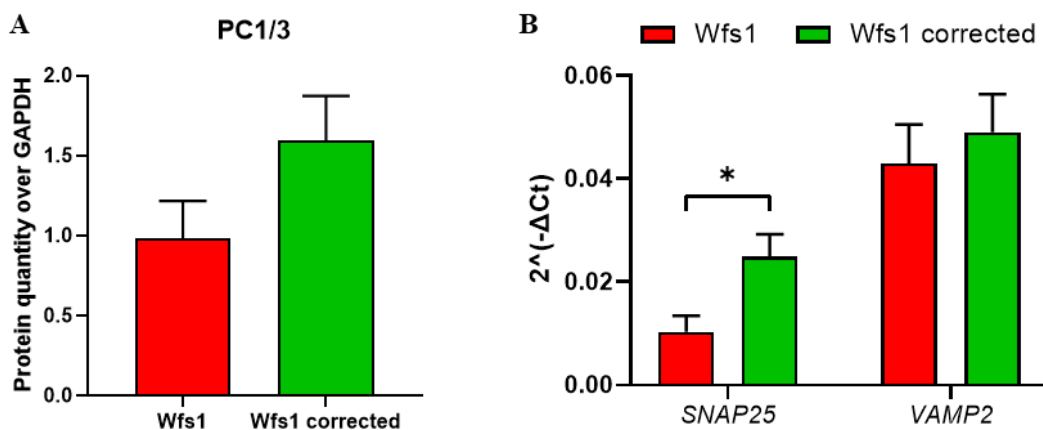
A) Insulin secretion in primary human islets, stimulated with high glucose alone or in combination with IBMX or Liraglutide $1\mu\text{M}$. B) Quantification of the AUC for the high glucose stimulation (minutes 3 to 40) as seen in A). C) Plot of insulin secretion during dynamic perfusion of the indicated secretagogues in iPSC-derived β cells. D) Quantification of the area under the curve (AUC) for the high glucose

+ IBMX stimulation (minutes 3 to 40) and for the whole curve (minutes 0 to 80), as seen in C). E) Plot of insulin secretion during dynamic perfusion of the indicated secretagogues. F) Quantification of the AUC for the high glucose + Liraglutide 1 μ M stimulation (minutes 3 to 40) and for the whole curve (minutes 0 to 80), as seen in E). G) Comparison of the glucose-stimulated and total insulin secretion in the two lines, with and without Liraglutide, expressed as a fold over Wfs1 values. H-I) Quantification of insulin secretion after chronic exposure to either TG (H) or TG+Liraglutide (I). Mean \pm SEM, N=3 for TG pretreatment, N=2 for TG+Liraglutide pretreatment.

To check if we could determine a molecular cause for the quantitative deficit in insulin secretion of Wfs1 β cells, we quantified relevant factors related to the process: PC1/3 enzyme and the expression of SNAP25 and VAMP2 genes (**Figure 36A-B**).

We observed a 30% reduction by Western blot in PC1/3 enzyme, which is crucial for proinsulin processing into insulin, although this was not statistically significant (p=0.15). Furthermore, we measured a statistically significant reduction in SNAP25 transcript in Wfs1 β cells compared to the corrected counterpart. SNAP25 and VAMP2 proteins are implicated in granule docking for secretion, the first one bound to the plasma membrane and the second one on insulin granules (Hou *et al*, 2009): an alteration in this balancing could explain the difference in secretory efficiency of Wfs1 cells.

Single Cell Transcriptomics confirmed the hypothesized alterations: we detected a marked downregulation of PCSK1 (coding for PC1/3 enzyme) and SNAP25 genes, while VAMP2 almost reached statistical significance, but the difference between the two lines is so thin that it probably does not imply a biological meaning (**Figure 36C**).



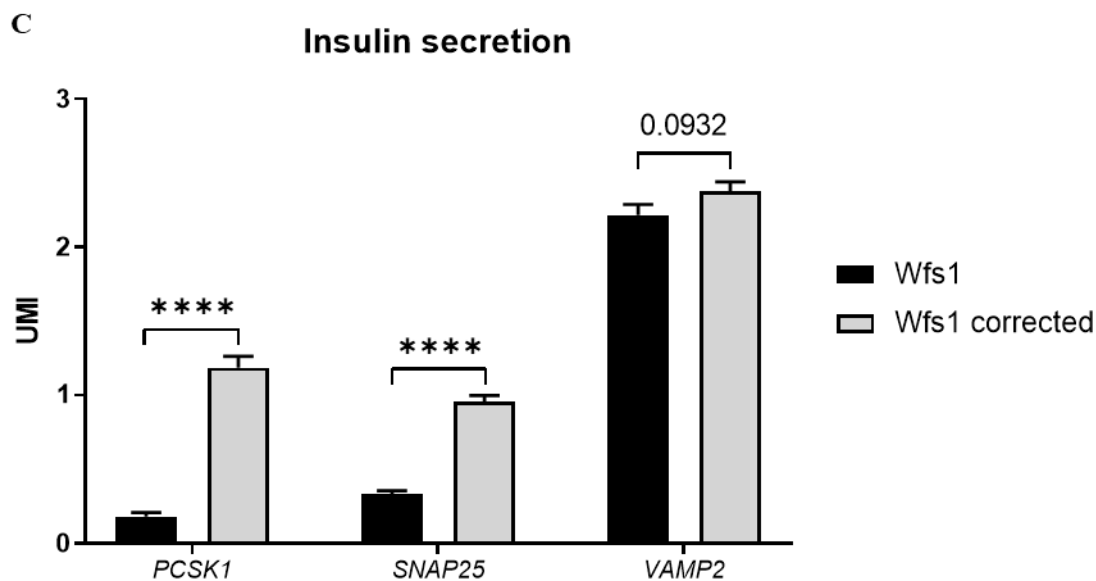


Figure 36. Quantification of secretion-related factors.

A) Protein quantification of PC1/3 enzyme. Mean±SEM, N=4. B) RT-qPCR quantification of SNAP25 and VAMP2 genes. Mean±SEM, N=5; * $p < 0.05$. C) Quantification from Single Cell Transcriptomics experiment evaluating the indicated insulin secretion-related genes in Wfs1 and Wfs1 corrected iPSC-derived β cells. Mean±SEM, N=831 for Wfs1, N=1140 for Wfs1 corrected; **** $p < 0.0001$.

5.11. Apoptosis

All the previous experiments demonstrated that Wfs1 cells, especially β cells, are extremely sensitive to stress induction and take aberrant countermeasures in order to overcome it; we now know that this affects their proper functionality, but we still must investigate the terminal outcome of all the previous processes: apoptosis or survival.

We opted to stimulate cells with TG and inflammatory cytokines treatment, using FACS to assess the lethality. We evaluated the percentage of cells that were positive for Annexin V, which is a marker of early apoptosis, and for Propidium Iodide (P.I.), which is a marker of late apoptosis or secondary necrosis (Crowley *et al*, 2016).

Our results indicate that Wfs1 iPSCs display a strong sensitivity to apoptosis induction: both TG and inflammatory cytokines induce a sharp upregulation of both cell death markers in Wfs1 cells, while Wfs1 corrected ones are more resistant. This is particularly evident for TG, for which we applied a stimulus of 8h followed by a recovery: we observed that TG has a similar effect on both genotypes in the short term, but after stressor removal Wfs1 cells keep dying, while Wfs1 corrected ones are able to recover

quickly and reenter the cell cycle, decreasing progressively the percentage of apoptotic cells. Concerning the inflammatory stimulus (IL1 β + IFN γ), Wfs1 iPSCs doubled their basal death rate after exposure, while Wfs1 corrected ones displayed a small and not statistically significant increase even after 48h of exposure (**Figure 37**).

These data suggest that loss of Wolframín impairs the ability of cells to reorganize and recover from stress in the long term: this is of great interest as it implicates that, while an acute stress induction may not show significant differences between the cell lines, repeated cycles of stimulation (on-and-off model) can highlight a differential tolerance that is uncovered in the long term.

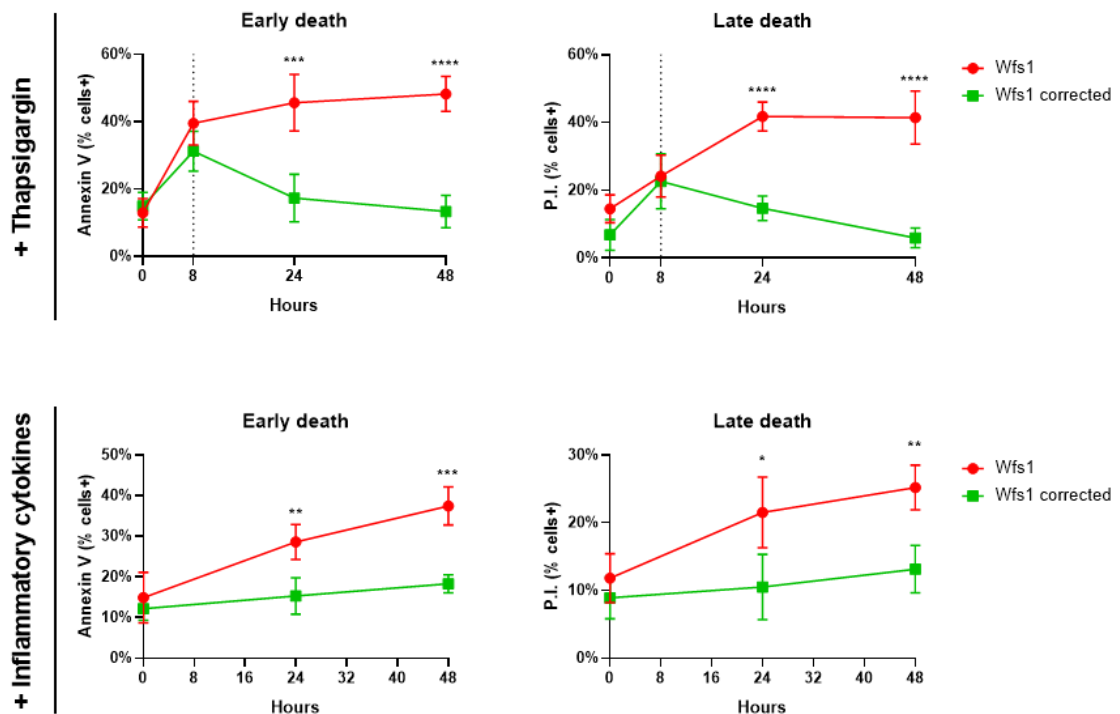


Figure 37. Apoptosis rate after stress induction in iPSCs.

iPSCs were treated for 8h with 100nM of TG to induce apoptosis, then the culture medium was switched to a fresh one without TG; cell death was assessed at the beginning of the experiment, after 8h of treatment and after 24h and 48h. Alternatively, iPSCs were treated with inflammatory cytokines (IL1 β 50U/ml +IFN γ 1000U/ml), analyzing cell death at time 0h, 24h and 48h of treatment. Mean \pm SEM, N=3; * p <0.05, ** p <0.01, *** p <0.001, **** p <0.0001.

In iPSC-derived β cells, we compared the effect of each stressor (TG or inflammatory cytokines) to the co-treatment with Liraglutide. First, we confirmed that Wfs1 β cells were more sensitive to exogenous stress induction, displaying significantly more Annexin V+ and P.I.+ cells than corrected ones; furthermore, we found that Liraglutide buffered

the excess of death given by the stressor: the co-treatment had an almost complete protective effect both in Wfs1 and in Wfs1 corrected cells, nullifying the genotype-dependent difference (**Figure 38**).

These data show that Wfs1 β cells poorly tolerate stress induction, both ER stress and inflammation: this can be prevented by concomitant treatment with Liraglutide, which protects cells from apoptosis induction.

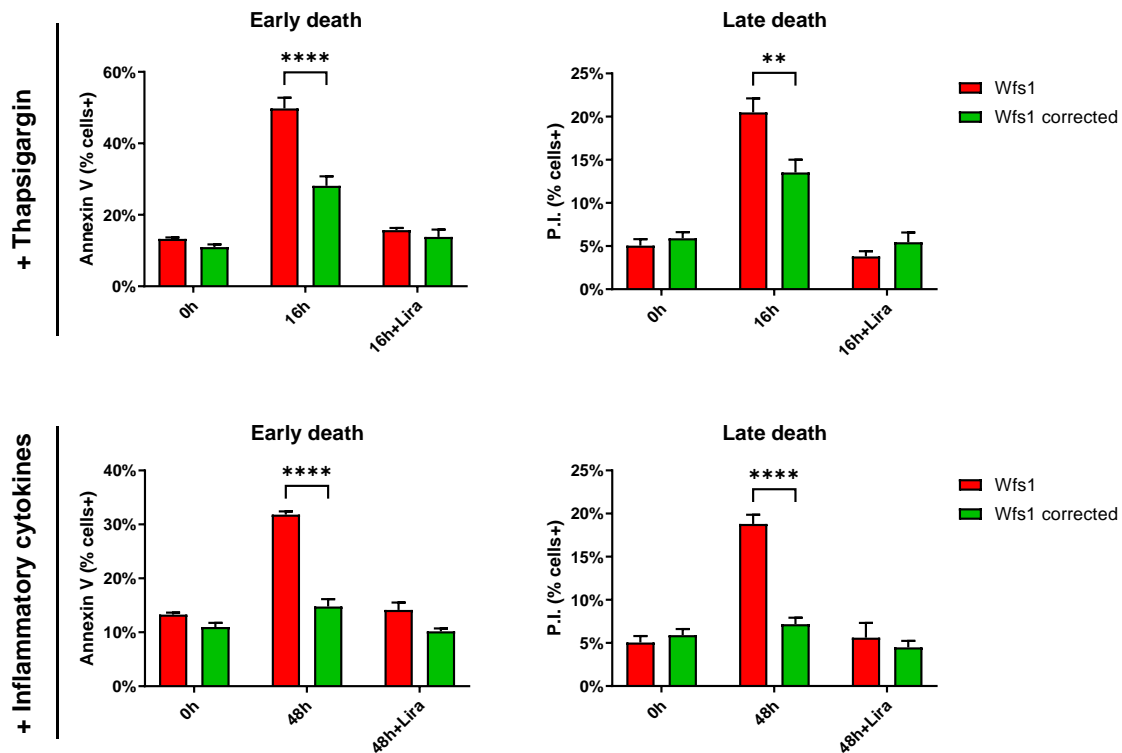


Figure 38. Apoptosis rate after stress induction in β cells.

β cells were treated for 16h with 50nM of TG with or without 1 μ M of Liraglutide; cell death was assessed at the beginning and at the end of the experiment. Alternatively, β cells were treated with inflammatory cytokines (IL1 β 50U/ml + IFN γ 1000U/ml + TNF α 10ng/ml) with or without 1 μ M of Liraglutide, analyzing cell death at time 0h and after 48h of treatment. Mean \pm SEM, N=2 for Wfs1 cells, N=4 for Wfs1 corrected cells; **p<0.01, **** p<0.0001.

6. Discussion

The aim of this thesis was to use iPSCs derived from a WS1 patient to study the molecular mechanisms underlying DM in the condition. To do so, we focused on two main states of iPSCs: their undifferentiated, pluripotent state, and the terminally differentiated into β cell one, as we tried to gain different pieces of information from both.

Concerning the state of the art, we were confronted with a very complex picture, as many groups throughout the years have tried to elucidate the mechanisms underlying WS1 pathogenesis: a lot of putative functions (and dysfunctions) of Wolframin have been proposed, at times in single papers without any further proof from external studies, and at times in very convincing ways, taking advantage of multiple models and cross-validation of many groups. Mostly, what appeared to be crucial was the choice of the model: to our knowledge, very few studies attempted to evaluate both the endocrinological and the neurological aspect of the disease, apart from clinical publications (Lu *et al*, 2014; Jagomäe *et al*, 2021; Seppa *et al*, 2021).

What can be gathered from literature is that some deficiencies are systematically found when investigated, like Ca^{++} mishandling and ER stress; some others might be cell type-specific, like mitochondrial involvement preferentially in skeletal muscle and neuronal tissues, and for some others the evidences are too scarce to deduct if they constitute an hallmark of the disease or an isolated finding (alterations in autophagy and protein trafficking). An ulterior complication is the use of animal models (rodents and zebrafish), which, while extremely useful for some studies, might not recapitulate the human disease with a sufficient grade of precision, as they intrinsically display differences in the phenotypic manifestations and biological players.

In this context, the selection of a strong model is crucial. We chose to use iPSCs and iPSC-derived β cells for two main reasons: on one hand they are extremely plastic and potentially allow the modelling of multiple affected tissues in a human background, and not in an animal one; on the other hand, they gave us the possibility to study a unique set of novel mutations in *WFS1*, which were patient-derived and held the potential to highlight a complex phenotype, made not by mere loss of the gene but to a more sophisticated pattern of mRNA and protein production.

Starting from reprogrammed patient-derived iPSCs, this intention to investigate the genetic aspect guided the first big challenge of the project. To our knowledge, this is the first attempt to characterize the transcriptional outcomes of a splice site mutation in WS1; a similar molecular characterization has been reported in WS2 (Cattaneo *et al*, 2017).

We found out that the c.316-1G>A mutation causes a loss of normal transcripts and the appearance of novel ones: this could only partially be predicted via bioinformatics tools, implicating some cell type-specific mechanisms that depend on chromatin conformation and transcription factors availability; in fact, different cell types appear to express different isoforms. It is extremely interesting to note that the same isoforms are expressed in the WT background, implying a degree of flexibility in the precision of the locus: healthy cells “accept” to lose a percentage of mRNA in non-canonical transcripts, suggesting that this mechanism might not be a simple error, but a potential tool to respond to a mutation and retain an incomplete protein, like ours, instead of fully losing Wolframin production.

As a consequence, we managed to describe the production of a residual protein, which could only be visualized by Western blot with one of the two available antibodies, named Wolframin B: the other one, Wolframin CST, is thought to recognize the lost epitope in the N-terminal and only reacts with the full length protein.

Since we described multiple splicing isoforms in the iPSCs of our patient, which is in open contrast with a report from another group on PBMCs (Panfili *et al*, 2021), we investigated PBMCs ourselves. In our hands, patient-derived PBMCs express at least two alternative splicing isoforms, compatible with the Splice3 and Splice4 that we characterized. It could be that our PCR conditions are less stringent and allow the amplification also of shorter, less frequent transcripts, without favoring the longer and more abundant amplicon (the WT form is always present, thanks to the contribution of the c.757A>T mutation-carrying allele).

A greater understanding of the complexity of the genetic system suggested to us that using an unrelated WT cell line as a control could not be stringent enough to investigate our WS1 model. Therefore, we designed a correction strategy targeting the acceptor splice site mutation upstream exon 4, producing an isogenic heterozygous match of the Wfs1 iPSCs.

Of course, a potential limitation of cells corrected in heterozygosity could be the risk of residual subclinical features in this model. As previously mentioned, carriers of WS1 have been suggested to bear a higher probability of developing multiple conditions, such as diabetes (Torres *et al*, 2001; Young *et al*, 2001; Martorell *et al*, 2003; Kato *et al*, 2003; Wasson & Permutt, 2008; Sandhu *et al*, 2009; Fawcett *et al*, 2010; Munshani *et al*, 2021).

We were comforted in our choice by the fact that a landmark paper for the field, the one published in 2020 by Urano and Millman's group (Maxwell *et al*, 2020), adopted the same strategy of only targeting one of the two alleles to generate their control cell lines.

Still, to address this issue, at the beginning of the project we compared an unrelated WT iPSC line, our Wfs1 cells and the corrected counterpart. The results, although preliminary, were quite encouraging: concerning ER stress parameters, our primary readout, corrected cells behaved in line with a WT genotype, with similar trends when compared to Wfs1.

In the differentiated cells, however, we got some intriguing results. We took advantage of previous differentiation experiments conducted on WT cells and we also performed new ones, in order to see potential differences in our hands. Unexpectedly, we demonstrated that Wfs1 cells had a higher and more consistent ability to differentiate into β cells at the end of the standard protocol than WT ones. This was surprising, and we reasoned that the genetic background, more than the mutation *per se*, could be the driving force of the difference. Consistently, corrected cells outperformed both Wfs1 and WT ones by means of differentiation capacity and insulin secretion ability.

Our observations cannot exclude that, compared to a double corrected situation, the heterozygous clones might still have some molecular or functional impairment: however, the control line in our possession was not able to answer the question and even raised concerns for the use of single cell lines as putative "universal" controls. Many factors can impact on differentiation efficiency, when considering the same protocol: age of the donor, cell type of origin, reprogramming strategy and efficiency, number of passages, acquired somatic mutations, genetic and epigenetic landscape (Carcamo-Orive *et al*, 2017; Lo Sardo *et al*, 2017; Volpato & Webber, 2020).

In light of this, we deemed it better to stick with the syngeneic corrected counterpart as a more stringent control for Wfs1 cells.

The genetics findings and the novel tool of corrected cells prompted us to investigate the molecular consequences of said mutations. We based our investigation on literature and sought after the most well characterized pathways, like ER stress, in the most readily available model, which is undifferentiated iPSCs.

Out of all the (several) genes and proteins tested, which comprise basically any aspect of ER stress response mediated by the UPR, we did not see any consistent alteration that could determine a pathological phenotype. Even application of a stressor, TG, did not highlight major differences among the two lines, denoting a comparable status in undifferentiated cells. This correlates with the clinical observation that the disease is rarely seen in early infancy and almost never at birth, apart from some congenital cases carrying major autosomal dominant mutations (De Franco *et al*, 2017): it is reasonable to speculate that early phases of embryonic development are independent from Wolframin presence, or they can better bypass its loss. Both explanations might be true: our data and data from others indicate that terminally differentiated cells express much more Wolframin than any other differentiation stage, and even then, there is no strict relationship between high expression levels and impaired function in the disease (see the case of hepatocytes).

On the contrary, Wfs1 iPSCs already exhibited alterations of autophagy: in response to stress, they failed to upregulate Beclin1 phosphorylation and *SQSTM1* transcription, suggesting that they do not implement autophagy as a survival mechanism after stressor stimulation. Such molecular switch loss could underlie the difference in survival capacity, measured by Annexin V+ and P.I.+ cell number upon TG or inflammatory cytokines exposure.

Generally speaking, we understood that iPSCs *per se* are not an appropriate model to investigate WS1 pathogenesis, although they gave us some insights into what to expect from our specific setting. Hence, we differentiated Wfs1 and Wfs1 corrected iPSCs into β cells *in vitro*.

The first readout we considered was actually the differentiation capacity of our cells. We measured conventional parameters of β cell identity, as previously done by our group (Pellegrini *et al*, 2018, 2021): however, we postulated that classical markers could be insufficient to discriminate specific endocrine subpopulations and their properties. To expand our analytical possibilities, we set up a Single Cell Transcriptomics experiment assessing the transcriptional profile of *Wfs1* and *Wfs1* corrected differentiated cells.

Overall, we detected a correct cluster composition at the end of differentiation, with a significant proportion of cells in the pancreatic endocrine lineage. However, we detected an imbalance in the formation of α , δ and γ cells and a distinct distribution of the β cell subpopulations, particularly of the $\beta 2$ and $\beta 3$ subtypes.

The most important take home message of this kind of analysis is that WS1-derived iPSCs, at least in our model, are able to differentiate a significant number of β cells, differently from other reports in literature (Maxwell *et al*, 2020): a similar result suggests that the alterations in β cell functionality do not stem from reduced formation of the cell type, but rather from the production of “badly equipped” β cells, which in the long term display malfunctions and undergo apoptosis. Alternatively, or in parallel to this, a malformation of the endocrine niche could determine a reduced survival and functionality also of the residual cell types.

Concerning ER stress response in iPSC-derived β cells, we found a significant downregulation of PERK and IRE1 α branches of the UPR, and no upregulation of the ATF6 branch. This is in contrast with previous reports in literature (Shang *et al*, 2014; Maxwell *et al*, 2020) and with the molecular link between Wolframin and ATF6, since Wolframin regulates the transcription factor’s stability and activity (Fonseca *et al*, 2010). This evidence suggests a non-canonical form of WS1, sporting a singular molecular profile and a generally mild phenotype: the hypothesis of a milder disease in response to the mutations has already been suggested and published, even with only clinical data as a support (Squitti *et al*, 2019).

Furthermore, we observed alterations in the basal activation of autophagy in *Wfs1* cells: the concomitant downregulation of *SQSTM1* and *MAP1LC3A* transcripts and of p62 protein suggest a lower level of induction of the process, and therefore the lack of proper machinery for autophagic flux performance. The conclusiveness of such results is,

however, limited by the lack of a direct measurement of autophagic turnover. We envision to perform additional experiments with Bafilomycin, a specific inhibitor of autophagosome-lysosome fusion, in order to address this issue and further strengthen our conclusions.

Another missing piece of information concerning autophagy is the relevance of specialized autophagic mechanisms in β cells. Crinophagy, the autophagic clearance of insulin granules, was reported early on in animal models (Halban & Wollheim, 1980) and is tightly linked with the secretory capacity of β cells, not only under starvation: different mediators intervene if the cargo of interest is proinsulin, insulin, or a misfolded isoform, and beneficially modulate the ER stress response (Pearson *et al*, 2021).

The proof of concept for ER-phagy actually happening in β cells was published just last year, outlining the PGRMC1-RTN3 complex as a mediator of mutant prohormone clearance from distinct domains in the ER (Chen *et al*, 2021). In the context of WS1, where there are no mutant prohormones but an increased amount of misfolded proteins, it is not known whether this specific mechanism may be conserved. Furthermore, other forms of selective autophagy, particularly mitophagy as already reported (Cagalinec *et al*, 2016; Wang *et al*, 2021b), may play a key role in the condition.

Stress induction in iPSC-derived β cells revealed a complex phenotype. On one hand, TG triggered ER stress response more in Wfs1 cells than in the corrected counterpart, especially after 8 hours. On the other hand, Wfs1 β cells make a greater effort to upregulate autophagy after TG treatment (increased *SQSTM1* transcript after 8h): however, the attempt does not seem to be effective, as at longer timepoints the clearance of p62 is much lower than the corrected counterpart, although not statistically significant. Collectively, our data suggest a poorly effective autophagic flux in Wfs1 β cells, also in response to stress: then again, Bafilomycin experiments will be needed to pinpoint the exact mechanisms involved in the phenomenon and, possibly, to suggest novel therapeutic targets.

Inflammatory cytokines did not seem to trigger the UPR, which is unusual: however, we must remember that inflammation-induced β cell death does not rely upon UPR activation (Åkerfeldt *et al*, 2008), and as such, we could be observing a timeframe in

which ER stress response is no longer a preponderant feature of the cell, independently from its survival rate.

In fact, all these molecular alterations converged in determining the switch between survival and apoptosis. Our data clearly show that Wfs1 β cells poorly tolerate stress induction and undergo apoptosis much more frequently than the corrected counterpart: interestingly, while ER stress has a measurable detrimental effect also on Wfs1 corrected cells, they seem almost insensitive to inflammation even after 48 hours of cytokine stimulation.

UPR and autophagy impairments are known to induce apoptosis in cells, but of course their alteration can extend beyond the dichotomy of survival and affect cell function. Evidences from patients tell us that not only affected β cells are reduced in number, which puts an extra load on survivors, but their physiology is also impaired. The double burden of dysfunction and death is the key factor in WS1 pathogenesis.

As suggested by literature, the tight interconnection of Wolframin with Ca^{++} biology and the centrality of Ca^{++} in β cell function brought us to investigate whether the ion dynamics were altered in our system. We postulated that any defect could represent the connecting ring between upstream, subclinical, primary mechanisms and downstream, functional, secondary ones. Ca^{++} flux quantification uncovered a severe impairment in synchronicity and control of timing, more than in Ca^{++} content *per se*. This is sustained by transcriptional deficits of ion channels: somehow, the molecular impairments of ER stress and autophagy that we measured at the basal stage already impact on proper structure of the β cell machinery, giving a subclinical impediment that, we postulate, grows in time to become clinically manifest as a WS1 symptom.

Ca^{++} alterations basically force anomalies in insulin secretion. Again, we observed a deficient secretory ability that could be explained by impaired Ca^{++} signalling alone, but instead has a complex molecular background: the processing enzyme PC1/3 and transcripts for the fusion complex are reduced. To summarize, insulin secretion impairment is due to both Ca^{++} alterations and to more primary phenomena, acting through a cascade effect where upstream glitches condition downstream function.

At this point, we postulate that two factors guide pathogenic processes in WS1-derived models: ER stress tolerance and functional load. In iPSCs, Wolframin expression and necessity for cell functionality are low, because the stem cell is not subject to a consistent ER stress burden in its normal life and therefore does not “invest” in energy-consuming systems to protect itself.

β cells and all pancreatic endocrine subpopulations, on the contrary, are the quintessence of a systematically stressed out cell type. In this system, Wolframin is highly present and orchestrates cell homeostasis not only in response to external stressors, but already at the basal level: its loss impacts on cell identity even before affecting function. We could even postulate that no truly mature pancreatic endocrine compartment can exist in the absence of Wolframin.

The production of a defective β cell is the preamble for WS1. ER stress and autophagy perturbations, which are present in an unstimulated context, influence cell performance both by physically acting on their interactors (the UPR affects Ca^{++} currents from the ER and autophagy inhibits proinsulin processing to insulin, for example) and by disrupting the transcriptional landscape. The double mechanism explains the severity of the conditions and the latent phase before clinical insurgence, as basal alterations can take up to years to manifest.

Figure 39 provides a graphical explanation of our hypothesis.

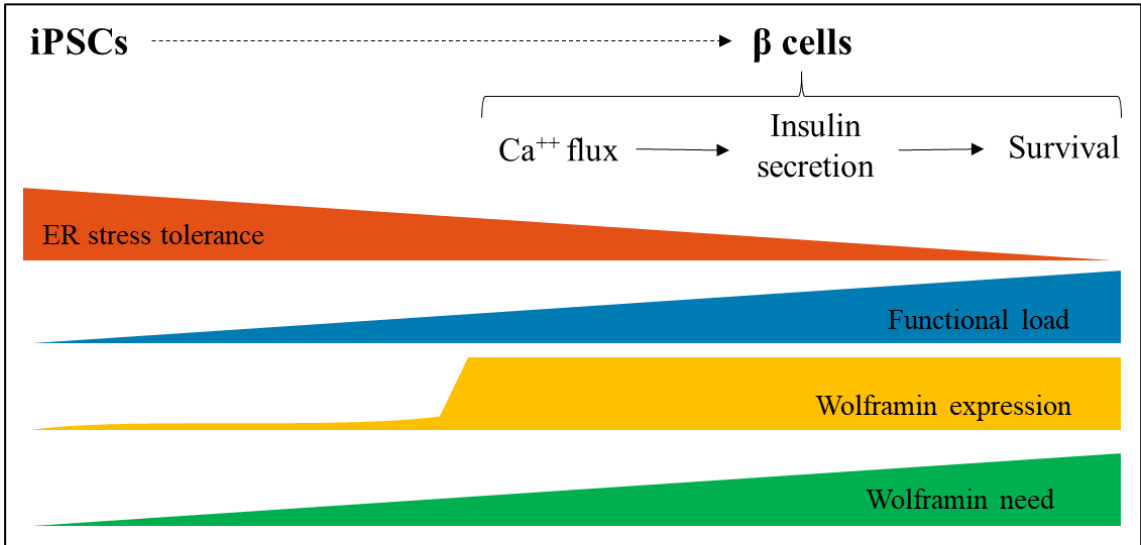


Figure 39. Model of WS1 pathogenesis.

In this context, we can also better understand the role of Liraglutide.

Liraglutide is an agonist of GLP-1R, whose endogenous ligands act in an acute way, but it also proved effective following chronic stimulation. The GLP-1R axis has pleiotropic effects at the cell level, thanks to its complex regulatory network, which mainly revolves around activation of cAMP signaling (Rowlands *et al*, 2018; Tomas *et al*, 2020).

Different modalities of administration are likely to trigger different beneficial effects: acute doses, for example given together with glucose during Ca^{++} measurements or secretion tests, will modulate downstream factors only at the post-translational level and have limited effects at the transcriptional one. Instead, chronic or chronic-like administration (at least a few hours long) will perform a deeper rewiring effect and affect metabolism and gene expression, particularly the CREB-dependent genes: they include pro-survival proteins and ER stress attenuators, mediating prevention of excessive UPR activation and oxidative stress damage. For example, concerning the link between Liraglutide and autophagy, it has been demonstrated that GLP-1R signalling has an apparent inhibitory effect: however, this is due to reduced load of misfolded proteins and increased efficiency of lysosomal degradation, which on the contrary indicates a more efficient performance of the autophagic flux (Lim *et al*, 2016). However, the precise mediators of the connection remain to be elucidated.

Such a complex and pleiotropic system explains why Liraglutide treatment has the potential to be so effective in WS1. Our results highlight that co-administration of Liraglutide with a stressor, TG or inflammatory cytokines, improves iPSC and iPSC-derived β cell survival. This is a downstream effect of a concerted fine-tuning of the cell, as we saw: it starts with alleviation of ER stress markers, autophagy modulation, normalization of Ca^{++} currents and upgrade of insulin secretion.

All in all, our *in vitro* data give an explanation as to why the drug was so effective in our patient of interest and demonstrate that our modelling system is appropriate for drug screening of relevant therapeutic compounds.

This work had the ambitious aim to shed light on a peculiar case of WS1, clarifying it from the genetic and pathogenic point of view. The greatest strength of our results is the

deepness reached, since we managed to explore and describe multiple mechanisms operating both in iPSCs and in β cells, even taking advantage of state-of-the-art techniques such as Single Cell Transcriptomics. On top of that, to our knowledge, this is the most thorough genetic characterization ever performed on a WS1 patient and one of the first syngeneic models ever created for the disease.

The strength, however, is also the major flaw. We are aware of the limitations of only focusing on a single clinical case, especially with a unique set of mutations: we must be very cautious in assuming that our observations can be automatically extended to the entire patient population.

Moreover, we directed our attention to β cells and not to neurons, the other most affected cell type: this was due to our consolidated expertise in the β cell field, but we recognize that our findings should be validated also in neuronal models.

Notwithstanding these considerations, our results contribute to a wider understanding of WS1 pathogenesis, highlighting that it is impossible to point the finger on a single, ancestral deficiency which would be the sole responsible for cell dysfunction: we must recognize that multiple pathways act in different tissues and models, possibly even in different patients. Our approach to therapy development for patients should stem from this awareness.

Accepting the multiplicity and complexity of the system, even if it makes findings more complicated to validate and assumptions more arduous to formulate, is the first step in understanding what we have been missing up until now and, most importantly, how to actually tackle WS1.

The answer, as it seems, is “it depends”.

7. Methods and Materials

7.1. Sequencing

Following the patient's referral to a geneticist for further examination, NGS was performed on a panel of 31 monogenic diabetes-related genes: ABCC8 (NM_000352), AIRE (NM_000383), BLK (NM_001715), CEL (NM_001807), CISD2 (NM_001008388), EIF2AK3 (NM_004836), FOXP3 (NM_014009), GATA4 (NM_002052), GATA6 (NM_005257), GCK (NM_000162), GLIS3 (NM_001042413), HNF1A (NM_000545), HNF1B (NM_000458), HNF4A (NM_000457), IER3IP1 (NM_016097), INS (NM_000207), ISL1 (NM_002202), KCNJ11 (NM_000525), KLF11 (NM_003597), MNX1 (NM_005515), NEUROD1 (NM_002500), NEUROG3 (NM_020999), PAX4 (NM_006193), PAX6 (NM_000280), PDX1 (NM_000209), PTF1A (NM_178161), RFX6 (NM_173560), SIRT1 (NM_012238), SLC19A2 (NM_006996), SLC29A3 (NM_018344), SLC2A2 (NM_000340), WFS1 (NM_006005).

Enrichment of fragments was performed with the TruSight One Sequencing kit; sequencing of coding regions and exon-intron junctions was done on NextSeq Illumina platform. Sanger sequencing was employed to confirm putative mutations of interest.

The software used for analysis were: BWA, Smith-Waterman Algorithm, freebayes, SnpSift - SnpEFF, MiSeq reporter. Results were compared to the following databases: NCBI dbSNP, 1000 Genomes, dbNSFP, ClinVar, LOVD. Variants present in more than 1% of the population with no clinical significance, polymorphisms, silent mutations, and mutations with low penetrance were filtered out from the results.

The following mutations were reported in heterozygosity in the *WFS1* gene, according to the Human Genome Variation Society guidelines (<http://varnomen.hgvs.org>, v20.05):

- c.316-1G>A, falling at the acceptor splice site upstream exon 4
- c.757A>T, inducing a premature stop codon resulting in the putative protein p.Lys253X

Such variants were previously unknown in literature and, according to the geneticist evaluation and clinical presentation, were deemed presumably pathogenic.

Another sequencing was performed to assess the exact sequence of the splice variants identified in WS1 cells. NGS was performed on complementary DNA (cDNA) samples

derived from the amplification of *WFS1* area comprised between exon 3 and exon 5. PCR was performed amplifying for up to 50 cycles in standard conditions, and derived PCR fragments were purified using Kit NucleoSpin PCR & Gel Clean-up (Macherey Nagel) according to the manufacturer's instructions. Samples were processed with the protocol "TruSeq Nano WGS" deriving 4×10^6 fragment clusters, 250nt long, via MiSeq_500_v2. Sequencing was performed on two Wfs1 iPSCs clones and one WT iPSCs clone.

7.2. Cell reprogramming

Written informed consent was obtained from the donor's parents for anonymized information to be used in scientific dissemination. Patient-derived iPSCs were generated by reprogramming the CD34⁺ fraction from PBMCs. Briefly, PBMCs were isolated from peripheral whole blood diluted with PBS (phosphate-buffered saline, Euroclone), layered over an equal volume of Ficoll®-Paque (Ficoll-Paque PREMIUM, Merck) in a Falcon tube and centrifuged for 30 minutes at 1000 rpm without brake. PBMCs were retrieved by manually collecting the ring between the upper, plasma layer and the lower, Ficoll®-Paque media. Part of the cells was frozen at -80°C for subsequent RNA and genomic DNA extraction. The remaining PBMCs were then cultured to ensure enrichment in the CD34⁺ fraction for optimal transduction efficiency.

Sendai virus commercial reprogramming kit (CytoTune-iPS Sendai Reprogramming Kit, ThermoFisher) was used according to the manufacturer's indications. Reprogrammed cells were cultivated initially on a MEFs (mouse embryonic fibroblasts) feeder layer: emerging clones were individually picked and expanded in mTeSR1 medium (STEMCELL Technologies) onto a Vitronectin coating (Vitronectin (VTN-N) Recombinant Human Protein, Truncated, ThermoFisher) at 500ng/cm².

Control iPSCs with WT genotype were already available and routinely employed in the lab: we took advantage of this cell line as a healthy control for preliminary screening of major alterations in iPSC and iPSC-derived β cell biology.

7.3. Cell culture

7.3.1. iPSCs and differentiation

Stable iPSC clones were cultured onto a Vitronectin coating at 500 ng/cm² in complete Essential 8 Flex medium (ThermoFisher) and dissociated with 0.5mM EDTA (Ambion)

for passaging every 3-4 days. Cells were routinely tested for mycoplasma contamination using MycoAlert™ Mycoplasma Detection Kit by Lonza, according to the manufacturer's instructions.

The karyotyping and aCGH analysis were performed by ISENET Biobanking service unit in Milan, Italy; all WS1-derived iPSC lines had normal karyotype.

Differentiation to pancreatic β cells was performed as already published by our group (Pellegrini *et al*, 2021), on one line of WT iPSCs, two lines of Wfs1 iPSCs and three lines of Wfs1 corrected iPSCs. Briefly, the following culture media were used as bases:

- M1 medium: MCDB131 (Gibco) + 8mM D-Glucose (Sigma) + 1.23g/l NaHCO₃ (Sigma) + 2% Bovin Serum Albumin (BSA, Sigma) + 0.25mM Vitamin C (Sigma) + 1% Pen/Strep (Lonza) + 1% Glutamine (Lonza);
- M2 medium: MCDB131 + 20mM D-Glucose + 1.754g/l NaHCO₃ + 2% BSA + 0.25mM Vitamin C + 10mg/ml Heparin (Sigma) + 1% Pen/Strep + 1% Glutamine.

All media were filter-sterilized through a 0.22 μ m bottle top filter (Corning). Medium changes were performed by adding small molecules and growth factors to the base media immediately before use, as follows:

- days 0–3: STEMdiff™ Definitive Endoderm Kit (STEMCELL), used following manufacturer's instructions
- days 4–6: M1 medium + 50ng/ml keratinocyte growth factor (KGF) (Peprotech, London, UK) + 1:50000 ITS-X (Invitrogen, Carlsbad, CA, USA)
- days 7, 8: M1 medium + 50ng/ml KGF + 0.25mM Sant1 (Sigma) + 2 μ M Retinoic acid (RA) (Sigma) + 500nM PdBU (Millipore) + 1:200 ITS-X + 200nM LDN193189 (only Day 7) (Sigma)
- days 9–13: M1 medium + 50ng/ml KGF + 0.25mM Sant1 + 100nM RA + 1:200 ITS-X + 2 μ M iBET-151 (Selleckchem)
- days 14–18: M2 medium + 0.25mM Sant1 + 100nM RA + 1mM XXI (Millipore) + 10mM Alk5i II (Selleckchem, Munich, Germany) + 1mM L-3,3',5'-Triiodothyronine (T3) (Sigma) + 20ng/ml Betacellulin (R&D) + 1:200 ITS-X

- days 19-25: CMRL 1066 (Mediatech) + 10% fetal bovine serum (FBS) (Lonza) + 1% Pen/Strep + 1% Glutamine + 10 μ M Alk5i II + 1 μ M T3 + 10mM Nicotinamide (Sigma) + 10 μ M H1152 (Euroclone)

For any drug treatment and in any case before terminal differentiation analyses, iPSC-derived β cells were detached using 0.5mM EDTA and relocated in 35mm or 60mm petri dishes, supplementing the culture medium with 100U/ml DNase I (Sigma); cells were let aggregate overnight on a shaker at 55 rpm. Treatments on iPSCs instead were performed in adhesion in standard coated culture plates; all drugs employed are listed in **Table 3**.

TG treatments lasted for 8 or 16 hours, while in rescue experiments TG was administered for 8 hours followed by 24 or 48 hours of recovery in fresh medium. Conditioning with inflammatory interleukins was performed for 24 or 48 hours. In all cases, Liraglutide co-treatment was performed for the same timing of the stressor treatment.

Drug	Supplier	Code	Stock solution
Thapsigargin	Sigma	T9033	7,68mM in DMSO
Liraglutide	DBA	HY-P0014	1mM in sterile water
rhIL-1 β	PeptoTech	200-01B	2000U/ml in PBS+3% BSA
rhIFN γ	PeptoTech	300-02	20000U/ml in PBS+3% BSA
rhTNF α	PeptoTech	300-01A	0.2 μ g/ μ l in PBS+3% BSA

Table 3. Drugs employed in vitro for cell treatments.
rh= recombinant human.

7.3.2. Human pancreatic islets

Human islets were isolated from the pancreas of cadaveric organ donors as described in literature (Ricordi *et al*, 1988); the procedure was performed in the Pancreatic Islet Processing Unit of Diabetes Research Institute at Ospedale San Raffaele. The use of human islet preparations discarded from clinical use is approved by the Institutional Review Board under the “European Consortium for Islet Transplantation human islet distribution program” supported by Juvenile Diabetes Research Foundation (2-RSC-

2019-724-I-X). Islet purity was assessed with dithizone (Sigma) staining; islets were kept in culture in Final Wash medium (SACCO) supplemented with 10% FBS, 1% Pen/Strep, 1% Glutamine, 10 μ M of Rock Inhibitor (Y-27632, Voden), 100U/ml DNase I, on a shaker at 55 rpm for up to a week.

7.3.3. *Fibroblasts*

Fibroblasts from a WS patient with known protein absence (genotype W189X/W189X) and a healthy control were a kind gift from Vania Broccoli's group at Ospedale San Raffaele. Cells were kept in Dulbecco's modified Eagle's medium (DMEM) with high glucose, supplemented with 10% FBS, 1% PenStrep, 1% Glutamine; cells were passaged with Trypsin (Lonza) every week.

7.4. Gene correction via CRISPR/Cas9

CRISPR/Cas9-mediated correction of the mutation located upstream exon 4 of *WFS1* gene was performed in patient-derived iPSCs.

Guide RNAs (gRNAs) were designed to induce genomic cleavage by Cas9 upstream the mutation site; GeneArt™ Precision gRNA Synthesis Kit (ThermoFisher) was employed for *in vitro* synthesis of the gRNAs, whose sequences are reported in **7.14, Primer table**. As donor templates for homologous recombination, single-strand oligodeoxynucleotides (ssODN) were used, designed to replace the entire locus including the point mutation and to destroy the protospacer adjacent motif (PAM) and seed sequence at the same time. This strategy was adopted in order to prevent multiple recombination reactions at the same locus.

To electroporate 5x10⁵ iPSCs, we used 20 μ g of Cas9 protein (TrueCut™ Cas9 Protein v2, ThermoFisher), 40 μ g of ssODN, 4 μ g of gRNAs and 2 μ g of pmaxGFP plasmid (Lonza), as a reporter. As controls, we kept the same cell line without electroporation nor reagents, electroporated without further reagents, and electroporated with pmaxGFP alone.

After electroporation, bulk cells were replated as usual and allowed to stabilize again. Five days later, using FACSARIA FUSION (BD), we sorted 4 GFP-positive cells per well in Vitronectin-coated 96-well plates; this allowed us to obtain almost only single

colonies in each well. To improve survival of sorted cells, they were cultured in Essential 8 Flex medium supplemented with 10% CloneR™ (STEMCELL).

Single colonies were picked and separately expanded until reaching at least 1×10^6 cells: at this point, part of the cells were pelleted, lysed, proteins were extracted and analyzed by Western Blot to confirm reexpression of wild type Wolframin.

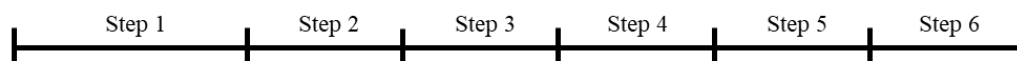
Six corrected clones were obtained. Karyotyping and aCGH analysis were performed by ISENET Biobanking service unit in Milan, Italy: one clone revealed severe karyotype alterations and was subsequently excluded.

7.5. Dynamic perfusion

Dynamic secretagogues stimulation of iPSC-derived β cells and primary human islets was performed using an automated perfusion system (BioRep® Perifusion V2.0.0), to evaluate the cells' ability to appropriately secrete insulin in response to stimuli. After the above described suspension culture, 200 absolute clusters per condition were picked for dynamic perfusion and resuspended in HEPES-buffered solution (125mM NaCl, 5.9mM KCl, 2.56mM CaCl₂, 1mM MgCl₂, 25mM HEPES, 0.1% BSA, pH 7.4), which was completed with the following conditions: low glucose, high glucose or high glucose \pm 50 μ M IBMX (Gibco) or high glucose \pm 1 μ M Liraglutide, 30mM KCl.

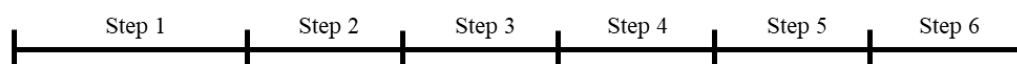
Stimuli were different according to the biology of the specific cell types, and they were applied in six steps as follows:

Primary human islets



Duration	60'	20'	20'	20'	20'	20'
Flux rate	30µl/min	100µl/min	100µl/min	100µl/min	100µl/min	100µl/min
Stimulus	2mM glucose	2mM glucose	20mM glucose ±IBMX or ± Liraglutide	2mM glucose	30mM KCl	2mM glucose

iPSC-derived β cells



Duration	60'	20'	20'	20'	20'	20'
Flux rate	30µl/min	100µl/min	100µl/min	100µl/min	100µl/min	100µl/min
Stimulus	0.5mM glucose	0.5mM glucose	11mM glucose ±IBMX or ± Liraglutide	0.5mM glucose	30mM KCl	0.5mM glucose

Perifusates were collected every minute; representative timepoints were quantified for insulin content by enzyme-linked immunosorbent assay kit (Mercodia), performed according to the manufacturer's instructions.

7.6. Protein extraction and Western blot

Pellets from at least 10^6 cells were lysed in M-PER™ Mammalian Protein Extraction Reagent supplemented with 5mM EDTA pH 8 and 1:100 Halt™ Protease Inhibitor Cocktail; proteins were extracted and quantified using Pierce™ Rapid Gold BCA Protein Assay Kit. Samples for Western blot were prepared from 15-30µg of protein per lane, formulated with 1:2 Novex™ Tris-Glycine SDS Sample Buffer and 1:10 NuPAGE Sample Reducing Agent.

Novex™ WedgeWell™ Tris-Glycine, 1.0 mm, Mini Protein Gels were employed for running, using appropriate polyacrylamide concentration and well number according to the number of samples and their concentration; PageRuler™ Plus Prestained Protein Ladder, 10 to 250 kDa were run in parallel as comparison for molecular weight. Novex Tris glycine SDS running buffer 10x was diluted in distilled water and used for running at 80-150V in Mini Gel Tank powered by PowerEase® 300W Power Supply. Blot Module Set was used for wet transfer on Polyvinylidene difluoride (PVDF) Transfer Membrane 0.45 µm, with Methanol-free Pierce™ 10x Western Blot Transfer Buffer, at 15V for 90'. Transfer efficiency was evaluated using Ponceau S (Sigma).

All washes were performed in Pierce™ TBS Tween™ 20 Buffer (TBST). Aspecific binding sites were blocked in skim milk resuspended to 5% in TBST for 1h at room temperature. Primary antibodies, as listed in section **7.13, Antibody table**, were incubated overnight at 4°C diluted in either 5% milk or 5% BSA. The following day, horseradish peroxidase (HRP)-conjugated secondary antibodies diluted 1:1000 in the same diluent as the corresponding primary antibody were incubated for 1h at room temperature. SuperSignal™ West Pico PLUS chemiluminescent substrate was used for chemiluminescence acquisition at ChemiDoc MP (Biorad). Quantification is expressed as the mean gray area of each band and was performed using ImageJ software (Rasband, W.S. (1997-2015) ImageJ. National Institutes of Health, Bethesda, Maryland, USA. <http://imagej.nih.gov/ij>).

All of the listed reagents and machineries were purchased from ThermoFisher unless otherwise specified.

7.7. RNA extraction, retrotranscription and PCR/RT-qPCR

RNA was extracted with mirVana Isolation Kit (Ambion) and quantified at the Epoch spectrophotometer, using Gen5 software (BioTek, Winooski, VT). After DNase (Invitrogen) treatment, 1µg of RNA was reverse transcribed to obtain cDNA with SuperScript IV RT (Invitrogen), according to the manufacturer's protocol. Gene-specific primers were synthesized and purchased from Eurofins Genomics or from TaqMan Gene Expression Assays (Applied Biosystems, Foster City, CA, USA): TaqMan assays and reagents are the same already reported in our previous papers (Pellegrini *et al*, 2018), while primers for use with PowerUp™ SYBR™ Green Master Mix are reported in **7.14**,

Primer table. All primers for use with SYBR Green system were designed to have the same annealing temperature (T_a) of 60°C.

RT-qPCR was performed with 5ng of cDNA per sample on 7900 Real-Time PCR System (Applied Biosystems). All results are reported as normalized over *GAPDH* expression and expressed as absolute normalized quantity ($2^{(-\Delta Ct)}$) or as a fold over a control ($2^{(-\Delta\Delta Ct)}$), as reported in specific figures.

To verify band size, PCR products were run on precast E-Gel™ Agarose Gels with SYBR™ Safe DNA Gel Stain, 2% (ThermoFisher); Generuler 100bp plus markers (ThermoFisher) were also run in parallel for size comparison.

7.8. FACS

Cells were detached with Trypsin, reduced to a single cell suspension and stained with Live/Dead Fixable Violet stain kit (ThermoScientifics) to exclude dead ones. Fixation was performed using Cytotfix/Cytoperm (Becton Dickinson, BD) and permeabilization with BD Phosflow™ Perm Buffer III (BD). A list of all antibodies used for FACS staining can be found at section **7.13, Antibody table**. For apoptosis assay, P.I. (Sigma) and FITC Annexin V Apoptosis Detection Kit I (BD) were used according to manufacturers' instructions.

Cells were read at cytometer FACS Canto (BD) and results were analyzed with FlowJo™ Software V.10 (FlowJo LLC, Ashland, Oregon, USA).

7.9. Immunofluorescence

To perform immunofluorescence, cells were passaged and replated directly onto appropriately coated Falcon™ Chambered Cell Culture Slides (ThermoFisher) and let grow until desired confluence. Then fixation was performed with 4% paraformaldehyde in PBS for 20' at RT or in cold MetOH at -20°C for 15', according to the primary antibody to be used; cells were subsequently washed in PBS and passed in Glycine 15mM for 5' at room temperature to minimize excessive crosslinking due to fixation.

Samples were then processed as follows:

- Permeabilization and blocking for 45' at room temperature in 5% FBS, 2% BSA, 0.4% TritonX-100 (Sigma) in PBS

- Primary antibody overnight at 4°C, diluted in 2% BSA in PBS as reported in section **7.13, Antibody Table**
- Secondary antibody for 1h at room temperature, diluted in 2% BSA in PBS as reported in section **7.13, Antibody Table** + nuclei counterstaining with Hoechst 33342 (ThermoScientific; 1:500).

Stained slides were acquired at Widefield Zeiss Axio Observer.Z1.

7.10. Ca⁺⁺ imaging

Ca⁺⁺ imaging experiments were performed *in vitro* on aggregated and replated iPSC-derived β cells. Cells were plated in Optical bottom plates, 96-well (Greiner) coated with Matrigel® Basement Membrane Matrix (Corning) and they were allowed to adhere for two to three days. To visualize Ca⁺⁺ distribution inside the cells, they were loaded with 1 μ M Fluo-4, AM, cell permeant (Invitrogen) diluted in the HEPES-buffered solution used for dynamic perfusion for 30' at 37°C.

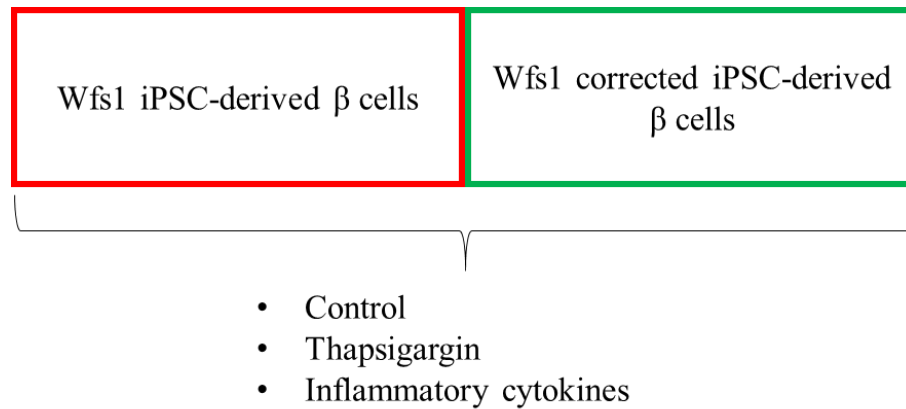
All videos were acquired at Widefield Zeiss Axio Observer.Z1. Fluo-4 was excited by a 488 laser (emission filter 500-550nm) and fluorescence signal was recorded every two seconds. After one minute of acclimation in order to minimize manipulation-induced mechanical stress, cells were challenged with secretagogues and their response was recorded for the total time indicated in each experiment.

For analysis, ImageJ v.1.44 was used. We selected a total of 20 responder cells from two independent experiments of each condition, by drawing the region of interest (ROI) inside the cytoplasmic region of the cell. The mean of fluorescence was normalized to the corresponding mean fluorescence value of the acclimation period (F_0). The change in fluorescence $\Delta F/F_0 = (F - F_0)/F$ was plotted as a function of time and cells were considered as responders if $\Delta F/F_0$ after stimulation was higher than two standard deviations from F_0 . All images were analyzed following background subtraction.

7.11. Single cell RNAseq

In order to tackle the complexity of iPSC-derived β cells and their response to cellular stresses, we set up a Single Cell Transcriptomics experiment. The whole experiment was planned, performed and analyzed in close collaboration with Dr. Giulia Scotti and Dr.

Francesca Giannese at the Center for Omics Sciences at Ospedale San Raffaele. The following conditions were evaluated:



Single cell transcriptomics were carried out following droplet-based Chromium 10X platform, kit version 3 protocol. Sequencing was performed on Illumina NovaSeq, obtaining about 150 millions of paired end reads per sample. Cellular barcodes corresponding to good-quality cells were identified and extracted using the UMItool pipeline: the top barcodes from all the samples were picked, then reads were aligned on the human genome hg38, Gencode version 31. For each sample, we filtered out cells with percentage of reads mapping on mitochondrial genes higher than 10%. Counts were log-normalized using the Seurat function “NormalizeData” with a scale factor of 10000. Data were then scaled using the “ScaleData” function, regressing on the number of Unique Molecular Identifier (UMI) and percentage of expressed mitochondrial genes. On scaled data, cell cycle scores were estimated through the “CellCycleScoring” function.

Dispersion values were calculated for each gene and transformed in the corresponding Z-scores. The most variable genes within each dataset were identified setting a cutoff of 1 over dispersion Z-scores and principal component analysis (PCA) was conducted on these sets of genes.

Selected cells were then analyzed using the workflow implemented in the Rpackage Seurat (v.4), in the R environment v.4.0.3. To identify cell populations, we applied UMAP dimensional reduction algorithm to identify similar expression profiles, and SNN unsupervised clustering algorithm, to further distinguish clusters based on top gene expression. Final clustering was obtained based on nPCs=50, resolution=0.5. Gene-cell count matrices were imported in R and analyzed by home-made scripts. Identification of

clusters and other sub-populations was inferred by comparing the top scored genes with the signatures reported in literature.

To maximize cluster homogeneity among all the genotypes and treatments considered, we derived a reference by integrating the two control samples (both Wfs1 and Wfs1 corrected), against which the other four conditions were compared and reclustered accordingly. Differential gene expression analysis was then applied to identify significantly differentially expressed genes within each cluster using a likelihood-ratio test for significance (adjusted p value <0.01) and a log2FC greater than 0.25. Only genes expressed by a fraction of cells higher than 25% in the considered population were tested.

The analysis of this experiment is still ongoing: for the sake of brevity, in this thesis we will only present and discuss data obtained from the two control samples, comparing expression of specific genes of interest in the endocrine compartment (both mature and immature), in order to exclude the influence of other cell types. The cells analyzed were distributed as shown in **Table 4**.

	<u>Wfs1</u>	<u>Wfs1 corrected</u>
Total cells	4061	2135
Endocrine cells	831	1140
α cells	10	63
γ cells	0	5
δ cells	2	18
Polyhormonal	23	41
β cells	633	397
β 1	612	377
β 2	17	3
β 3	4	17
β 4	0	0

Table 4. Repartition of cells from control samples of the Single Cell Transcriptomics experiment.

7.12. Statistical analysis

GraphPad Prism software (9.0.1 version) was employed to perform statistical analyses. Student's unpaired t-test was used for the comparison of two groups and one variable, while for multiple variables, Two-way ANOVA with Šidák's correction for multiple comparisons test was applied. In all cases, a p-value below 0.05 was considered statistically significant. Data are graphed as mean±standard error of the mean (SEM), unless otherwise specified.

7.13. Antibody table

Antibody	Species	Supplier	Code	Use	Dilution	MW
ATF4	Rabbit	Abcam	ab184909	WB	1:1500 Milk	55kDa
ATF6	Mouse	Abcam	ab122897	WB	1:500 Milk	55-90kDa
Beclin	Rabbit	Cell Signalling	#3495	WB	1:1000 BSA 5%	60kDa
p-Beclin	Rabbit	Cell Signalling	#14717	WB	1:1000 BSA 5%	60kDa
BiP/GRP78	Rabbit	Cell Signalling	#3177	WB	1:2000 Milk	78kDa
Calnexin	Rabbit	Cell Signalling	#2679	WB	1:1000 Milk	90kDa
Chromogranin A	Rabbit	Abcam	ab15160	IF	1:200	n.a.
CXCR4	Mouse	BD	557145 PE	FACS	6µl x 10 ⁶ cells	n.a.
eIF2α	Mouse	Abcam	ab5369	WB	1:500 Milk	36kDa
p-eIF2α	Rabbit	Cell Signalling	#3597	WB	1:1000 BSA 5%	38kDa
ERO1α	Rabbit	Cell Signalling	#3264	WB	1:1000 Milk	60kDa
GAPDH	Mouse	Abcam	ab8245	WB	1:5000 Milk	36kDa
Insulin	Guinea pig	Dako	A0564	IF	1:200	n.a.

Insulin	Mouse	BD	T56-706 Alexa- Fluor647	FACS	2 μ l x 10 ⁶ cells	n.a.
IRE1 α	Rabbit	Cell Signalling	#3294	WB	1:1000 Milk	130kDa
p-IRE1 α	Rabbit	Abcam	ab124945	WB	1:2000 BSA 5%	110kDa
LC3A/B	Rabbit	Cell Signalling	#12741	WB	1:1000 Milk	14- 16kDa
NANOG	Goat	Abcam	AF1997	IF	1:20	n.a.
NKX6.1	Mouse	R&D	MAB5857	IF	1:100	n.a.
NKX6.1	Mouse	BD	R11-560 PE	FACS	5 μ l x 10 ⁶ cells	n.a.
OCT4	Mouse	Novus	NBP2-15052	IF	1:100	n.a.
OCT4	Mouse	BD	40/Oct3 Alexa- Fluor647	FACS	4 μ l x 10 ⁶ cells	n.a.
PC1/3	Rabbit	Abcam	ab220363	WB	1:1000 Milk	84kDa
PDX1	Mouse	BD	658A5 Alexa- Fluor488	FACS	5 μ l x 10 ⁶ cells	n.a.
Somatostatin	Rat	Abcam	AB30788	IF	1:100	n.a.
SOX2	Mouse	Biotechne	MAB2018	IF	1:200	n.a.
Wolframin (679-783aa)	Sheep	Biotechne	AF7417	WB	1:200 Milk	100kDa
Wolframin (Ala43)	Rabbit	Cell Signalling	#8749	WB	1:1000 Milk	100kDa
XBP-1s	Rabbit	Cell Signalling	#12782	WB	1:1000 Milk	60kDa
HRP- conjugated anti-mouse	Goat	R&D	HAF007	WB	1:1000	n.a.
HRP- conjugated anti-rabbit	Goat	R&D	HAF008	WB	1:1000	n.a.

HRP-conjugated anti-sheep	Donkey	R&D	HAF016	WB	1:1000	n.a.
488 anti-mouse	Goat	AlexaFluor	A32723	IF	1:500	n.a.
488 anti-rabbit	Goat	AlexaFluor	A32731	IF	1:500	n.a.
488 anti-goat	Donkey	AlexaFluor	A32814	IF	1:500	n.a.
546 anti-mouse	Goat	AlexaFluor	A-11030	IF	1:500	n.a.
546 anti-goat	Rabbit	AlexaFluor	A-21085	IF	1:500	n.a.

7.14. Primer table

Gene (Protein)	Forward	Reverse
<i>ATF3</i>	ATGATGCTTCAACACCCAGG	TTTCGGCACTTTGCAGCTG
<i>ATF4</i>	GTTCTCCAGCGACAAGGCTA	ATCCTGCTTGCTGTTGTTGG
<i>ATF5</i>	GCTCGTAGACTATGGGAAACTCC	CATCCAGTCAGAGAAGCCATCAC
<i>ATF6</i>	CAGACAGTACCAACGCTTATGCC	GCAGAACTCCAGGTGCTTGAAG
<i>ATG10</i>	GGTGATAGTTGGGAATGGAGACC	GTCTGTCCATGGGTAGATGCTC
<i>ATG12</i>	GGGAAGGACTTACGGATGTCTC	AGGAGTGTCTCCCACAGCCTTT
<i>BECN1</i>	CTGGACACTCAGCTCAACGTCA	CTCTAGTGCCAGCTCCTTTAGC
<i>CACNA1D</i>	CTTCGACAACGTCCTCTCTGCT	GCCGATGTTCTCTCCATTCGAG
<i>DDIT3 (CHOP)</i>	AGAACCAGGAAACGGAAACAGA	TCTCCTTCATGCGCTGCTTT
<i>EDEMI</i>	CAAGTGTGGGTACGCCACG	AAAGAAGCTCTCCATCCGGTC
<i>EIF2AK3 (PERK)</i>	GTCCCAAGGCTTTGGAATCTGTC	CCTACCAAGACAGGAGTTCTGG
<i>ERN1 (IRE1α)</i>	CCGAACGTGATCCGCTACTTCT	CGCAAAGTCCTTCTGCTCCACA
<i>GAPDH</i>	GTCTCCTCTGACTTCAACAGCG	ACCACCCTGTTGCTGTAGCCAA

<i>HERPUDI</i>	TACTCCTCCCTGAGCAGATTCC	TTTCAGGATCAGTGCCTTCCTGT
<i>HSPA5</i> (BiP)	TGTTCAACCAATTATCAGCAAAC C	TTCTGCTGTATCCTCTTCACCAGT
<i>HYOU1</i>	AGGGCATCAAGGCTCACTTC	TGGTGTTGCCAAGTTTGGTG
<i>PDIA4</i>	CTCCAGAACCCAGGAAGAAATTG	CTTCTCATACTCGGGGGCAA
<i>SELIL</i>	GTGGGGCTTTTGTGAAACTGAA	TGACACTCTCTCCAGGGCTT
<i>SNAP25</i>	CGTCGTATGCTGCAACTGGTTG	GGTTCATGCCTTCTTCGACACG
<i>SQSTM1</i> (p62)	TGCCCAGACTACGACTTGTG	AGTGTCCGTGTTTCACCTTCC
<i>VAMP2</i>	CTCCAAACCTCACCAGTAACAGG	AGCTCCGACAGCTTCTGGTCTC
<i>WFS1_ex3</i>	GGGCCTACAAAGGGAGACAT	-
<i>WFS1_ex4</i>	GGCGACACGGATTGAAGAACT	AGTTCTTCATCCGTGTGC
<i>WFS1_ex5</i>	-	CCAGTACATGACCAGGGCTG
<i>WFS1_ex4_gR</i> <i>NA</i>	TAATACGACTCACTATAGGAGTTC TTCATCCGTG	TTCTAGCTCTAAAACGCGACACGG ATGAAGAAC
<i>WFS1_ex7_gR</i> <i>NA</i>	TAATACGACTCACTATAGAGCCAA GAACTACATC	TTCTAGCTCTAAAACGCGGATGT AGTTCTTGG
<i>WFS1_hr</i>	CTTCCTCCTCACCCAGCCTG	GGGTCTTGGTCACTCACCTT
<i>XBPI spliced</i>	CTGCCAGAGATCGAAAGAAGGC	CTCCTGGTTCTCAACTACAAGGC

8. References

- Abreu D, Asada R, Revilla JMP, Lavagnino Z, Kries K, Piston DW & Urano F (2020) Wolfram syndrome 1 gene regulates pathways maintaining beta-cell health and survival. *Lab Invest* 100: 849–862
- Abreu D, Stone SI, Pearson TS, Bucelli RC, Simpson AN, Hurst S, Brown CM, Kries K, Onwumere C, Gu H, *et al* (2021) A phase Ib/IIa clinical trial of dantrolene sodium in patients with Wolfram syndrome. *JCI Insight* 6
- Abreu D & Urano F (2019) Current Landscape of Treatments for Wolfram Syndrome. *Trends Pharmacol Sci* 40: 711–714
- Adachi Y, Yamamoto K, Okada T, Yoshida H, Harada A & Mori K (2008) ATF6 Is a Transcription Factor Specializing in the Regulation of Quality Control Proteins in the Endoplasmic Reticulum. *CELL Struct Funct* 33: 75–89
- Agulnick A, Ambruzs DM, Moorman M, Bhoumik A, Cesario RM, Payne JK, Kelly JR, Haakmeester C, Srijemac R, Wilson JN, *et al* (2015) Insulin-Producing Endocrine Cells Differentiated In Vitro From Human Embryonic Stem Cells Function in Macroencapsulation Devices In Vivo. *Stem Cells Transl Med* 4: 1214–1222
- Åkerfeldt MC, Howes J, Chan JY, Stevens VA, Boubenna N, McGuire HM, King C, Biden TJ & Laybutt DR (2008) Cytokine-Induced β -cell death is independent of endoplasmic reticulum stress signaling. *Diabetes* 57: 3034–3044
- Akiyama M, Hatanaka M, Ohta Y, Ueda K, Yanai A, Uehara Y, Tanabe K, Tsuru M, Miyazaki M, Saeki S, *et al* (2009) Increased insulin demand promotes while pioglitazone prevents pancreatic beta cell apoptosis in *Wfs1* knockout mice. *Diabetologia* 52: 653–663
- Alimadadi A, Ebrahim-Habibi A, Abbasi F, Amoli MM, Sayahpour FA & Larijani B (2011) Novel mutations of wolframin: A report with a look at the protein structure. *Clin Genet* 79: 96–99
- Aloi C, Salina A, Pasquali L, Lugani F, Perri K, Russo C, Tallone R, Ghiggeri GM, Lorini R & D'Annunzio G (2012) Wolfram syndrome: New mutations, different phenotype. *PLoS One* 7: 121–123
- Amodio G, Venditti R, De Matteis MA, Moltedo O, Pignataro P & Remondelli P (2013) Endoplasmic reticulum stress reduces COPII vesicle formation and modifies Sec23a cycling at ERESs. *FEBS Lett* 587: 3261–3266

- Amr S, Heisey C, Zhang M, Xia XJ, Shows KH, Ajlouni K, Pandya A, Satin LS, El-Shanti H & Shiang R (2007) A homozygous mutation in a novel zinc-finger protein, ERIS, is responsible for Wolfram syndrome 2. *Am J Hum Genet* 81: 673–683
- Angebault C, Fauconnier J, Patergnani S, Rieusset J, Danese A, Affortit CA, Jagodzinska J, Mégy C, Quiles M, Cazevieille C, *et al* (2018) ER-mitochondria cross-talk is regulated by the Ca²⁺ sensor NCS1 and is impaired in Wolfram syndrome. *Sci Signal* 11
- Appenzeller-Herzog C, Riemer J, Zito E, Chin KT, Ron D, Spiess M & Ellgaard L (2010) Disulphide production by Ero1 α -PDI relay is rapid and effectively regulated. *EMBO J* 29: 3318–3329
- Ariyasu D, Yoshida H & Hasegawa Y (2017) Endoplasmic Reticulum (ER) Stress and Endocrine Disorders. *Int J Mol Sci* 2017, Vol 18, Page 382 18: 382
- De Azua IR, Scarselli M, Rosemond E, Gautam D, Jou W, Gavrilova O, Ebert PJ, Levitt P & Wess J (2010) RGS4 is a negative regulator of insulin release from pancreatic beta-cells in vitro and in vivo. *Proc Natl Acad Sci U S A* 107: 7999–8004
- Bababeygy SR, Wang MY, Khaderi KR & Sadun AA (2012) Visual improvement with the use of idebenone in the treatment of wolfram syndrome. *J Neuro-Ophthalmology* 32: 386–389
- Bainbridge JWB, Mehat MS, Sundaram V, Robbie SJ, Barker SE, Ripamonti C, Georgiadis A, Mowat FM, Beattie SG, Gardner PJ, *et al* (2015) Long-Term Effect of Gene Therapy on Leber's Congenital Amaurosis. *N Engl J Med* 372: 1887–1897
- Balboa D, Barsby T, Lithovius V, Saarimäki-Vire J, Omar-Hmeadi M, Dyachok O, Montaser H, Lund P-E, Yang M, Ibrahim H, *et al* (2022) Functional, metabolic and transcriptional maturation of human pancreatic islets derived from stem cells. *Nat Biotechnol*
- Balboa D, Saarimäki-Vire J & Otonkoski T (2019) Concise Review: Human Pluripotent Stem Cells for the Modeling of Pancreatic β -Cell Pathology. *Stem Cells* 37: 33–41
- Ballinger SW, Shoffner JM, Hedaya E V., Trounce I, Polak MA, Koontz DA & Wallace DC (1992) Maternally transmitted diabetes and deafness associated with a 10.4 kb mitochondrial DNA deletion. *Nat Genet* 1: 11–15
- Ban H, Nishishita N, Fusaki N, Tabata T, Saeki K, Shikamura M, Takada N, Inoue M, Hasegawa M, Kawamata S, *et al* (2011) Efficient generation of transgene-free human induced pluripotent stem cells (iPSCs) by temperature-sensitive Sendai virus vectors. *Proc Natl Acad Sci U S A* 108: 14234–14239

- Barrett T, Bunday SE & Macleod AF (1995) (DIDMOAD) syndrome UK nationwide study of Wolfram. *Lancet* 346: 1458–1463
- Batjargal K, Tajima T, Jimbo EF & Yamagata T (2020) Effect of 4-phenylbutyrate and valproate on dominant mutations of WFS1 gene in Wolfram syndrome. *J Endocrinol Invest*: 2–10
- Battista M, Cascavilla ML, Grosso D, Borrelli E, Frontino G, Amore G, Carbonelli M, Bonfanti R, Rigamonti A, Barresi C, *et al* (2022) Retinal vascular impairment in Wolfram syndrome: an optical coherence tomography angiography study. *Sci Reports* 2022 121 12: 1–8
- Belmont PJ, Tadimalla A, Chen WJ, Martindale JJ, Thuerauf DJ, Marcinko M, Gude N, Sussman MA & Glembotski CC (2008) Coordination of Growth and Endoplasmic Reticulum Stress Signaling by Regulator of Calcineurin 1 (RCAN1), a Novel ATF6-inducible Gene. *J Biol Chem* 283: 14012
- Bernales S, McDonald KL & Walter P (2006) Autophagy counterbalances endoplasmic reticulum expansion during the unfolded protein response. *PLoS Biol* 4: 2311–2324
- Berry V, Gregory-Evans C, Emmett W, Waseem N, Raby J, Prescott D, Moore AT & Bhattacharya SS (2013) Wolfram gene (WFS1) mutation causes autosomal dominant congenital nuclear cataract in humans. *Eur J Hum Genet* 21: 1356–1360
- Bonnet Wersinger D, Benkafadar N, Jagodzinska J, Hamel C, Tanizawa Y, Lenaers G & Delettre C (2014) Impairment of visual function and retinal ER stress activation in Wfs1-deficient mice. *PLoS One* 9: 97222
- Bourgeois S, Sawatani T, Van Mulders A, De Leu N, Heremans Y, Heimberg H, Cnop M & Staels W (2021) Towards a Functional Cure for Diabetes Using Stem Cell-Derived Beta Cells: Are We There Yet? *Cells* 10 doi:10.3390/cells10010191 [PREPRINT]
- Boye SE, Boye SL, Lewin AS & Hauswirth WW (2013) A Comprehensive Review of Retinal Gene Therapy. *Mol Ther* 21: 509
- Brusko TM, Russ HA & Stabler CL (2021) Strategies for durable β cell replacement in type 1 diabetes. *Science (80-)* 373: 516–522
- Bueno GE, Ruiz-Castañeda D, Martínez JR, Muñoz MR & Alascio PC (2018) Natural history and clinical characteristics of 50 patients with Wolfram syndrome. *Endocrine* 61: 440–446
- Bunday S, Poulton K, Whitwell H, Curtis E, Brown IAR & Fielder AR (1992) Mitochondrial

- abnormalities in the DIDMOAD syndrome. *J Inherit Metab Dis* 15: 315–319
- Cagalinec M, Liiv M, Hodurova Z, Hickey MA, Vaarmann A, Mandel M, Zeb A, Choubey V, Kuum M, Safiulina D, *et al* (2016) Role of Mitochondrial Dynamics in Neuronal Development: Mechanism for Wolfram Syndrome. *PLoS Biol* 14: 1–28
- Cano A, Rouzier C, Monnot S, Chabrol B, Conrath J, Lecomte P, Delobel B, Boileau P, Valero R, Procaccio V, *et al* (2007) Identification of novel mutations in WFS1 and genotype-phenotype correlation in Wolfram syndrome. *Am J Med Genet A* 143A: 1605–1612
- Cao Y & Zhang L (2013) A Smurf1 tale: Function and regulation of an ubiquitin ligase in multiple cellular networks. *Cell Mol Life Sci* 70: 2305–2317
- Carcamo-Orive I, Hoffman GE, Cundiff P, Beckmann ND, D’Souza SL, Knowles JW, Patel A, Papatsenko D, Abbasi F, Reaven GM, *et al* (2017) Analysis of Transcriptional Variability in a Large Human iPSC Library Reveals Genetic and Non-genetic Determinants of Heterogeneity. *Cell Stem Cell* 20: 518-532.e9
- Cardenas-Diaz FL & Cardenas FL (2018) Modeling Monogenic Diabetes Mody3 Using Human Pluripotent Stem Cells.
- Carreras-Sureda A, Jaña F, Urra H, Durand S, Mortenson DE, Sagredo A, Bustos G, Hazari Y, Ramos-Fernández E, Sassano ML, *et al* (2019) Non-canonical function of IRE1 α determines mitochondria-associated endoplasmic reticulum composition to control calcium transfer and bioenergetics. *Nat Cell Biol* 21
- Cattaneo M, La Sala L, Rondinelli M, Errichiello E, Zuffardi O, Puca AA, Genovese S & Ceriello A (2017) A donor splice site mutation in CISD2 generates multiple truncated, non-functional isoforms in Wolfram syndrome type 2 patients. *BMC Med Genet* 18: 1–8
- Chausseot A, Bannwarth S, Rouzier C, Vialettes B, Mkadem SA El, Chabrol B, Cano A, Labauge P & Paquis-Flucklinger V (2011) Neurologic features and genotype-phenotype correlation in Wolfram syndrome. *Ann Neurol* 69: 501–508
- Chen YJ, Knupp J, Arunagiri A, Haataja L, Arvan P & Tsai B (2021) PGRMC1 acts as a size-selective cargo receptor to drive ER-phagic clearance of mutant prohormones. *Nat Commun* 12
- Coppieters KT, Dotta F, Amirian N, Campbell PD, Kay TWH, Atkinson MA, Roep BO & von Herrath MG (2012) Demonstration of islet-autoreactive CD8 T cells in insulitic lesions from recent onset and long-term type 1 diabetes patients. *J Exp Med* 209: 51–60

- Crouzier L, Danese A, Yasui Y, Richard EM, Liévens J-C, Patergnani S, Couly S, Diez C, Denus M, Cubedo N, *et al* (2022) Activation of the sigma-1 receptor chaperone alleviates symptoms of Wolfram syndrome in preclinical models. *Sci Transl Med* 14: 3763
- Crowley LC, Marfell BJ, Scott AP & Waterhouse NJ (2016) Quantitation of apoptosis and necrosis by annexin V binding, propidium iodide uptake, and flow cytometry. *Cold Spring Harb Protoc* 2016: 953–957
- Csordás G, Weaver D & Hajnóczky G (2018) Endoplasmic Reticulum–Mitochondrial Contactology: Structure and Signaling Functions. *Trends Cell Biol* 28: 523–540
- D’Amour KA, Bang AG, Eliazar S, Kelly OG, Agulnick AD, Smart NG, Moorman MA, Kroon E, Carpenter MK & Baetge EE (2006) Production of pancreatic hormone-expressing endocrine cells from human embryonic stem cells. *Nat Biotechnol* 24: 1392–1401
- Danielpur L, Sohn YS, Karmi O, Fogel C, Zinger A, Abu-Libdeh A, Israeli T, Riahi Y, Pappo O, Birk R, *et al* (2016) GLP-1-RA corrects mitochondrial labile iron accumulation and improves β -cell function in type 2 wolfram syndrome. *J Clin Endocrinol Metab* 101: 3592–3599
- Davis S, Wang J, Zhu M, Stahmer K, Lakshminarayan R, Ghassemian M, Jiang Y, Miller EA & Ferro-Novick S (2016) Sec24 phosphorylation regulates autophagosome abundance during nutrient deprivation. *Elife* 5
- Deiss D, Diederich S & Kordonouri O (2011) [Successful treatment with liraglutide in type 1 diabetes and MODY]. *Dtsch Med Wochenschr* 136: 1116–1120
- Delépine M, Nicolino M, Barrett T, Golamaully M, Mark Lathrop G & Julier C (2000) EIF2AK3, encoding translation initiation factor 2- α kinase 3, is mutated in patients with Wolcott-Rallison syndrome. *Nat Genet* 25: 406–409
- Delprat B, Maurice T & Delettre C (2018) Wolfram syndrome: MAMs’ connection? *Cell Death Dis* 9: 364
- Delvecchio M, Iacoviello M, Pantaleo A & Resta N (2021) Clinical spectrum associated with wolfram syndrome type 1 and type 2: A review on genotype–phenotype correlations. *Int J Environ Res Public Health* 18: 4796
- Docena MK, Faiman C, Stanley CM & Pantalone KM (2014) Mody-3: novel HNF1A mutation and the utility of glucagon-like peptide (GLP)-1 receptor agonist therapy. *Endocr Pract* 20: 107–111

- Dorrell C, Schug J, Canaday PS, Russ HA, Tarlow BD, Grompe MT, Horton T, Hebrok M, Streeter PR, Kaestner KH, *et al* (2016) Human islets contain four distinct subtypes of β cells. *Nat Commun* 7: 1–9
- El-Shanti, Lidral, Jarrah, Druhan & Ajlouni (2000) Homozygosity mapping identifies an additional locus for Wolfram syndrome on chromosome 4q. *Am J Hum Genet* 66: 1229–1236
- Elek Z, Németh N, Nagy G, Németh H, Somogyi A, Hosszúfalusi N, Sasvári-Székely M & Rónai Z (2015) Micro-RNA binding site polymorphisms in the WFS1 gene are risk factors of diabetes mellitus. *PLoS One* 10: 1–17
- Evans MJ & Kaufman MH (1981) Establishment in culture of pluripotential cells from mouse embryos. *Nature* 292: 154–156
- De Falco M, Manente L, Lucariello A, Baldi G, Fiore P, Laforgia V, Baldi A, Iannaccone A & De Luca A (2012) Localization and distribution of wolframin in human tissues. *Front Biosci* 1: 1986–1998
- Fawcett KA, Wheeler E, Morris AP, Ricketts SL, Hallmans G, Rolandsson O, Daly A, Wasson J, Permutt A, Hattersley AT, *et al* (2010) Detailed investigation of the role of common and low-frequency WFS1 variants in type 2 diabetes risk. *Diabetes* 59: 741–746
- Fiorese CJ, Schulz AM, Lin YF, Rosin N, Pellegrino MW & Haynes CM (2016) The Transcription Factor ATF5 Mediates a Mammalian Mitochondrial UPR. *Curr Biol* 26: 2037–2043
- Flahou C, Morishima T, Takizawa H & Sugimoto N (2021) Fit-For-All iPSC-Derived Cell Therapies and Their Evaluation in Humanized Mice With NK Cell Immunity. *Front Immunol* 12 doi:10.3389/fimmu.2021.662360 [PREPRINT]
- Fonseca SG, Burcin M, Gromada J & Urano F (2009) Endoplasmic reticulum stress in β -cells and development of diabetes. *Curr Opin Pharmacol* 9: 763–770
- Fonseca SG, Fukuma M, Lipson KL, Nguyen LX, Allen JR, Oka Y & Urano F (2005) WFS1 is a novel component of the unfolded protein response and maintains homeostasis of the endoplasmic reticulum in pancreatic β -cells. *J Biol Chem* 280: 39609–39615
- Fonseca SG, Ishigaki S, Osowski CM, Lu S, Lipson KL, Ghosh R, Hayashi E, Ishihara H, Oka Y, Permutt MA, *et al* (2010) Wolfram syndrome 1 gene negatively regulates ER stress signaling in rodent and human cells. *J Clin Invest* 120: 744–755

- Fonseca SG, Urano F, Weir GC, Gromada J & Burcin M (2012) Wolfram syndrome 1 and adenylyl cyclase 8 interact at the plasma membrane to regulate insulin production and secretion. *Nat Cell Biol* 14: 1105–1112
- De Franco E, Flanagan SE, Yagi T, Abreu D, Mahadevan J, Johnson MB, Jones G, Acosta F, Mulaudzi M, Lek N, *et al* (2017) Dominant ER stress-inducing WFS1 mutations underlie a genetic syndrome of neonatal/infancy-onset diabetes, congenital sensorineural deafness, and congenital cataracts. *Diabetes* 66: 2044–2053
- De Franco E, Lytrivi M, Ibrahim H, Montaser H, Wakeling MN, Fantuzzi F, Patel K, Demarez C, Cai Y, Igoillo-Esteve M, *et al* (2020) YIPF5 mutations cause neonatal diabetes and microcephaly through endoplasmic reticulum stress. *J Clin Invest* 130: 6338–6353
- Frontino G, Raouf T, Canarutto D, Tirelli E, Di Tonno R, Rigamonti A, Cascavilla LM, Baldoli C, Scotti R, Bonfanti R, *et al* (2021) Off-label Liraglutide use in children with Wolfram Syndrome type 1: extensive characterization of four patients. [PREPRINT]
- Fu S, Yalcin A, Lee GY, Li P, Fan J, Arruda AP, Pers BM, Yilmaz M, Eguchi K & Hotamisligil GS (2015) Phenotypic assays identify a small molecule modulator of the unfolded protein response with anti-diabetic activity. *Sci Transl Med* 7: 292–98
- Fukuoka H, Kanda Y, Ohta S & Usami SI (2007) Mutations in the WFS1 gene are a frequent cause of autosomal dominant nonsyndromic low-frequency hearing loss in Japanese. *J Hum Genet* 52: 510–515
- Gharanei S, Zatyka M, Astuti D, Fenton J, Sik A, Nagy Z & Barrett TG (2013) Vacuolar-type H⁺-ATPase V1A subunit is a molecular partner of Wolfram syndrome 1 (WFS1) protein, which regulates its expression and stability. *Hum Mol Genet* 22: 203–217
- González-González JG, Díaz González-Colmenero A, Millán-Alanís JM, Lytvyn L, Solis RC, Mustafa RA, Palmer SC, Li S, Hao Q, Alvarez-Villalobos NA, *et al* (2021) Values, preferences and burden of treatment for the initiation of GLP-1 receptor agonists and SGLT-2 inhibitors in adult patients with type 2 diabetes: A systematic review. *BMJ Open* 11
- Gonzalez CD, Lee MS, Marchetti P, Pietropaolo M, Towns R, Vaccaro MI, Watada H & Wiley JW (2011) The emerging role of autophagy in the pathophysiology of diabetes mellitus. *Autophagy* 7: 2–11 doi:10.4161/auto.7.1.13044 [PREPRINT]
- Gornalusse GG, Hirata RK, Funk SE, Riobos L, Lopes VS, Manske G, Prunkard D, Colunga

- AG, Hanafi LA, Clegg DO, *et al* (2017) HLA-E-expressing pluripotent stem cells escape allogeneic responses and lysis by NK cells. *Nat Biotechnol* 35: 765–772
- Gromada J, Bark C, Smidt K, Efanov AM, Janson J, Mandic SA, Webb D-L, Zhang W, Meister B, Jeromin A, *et al* (2005) Neuronal calcium sensor-1 potentiates glucose-dependent exocytosis in pancreatic β cells through activation of phosphatidylinositol 4-kinase β . *Proc Natl Acad Sci* 102: 10303–10308
- Grzela DP, Marciniak B & Pulaski L (2020) Characterization of an induced pluripotent stem cell line (IMBPASi001-A) derived from fibroblasts of a patient affected by Wolfram Syndrome. *Stem Cell Res* 46: 101858
- Gubas A & Dikic I (2021) A Guide To... The regulation of selective autophagy receptors. *FEBS J*
- Guo X, Shen S, Song S, He S, Cui Y, Xing G, Wang J, Yin Y, Fan L, He F, *et al* (2011) The E3 ligase Smurf1 regulates Wolfram syndrome protein stability at the endoplasmic reticulum. *J Biol Chem* 286: 18037–18047
- Gurdon JB, Elsdale TR & Fischberg M (1958) Sexually mature individuals of *Xenopus laevis* from the transplantation of single somatic nuclei. *Nature* 182: 64–65
- Hakonen E, Chandra V, Fogarty CL, Yu NYL, Ustinov J, Katayama S, Galli E, Danilova T, Lindholm P, Vartiainen A, *et al* (2018) MANF protects human pancreatic beta cells against stress-induced cell death. *Diabetologia* 61: 2202–2214
- Halban PA & Wollheim CB (1980) Intracellular degradation of insulin stores by rat pancreatic islets in vitro. An alternative pathway for homeostasis of pancreatic insulin content. *J Biol Chem* 255: 6003–6006
- Haller C, Piccand J, De Franceschi F, Ohi Y, Bhoumik A, Boss C, De Marchi U, Jacot G, Metairon S, Descombes P, *et al* (2019) Macroencapsulated Human iPSC-Derived Pancreatic Progenitors Protect against STZ-Induced Hyperglycemia in Mice. *Stem Cell Reports* 12: 787–800
- Hamel C, Jagodzinska J, Bonner-Wersinger D, Koks S, Seveno M & Delettre C (2017) Advances in gene therapy for Wolfram syndrome. *Acta Ophthalmol* 95
- Hara T, Mahadevan J, Kanekura K, Hara M, Lu S & Urano F (2014) Calcium efflux from the endoplasmic reticulum leads to β -cell death. *Endocrinology* 155: 758–768
- Harding HP, Novoa I, Zhang Y, Zeng H, Wek R, Schapira M & Ron D (2000) Regulated

- translation initiation controls stress-induced gene expression in mammalian cells. *Mol Cell* 6: 1099–1108
- Hardy C, Khanim F, Torres R, Scott-Brown M, Seller A, Poulton J, Collier D, Kirk J, Polymeropoulos M, Latif F, *et al* (1999) Clinical and molecular genetic analysis of 19 Wolfram syndrome kindreds demonstrating a wide spectrum of mutations in WFS1. *Am J Hum Genet* 65: 1279–1290
- Hatanaka M, Tanabe K, Yanai A, Ohta Y, Kondo M, Akiyama M, Shinoda K, Oka Y & Tanizawa Y (2011) Wolfram syndrome 1 gene (WFS1) product localizes to secretory granules and determines granule acidification in pancreatic β -cells. *Hum Mol Genet* 20: 1274–1284
- Hellman M, Arumäe U, Yu LY, Lindholm P, Peränen J, Saarma M & Permi P (2011) Mesencephalic astrocyte-derived neurotrophic factor (MANF) has a unique mechanism to rescue apoptotic neurons. *J Biol Chem* 286: 2675–2680
- Henderson MJ, Trychta KA, Yang SM, Bäck S, Yasgar A, Wires ES, Danchik C, Yan X, Yano H, Shi L, *et al* (2021) A target-agnostic screen identifies approved drugs to stabilize the endoplasmic reticulum-resident proteome. *Cell Rep* 35: 109040
- De Heredia ML, Cléries R & Nunes V (2013) Genotypic classification of patients with Wolfram syndrome: Insights into the natural history of the disease and correlation with phenotype. *Genet Med* 15: 497–506
- Hershey T, Lugar HM, Shimony JS, Rutlin J, Koller JM, Perantie DC, Paciorkowski AR, Eisenstein SA, Permutt MA & Group the WUWS (2012) Early Brain Vulnerability in Wolfram Syndrome. *PLoS One* 7: e40604
- Hetz C, Martinon F, Rodriguez D & Glimcher LH (2011) The unfolded protein response: Integrating stress signals through the stress sensor IRE1 α . *Physiol Rev* 91: 1219–1243
- Hildebrand MS, Sorensen JL, Jensen M, Kimberling WJ & Smith RJH (2008) Autoimmune disease in a DFNA6/14/38 family carrying a novel missense mutation in WFS1. *Am J Med Genet Part A* 146: 2258–2265
- Hofmann S, Philbrook C, Gerbitz KD & Bauer MF (2003) Wolfram syndrome: Structural and functional analyses of mutant and wild-type wolframin, the WFS1 gene product. *Hum Mol Genet* 12: 2003–2012
- Hogrebe NJ, Augsornworawat P, Maxwell KG, Velazco-Cruz L & Millman JR (2020)

- Targeting the cytoskeleton to direct pancreatic differentiation of human pluripotent stem cells. *Nat Biotechnol* 38: 460–470
- Hogrebe NJ, Maxwell KG, Augsornworawat P & Millman JR (2021) Generation of insulin-producing pancreatic β cells from multiple human stem cell lines. *Nat Protoc* 2021 169 16: 4109–4143
- Hou JC, Min L & Pessin JE (2009) Insulin Granule Biogenesis, Trafficking and Exocytosis. *Vitam Horm* 80: 473–506
- Huang CJ, Gurlo T, Haataja L, Costes S, Daval M, Ryazantsev S, Wu X, Butler AE & Butler PC (2010) Calcium-activated Calpain-2 Is a Mediator of Beta Cell Dysfunction and Apoptosis in Type 2 Diabetes. *J Biol Chem* 285: 339–348
- Idevall-Hagren O & Tengholm A (2020) Metabolic regulation of calcium signaling in beta cells. *Semin Cell Dev Biol* 103: 20–30 doi:10.1016/j.semcdb.2020.01.008 [PREPRINT]
- Inoue H, Tanizawa Y, Wasson J, Behn P, Kalidas K, Bernal-Mizrachi E, Mueckler M, Marshall H, Donis-Keller H, Crock P, *et al* (1998) A gene encoding a transmembrane protein is mutated in patients with diabetes mellitus and optic atrophy (Wolfram syndrome). *Nat Genet* 20: 143–148
- Ishihara H, Takeda S, Tamura A, Takahashi R, Yamaguchi S, Takei D, Yamada T, Inoue H, Soga H, Katagiri H, *et al* (2004) Disruption of the WFS1 gene in mice causes progressive β -cell loss and impaired stimulus - Secretion coupling in insulin secretion. *Hum Mol Genet* 13: 1159–1170
- Jackson MJ, Bindoff LA, Weber K, Wilson JN, Ince P, Alberti KGMM & Turnbull DM (1994) Biochemical and molecular studies of mitochondrial function in diabetes insipidus, diabetes mellitus, optic atrophy, and deafness. *Diabetes Care* 17: 728–733
- Jagomäe T, Seppa K, Reimets R, Pastak M, Plaas M, Hickey MA, Kukker KG, Moons L, De Groef L, Vasar E, *et al* (2021) Early Intervention and Lifelong Treatment with GLP1 Receptor Agonist Liraglutide in a Wolfram Syndrome Rat Model with an Emphasis on Visual Neurodegeneration, Sensorineural Hearing Loss and Diabetic Phenotype. *Cells* 10: 3193
- Johnston NR, Mitchell RK, Haythorne E, Pessoa MP, Semplici F, Ferrer J, Piemonti L, Marchetti P, Bugliani M, Bosco D, *et al* (2016) Beta Cell Hubs Dictate Pancreatic Islet Responses to Glucose. *Cell Metab* 24: 389–401

- Juliana CA, Yang J, Rozo A V., Good A, Groff DN, Wang SZ, Green MR & Stoffers DA (2017) ATF5 regulates β -cell survival during stress. *Proc Natl Acad Sci U S A* 114: 1341–1346
- Kakiuchi C, Ishigaki S, Osowski CM, Fonseca SG, Kato T & Urano F (2009) Valproate, a mood stabilizer, induces WFS1 expression and modulates its interaction with ER stress protein GRP94. *PLoS One* 4
- Kakiuchi C, Ishiwata M, Hayashi A & Kato T (2006) XBP1 induces WFS1 through an endoplasmic reticulum stress response element-like motif in SH-SY5Y cells. *J Neurochem* 97: 545–555
- Kakoi S, Yorimitsu T & Sato K (2013) COPII machinery cooperates with ER-localized Hsp40 to sequester misfolded membrane proteins into ER-associated compartments. *Mol Biol Cell* 24: 633–642
- Karasik A, O’Hara C, Srikanta S, Swift M, Soeldner JS, Kahn CR & Herskowitz RD (1989) Genetically programmed selective islet β -cell loss in diabetic subjects with Wolfram’s syndrome. *Diabetes Care* 12: 135–138
- Kato T, Iwamoto K, Washizuka S, Mori K, Tajima O, Akiyama T, Nanko S, Kunugi H & Kato N (2003) No association of mutations and mRNA expression of WFS1/wolframin with bipolar disorder in humans. *Neurosci Lett* 338: 21–24
- Ke M, Chong C-M, Zeng H, Huang M, Huang Z, Zhang K, Cen X, Lu J-H, Yao X, Qin D, *et al* (2020) Azoramide protects iPSC-derived dopaminergic neurons with PLA2G6 D331Y mutation through restoring ER function and CREB signaling. *Cell Death Dis* 2020 112 11: 1–14
- Keenan HA, Sun JK, Levine J, Doria A, Aiello LP, Eisenbarth G, Bonner-Weir S & King GL (2010) Residual insulin production and pancreatic β -cell turnover after 50 years of diabetes: Joslin medalist study. *Diabetes* 59: 2846–2853
- Khanim F, Kirk J, Latif F & Barrett TG (2001) WFS1/wolframin mutations, wolfram syndrome, and associated diseases. *Hum Mutat* 17: 357–367
- Kinsley BT, Swift M, Dumont RH & Swift RG (1995) Morbidity and mortality in the Wolfram syndrome. *Diabetes Care* 18: 1566–1570
- Kocaturk NM & Gozuacik D (2018) Crosstalk between mammalian autophagy and the ubiquitin-proteasome system. *Front Cell Dev Biol* 6: 128 doi:10.3389/fcell.2018.00128

[PREPRINT]

- Kondo M, Tanabe K, Amo-Shiinoki K, Hatanaka M, Morii T, Takahashi H, Seino S, Yamada Y & Tanizawa Y (2018) Activation of GLP-1 receptor signalling alleviates cellular stresses and improves beta cell function in a mouse model of Wolfram syndrome. *Diabetologia* 61: 2189–2201
- Kranjc T, Dempsey E, Cagney G, Nakamura N, Shields DC & Simpson JC (2017) Functional characterisation of the YIPF protein family in mammalian cells. *Histochem Cell Biol* 147: 439–451
- Kranz P, Neumann F, Wolf A, Classen F, Pomsch M, Ocklenburg T, Baumann J, Janke K, Baumann M, Goepelt K, *et al* (2017) PDI is an essential redox-sensitive activator of PERK during the unfolded protein response (UPR). *Cell Death Dis* 2017 88 8: e2986–e2986
- Ku HC & Cheng CF (2020) Master Regulator Activating Transcription Factor 3 (ATF3) in Metabolic Homeostasis and Cancer. *Front Endocrinol (Lausanne)* 11: 556
doi:10.3389/fendo.2020.00556 [PREPRINT]
- Lang H, Xiang Y, Lin N, Ai Z, You Z, Xiao J, Liu D & Yang Y (2018) Identification of a Panel of MiRNAs as Positive Regulators of Insulin Release in Pancreatic B-Cells. *Cell Physiol Biochem* 48: 185–193
- Lee H, Lee YS, Harenda Q, Pietrzak S, Oktay HZ, Schreiber S, Liao Y, Sonthalia S, Cieccko AE, Chen YG, *et al* (2020) Beta Cell Dedifferentiation Induced by IRE1 α Deletion Prevents Type 1 Diabetes. *Cell Metab* 31: 822-836.e5
- Lemaire K & Schuit F (2012) Integrating insulin secretion and ER stress in pancreatic β -cells. *Nat Cell Biol* 14: 979–981
- Li G, Mongillo M, Chin KT, Harding H, Ron D, Marks AR & Tabas I (2009) Role of ERO1- α -mediated stimulation of inositol 1,4,5-triphosphate receptor activity in endoplasmic reticulum stress-induced apoptosis. *J Cell Biol* 186: 783–792
- Li J, Ni M, Lee B, Barron E, Hinton DR & Lee AS (2008) The unfolded protein response regulator GRP78/BiP is required for endoplasmic reticulum integrity and stress-induced autophagy in mammalian cells. *Cell Death Differ* 15: 1460–1471
- Lim SW, Jin L, Jin J & Yang CW (2016) Effect of Exendin-4 on Autophagy Clearance in Beta Cell of Rats with Tacrolimus-induced Diabetes Mellitus. *Sci Reports* 2016 61 6: 1–15
- Lin TK, Lin KJ, Lin HY, Lin KL, Lan MY, Wang PW, Wang TJ, Wang FS, Tsai PC, Liou CW,

- et al* (2021) Glucagon-Like Peptide-1 Receptor Agonist Ameliorates 1-Methyl-4-Phenyl-1,2,3,6-Tetrahydropyridine (MPTP) Neurotoxicity Through Enhancing Mitophagy Flux and Reducing α -Synuclein and Oxidative Stress. *Front Mol Neurosci* 14
- Loncke J, Vervliet T, Parys JB, Kaasik A & Bultynck G (2021) Uniting the divergent Wolfram syndrome-linked proteins WFS1 and CISD2 as modulators of Ca²⁺ signaling. *Sci Signal* 14: eabc6165
- Lu S, Kanekura K, Hara T, Mahadevan J, Spears LD, Osowski CM, Martinez R, Yamazaki-Inoue M, Toyoda M, Neilson A, *et al* (2014) A calcium-dependent protease as a potential therapeutic target for Wolfram syndrome. *Proc Natl Acad Sci U S A* 111: E5292–E5301
- Lugar HM, Koller JM, Rutlin J, Eisenstein SA, Neyman O, Narayanan A, Chen L, Shimony JS & Hershey T (2019) Evidence for altered neurodevelopment and neurodegeneration in Wolfram syndrome using longitudinal morphometry. *Sci Rep* 9: 1–11
- Ma EL & Sadun AA (2021) LHON. *Orphanet Encycl*
- Mahadevan J, Morikawa S, Yagi T, Abreu D, Lu S, Kanekura K, Brown CM & Urano F (2020) A soluble endoplasmic reticulum factor as regenerative therapy for Wolfram syndrome. *Lab Investig*
- Martin GR (1981) Isolation of a pluripotent cell line from early mouse embryos cultured in medium conditioned by teratocarcinoma stem cells. *Proc Natl Acad Sci U S A* 78: 7634–7638
- Martorell L, Gómez Zaera M, Valero J, Serrano D, Figuera L, Joven J, Labad A, Vilella E & Nunes V (2003) The WFS1 (Wolfram syndrome 1) is not a major susceptibility gene for the development of psychiatric disorders. *Psychiatr Genet* 13: 29–32
- Maxwell KG, Augsornworawat P, Velazco-Cruz L, Kim MH, Asada R, Hoglebe NJ, Morikawa S, Urano F & Millman JR (2020) Gene-edited human stem cell-derived β cells from a patient with monogenic diabetes reverse preexisting diabetes in mice. *Sci Transl Med* 12
- Maxwell KG & Millman JR (2021) Applications of iPSC-derived beta cells from patients with diabetes. *Cell Reports Med* 2: 100238
- Mirrahimi M, Safi S, Mohammadzadeh M, Doozandeh A & Suri F (2021) Variable Expressivity of Wolfram Syndrome in a Family with Multiple Affected Subjects. *J Ophthalmic Vis Res*
- Mishra R, Chen BS, Richa P & Yu-Wai-Man P (2021) Wolfram syndrome: new pathophysiological insights and therapeutic strategies. *Ther Adv Rare Dis* 2:

263300402110395

- Mizushima N, Yoshimori T & Levine B (2010) Methods in Mammalian Autophagy Research. *Cell* 140: 313–326
- La Morgia C, Maresca A, Amore G, Gramegna LL, Carbonelli M, Scimonelli E, Danese A, Patergnani S, Caporali L, Tagliavini F, *et al* (2020) Calcium mishandling in absence of primary mitochondrial dysfunction drives cellular pathology in Wolfram Syndrome. *Sci Rep* 10: 1–15
- Morikawa S, Blacher L, Onwumere C & Urano F (2022) Loss of Function of WFS1 Causes ER Stress-Mediated Inflammation in Pancreatic Beta-Cells. *Front Endocrinol (Lausanne)* 0: 417
- Morita S, Villalta SA, Feldman HC, Register AC, Rosenthal W, Hoffmann-Petersen IT, Mehdizadeh M, Ghosh R, Wang L, Colon-Negron K, *et al* (2017) Targeting ABL-IRE1 α Signaling Spares ER-Stressed Pancreatic β Cells to Reverse Autoimmune Diabetes
- Mozzillo E, Delvecchio M, Carella M, Grandone E, Palumbo P, Salina A, Aloï C, Buono P, Izzo A, D'Annunzio G, *et al* (2014) A novel CISD2 intragenic deletion, optic neuropathy and platelet aggregation defect in Wolfram syndrome type 2. *BMC Med Genet* 15
- Munshani S, Ibrahim EY, Domenicano I & Ehrlich BE (2021) The Impact of Mutations in Wolframin on Psychiatric Disorders. *Front Pediatr* 9: 1131
- Nair GG, Liu JS, Russ HA, Tran S, Saxton MS, Chen R, Juang C, Li M lan, Nguyen VQ, Giacometti S, *et al* (2019) Recapitulating endocrine cell clustering in culture promotes maturation of human stem-cell-derived β cells. *Nat Cell Biol* 21: 263–274
- Nami F, Ramezankhani R, Vandenabeele M, Vervliet T, Vogels K, Urano F & Verfaillie C (2021) Fast and Efficient Generation of Isogenic Induced Pluripotent Stem Cell Lines Using Adenine Base Editing. *Cris J* 4: 502–518
- Newman NJ, Yu-Wai-Man P, Carelli V, Moster ML, Biousse V, Vignal-Clermont C, Sergott RC, Klopstock T, Sadun AA, Barboni P, *et al* (2021) Efficacy and Safety of Intravitreal Gene Therapy for Leber Hereditary Optic Neuropathy Treated within 6 Months of Disease Onset. *Ophthalmology* 128: 649–660
- Nguyen LD, Fischer TT, Abreu D, Arroyo A, Urano F & Ehrlich BE (2020) Calpain inhibitor and ibudilast rescue β cell functions in a cellular model of Wolfram syndrome. *Proc Natl Acad Sci U S A* 117: 17389–17398

- Nkonge KM, Nkonge DK & Nkonge TN (2020) The epidemiology, molecular pathogenesis, diagnosis, and treatment of maturity-onset diabetes of the young (MODY). *Clin Diabetes Endocrinol* 6: 1–10
- Ontario Health Quality (2015) Pancreas Islet Transplantation for Patients With Type 1 Diabetes Mellitus: A Clinical Evidence Review. *Ont Health Technol Assess Ser* 15: 1–84 ([/pmc/articles/PMC4664938/](#)) [PREPRINT]
- Osman AA, Saito M, Makepeace C, Permutt MA, Schlesinger P & Mueckler M (2003) Wolframin Expression Induces Novel Ion Channel Activity in Endoplasmic Reticulum Membranes and Increases Intracellular Calcium. *J Biol Chem* 278: 52755–52762
- Paganoni S, Macklin E, Hendrix S, Berry J, Elliott M, Maiser S, Karam C, Caress J, Owegi M, Quick A, *et al* (2020) Trial of Sodium Phenylbutyrate-Taurursodiol for Amyotrophic Lateral Sclerosis. *N Engl J Med* 383: 919–930
- Pallotta MT, Tascini G, Crispoldi R, Orabona C, Mondanelli G, Grohmann U & Esposito S (2019) Wolfram syndrome, a rare neurodegenerative disease: from pathogenesis to future treatment perspectives. *J Transl Med* 17: 1–12
- Panfili E, Mondanelli G, Orabona C, Belladonna ML, Gargaro M, Fallarino F, Orecchini E, Prontera P, Proietti E, Frontino G, *et al* (2021) Novel mutations in the WFS1 gene are associated with Wolfram syndrome and systemic inflammation. *Hum Mol Genet* 30: 265–276
- Pavelka M & Roth J (2015) The Cytoplasm: The Secretory System. *Funct Ultrastruct*: 34–115
- Pearson GL, Gingerich MA, Walker EM, Biden TJ & Soleimanpour SA (2021) A Selective Look at Autophagy in Pancreatic β -Cells. *Diabetes* 70: 1229–1241
- Pellegrini S, Manenti F, Chimienti R, Nano R, Ottoboni L, Ruffini F, Martino G, Ravassard P, Piemonti L & Sordi V (2018) Differentiation of Sendai Virus-Reprogrammed iPSC into β Cells, Compared with Human Pancreatic Islets and Immortalized β Cell Line. *Cell Transplant* 27: 1548–1560
- Pellegrini S, Pipitone GB, Cospito A, Manenti F, Poggi G, Lombardo MT, Nano R, Martino G, Ferrari M, Carrera P, *et al* (2021) Generation of β Cells from iPSC of a MODY8 Patient with a Novel Mutation in the Carboxyl Ester Lipase (CEL) Gene . *J Clin Endocrinol Metab* doi:10.1210/clinem/dgaa986 [PREPRINT]
- Philbrook C, Fritz E & Weiher H (2005) Expressional and functional studies of Wolframin, the

- gene function deficient in Wolfram syndrome, in mice and patient cells. *Exp Gerontol* 40: 671–8
- Pourtoy-Brasselet S, Sciauvaud A, Boza-Moran M-G, Cailleret M, Jarrige M, Polvèche H, Polentes J, Chevet E, Martinat C, Peschanski M, *et al* (2021) Human iPSC-derived neurons reveal early developmental alteration of neurite outgrowth in the late-occurring neurodegenerative Wolfram syndrome. *Am J Hum Genet*
- Pugliese A (2017) Autoreactive T cells in type 1 diabetes. *J Clin Invest* 127: 2881–2891
- Ramzy A, Thompson DM, Ward-Hartstonge KA, Ivison S, Cook L, Garcia R V., Loyal J, Kim PTW, Warnock GL, Levings MK, *et al* (2021) Implanted pluripotent stem-cell-derived pancreatic endoderm cells secrete glucose-responsive C-peptide in patients with type 1 diabetes. *Cell Stem Cell* 28: 2047-2061.e5
- Rashid HO, Yadav RK, Kim HR & Chae HJ (2015) ER stress: Autophagy induction, inhibition and selection. *Autophagy* 11: 1956–1977
- Reinbothe TM, Alkayyali S, Ahlqvist E, Tuomi T, Isomaa B, Lyssenko V & Renström E (2013) The human L-type calcium channel Cav1.3 regulates insulin release and polymorphisms in CACNA1D associate with type 2 diabetes. *Diabetologia* 56: 340–349
- Ricketts C, Zatyka M & Barrett T (2006) The characterisation of the human Wolfram syndrome gene promoter demonstrating regulation by Sp1 and Sp3 transcription factors. *Biochim Biophys Acta - Gene Struct Expr* 1759: 367–377
- Ricordi C, Lacy PE, Finke EH, Olack BJ, Scharp DW & Bjo S (1988) Automated Method for Isolation of Human Pancreatic Islets From the Departments of Pathology. *Diabetes* 37: 413–420
- Rieusset J (2018) The role of endoplasmic reticulum-mitochondria contact sites in the control of glucose homeostasis: An update. *Cell Death Dis* 9: 1–12
- Riggs AC, Bernal-Mizrachi E, Ohsugi M, Wasson J, Fatrai S, Welling C, Murray J, Schmidt RE, Herrera PL & Permutt MA (2005) Mice conditionally lacking the Wolfram gene in pancreatic islet beta cells exhibit diabetes as a result of enhanced endoplasmic reticulum stress and apoptosis. *Diabetologia* 48: 2313–2321
- Rigoli L & Di Bella C (2012) Wolfram syndrome 1 and Wolfram syndrome 2. *Curr Opin Pediatr* 24: 512–517
- Rigoli L, Bramanti P, Di Bella C & De Luca F (2018) Genetic and clinical aspects of Wolfram

- syndrome 1, a severe neurodegenerative disease. *Pediatr Res* 83: 921–929
- Rigoli L, Lombardo F & Di Bella C (2011) Wolfram syndrome and WFS1 gene. *Clin Genet* 79: 103–117
- Riolobos L, Hirata RK, Turtle CJ, Wang PR, Gornalusse GG, Zavajlevski M, Riddell SR & Russell DW (2013) HLA engineering of human pluripotent stem cells. *Mol Ther* 21: 1232–1241
- Rodriguez-Castro KI, Hevia-Urrutia FJ & Sturniolo GC (2015) Wilson’s disease: A review of what we have learned. *World J Hepatol* 7: 2859–2870 doi:10.4254/wjh.v7.i29.2859 [PREPRINT]
- Rohayem J, Ehlers C, Wiedemann B, Holl R, Oexle K, Kordonouri O, Salzano G, Meissner T, Burger W, Schober E, *et al* (2011) Diabetes and neurodegeneration in Wolfram syndrome: A multicenter study of phenotype and genotype. *Diabetes Care* 34: 1503–1510
- Rondinelli M, Novara F, Calcaterra V, Zuffardi O & Genovese S (2015) Wolfram syndrome 2: a novel CISD2 mutation identified in Italian siblings. *Acta Diabetol* 52: 175–178
- Rouzier C, Moore D, Delorme C, Lacas-Gervais S, Ait-El-Mkadem S, Fragaki K, Burté F, Serre V, Bannwarth S, Chaussenot A, *et al* (2017) A novel CISD2 mutation associated with a classical Wolfram syndrome phenotype alters Ca²⁺ homeostasis and ER-mitochondria interactions. *Hum Mol Genet* 26: 1599
- Rowlands J, Heng J, Newsholme P & Carlessi R (2018) Pleiotropic Effects of GLP-1 and Analogs on Cell Signaling, Metabolism, and Function. *Front Endocrinol (Lausanne)* 9: 672 doi:10.3389/fendo.2018.00672 [PREPRINT]
- Rubinsztein DC, Shpilka T & Elazar Z (2012) Mechanisms of autophagosome biogenesis. *Curr Biol* 22: R29–R34 doi:10.1016/j.cub.2011.11.034 [PREPRINT]
- Sabatini P V., Speckmann T & Lynn FC (2019) Friend and foe: β -cell Ca²⁺ signaling and the development of diabetes. *Mol Metab* 21: 1–12 doi:10.1016/j.molmet.2018.12.007 [PREPRINT]
- Salem V, Silva LD, Suba K, Georgiadou E, Neda Mousavy Gharavy S, Akhtar N, Martin-Alonso A, Gaboriau DCA, Rothery SM, Stylianides T, *et al* (2019) Leader β -cells coordinate Ca²⁺ dynamics across pancreatic islets in vivo. *Nat Metab* 1: 615–629
- Samara A, Lugar HM, Hershey T & Shimony JS (2020) Longitudinal assessment of neuroradiologic features in wolfram syndrome. *Am J Neuroradiol* 41: 2364–2369

- Samara AA, Rahn R, Neyman O, Park KY, Samara AA, Marshall B, Dougherty J & Hershey T (2019) Developmental hypomyelination in Wolfram syndrome: New insights from neuroimaging and gene expression analyses. *Orphanet J Rare Dis* 14: 1–14
- Sandhu MS, Weedon MN, Fawcett KA, Wasson J, Debenham L, Daly A, Lango H, Frayling TM, Neumann RJ, Sherva R, *et al* (2009) Common variants in WFS1 confer risk of type 2 diabetes. *Eur PMC Funders Gr* 39: 951–953
- Lo Sardo V, Ferguson W, Erikson GA, Topol EJ, Baldwin KK & Torkamani A (2017) Influence of donor age on induced pluripotent stem cells. *Nat Biotechnol* 35: 69–74
- Schäffer DE, Iyer LM, Burroughs AM & Aravind L (2020) Functional Innovation in the Evolution of the Calcium-Dependent System of the Eukaryotic Endoplasmic Reticulum. *Front Genet* 11: 1–17
- Schröder M (2006) The Unfolded Protein Response. *Mol Biotechnol* 34: 279–290
- Scully KJ & Wolfsdorf JI (2021) Efficacy of GLP-1 Agonist Therapy in Autosomal Dominant WFS1-Related Disorder: A Case Report. *Horm Res Paediatr* 93: 409–414
- Sedman T, Rünkorg K, Krass M, Luuk H, Plaas M, Vasar E & Volke V (2016) Exenatide Is an Effective Antihyperglycaemic Agent in a Mouse Model of Wolfram Syndrome 1. *J Diabetes Res* 2016
- Seppa K, Jagomäe T, Kukker KG, Reimets R, Pastak M, Vasar E, Terasmaa A & Plaas M (2021) Liraglutide, 7,8-DHF and their co-treatment prevents loss of vision and cognitive decline in a Wolfram syndrome rat model. *Sci Rep* 11: 1–14
- Seppa K, Toots M, Reimets R, Jagomäe T, Koppel T, Pallase M, Hasselholt S, Krogsbæk Mikkelsen M, Randel Nyengaard J, Vasar E, *et al* (2019) GLP-1 receptor agonist liraglutide has a neuroprotective effect on an aged rat model of Wolfram syndrome. *Sci Rep* 9: 1–13
- Shang L, Hua H, Foo K, Martinez H, Watanabe K, Zimmer M, Kahler DJ, Freeby M, Chung W, LeDuc C, *et al* (2014) β -cell dysfunction due to increased ER stress in a stem cell model of wolfram syndrome. *Diabetes* 63: 923–933
- Shapiro AMJ, Pokrywczynska M & Ricordi C (2016) Clinical pancreatic islet transplantation. *Nat Rev Endocrinol* 2016 135 13: 268–277
- Shapiro AMJ, Thompson D, Donner TW, Bellin MD, Hsueh W, Pettus J, Wilensky J, Daniels M, Wang RM, Brandon EP, *et al* (2021) Insulin expression and C-peptide in type 1

- diabetes subjects implanted with stem cell-derived pancreatic endoderm cells in an encapsulation device. *Cell Reports Med* 2: 100466
- Shen J, Snapp EL, Lippincott-Schwartz J & Prywes R (2005) Stable Binding of ATF6 to BiP in the Endoplasmic Reticulum Stress Response. *Mol Cell Biol* 25: 921–932
- Shen ZQ, Huang YL, Teng YC, Wang TW, Kao CH, Yeh CH & Tsai TF (2021) CISD2 maintains cellular homeostasis. *Biochim Biophys Acta - Mol Cell Res* 1868: 118954 doi:10.1016/j.bbamcr.2021.118954 [PREPRINT]
- Sitia R, Van Anken E, Tade L, Danieli A, Christianson J, Vitale M, Valetti C, Orsi A, Rato C, Bakunts A, *et al* (2019) Inadequate BiP availability defines endoplasmic reticulum stress. *Elife*: 1–17
- Skoczek D, Dulak J & Kachamakova-Trojanowska N (2021) Maturity Onset Diabetes of the Young—New Approaches for Disease Modelling. *Int J Mol Sci* 22
- Smith CJA, Crock PA, King BR, Meldrum CJ & Scott RJ (2004) Phenotype-genotype correlations in a series of wolfram syndrome families. *Diabetes Care* 27: 2003–2009
- Song S, Tan J, Miao Y & Zhang Q (2018) Crosstalk of ER stress-mediated autophagy and ER-phagy: Involvement of UPR and the core autophagy machinery. *J Cell Physiol* 233: 3867–3874
- La Spada A, Ntai A, Genovese S, Rondinelli M, De Blasio P & Biunno I (2018) Generation of Human-Induced Pluripotent Stem Cells from Wolfram Syndrome Type 2 Patients Bearing the c.103 + 1G>A *CISD2* Mutation for Disease Modeling. *Stem Cells Dev* 27: 287–295
- Squitti R, Cerchiaro G, Giovannoni I, Francalanci P, Siotto M, Maffei P & Rongioletti MC (2019) A case of a mild Wolfram Syndrome with concomitant ATP7B mutation. 1–8
- Stone SI, Abreu D, McGill JB & Urano F (2020) Monogenic and syndromic diabetes due to endoplasmic reticulum stress. *J Diabetes Complications*: 107618
- Strom TM, Hörtnagel K, Hofmann S, Gekeler F, Scharfe C, Rabl W, Gerbitz KD & Meitinger T (1998) Diabetes insipidus, diabetes mellitus, optic atrophy and deafness (DIDMOAD) caused by mutations in a novel gene (wolframin) coding for a predicted transmembrane protein. *Hum Mol Genet* 7: 2021–2028
- Takahashi K, Tanabe K, Ohnuki M, Narita M, Ichisaka T, Tomoda K & Yamanaka S (2007) Induction of Pluripotent Stem Cells from Adult Human Fibroblasts by Defined Factors. *Cell* 131: 861–872

- Takahashi K & Yamanaka S (2006) Induction of Pluripotent Stem Cells from Mouse Embryonic and Adult Fibroblast Cultures by Defined Factors. *Cell* 126: 663–676
- Takeda K, Inoue H, Tanizawa Y, Matsuzaki Y, Oba J, Watanabe Y, Shinoda K & Oka Y (2001) WFS1 (Wolfram syndrome 1) gene product: predominant subcellular localization to endoplasmic reticulum in cultured cells and neuronal expression in rat brain. *Hum Mol Genet* 10: 477–484
- Takei D, Ishihara H, Yamaguchi S, Yamada T, Tamura A, Katagiri H, Maruyama Y & Oka Y (2006) WFS1 protein modulates the free Ca²⁺-concentration in the endoplasmic reticulum. *FEBS Lett* 580: 5635–5640
- Tamborlane W V., Barrientos-Pérez M, Fainberg U, Frimer-Larsen H, Hafez M, Hale PM, Jalaludin MY, Kovarenko M, Libman I, Lynch JL, *et al* (2019) Liraglutide in Children and Adolescents with Type 2 Diabetes. *N Engl J Med* 381: 637–646
- Tanji Y, Yamaguchi S, Ishigaki Y, Katagiri H, Oka Y & Ishihara H (2015) DPP-4 Inhibition Ameliorates Pancreatic β -Cell Failure and Improves Glucose Tolerance in the Mouse Model of Wolfram Syndrome. *J Diabetes Mellit* 05: 72–80
- Tarcin G, Turan H, Dagdeviren Cakir A, Ozer Y, Aykut A, Alpman Durmaz A, Ercan O & Evliyaoglu O (2021) Different clinical entities of the same mutation: A case report of three sisters with Wolfram syndrome and efficacy of dipeptidyl peptidase-4 inhibitor therapy. *J Pediatr Endocrinol Metab* 34: 1049–1053
- Terakawa A, Chujo D, Yasuda K, Ueno K, Nakamura T, Hamano S, Ohsugi M, Tanabe A, Ueki K & Kajio H (2020) Maturity-Onset diabetes of the young type 5 treated with the glucagon-like peptide-1 receptor agonist: A case report. *Medicine (Baltimore)* 99: e21939
- Theiner T, Jacobo-Piqueras N, Ortner NJ, Geisler SM & Tuluc P (2022) CaV1.3 L-type Ca²⁺ channel modulates pancreatic β -cell electrical activity and survival. *J Gen Physiol* 154
- Thomson JA, Itskovitz-Eldor J, Shapiro S, Waknitz M, Swiergiel J, Marshall V & Jones J (1998) Embryonic stem cell lines derived from human blastocysts. *Science (80-)* 282: 1145–1147
- Tomas A, Jones B & Leech C (2020) New Insights into Beta-Cell GLP-1 Receptor and cAMP Signaling. *J Mol Biol* 432: 1347–1366
- Toots M, Reimets R, Plaas M & Vasar E (2019) Muscarinic Agonist Ameliorates Insulin Secretion in Wfs1-Deficient Mice. *Can J Diabetes* 43: 115–120

- Toots M, Seppa K, Jagomäe T, Koppel T, Pallase M, Heinla I, Terasmaa A, Plaas M & Vasar E (2018) Preventive treatment with liraglutide protects against development of glucose intolerance in a rat model of Wolfram syndrome. *Sci Rep* 8: 1–10
- Torres R, Leroy E, Hu X, Katrivanou A, Gourzis P, Papachatzopoulou A, Athanassiadou A, Beratis S, Collier D & Polymeropoulos MH (2001) Mutation screening of the Wolfram syndrome gene in psychiatric patients. *Mol Psychiatry* 6: 39–43
- Tranebjærg L, Barrett T & Dahl N (2020) WFS1 Wolfram Syndrome Spectrum Disorder. In *GeneReviews*® pp 1–27.
- Ueda K, Kawano J, Takeda K, Yujiri T, Tanabe K, Anno T, Akiyama M, Nozaki J, Yoshinaga T, Koizumi A, *et al* (2005) Endoplasmic reticulum stress induces Wfs1 gene expression in pancreatic β -cells via transcriptional activation. *Eur J Endocrinol* 153: 167–176
- Urakami T, Habu M, Okuno M, Suzuki J, Takahashi S & Yorifuji T (2015) Three years of liraglutide treatment offers continuously optimal glycemic control in a pediatric patient with maturity-onset diabetes of the young type 3. *J Pediatr Endocrinol Metab* 28: 327–331
- Urano F (2016) Wolfram Syndrome: Diagnosis, Management, and Treatment. *Curr Diab Rep* 16: 1–8 doi:10.1007/s11892-015-0702-6 [PREPRINT]
- Urrea H, Dufey E, Lisbona F, Rojas-Rivera D & Hetz C (2013) When ER stress reaches a dead end. *Biochim Biophys Acta - Mol Cell Res* 1833: 3507–3517
- Valéro R, Bannwarth S, Roman S, Paquis-Flucklinger V & Vialettes B (2008) Autosomal dominant transmission of diabetes and congenital hearing impairment secondary to a missense mutation in the WFS1 gene. *Diabet Med* 25: 657–661
- Vantyghem M-C, de Koning EJP, Pattou F & Rickels MR (2019) Advances in β -cell replacement therapy for the treatment of type 1 diabetes. *Lancet* 394: 1274–1285
- Vattem KM, Dele M, Rainbow LA, Lecoq A, Shaw NJ, Robert J, Rooman R, Diatloff-zito C, Michaud JL, Bin-abbas B, *et al* (2004) Wolcott-Rallison Syndrome Clinical, Genetic, and Functional Study of EIF2AK3 Mutations and Suggestion of Genetic Heterogeneity. *Diabetes* 53
- Velazco-Cruz L, Song J, Maxwell KG, Goedegebuure MM, Augsornworawat P, Hogrebe NJ & Millman JR (2019) Acquisition of Dynamic Function in Human Stem Cell-Derived β Cells. *Stem Cell Reports* 12: 351–365
- Volpato V & Webber C (2020) Addressing variability in iPSC-derived models of human

- disease: Guidelines to promote reproducibility. *DMM Dis Model Mech* 13
doi:10.1242/dmm.042317 [PREPRINT]
- Vora AJ, Lilleyman JS, Bunday S, Fielder A & Poulton K (1993) Wolfram syndrome: mitochondrial disorder. *Lancet* 342: 1059–1060 doi:10.1016/0140-6736(93)92918-J [PREPRINT]
- Wang CH, Kao CH, Chen YF, Wei YH & Tsai TF (2014) Cisd2 mediates lifespan: Is there an interconnection among Ca²⁺ homeostasis, autophagy, and lifespan? *Free Radic Res* 48: 1109–1114
- Wang L, Liu H, Zhang X, Song E, Wang Y, Xu T & Li Z (2021a) WFS1 functions in ER export of vesicular cargo proteins in pancreatic β -cells. *Nat Commun* 12: 6996
- Wang M, Wan C, He T, Han C, Zhu K, Waddington JL & Zhen X (2021b) Sigma-1 receptor regulates mitophagy in dopaminergic neurons and contributes to dopaminergic protection. *Neuropharmacology* 196
- Wang X, Ma M, Teng J, Che X, Zhang W, Feng S, Zhou S, Zhang Y, Wu E & Ding X (2015) Valproate attenuates 25-kDa C-terminal fragment of TDP-43-induced neuronal toxicity via suppressing endoplasmic reticulum stress and activating autophagy. *Int J Biol Sci* 11: 752–761
- Wang X, Maxwell KG, Wang K, Bowers DT, Flanders JA, Liu W, Wang L-H, Liu Q, Liu C, Naji A, *et al* (2021c) A nanofibrous encapsulation device for safe delivery of insulin-producing cells to treat type 1 diabetes. *Sci Transl Med* 13: eabb4601
- Wasson J & Permutt MA (2008) Candidate gene studies reveal that the WFS1 gene joins the expanding list of novel type 2 diabetes genes. *Diabetologia* 51: 391–393
doi:10.1007/s00125-007-0920-9 [PREPRINT]
- Wiley SE, Andreyev AY, Divakaruni AS, Karisch R, Perkins G, Wall EA, van der Geer P, Chen YF, Tsai TF, Simon MI, *et al* (2013) Wolfram Syndrome protein, Miner1, regulates sulphhydryl redox status, the unfolded protein response, and Ca²⁺ homeostasis. *EMBO Mol Med* 5: 904–918
- Wilf-Yarkoni A, Shor O, Fellner A, Hellmann MA, Pras E, Yonath H, Shkedi-Rafid S, Basel-Salmon L, Bazak L, Eliahou R, *et al* (2021) Mild Phenotype of Wolfram Syndrome Associated With a Common Pathogenic Variant Is Predicted by a Structural Model of Wolframin. *Neurol Genet* 7: e578

- Wolfram DJ & Wagener HP (1938) Diabetes Mellitus and Simple Optic Atrophy among Siblings: Report on Four Cases. 715–71
- Wolfram Syndrome Guideline Development Group (2014) Management of Wolfram Syndrome: A Clinical Guideline
- Wright J, Birk J, Haataja L, Liu M, Ramming T, Weiss MA, Appenzeller-Herzog C & Arvan P (2013) Endoplasmic reticulum oxidoreductin-1 α (Ero1 α) improves folding and secretion of mutant proinsulin and limits mutant proinsulin-induced endoplasmic reticulum stress. *J Biol Chem* 288: 31010–31018
- Yamada T, Ishihara H, Tamura A, Takahashi R, Yamaguchi S, Takei D, Tokita A, Satake C, Tashiro F, Katagiri H, *et al* (2006) WFS1-deficiency increases endoplasmic reticulum stress, impairs cell cycle progression and triggers the apoptotic pathway specifically in pancreatic β -cells. *Hum Mol Genet* 15: 1600–1609
- Yamaguchi S, Ishihara H, Tamura A, Yamada T, Takahashi R, Takei D, Katagiri H & Oka Y (2004) Endoplasmic reticulum stress and N-glycosylation modulate expression of WFS1 protein. *Biochem Biophys Res Commun* 325: 250–256
- Yamaguchi S, Ishihara H, Yamada T, Tamura A, Usui M, Tominaga R, Munakata Y, Satake C, Katagiri H, Tashiro F, *et al* (2008) ATF4-Mediated Induction of 4E-BP1 Contributes to Pancreatic β Cell Survival under Endoplasmic Reticulum Stress. *Cell Metab* 7: 269–276
- Yan Y, Rato C, Rohland L, Preissler S & Ron D (2019) MANF antagonizes nucleotide exchange by the endoplasmic reticulum chaperone BiP. *Nat Commun* 10
- Yin JJ, Li YB, Wang Y, Liu GD, Wang J, Zhu XO & Pan SH (2012) The role of autophagy in endoplasmic reticulum stress-induced pancreatic β cell death. *Autophagy* 8
- Young TL, Ives E, Lynch E, Person R, Snook S, MacLaren L, Cator T, Griffin A, Fernandez B, Lee MK, *et al* (2001) Non-syndromic progressive hearing loss DFNA38 is caused by heterozygous missense mutation in the Wolfram syndrome gene WFS1. *Hum Mol Genet* 10: 2509–2514
- Yu J, Li T, Liu Y, Wang X, Zhang J, Wang X, Shi G, Lou J, Wang L, Wang C, *et al* (2020) Phosphorylation switches protein disulfide isomerase activity to maintain proteostasis and attenuate ER stress. *EMBO J* 39: e103841
- Yurimoto S, Hatano N, Tsuchiya M, Kato K, Fujimoto T, Masaki T, Kobayashi R & Tokumitsu H (2009) Identification and characterization of wolframin, the product of the Wolfram

syndrome gene (WFS1), as a novel calmodulin-binding protein. *Biochemistry* 48: 3946–3955

Zatyka M, Da Silva Xavier G, Bellomo EA, Leadbeater W, Astuti D, Smith J, Michelangeli F, Rutter GA & Barrett TG (2015) Sarco(endo)plasmic reticulum atpase is a molecular partner of wolfram syndrome 1 protein, which negatively regulates its expression. *Hum Mol Genet* 24: 814–827

Zhang D, Jiang W, Liu M, Sui X, Yin X, Chen S, Shi Y & Deng H (2009) Highly efficient differentiation of human ES cells and iPS cells into mature pancreatic insulin-producing cells. *Cell Res* 19: 429–438

Zhang L, Zhang L, Li Y, Li L, Melchiorson JU, Rosenkilde M & Hölscher C (2020) The Novel Dual GLP-1/GIP Receptor Agonist DA-CH5 Is Superior to Single GLP-1 Receptor Agonists in the MPTP Model of Parkinson's Disease. *J Parkinsons Dis* 10: 523–542

Zhu Z, Li Q V., Lee K, Rosen BP, González F, Soh CL & Huangfu D (2016) Genome Editing of Lineage Determinants in Human Pluripotent Stem Cells Reveals Mechanisms of Pancreatic Development and Diabetes. *Cell Stem Cell* 18: 755–768

Zinszner H, Kuroda M, Wang X, Batchvarova N, Lightfoot RT, Remotti H, Stevens JL & Ron D (1998) CHOP is implicated in programmed cell death in response to impaired function of the endoplasmic reticulum. *Genes Dev* 12: 982

Silvia Turchio